UNIVERSITAT POLITÈCNICA DE CATALUNYA

Wake-up Radio Systems: Design, Development, Performance Evaluation and Comparison to Conventional Medium Access Control Protocols for Wireless Sensor Networks

by

Joaquim Oller i Bosch

A thesis submitted in partial fulfillment for the
degree of Doctor of Philosophy

in the
Escola Tècnica Superior d'Enginyeria de Telecomunicació de Barcelona
Departament d'Enginyeria Telemàtica

PhD Advisor: Jordi Casademont i Serra
January 2015

UNIVERSITAT POLITÈCNICA DE CATALUNYA
BARCELONATECH
Escola de Doctorat

Acta de qualificació de tesi doctoral

Curs acadèmic:

Nom i cognoms

Programa de doctorat

Unitat estructural responsable del programa

Resolució del Tribunal

Reunit el Tribunal designat a l'efecte, el doctorand / la doctoranda exposa el tema de la seva tesi doctoral titulada

_____

_____.

Acabada la lectura i després de donar resposta a les qüestions formulades pels membres titulars del tribunal, aquest atorga la qualificació:

☐ NO APTE ☐ APROVAT ☐ NOTABLE ☐ EXCEL·LENT

(Nom, cognoms i signatura) President/a	(Nom, cognoms i signatura) Secretari/ària

(Nom, cognoms i signatura) Vocal	(Nom, cognoms i signatura) Vocal	(Nom, cognoms i signatura) Vocal

_____, _____ d'/de _____ de _____

El resultat de l'escrutini dels vots emesos pels membres titulars del tribunal, efectuat per l'Escola de Doctorat, a instància de la Comissió de Doctorat de la UPC, atorga la MENCIÓ CUM LAUDE:

☐ SÍ ☐ NO

(Nom, cognoms i signatura) President de la Comissió Permanent de l'Escola de Doctorat	(Nom, cognoms i signatura) Secretari de la Comissió Permanent de l'Escola de Doctorat

Barcelona, _____ d'/de _____ de _____

Declaration of Authorship

I, Joaquim Oller Bosch, declare that this thesis titled, 'Wake-up Radio Systems: Design, Development, Performance Evaluation and Comparison to Conventional Medium Access Control Protocols for Wireless Sensor Networks' and the work presented in it are my own. I confirm that:

- This work was done wholly or mainly while in candidature for a research degree at this University.
- Where any part of this thesis has previously been submitted for a degree or any other qualification at this University or any other institution, this has been clearly stated.
- Where I have consulted the published work of others, this is always clearly attributed.
- Where I have quoted from the work of others, the source is always given. With the exception of such quotations, this thesis is entirely my own work.
- I have acknowledged all main sources of help.
- Where the thesis is based on work done by myself jointly with others, I have made clear exactly what was done by others and what I have contributed myself.

Signed: _____

Date: _____

UNIVERSITAT POLITÈCNICA DE CATALUNYA

Abstract

Escola Tècnica Superior d'Enginyeria de Telecomunicació de Barcelona
Departament d'Enginyeria Telemàtica

Doctor of Philosophy

by Joaquim Oller i Bosch

This thesis arises from the need of improving the energy efficiency of radio communications in low-power applications such as Wireless Sensor Networks. During the last years, the traditional paradigm employed by this type of networks has been duty-cycling, which suffers from several issues such as overhearing and idle listening.

This work presents a research developed in the field of Wake-up Radio (WuR) systems in an incremental fashion; from the very basic concepts in low-power communications, microcontrollers, wake-up receivers (WuRx) and transmitters (WuTx), up to two complete designs of WuR systems, which are thoroughly analyzed along the thesis in terms of numerous metrics. The thesis also exhaustively describes the kind of applications that may benefit from WuR systems.

Node addressing is a crucial feature in WuR systems. Thus, this thesis also presents, develops and analyzes several of these addressing mechanisms for WuR systems.

A complete state-of-the-art is also presented in the thesis comprising a complete overview of most relevant WuR systems as of 2014. Such systems are analyzed in detail and their features and architectures compared to the two designs previously mentioned.

To be able to study the performance of networks with a high number of concurrent nodes, this thesis also provides a complete framework for simulating and comparing WuR systems to traditional duty-cycled MAC approaches. The evaluated protocols are among the most known and used in the research literature. Regarding commercial systems, this thesis also analyzes and evaluates the performance of Bluetooth Low Energy (BLE), a low-power MAC protocol which in certain cases proves to fit several applications better than WuR.

Finally, this thesis solves the issue of the need for custom wake-up transmitters, as required by most WuR systems, by presenting a design that enables any IEEE 802.11-enabled device to be used as a WuTx without requiring any hardware modification. This idea effectively allows extending WuR systems to a whole new area of customer-oriented applications.

Acknowledgements

This work would have not been possible without the support from my family, and Rut. Thank you everybody.

I would also like to thank my research partners at the Wireless Networks Group. Thanks to Dr. Ilker Demirkol and Prof. Josep Paradells for their wise contributions.

Thanks to the Institut für Mikrosystemtechnik - IMTEK at Albert-Ludwigs-Universität, Freiburg: Dr. Joan Albesa, Dr. Gerd Ulrich Gamm, Dr. Fabian Höflinger and Prof. Leonhard Reindl. It was a pleasure to work and learn with you.

Thanks to Martí Fàbregas at Universitat de Girona and to Robert Martín, from Cassà de la Selva.

Last but not least, special thanks to my PhD Advisor: Dr. Jordi Casademont.

Contents

List of Figures

Chapter 1

Chapter 2

Chapter 5

Chapter 6

Chapter 7

Chapter 8

Source Codes

Abbreviations

A

ACK	**ACK**nowledgment
ACLK	**A**uxiliar **CL**oc**K**
ACM	**A**ssociation for **C**omputing **M**achinery
AES	**A**dvanced **E**ncryption **S**tandard
AP	**A**ccess **P**oint
ASCII	**A**merican **S**tandard **C**ode for **I**nformation **I**nterchange
ASK	**A**mplitude **S**hift **K**eying
ATT	**ATT**ribute (Protocol)

B

BER	**B**it **E**rror **R**ate
BLE	**B**luetooth **L**ow **E**nergy

C

CCA	**C**lear **C**hannel **A**ssessment
CPU	**C**entral **P**rocessing **U**nit
CRC	**C**yclic **R**edundancy **C**heck
CS	**C**arrier **S**ense

D

DCF	**D**istributed **C**oordination **F**unction
DIFS	**D**CF **I**nterframe **S**pace

F

FPGA	**F**ield **P**rogrammable **G**ate **A**rray
FSO	**F**ree **S**pace **O**ptics

G

GAP	**G**eneric **A**ccess **P**rofile
GATT	**G**eneric **A**ttribute **P**rofile
GPIO	**G**eneral **P**urpose **I**nput **O**uput
GPS	**G**lobal **P**ositioning **S**ystem
GSM	**G**lobal **S**ystem for **M**obile **C**ommunications

I

IC	**I**ntegrated **C**ircuit
IEEE	**I**nstitute of **E**lectrical and **E**lectronics **E**ngineers
IET	**I**nstitution of **E**ngineering and **T**echnology
IETF	**I**nternet **E**ngineering **T**ask **F**orce
IF	**I**ntermediate **F**requency
IFS	**I**nter**F**rame **S**pace
ILRO	**I**njection-**L**ocked **R**ing **O**scillators
IP	**I**nternet **P**rotocol
IRQ	**I**nterrupt **R**e**Q**uest
ISR	**I**nterrupt **S**ervice **R**equest

J

JCR	**J**ournal **C**itation **R**eport

L

LAN	**L**ocal **A**rea **N**etwork
LED	**L**ight **E**mitting **D**iode
LF	**L**ow **F**requency
LPM	**L**ow **P**ower **M**ode
LTK	**L**ong **T**erm **K**ey

M

MAC	**M**edium **A**ccess **C**ontrol
MCU	**M**icro**C**ontroller **U**nit
MIC	**M**essage **I**ntegrity **C**heck

N

NFC	**N**ear **F**ield **C**ommunication
NIC	**N**etwork **I**nterface **C**ard
NWK	**N**et**W**or**K**

O

OOK	**O**n-**O**ff **K**eying

P

PC	**P**ersonal **C**omputer, also **P**ower **C**ontrol
PDR	**P**acket **D**elivery **R**atio
PDU	**P**acket **D**atagram **U**nit
PPM	**P**ulse **P**osition **M**odulation

R

RF	**R**adio-**F**requency
RFID	**R**adio **F**requency **ID**entification
RI	**R**eceiver **I**nitiated
RSSI	**R**eceived **S**ignal **S**trength **I**ndicator
RTC	**R**eal **T**ime **C**lock
RTID	**R**adio **T**riggered **ID**entification

S

SAW	**S**urface **A**coustic **W**avelength
SCM	**S**ub**C**arrier **M**odulation
SMA	**S**ub**M**iniature version **A**
SMP	**S**ecurity **M**anager **P**rotocol
SPI	**S**erial **P**eripheral **I**nterface
STK	**S**hort **T**erm **K**ey

T

TK	**T**emporary **K**ey

U

UHF	**U**ltra **H**igh **F**requency

V

VLO	**V**ery **L**ow-power **O**scillator
VM	**V**oltage **M**ultiplier
VSWR	**V**oltage **S**tanding **W**ave **R**atio

W

WBAN	**W**ireless **B**ody **A**rea **N**etwork
WG	**W**orking **G**roup
WHAN	**W**ireless **H**ome **A**utomation **N**etwork
WSN	**W**ireless **S**ensor **N**etwork
WuC	**W**ake-up **C**all
WuR	**W**ake-up **R**adio
WuRx	**W**ake-up **R**eceiver (**Rx**)
WuTx	**W**ake-up **T**ransmitter (**Tx**)

1 Introduction to Low-Power Wireless Communications & MicroControllers

As of 2014, low-power radios represent one of the most active research areas in the field of wireless communications. Accordingly, new ecosystems of technical terms periodically appear in the literature in order to describe new particular features or capabilities, improved electronic designs or novel devices' classifications. To properly introduce such particular terminology, and for the sake of maximum comprehension, this thesis provides an introductory chapter related to wireless communications, wireless transceivers, low-power electronic components, communication protocols and wake-up systems. In addition to presenting these concepts, the current chapter also describes the interactions between them, as well as the different operational paradigms they enable. However, experienced readers may choose to skip the following pages up to section 1.6, where the Wake-up Radio concept is introduced.

Contents

1.1 Introduction

Data in a wireless system is actually transmitted and/or received by means of *transceivers*, an electronic component that includes the circuitry for both transmission and reception functions in a single Integrated Circuit (IC), or chip. Nowadays' cell phones contain different transceivers for GSM, Bluetooth, IEEE 802.11, Near Field Communication (NFC), etc. To achieve maximum communication distances in a wireless system, a transceiver commonly attaches an *antenna*. Antennas, or antennae as in its Latin plural form, propagate and receive

electromagnetic radio waves at a given frequency. Thus, the transceiver converts bits of data from an electronic device to radio waves to be radiated by an antenna, and vice versa. Figure 1.1 depicts some of the basic components in a wireless system.

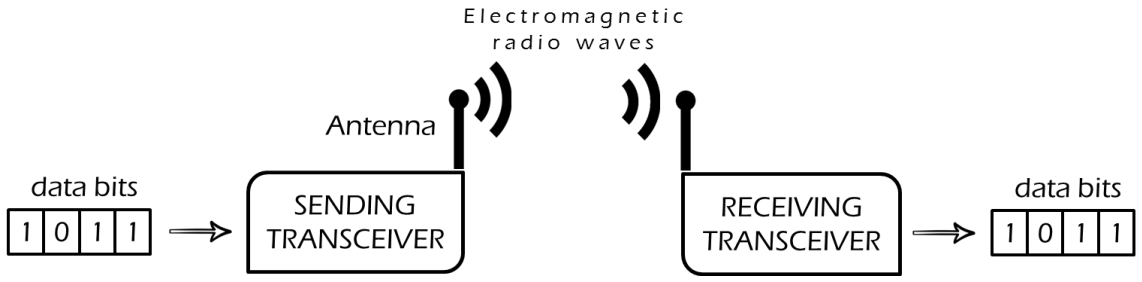

Figure 1.1: Elements of a basic wireless system.

Transceivers require electrical current to operate. Basically, provided that they are correctly attached, or matched, to an antenna, the maximum communication distance they enable is proportional to the amount of current they employ. At the same time, this amount of current is inversely proportional to the lifetime of the battery of the electronic device that includes the wireless transceiver. Thus, the ideal transceiver should consume very little amount of electrical current while allowing for adjustable communication distances in order to fit the largest number of applications possible. In addition, such transceiver should transmit and receive information at very high speed. However, achieving both of the previous requirements is not possible. Devices capable of communicating fast and at long distances require energy-demanding electronic components, such as power amplifiers, between the transceiver and the antenna. At the same time, devices featuring low current consumption values usually provide simplified circuitry, reduced communication distances and low bit-rates. Hence, depending on the intended application, the adequate transceiver design strongly differs.

1.1.1 Choosing an Adequate Wireless Technology

There is an infinite number of ways of looking at existing wireless technologies, e.g., based on their maximum bit-rates, their presence in consumer electronic devices, their memory requirements, their programming capabilities, the different types of networks they may build, etc. These classifications certainly narrows the possible candidate technologies for a certain application. However, performing selection based on the previous criteria does not guarantee the final candidate choice completely fits the purpose of a certain application. For example, several wireless technologies such as IEEE 802.11, Bluetooth and IEEE 802.15.4 / ZigBee present common parameters like an operational frequency of 2.4 GHz. However, they certainly do not fit the same application areas.

Instead, a more efficient approach to consider wireless technologies is from an application point of view from the very beginning, putting system's purpose and context first. This allows quickly chopping the branches of the selection tree in order to identify the most suitable

technology for a certain application. For example, when considering an application for wireless access to Internet, it is immediate to think about IEEE 802.11. However, for applications comprising wireless body area devices, such as medical electrocardiograms or music headsets, Bluetooth is the most usual choice. Finally, IEEE 802.15.4 / ZigBee technologies find its application area in wireless home networks like domotics.

An application-oriented selection even allows omitting some of the technical aspects of candidate technologies. That is, up to a degree, the selection may be performed without even taking into account several aspects of the different wireless technologies. In other words, an application-oriented classification gives extra preference to the suitability and applicability of a wireless technology over other aspects such as the frequency or the maximum bit-rate value it features.

Thus, the selection of a technology presents a trade-off between the expected application's wireless performance and the application's nature. For example, the three technologies previously mentioned implicitly include an underlying tendency; as applications increase their complexity, devices tend to consume more power. Hence, from an operational point of view, an IEEE 802.11 transceiver has to be aware of keeping its synchronization with the network's Access Point (AP), scan surrounding wireless networks, receive large amounts of streaming data and multiplex the different requirements upcoming from the user's terminal, among other functions. Differently, traditional Bluetooth is commonly employed in applications where the transceiver interacts with a reduced number of nodes, mostly just one. Contrasting to IEEE 802.11, two devices involved in a Bluetooth communication usually run a single application, like transferring a file or streaming audio. Finally, IEEE 802.15.4 / ZigBee devices form networks which usually require very few interaction among nodes compared to the previous two examples. These interactions may range from once every 30 seconds to once a day. Because of this latter lower application complexity, less energy is required.

Even without numerical calculations, it is immediate to see how heterogeneous are the battery requirements for these three example technologies. Thus, both the technology and its associated battery requirements are factors that must be accounted altogether when designing a wireless application.

1.2 First Insights on Low-Power Wireless Chipsets

Many wireless transceivers hold the low-power label in the literature. However, the low-power feature of a wireless technology is extremely relative and has to be put in context. For example, can IEEE 802.11 be considered energy-efficient? Yes, indeed it is for large data transfer thanks to the high bit-rates it allows for. However, can IEEE 802.11 be considered low-power? No, it cannot, because of its high electrical current peaks when transmitting and the complex circuitry and software it requires for its operation.

The capability of a technology to be considered as low-power directly relates to the intended device's battery. Following the previous example, IEEE 802.11 operation presumes a considerable back-end, like a laptop battery, commonly charged by means of an Alternating Current (AC) power supply. Under these comfortable conditions, IEEE 802.11 is undoubtedly the most adequate wireless technology. However, for low-power applications as the ones in this thesis, an essential requirement for any candidate technology is to operate on low-performance batteries such as the CR2032 Manganese Dioxide Lithium coin cell in Figure 1.2, or even completely bypassing the need for such battery if energy harvesting strategies are considered. Clearly, IEEE 802.11 does not easily comply this requirement.

Figure 1.2: A CR2032 coin cell battery.

Nowadays, low-power solutions target applications for which the capabilities of IEEE 802.11 are oversized. Numerically, technologies truly designed with low-power in mind like IEEE 802.15.4 / ZigBee, Bluetooth and ANT, among others, usually present peak current consumption values around 15 mA, which makes them suitable to operate on batteries such as CR2032. For higher peak current demands, such as the ones in NFC or IEEE 802.11 of up to 50 mA and 116 mA respectively [8], the lifetime of coin cell batteries quickly degrades [9].

Transceivers' peak current demands indeed affect to the suitability of a wireless technology for a certain application because of their effect on the battery requirements. However, it is even more important to quantify the average energy profile presented by a wireless technology when not dealing with application data. For maximum energy savings, when the transceiver is said to be *idle*, i.e., not receiving or transmitting, it must enter *sleep mode*. In sleeping state, electronic components require current in the order of magnitude of µA, that is, thousands of times less than the mA employed when actively transmitting or receiving data. This improvement factor becomes essential in low-power applications, examples of which are Wireless Sensor Networks (WSN) and Wireless Body Area Networks (WBAN).

The simplest *Wireless Sensor node* may be understood as a temperature sensor to which a wireless transceiver is attached. The common operation of such wireless sensors consists in sending the measured temperature and, afterwards, entering sleep mode in order to save energy. In an example application, the node is not permanently active but transmits data only during 100 ms once every 30 seconds. To perform such transmission, the node requires 15 mA of electrical current. When the sensor node is not transmitting it enters sleep mode, where it only requires 10 µA of electrical current, and remains in this low-power state until the next

data transmission. Thus, the average current consumption is obtained by simply weighting current consumption by the time duration of the two different possible states of the sensor node over the full time period:

$$\frac{(0.1\ \text{s} \times 15\ \text{mA}) + (29.9\ \text{s} \times 0.01\ \text{mA})}{30\ \text{s}} = 76\ \mu\text{A} = 0.076\ \text{mA}$$

By considering a typical 230 mAh capacity of a cell coin battery, the presented application case features an approximate battery lifetime of:

$$\frac{230\ \text{mAh}}{0.076\ \text{mA}} = 3026\ \text{hours} = 126\ \text{days}$$

Similar calculations can be performed in case the sensor is not notifying a temperature measure, but receiving it. In any case, the sensor is only active during a small portion of the total time. In this example, the sensor is active for 100 milliseconds every 30 seconds. By dividing these two values, the ratio of time the sensor is duty can be obtained, in this case:

$$\frac{0.1\ \text{s}}{30\ \text{s}} \times 100 = 0.3\%$$

The previous relation is commonly known as the *duty cycle ratio* of the sensor, and represents the energy savings allowed by the alternating sleep / active strategy when compared to an always-on approach. In this example, the application features a periodicity of 30 seconds. This value is realistic and in fact close to the maximum periodicity limit of Bluetooth Low Energy, also known as Bluetooth Smart or BLE, in which one notifying sensor node, e.g. a humidity sensor, may sleep for up to 32 seconds between two active periods of the wireless transceiver. However, BLE active periods are shorter than 100 ms, which allows this technology to present extended battery lifetimes.

Instead, if no duty cycle strategy is considered in a wireless sensor node, the battery is depleted much quicker. For example, a wireless transceiver which is left activated to receive remote frames requires about 20 mA in average. Considering a battery capacity of 230 mAh, this means only 11.5 hours of battery lifetime.

1.3 First Insights on Low-Power MCUs

This section emphasizes on an intentionally obviated element in previous sections, which is the MicroController Unit (MCU). The MCU is the processing core of the wireless node, and is attached by some interface to sensors, displays, keyboards, etc., and by some other to the wireless transceiver. Connection of the MCU is shown in Figure 1.3 as an updated version of Figure 1.1:

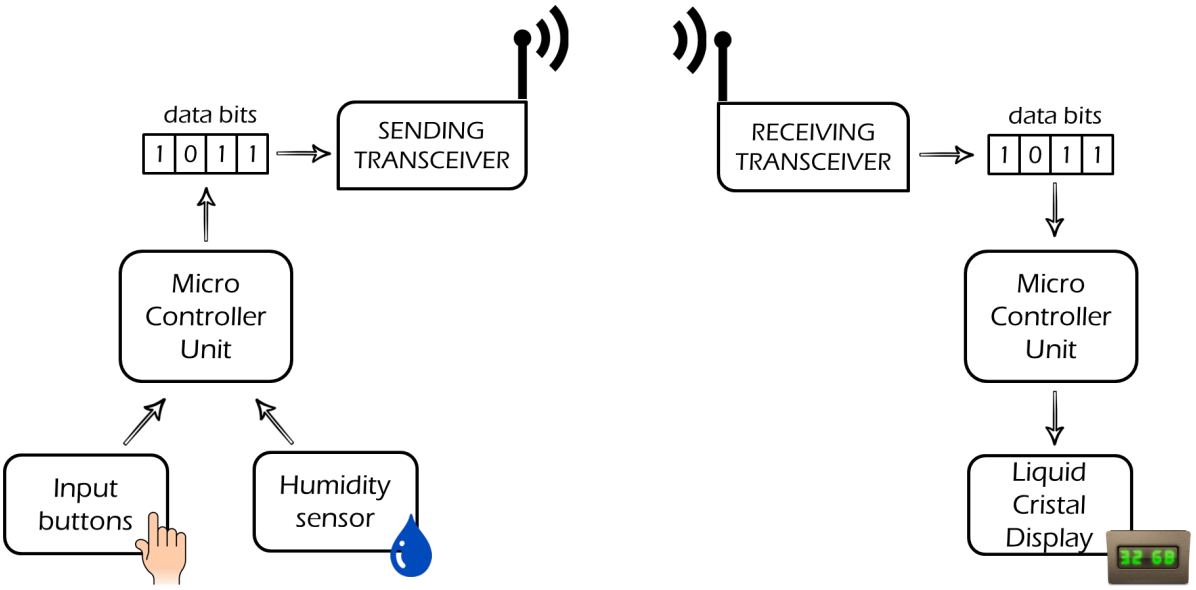

Figure 1.3: Elements of a basic wireless system (II).

The MCU is in charge of all processing tasks in the node but the ones performed by the data transceiver. These tasks vary depending on the designed application. Concretely, in a wireless sensor node, the MCU may:

→ Obtain the incoming data from attached sensors, or transducers, that measure humidity, radiation, pollution, button presses, etc.

→ Configure the transceiver's transmission / reception parameters like bit-rate, operational frequency, number of bytes per frame, etc.

→ Provide the data to be transmitted to the transceiver, e.g., the last 10 measurements from sensors, or a text message entered by an attached input keyboard.

→ Collect data sent from remote nodes and received by the transceiver, and present it to display interfaces.

→ Be award of event timers, i.e., configurable alarms that trigger after a finite number of seconds. The duty cycle timer is an example of this.

→ Set the transceiver from active to sleep mode, and vice versa, in order to save energy.

The previous functions are performed in a logical sequence in the diagram in Figure 1.4, which represents an example action flow for a MCU of a wireless sensor node. It can be seen that, once initialization part performs correctly, the MCU enters an infinite but controlled loop where it periodically obtains measurements from sensors, activates the wireless transceiver to transmit them as well as to check if there are incoming communications and, finally, disables every electronic component in the node until the next measurement.

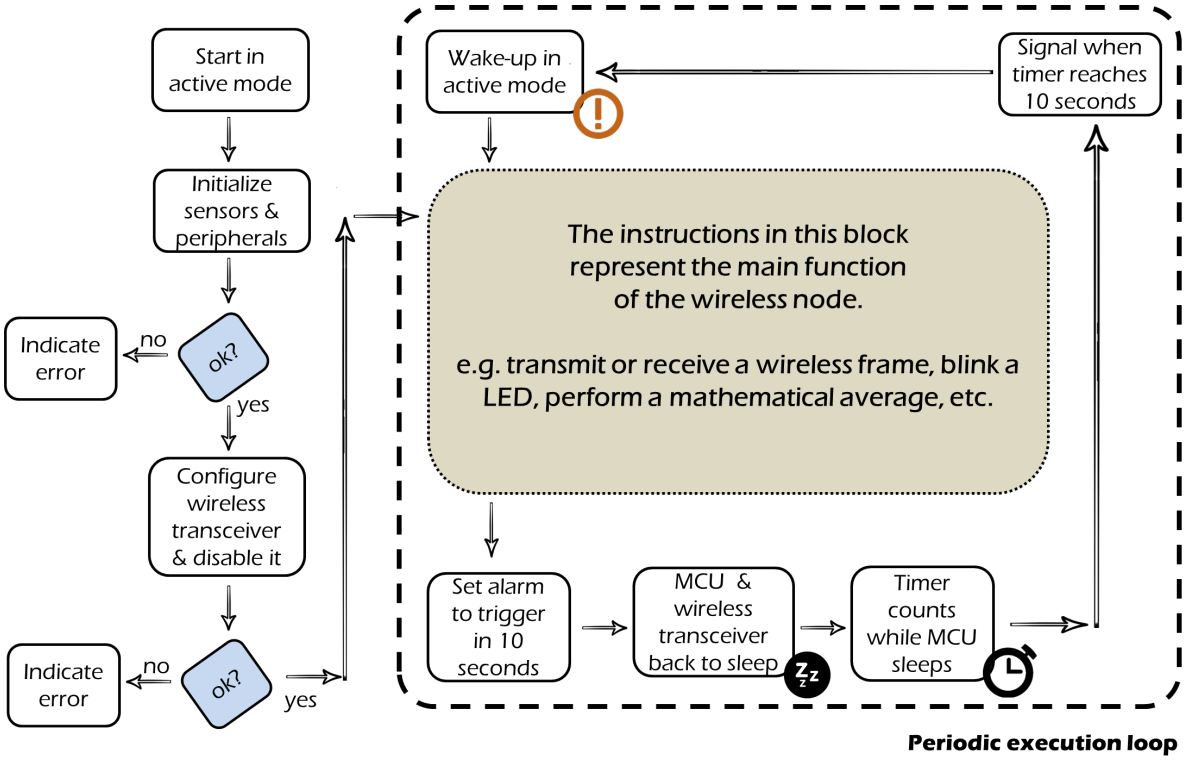

Figure 1.4: Example execution flow of the MCU in a wireless sensor node.

For maximum energy efficiency, it is important that a MCU is designed from scratch with low-power purposes in mind. However, this does not necessarily imply these MCUs are expensive, but even the other way around, since low-power strongly interrelates with circuitry complexity. For example, a 16 MHz MSP430G2553 low-power MCU from Texas Instruments enables wireless sensor node designs while costing less than 1 $ when bought in volume. Code 1.1 is a simple working snippet for this MCU implementing a periodic timed loop as the one in Figure 1.4.

The MCU in the example Code 1.1 simply blinks a Light Emitting Diode (LED) on and off alternatively. The code's only difficulty is the naming convention, since each MCU follows its own terminology for internal hardware registers, pins, etc. The same program can be written analogously for another MCU and the structure would be similar. Code 1.1 first makes sure to stop an internal timer of the MCU that constantly checks if the program's execution hangs. That is, it stops the WatchDog timer, as it is called, from guarding. Next, it sets a General Purpose Input Output (GPIO) pin of the MCU as output. This pin is concretely the first pin on port 1, P1.1, to which a LED is connected. Afterwards, the program configures a timer to start counting. Finally, the MCU is set in a state to not run any task but to be aware of interrupts from the previous interval alarm timer may appear. When such interrupt takes place, the MCU simply toggles the LED attached to its output pin.

Numerically, Code 1.1 consumes 56 µA in average when the MCU feeds a clock frequency

```c
#include <msp430g2553.h>
#include <stdint.h>

int main(void) {
    /* configure WatchDog Timer */
    WDTCTL = WDTPW + WDTHOLD;
    // configure in/output pins
    P1DIR |= 0x01;
    // configure SMCLK, counter mode, and the interrupt from timer
    TACTL = TASSEL_2 + MC_2 + TAIE;

    // enable interrupts to MCU
    _BIS_SR(LPM0_bits + GIE);
}

// Timer_A3 Interrupt Vector (TA0IV) handler
#pragma vector=TIMER0_A1_VECTOR
__interrupt void Timer_A(void) {
    switch (TA0IV) {
    case 10:
        P1OUT ^= 0x01;  // toggle LED
        break;
    }
}
```

Code 1.1: Blinking a LED in a low-power MCU.

of 1 MHz to the timer. The line toggling the LED status is the only part of the code where the MCU is active after the configuration phase and its current consumption is simply ignored in this example because the active period code content logically varies among applications. In fact, the timer code is precisely the adequate location to include the transceiver's activation in a duty-cycled application.

Besides hardware, software also plays an important role in energy saving purposes. A similar but more energy efficient variant of the previous Code 1.1 only requires changing the following two statements:

```c
TACTL = TASSEL_2 + MC_2 + TAIE;
_BIS_SR(LPM0_bits + GIE);
```

To the following Code 1.2:

```c
TACTL = TASSEL_1 + MC_2 + TAIE;
_BIS_SR(LPM3_bits + GIE);
```

Code 1.2: Optimizing the code for blinking a LED in a low-power MCU.

Modified lines in Code 1.2 provoke the low-power MCU to not use its internal oscillator to feed the timer, but a dedicated external crystal oscillator. This allows the MCU for a higher degree of sleeping, since now the counting is provided to the timer by another element. Notice the switch of the sleeping mode of the MCU from LPM0 to LPM3, where LPM stands for Low-Power Mode. Different low-power modes imply different amount of circuitry such as

clocks left active in the MCU, thus different current consumption values. By just applying the changes in Code 1.2, the previous code consumes less than 0.8 µA, 0.5 µA of which are due to the crystal oscillator. That is, Code 1.2 allows a battery to last for 70 times more than Code 1.1, a drastic improvement factor for low-profile batteries such as cell coin ones.

Only a deep knowledge of the employed MCUs allows for power-optimized software design. As another example, a single misconfigured output pin leads the MCU to require up to additional 77 µA.

1.4 Best Practices on Low-Power Wireless Applications

Previous Sections 1.2 and 1.3 provide introductory concepts for designs comprising low-power MCUs and wireless transceivers. This two-element combination is so common that manufacturers provide integrated circuits with both modules in a single package. For example, the Texas Instruments' CC430 is basically the combination of one low-power CC1101 wireless transceiver and one MSP430 low-power MCU.

Low-power MCUs and transceivers are the building blocks of any sensor node but, as seen, also the software design plays a crucial role. What follows is a list of considerations that any energy-aware wireless sensor node must take into account when implementing an application:

- → Use the lowest possible duty cycle. A common strategy consists in only sending a data frame when new measures exceed a threshold. For example, if a room temperature range lies within values from 21 °C to 22.5°C during all day, a node may only notify when measured data falls out of this range.
- → Avoid function calls and iterative codes, or bucles, when possible.
- → Minimize receive times in order to reduce the amount of time radio is in active state.
- → Quickly discard packets not intended for the current wireless node in order to avoid triggering energy-demanding data decoding procedures in the transceiver.
- → Be aware of the received power. Wireless transceivers provide a Received Signal Strength Indicator (RSSI) in order to estimate the distance remote transmitters are at to accordingly reduce the transmit power for sending data back when required.
- → Minimize transmitting power. Since usually the transmitting time cannot be reduced because of bit-rate limitations, reducing its associated output power provides the best way to save energy. For example, output powers of a CC1101 radio transceiver of +12 dBm, +10 dBm, 0 dBm and -6 dBm require respective current amounts of 34.2 mA, 30 mA, 16.8 mA and 16.4 mA. Depending on if the wireless application runs in a room or in a wide open field, adjusting the output power level may represent a big difference in battery lifetime.

→ Aggregate non-critical data in order to avoid transmissions consisting on few bytes, as well as to reduce the number of internal communication procedures between the MCU and the wireless transceiver. Also, different wireless transceivers provide different transition times between their states. By knowing these transitions when designing the node's source code, residual energy may be saved.

→ Besides application data, also underlying communications are to be considered. For example, a wireless technology relying on keep-alive messages, or control messages carrying no data but sent between stations to check for respective reachability or presence, provides lower battery lifetimes than others avoiding its use.

Thus, taking the aforementioned points into account, the MCU execution flow diagram in Figure 1.4 is updated in Figures 1.5a and 1.5b for the respective wireless transmitting and receiving roles of a low-power, duty-cycled application.

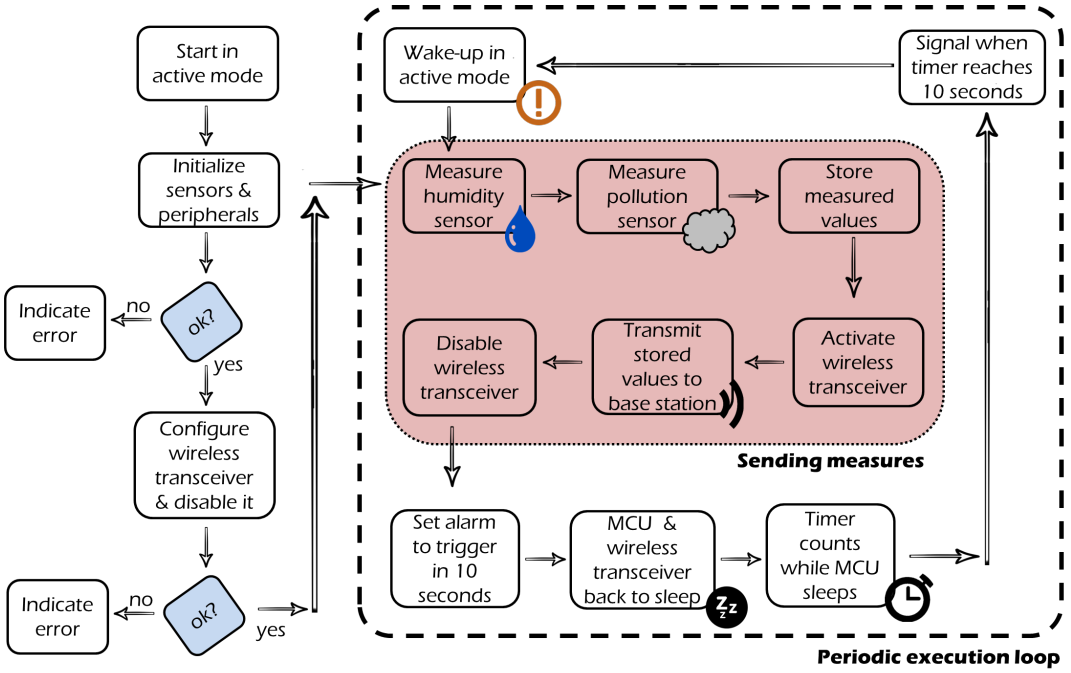

(a)

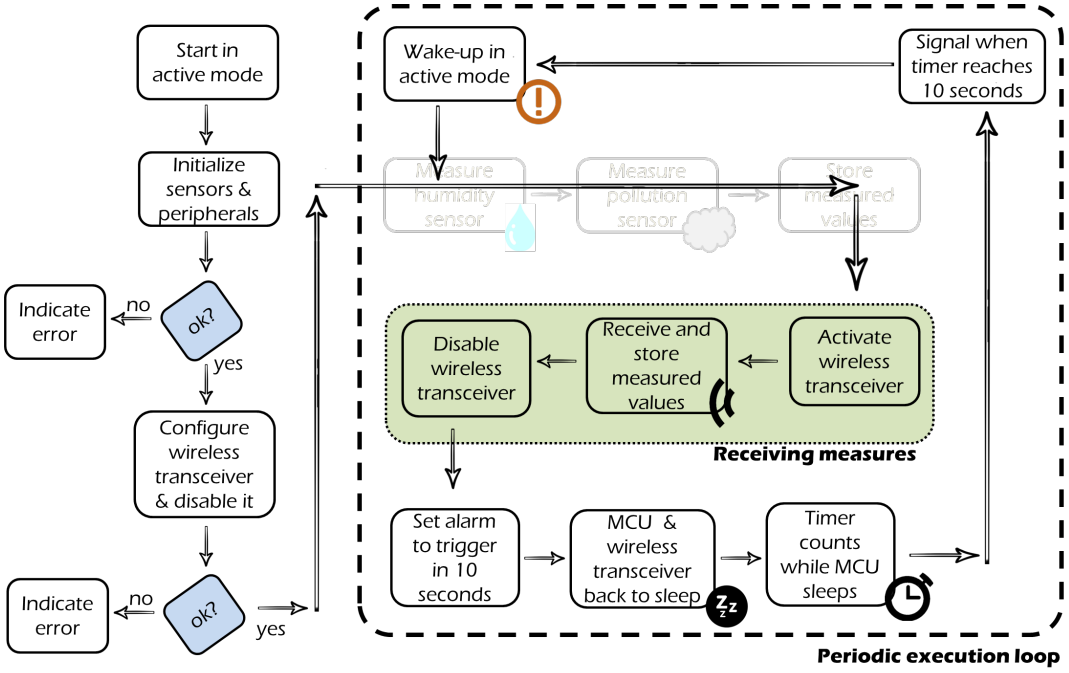

(b)

Figure 1.5: MCU execution flows for (a) transmitter and (b) receiver nodes.

While correct, execution flows in Figures 1.5b and 1.5a overlook an important synchronization issue in real applications related to how the nodes perform the wireless communication. There is no guarantee that distant nodes in an application will wake-up at the same time. For example, if the transmitting node periodically wakes up in the middle of the cyclic process, that is, at second number 5 of each 10 seconds interval, and the receiver node wakes up, at

second number 8 of each 10 seconds interval, they clearly do not coincide active at the same time, thus communication seems infeasible. Hence, there is a need for a so-called *rendezvous* mechanism that allows nodes to synchronize for wireless communication to take place.

1.5 Rendezvous Schemes for Wireless Communications

In this section, three different approaches for achieving node rendezvous are introduced, each of them providing different performance degrees.

Rendezvous schemes always represent a trade-off between time and energy. The first possible rendezvous scheme is as energy-consuming as time immediate. Simply, if no duty-cycling strategy is considered, the receiver is permanently active. In this way, when the transmitter sends a wireless frame, it is received with high probability. This approach is the less energy-efficient among the possible, but at the same time it is logically the one providing the highest data-rates and fastest response time.

On the other hand, if some degree of duty-cycling is employed, a way to assure that the participant nodes in a communication are active at the same time must be contemplated. There are numerous strategies for solving this issue. Some of them rely on the presence of one master node to coordinate communications, while others, so called *ad-hoc*, consider all nodes as equal entities. In the latter category, the most employed approach is based on repetition. For example, if nodes have a duty cycle period of 1 second, a transmitter node may choose to continuously transmit the intended packet during this entire time period. This way, whenever the receiver wakes up, it will receive the packet. Due to packet transmissions occurring few times in Wireless Sensor Networks (WSN) compared to the number of medium listening procedures, this approach really allows for energy savings and, in fact, is the default implementation in operating systems designed for wireless sensor nodes. Since they have to do with how nodes interact with the wireless medium, these approaches are called Medium Access Control (MAC) protocols. Since node rendezvous between transmitters and receivers presents a technical challenge, and therefore is a common subject in WSN studies under the naming to MAC protocols for WSN [10–13].

However, while MAC protocols indeed help in achieving longer battery lifetimes, they still suffer from several drawbacks summarized next:

→ *Idle listening*, which occurs when a node is in reception state but no communication is present in the channel. Even if the duty-cycling mechanism effectively reduces idle listening, it does not fully remove it.

→ *Overhearing*, which occurs when a communication is received by a node, yet it is not intended for that node.

→ Timing issues such as latency in data transactions, since communication is delayed up to the moment the receiver is ready to process the data.

Thus, the optimum approach should be able to combine the best aspects of the previous two. First, it should introduce few latency. Second, it should be energy-efficient. Therefore, the third solution should include a way for the transmitter node to wake up the remote receiver node just before sending the wireless data frame. This approach is enabled by the use of Wake-up Radio (WuR), which enables a pure asynchronous, on-demand communication mechanism. By attaching a secondary ultra-low power receiver, so-called wake-up receiver, to a wireless device, its main MCU and data transceiver can be switched to its lowest power sleep mode. Both are only activated when required by an interrupt generated due to a special RF signal sent from another node. With such a radio-triggered circuit, nodes may stay asleep until their intervention is really required.

This last approach, introduced in next section 1.6, is effectively the most energy efficient of them all, since there is no better way to maximize energy efficiency than waking up nodes only when there is really necessary. As it is logical, in order to provide higher energy savings than duty-cycled approaches, such secondary wireless wake-up receiver has to consume several times less power than traditional wireless transceivers.

The first relevant papers describing and implementing the wake-up strategy came out in 2009, and they basically propose the hardware design of these energy-efficient secondary receivers, so-called wake-up receivers, and their performance analysis.

1.6 Introduction to Wake-up Receivers

In WuR systems, as illustrated in Figure 1.6, a node initiating a communication first sends a Wake-up Call (WuC) by means of its Wake-up Transmitter (WuTx), to the Wake-up Receiver (WuRx) of a remote node to activate it in an on-demand manner. Until the reception of the WuC, the node's MCU and main data communication radio remain in deep sleep.

The wake-up approach enables energy savings in plenty of different applications, e.g., retrieving information from environmental pollution sensors placed in a city by a mobile collector node, or activating a sleeping wireless AP.

Quantitative evaluations, e.g., [14, 15], prove the efficiency and benefits of WuR. Wake-up Radio systems reduce or even eliminate the aforementioned energy inefficiency of duty-cycling. As previously mentioned, during the active period of duty-cycled nodes where listening and transmitting take place, the node's MCU and main data transceiver present current consumption values in the order of mA. Even for theoretically low duty cycle settings such as 1%, this behavior implies constant energy waste during the active state. In contrast, WuR systems allow nodes to present a constant current consumption value in the order of μA during the time their intervention is not required, significantly dividing by 1000 the energy waste caused by idle listening. In addition, if a WuR system features a so-called addressing mechanism also the overhearing issue is resolved, since it is possible to wake up a single node among several of them. Finally, since the wake-up procedure can be performed in a short time, the latency

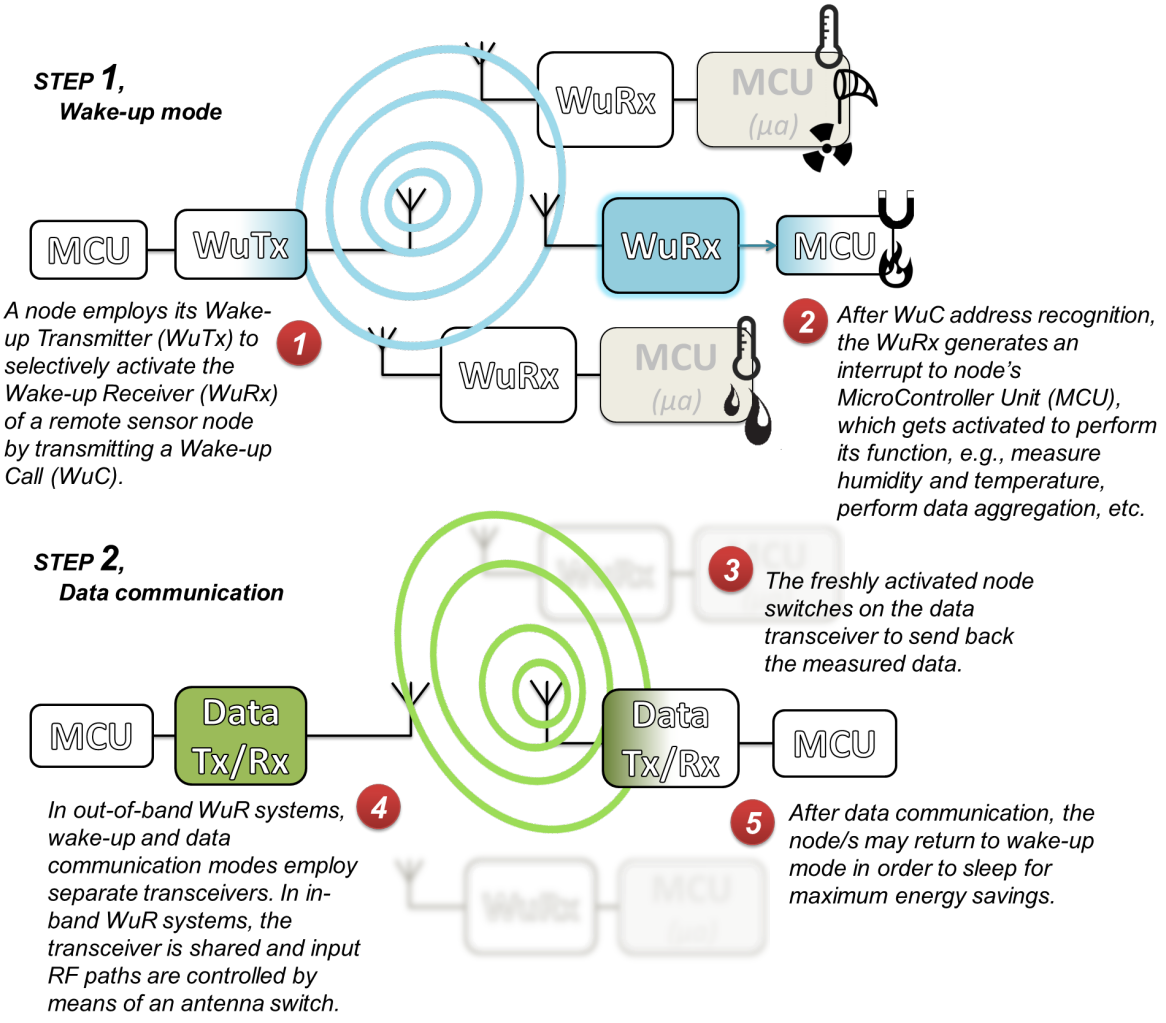

Figure 1.6: The Wake-up Radio paradigm.

duty-cycled systems suffer from is diminished. On the other hand, WuR systems present the disadvantage of requiring the design of an additional, energy-restricted hardware for WuRx, as well as to contemplate a mechanism for the WuTx to generate the WuCs.

However, WuR systems present additional benefits, such as being easier to program in terms of software. To begin with, they provide implicit synchronization. Because of this, no clocks have to be taken into account, since the node originating the communication explicitly activates the remote sleeping node. Therefore, timers can be stopped for further energy savings. In Code 1.2 for duty-cycled systems, LPM3 of the MCU is employed. Instead, when featuring a WuRx as in the example Code 1.3 , the MCU sleeps down to LPM4 levels for minimum consumption. Differently to LPM3, in LPM4 even the MCU's timers are disabled. As a second advantage, the system's programmer simply considers a WuRx in the same manner as interrupts from an input push button. In fact, because the latter, the reason of the interrupt is not even explicitly indicated but simply named as a `WAKEUP_INT` attached to pin P1.3.

```
// #includes contain names for registers, constants, etc.
#include <msp430g2553.h>

#define WAKEUP_INT BIT3

int main(void)
{
    WDTCTL = WDTPW + WDTHOLD;    // Stop watchdog timer
    P1DIR = 0x01;                // P1.0 output, else input
    P1OUT =  WAKEUP_INT;         // P1.3 set, else reset
    P1REN |= WAKEUP_INT;         // P1.3 pullup
    P1IE  |= WAKEUP_INT;         // P1.3 interrupt enabled
    P1IES |= WAKEUP_INT;         // P1.3 Hi/lo edge
    P1IFG &= ~WAKEUP_INT;        // P1.3 IFG cleared

    // Enter LPM4
    // enabling interrupts to wake-up the MCU
    __bis_SR_register(LPM4_bits + GIE);
}

// Port 1 interrupt service routine
#pragma vector=PORT1_VECTOR
__interrupt void Port_1(void)
{
    P1OUT ^= 0x01;           // LED at P1.0 = toggle
    P1IFG &= ~WAKEUP_INT;    // P1.3 IFG cleared
}
```

Code 1.3: Code to attend a Wake-up Interrupt.

Code 1.3 first defines MCU unused pins as outputs in order to save power. Next, it configures an input pin to be used WuRx or button interrupts. Afterwards, it enters LPM4, where the MCU only requires 0.1 µA to operate instead of the 0.8 µA in LPM3 for duty-cycled systems in Code 1.2. In addition, the latter have to account the energy to periodically wake-up the transceiver, which cannot be neglected. Instead, the current consumption in Code 1.3 is much better than the one of Code 1.2, since the whole WuRx lies in the µA order as long as the MCU sleeps in LPM4, enabling optimal energy savings. When in LPM4, since no timers are enabled, the MCU may only be activated by means of an interrupt. As in previous examples, when the MCU detects the interrupt it signals such condition by blinking a LED and returns to sleep mode.

WuR system designs may strongly differ depending on the application. A system to collect remote information from sensors placed 20 meters away may certainly benefit of a different design than a WuR system designed for WBAN. However, independently of the application, the following list summarizes the common requirements that a WuR system should satisfy:

→ The amount of energy used by nodes equipped with a radio-triggered mechanism must be approximately equal to energy consumed in the lowest MCU sleep mode.

→ A node equipped with a radio-triggered mechanism has to wake-up with minimum latency after receiving a wake-up call in order to minimize the overall active time.

→ WuTx retransmissions are costly in terms of latency and energy. Thus, intended nodes must not miss any WuC. Also, if a wake-up addressing mechanism is implemented, a WuRx must not generate a wake-up interrupt in the case that a correctly constructed WuC is detected but not destined to the current node.

→ Background noise and signals that can result in false positives for WuC have to be taken into account and filtered. Unnecessary activations of nodes detract the wake-up strategy purpose.

→ WuTx must comply with frequency regulations and present low economic cost. Such two conditions can be difficult to achieve with battery-constrained WuRx, which implicitly requires employing more transmission power at the WuTx. Introducing some active components indeed helps in lowering the transmission power required and extending the range, but in turn implies higher monetary and energy costs. The additional WuRx hardware cost should be less than 5%-15% of the cost of a complete node [16].

→ Finally, WuC detection distances should be at least 10 m to support different type of applications [17].

A properly designed WuR system must target to comply with the low-power concepts and requirements presented in the current chapter. In the following chapter 2, both one WuTx and one WuRx designs of a successful prototype of a WuR system are analyzed for several metrics and its application areas clearly specified. Chapter 2 also contains a comparison to a commercial system to illustrate the performance benefits and possibilities of the developed WuR system over pre-existing designs.

2 Design, Development & Performance Evaluation of a Low-Cost, Low-Power Wake-Up Radio System for WSN

This chapter 2 presents a complete WuR system that targets simplicity in design for the monetary cost and flexibility concerns, along with a good operation range and very low power consumption. Both the transmitter, or WuTx, and the receiver, or WuRx, are presented with accompanying physical experiments for several design alternatives. A detailed analysis of the end system is provided in terms of both operational distance (more than $10\,\mathrm{m}$*) and current consumption (less than* $1\,\mu\mathrm{A}$*). As a reference, a commercial WuR system is analyzed and compared to the presented one, by expressing the trade-offs and advantages of both designs.*

This chapter is organized as follows: section 2.1 depicts the designs of a Sub-microAmpere Wake-up Receiver (SμA-WuRx) and its corresponding WuTx. Next, section 2.2 presents the assessments of different design choices through evaluations of the operational range, current consumption and the timing behavior. Section 2.3 introduces and provides a similar analysis for a commercial WuR solution. Finally, section 2.4 provides a comparison between both the proposed and the commercial WuR systems and concludes the chapter.[1]

Contents

[1] The current chapter is based on and extends the work contained in the following JCR Q1 (2012) publication: ≪J. Oller, I. Demirkol, J. Paradells, and J. Casademont, 'Design, Development and Performance Evaluation of a Low-Cost, Low-Power Wake-Up Radio System for Wireless Sensor Networks', ACM Trans. Sens. Networks, vol. 10, no. 1, 2013.≫.

2.1 Proposed WuRx and WuTx Designs

Energy efficient operation is currently the most effort-demanding research challenge for WSN. As mentioned in chapter 1, a common method for energy saving is duty-cycling, which extends battery lifetime, yet, incurs several types of energy wastes. A promising alternative to duty-cycled operation is the use of Wake-up Radio or WuR, where the main MCU and wireless transceiver of a node, i.e., the two most energy consuming elements, are kept in sleep mode until a special signal from another node is received by an attached, secondary, ultra-low power receiver. Next, this so-called wake-up receiver, or WuRx, generates an interrupt to activate the main MCU and the main radio.

In this section, a WuR system targeting low cost and flexible design is presented. The WuRx achieves a current consumption below 1 µA, so its called SubµA-WuRx, or SµA-WuRx, and a physical design very easy to reproduce, while still affordable from the economic point of view and modifiable in several aspects. Regarding the WuTx, various factors affecting its design are analyzed along with the changes in operational distance they imply.

2.1.1 WuRx Design

The SµA-WuRx implements an 868 MHz wake-up circuit based on voltage rectification, which concept is shown in Figure 2.1. In Figure 2.1a, Vin models the WuRx antenna. As shown in Figure 2.1b, a capacitor and a diode effectively detect and extract the *envelope* of a high frequency Vin signal. This is the basis of most WuRx designs, which work with low frequency signals that can be managed with simplistic circuitry.

The circuit schematic for the complete SµA-WuRx is given in Figure 2.2a. Because the RF energy collected at the antenna from the WuC is very weak, a multi-stage voltage multiplier (VM) schema is employed. Simulation of this design is conducted in Ansys HFSS electromagnetic simulation software and displayed in Figure 2.2b, where Va, Vin, and Vo stand for voltage level at the antenna, at the VM input and at the VM output, respectively.

In Figure 2.2b, by concatenating the scheme in Figure 2.1a, the envelope of the Vin signal is rectified and progressively increased due to the effect of the diodes and capacitors, respectively. The resulting signal after envelope detection is labeled in Figure 2.2b as Vo. After several microseconds, such signal is suitable to be employed as an interrupt in an input pin of a MCU, as introduced in chapter 1, section 1.6. Theoretically, the digital comparator input voltage is equal to 5 Vm, which stands for having 5 times (the number of VM stages) more voltage at the output of the VM than at the input. A digital comparator (Maxim MAX9119) is placed at the end of the schema, being the only active component in the system, with a current consumption

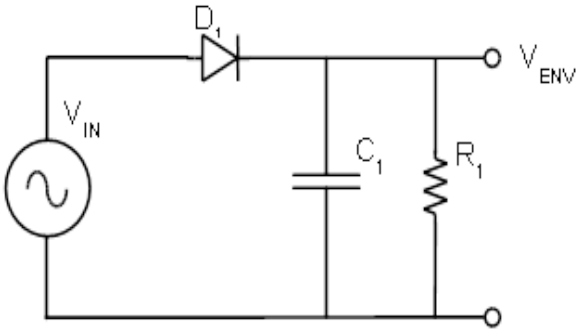

(a)

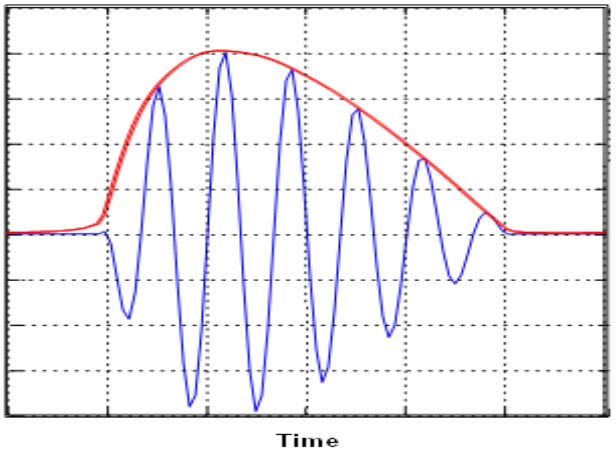

(b)

Figure 2.1: (a) Basic envelope detector; (b) input (blue) and output (red) waveforms. [1].

of 350 nA. The comparator's threshold voltage is extracted from the voltage divider formed by R2 and R3, which consumes 526 nA. The final envelope signal coming from the antenna is presented at R1 terminals. For each VM stage, two 8 pF capacitors and two HSMS-285Y Schottky diodes are used.

The SμA-WuRx features a 868 MHz ANT-868-SP antenna [18], which is a low-cost, compact footprint antenna suitable for wireless sensor devices. The technical details of the antenna, as well as of the Surface Acoustic Wavelength (SAW) filter employed after it, are shown in Table 2.1.

Figure 2.3a shows the SμA-WuRx hardware prototype. The measured antenna's return losses S_{11} are plotted in Figure 2.3b, where *Plac.* labels represent different placements of the antenna on a 3.81 cm x 4 cm board. Measurements are obtained by employing an Agilent Technologies E8364B PNA Network Analyzer.

Variations of the frequency response show that the placement of the antenna on the WuRx board is an important factor. In fact, the manufacturer's datasheet recommends a 3.81 cm x 8.32 cm ground plane, but such value would mean too much physical space in small devices.

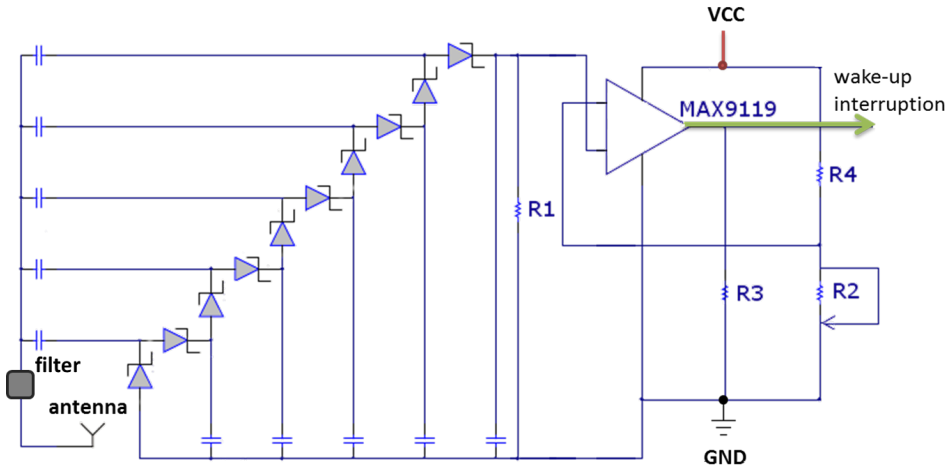

(a)

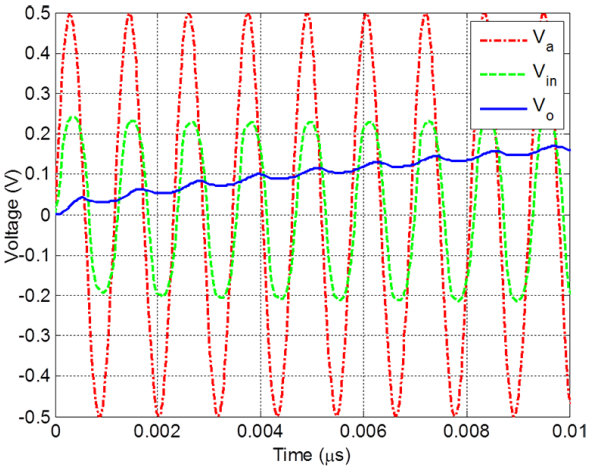

(b)

Figure 2.2: (a) The SµA-WuRx circuit design; (b) five-stage VM rectified output (Vo).

ANT-868-SP	
Center Frequency	868 MHz
Bandwitdh	35 MHz
Wavelength	1/4 λ
VSWR	< 1.9
Impedance	50 Ω
Gain	0.77 dBi
Mounting	Surface

EPCOS B3715	
Center Frequency	869 MHz
Max. insertion loss	3.1 dB
Attenuation < 868 MHz	min 20 dB, max 41 dB
Attenuation > 868 MHz	min 35 dB, max 47 dB

Table 2.1: Characteristics of the SµA-WuRx antenna and SAW filter.

After assembling, the SµA-WuRx features a sensitivity value of around -45 dBm. As a comparison, such value is slightly higher than some commercial WuRx designs like the ATA5283 proposal from Atmel [19]. When a WuC is detected by the 868 MHz antenna (1) in Figure 2.3a, and if the threshold of the comparator (5) placed at the end of the SµA-WuRx is surpassed, the mote's microcontroller attached to the output GPIO pin (4) is triggered on.

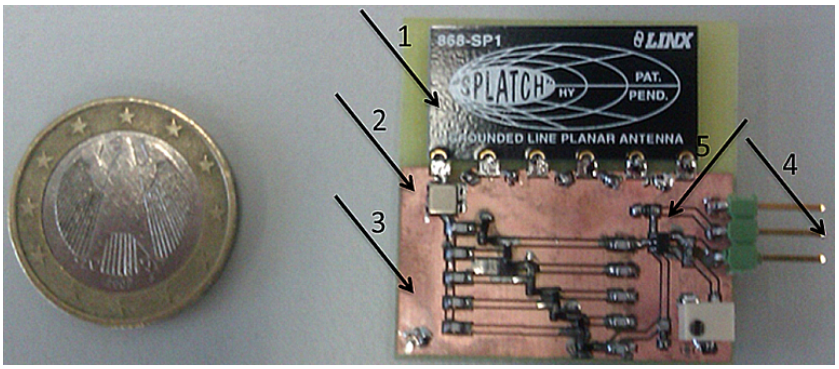

(a)

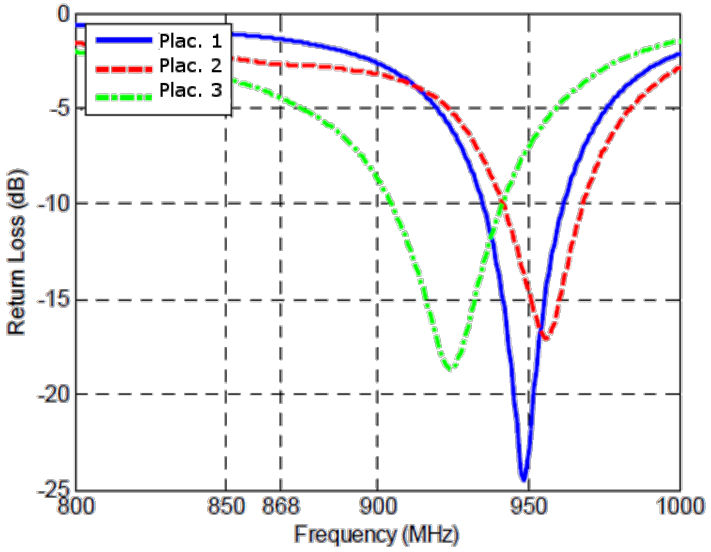

(b)

Figure 2.3: (a) A 5-stage SµA-WuRx. In the image: 1 - antenna, 2 - SAW filter, 3 - voltage multiplier, 4 - wake-up interrupt output pin, 5 - comparator. (b) Return loss variances of the ANT-868-SP antenna depending on physical placement.

The WuC is shown from the signal point of view in Figure 2.4, where the lower trace represents the signal just before the comparator. The upper trace presents the signal at the output pin in Figure 2.3a. The signal shown consists of the word *wakeup* encoded in ASCII. The figure shows how the diodes and capacitor values are properly dimensioned to manage the WuC, which consists of some initial '1' padding bits, as well of the 42 bits of the 6 ASCII characters. The time duration of each of the bits is 1 ms, which implies a wake-up bit-rate of 1 kbps. This bit duration value can be decreased if needed, but usually WuR systems do not require high bit-rates, since large data transfers are performed by the main interfaces of the nodes when activated.

The SµA-WuRx prototype presents a low monetary cost due to the use of common off-the-shelf components. A market survey yielded a total cost of lower than 3 € for a prototype. Furthermore, the entire WuR system provides high flexibility since no restrictions exists regarding the transmitter side, i.e., any 868 MHz transceiver can be employed. Moreover, the

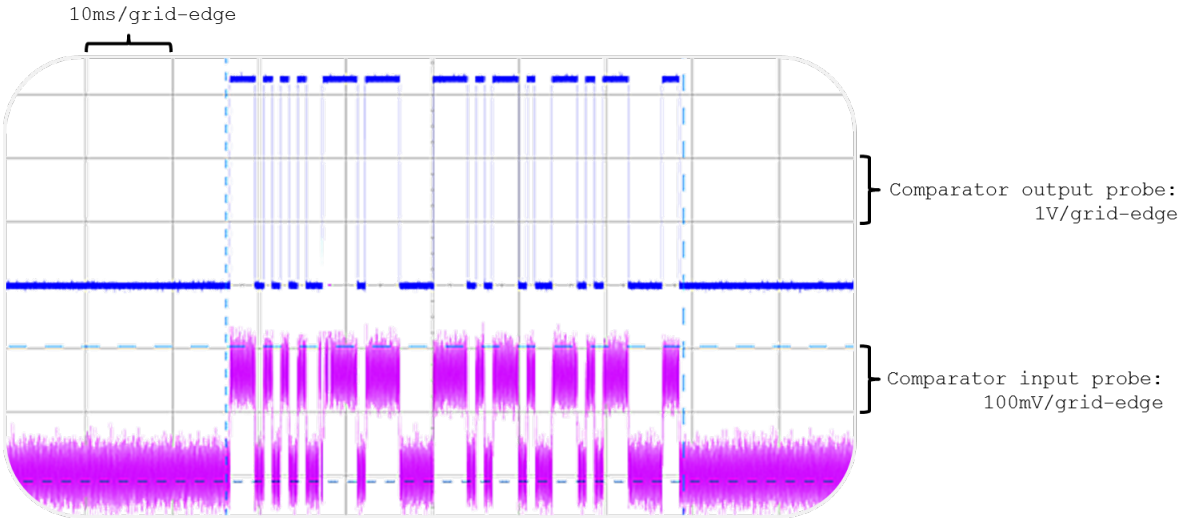

Figure 2.4: A WuC as received by the SμA-WuRx. Bottom signal shows the comparator's input; top signal shows the comparator's output.

WuRx hardware design can be modified in several ways conveniently, as studied in section 2.2. For example, if an environment without radio interferences is expected, the filter at the input of the SμA-WuRx can be omitted to achieve better operational range. On the other hand, if long range is not critical for the deployed application, the comparator threshold of the SμA-WuRx can be increased through the potentiometer R2, which in turn reduces the effect of interference and noise.

By default, the SμA-WuRx does not provide an addressing feature to be able to wake-up a specific receiver among many[2]. However, in a scenario comprising a broadcast scheme or in applications where nodes are distant enough, the addressing mechanism is dispensable.

2.1.2 WuTx Design

The WuTx employed to wake-up the SμA-WuRx consists of an 868 MHz AdeunisRF ARF7243A module attached to the output pins of a WSN mote developed by the Wireless Networks Group at Universitat Politecnica de Catalunya [20]. The specifications of the transmitter module [21] and the antenna [22] of the WuTx are given in Table 2.2.

ANT-868-CW-QW	
Center Frequency	868 MHz
Frequency Range	750 - 950 MHz
VSWR	< 1.9
Impedance	50 Ω
Gain	0.50 dBi
Mounting	SMA

AdeunisRF ARF7243A	
Center Frequency	869.525 MHz
Output power	25 to 500 mW
Modulation	ASK
VCC	2.7 to 5 V
Current Consumption	150 to 600 mA

Table 2.2: Characteristics of the antenna and transceiver employed in the WuTx.

[2]Next Chapter contains an implementation to solve this issue.

The output power of the ARF7243A of the WuTx hardware prototype in Figure 2.5 can be adjusted from 25 mW to 500 mW in order to comply with radio spectrum regulations. Up to 10% duty cycle is allowed in Europe when working at 869.525 MHz and 500 mW, i.e., +27 dBm. During the WuTx output power tests, a 30 dB attenuator is used to protect the measurement equipment. Figure 2.5b depicts the maximum transmission power of the WuTx measured by a Rohde & Schwarz FSL6 spectrum analyzer.

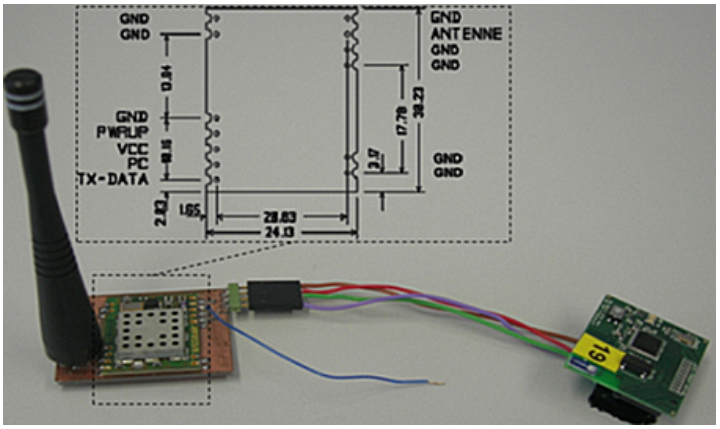

(a)

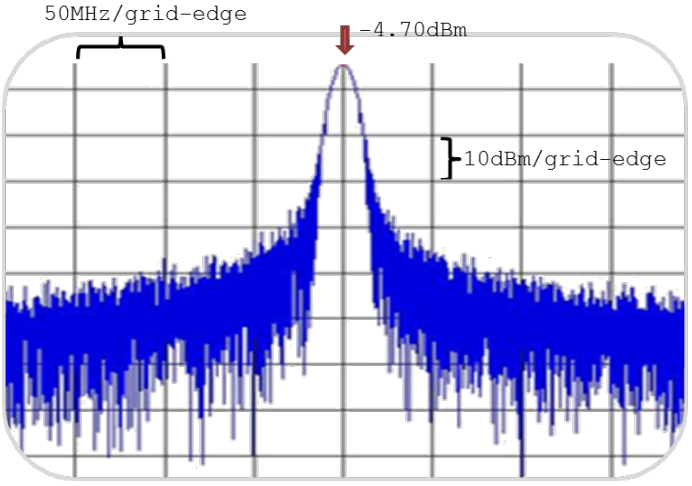

(b)

Figure 2.5: (a) The 868 MHz WuTx attached to a WSN mote. (b) Measurement of the output power of the WuTx considering a 30 dB attenuator.

Note the -4.70 dBm value in Figure 2.5b, which shows that the output of the ARF7243A satisfies the power regulation value for the 868 MHz band in Europe. Finally, as in the WuRx case, it is observed that the antenna return loss strongly depends on the WuTx ground plane size and/or the antenna placement on the ground plane. Section 2.2.2.3 analyzes this effect.

2.2 Performance Evaluation of the Developed WuR System

In order to obtain the maximum performance for the WuR system without violating the electromagnetic interference regulations, there is a need to quantify the relation between the output power and the power-adjusting mechanisms provided by the WuTx. This section presents the characterization of this relation, which is crucial for realistic operational range evaluations.

As a general rule, the output power increases accordingly to the supply voltage, so does the current consumption. But while this is the most important factor in determining the operational range of the WuR system, it is not the only one. However, there are several other factors that can affect the operational range. For example, by varying the size of the WuTx ground plane, its radiation pattern gets affected and so is the achieved maximum operational distance. In addition, the use of a SAW filter at the input of the WuRx, while offering higher immunity to interferences that can provoke a false wake-up positive, results in some gaps along the maximum operational distance. Another aspect to study is the number of VM stages in the WuRx, as it must achieve an optimum balance between the performance and the amount of circuitry. Depending on whether the WuR system is deployed in an outdoor or indoor scenario also affects the performance of the WuR system as well, due to different signal propagations. Finally, the effect of the antenna type on the operational distances plays an important role. All these factors are characterized through field tests in this section.

2.2.1 Current and Power Consumption Evaluations

The transmitter in the WuTx provides two ways of adjusting the output power. The first one consists in a Power Control (PC) pin, shown and left unconnected in Figure 2.5a. The second one consists in directly adjusting the VCC value of the device, which requires less circuitry. However, these two mechanisms are mutually exclusive. In other words, if the PC pin is used VCC variation has no effect on the output power (as long it is not decreased more than the voltage the device needs) and vice versa. Empirically, while the PC pin variation seems to be the most flexible approach for output power control, in practice it requires managing an extra GPIO and does not behave as stable as using VCC adjustment. Hence, VCC variation is chosen as the power adjustment strategy.

Figure 2.6 shows the output power value in dBm and the associated current consumption for both approaches. As previously mentioned, the 30 dB value stands for the attenuator placed for protection purposes.

If for the allowed output power the WuR system provides an unsatisfactory operational range, a total or partial redesign has to be considered. As shown in Figure 2.6, under the default WuTx configuration, even for the highest VCC values the output power does not surpass the legal +27 dBm limit. Concretely, for the highest VCC value of 5 V, the output

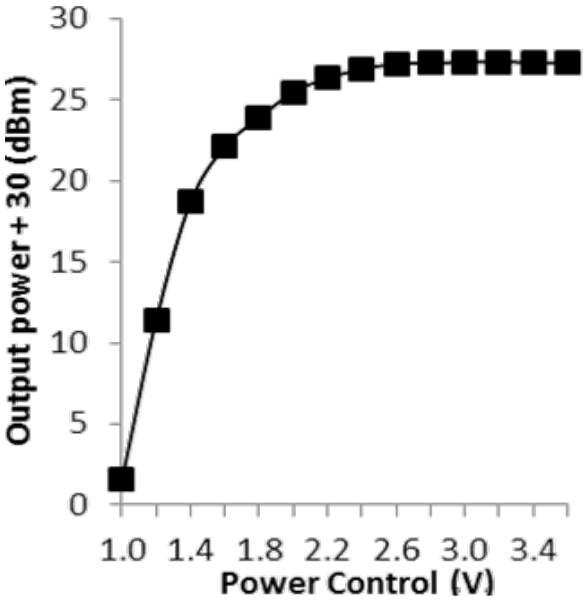

(a)

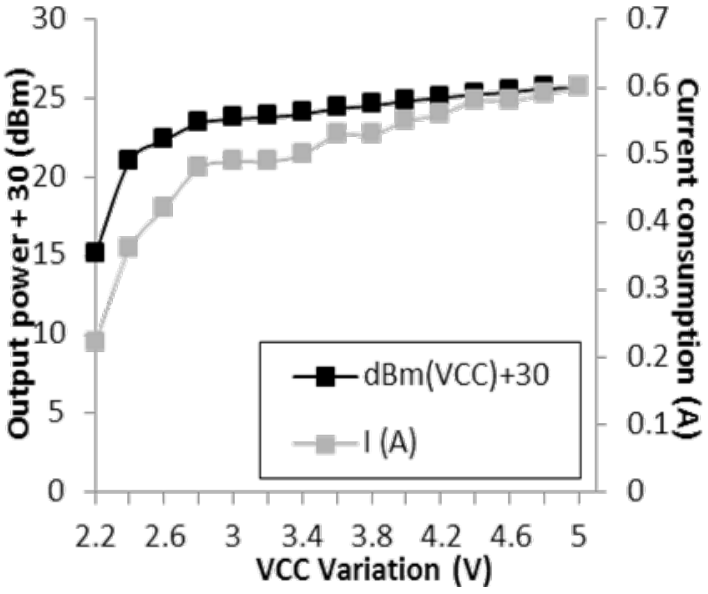

(b)

Figure 2.6: WuTx output power controlled by using (a) the PC pin; (b) VCC variation.

power is observed to be +25.66 dBm. Hence, as long as the WuTx does not employ an antenna with a gain higher than 27 - 25.66 = 1.34 dB, the system operates properly. As shown in Table 2.2, the antenna used for WuTx default configuration fits this requirement.

Regarding the receiver side, the SμA-WuRx is found to feature a current consumption of just 0.9 μA by employing a Kyoritsu K-1011 multimeter capable of performing measurements down to 0.1 μA. For higher precision, a simple circuit is used with accurately measured resistor and voltage values. This way, a current consumption of 890 nA is obtained by applying Ohm's law.

2.2.2 Operational Range Evaluations

To quantify the wake-up probabilities achieved by the WuR system in real applications, the WuTx is fixed at a coherent height of 100 cm and the SμA-WuRx is displaced vertically and horizontally relative to the WuTx, in steps of 20 cm and 25 cm, respectively. Hence, a grid of WuC detection results is built for each configuration under evaluation. Each of the figures in the current section show WuC detection results along with the settings applied for the WuRx and WuTx boards.

In the range evaluations, the SμA-WuRx is attached to the input pin of an IEEE 802.15.4-compliant mote developed by the Wireless Networks Group at Universitat Politècnica de Catalunya [20]. The WSN mote generates a single IEEE 802.15.4 frame every time it detects an interrupt on its input pin. Next, it immediately returns to its deepest low-power mode, in which the MCU presents a current consumption of just 0.4 μA. The WuTx sends once WuC per second and response frames are captured by an IEEE 802.15.4 sniffer for statistical purposes. 100 WuC are sent per each grid point.

2.2.2.1 Reference Scenario

The first operational range test is performed by applying VCC = 5 V to the WuTx and sending the word *wakeup* through its data pin. These initial measurements establish a reference operational behavior to compare the subsequent device modifications to. Attention has to be paid to the x-axis of each results graph in following sections, because different distance limits are achieved by the WuR system for different configurations.

Three operational zones are defined for the figures in this section based on the ratio of IEEE 802.15.4 frames sent as a result of received WuCs. *Zone1* implies a consistent reception of the WuCs and consequent activation of the SμA-WuRx, and is represented by the white color in the figures. In *Zone2*, which is represented by gray color in the figures, certain WuCs are detected, but the reception is not infallible. Finally, in *Zone3* the WuRx does not get activated by any of the WuCs, which is represented by the black color in the figures. The wake-up zones observed from the reference field test are depicted in Figure 2.7. Along the section, the summary of the reference scenario settings are shown in the figures' caption.

Several gaps along the operational distance are observed in Figure 2.7, possibly due to the fact that to save physical space due to application requirements, the antenna in the WuTx design is not placed on a 10 cm x 10 cm ground plane acting as signal's counterpoise as recommended by the manufacturer but on a smaller one (4.3 cm x 3.3 cm), a circumstance which distorts the radiation pattern. The observed maximum operational range is around 3.40 m. These results represent at the same tens of times less distance than for traditional wireless data transceivers while requiring thousands of times less energy. Results from Figure 2.7 also allow identifying an interesting behavior; due the the WuC reflection by the floor, the lower the WuRx heights, the better the results. This multipath effect is even more noticeable in

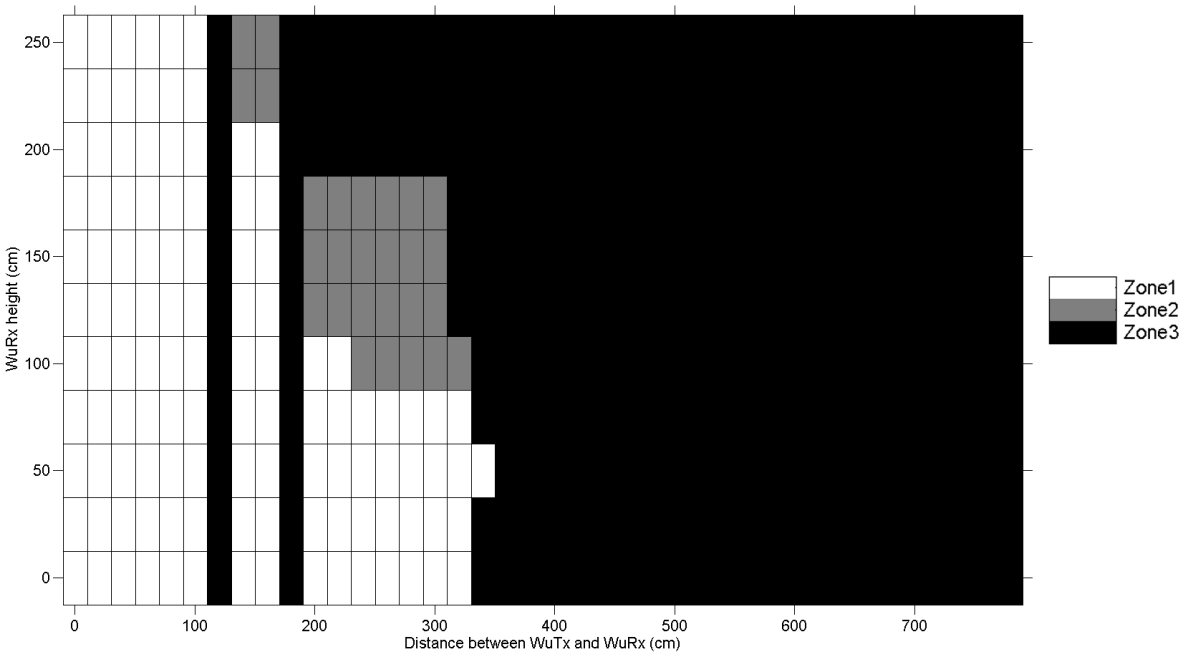

Figure 2.7: Observed wake-up zones for the reference outdoor WuR test. WuTx: Small (4.3 cm x 3.3 cm) ground plane, VCC = 5 V, antenna gain = 0.5 dBi. SμA-WuRx: 3.81 cm x 4 cm ground plane, SAW filter, five-stage VM.

indoor environments, as can be seen in Figure 2.8, which shows the results of the same test setup in an indoor space scenario.

The general wake-up behavior is more homogeneous in indoor than for outdoor scenarios. Although, as for the outdoor scenario, there are *Zone3* gaps between locations with persistent reception (*Zone1*), in this environment these are scattered in a wider range and in a more unpredictable way. In fact, due to the multipath effect, the indoor measurements show WuRx responses up to 9 meters, although omitted in the figure for being too occasional.

2.2.2.2 The Effect of the SAW Filter

To observe the effect of including a SAW filter at the input of the VM, such filter is removed. The motivation of this modification is checking the necessity of the filter in different environments. This variation makes the whole SμA-WuRx more vulnerable to radio communications in the adjacent frequencies such as GSM but, in turn, allows longer operational distances. As shown in Figure 2.9, removing the filter effectively increases the operational range achieved of the reference scenario in section 2.2.2.1 while smoothing the gaps out. The reason is the removal of the 3 dB insertion loss due to the SAW filter.

The interference rejection by the SAW filter is observed in practice as follows. When present, a cell phone in communication has to be placed closer than 15 cm to activate the WuRx circuit, which generates a false wake-up. When placed further, the SμA-WuRx is not activated. If instead the filter is removed, an operating cell phone two meters away can easily

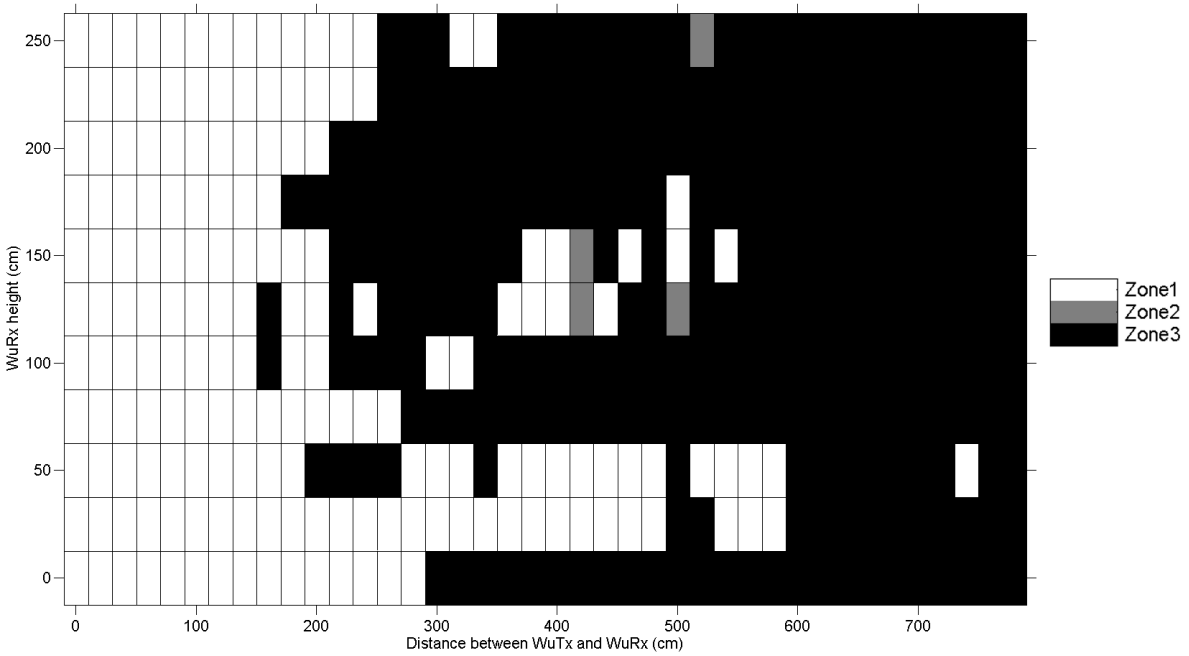

Figure 2.8: Wake-up zones for the indoor scenario. WuTx: Small (4.3 cm x 3.3 cm) ground plane, VCC = 5 V, antenna gain = 0.5 dBi. SμA-WuRx: 3.81 cm x 4 cm ground plane, SAW filter, five-stage VM.

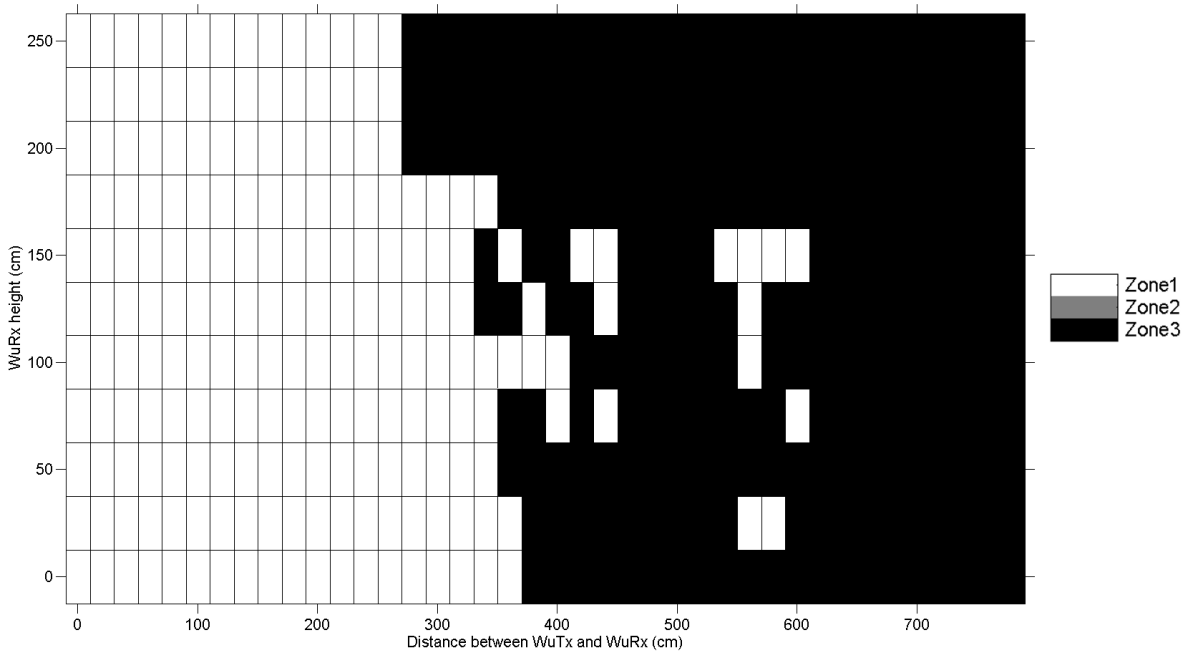

Figure 2.9: Wake-up zones for the outdoor scenario when removing the SAW filter in the SμA-WuRx. WuTx: Small (4.3 cm x 3.3 cm) ground plane, VCC = 5 V, antenna gain = 0.5 dBi. SμA-WuRx: 3.81 cm x 4 cm ground plane, no SAW filter, five-stage VM.

activate the circuit and provoke a false positive. These false positives can be diminished by increasing the potentiometer value in the comparator's threshold input (R2 in Figure 2.2a), which in turn decreases the WuC detection range. In fact, the SAW filter can be dispensable

in isolated or rural application scenarios where nearby interference sources are not expected.

Theoretically, removing the SAW filter and placing an inductance at the entrance of the VM to best match the RF impedance should translate to better range results, but in empiric tests it does not change the overall behavior in a great way. A 14.5 nH series inductance is placed after the SAW filter in order to compensate the capacitive behavior of the VM circuit. However, in the conducted tests placing or not such inductance does not affect significantly the wake-up probabilities of the SμA-WuRx.

2.2.2.3 The Effect of the WuTx Ground Plane

In this subsection, a test is conducted with a ground plane larger than the one in the reference configuration for the WuTx to identify the effects of such plane on the performance of the WuR system. The ground plane size is increased up to 10 cm x 10 cm, which is the recommended size in the datasheet of the ANT-868-CW-QW antenna used in the WuTx, yet may be not suitable for every application. As shown in Figure 2.10, by employing a larger ground plane in the WuTx, the whole system appears to improve substantially in terms of operational distance.

As a general rule, the larger the ground plane size of an antenna, the longer the horizontal operational range achieved. The maximum x-axis value achieved in Figure 2.10 reaffirms this assertion.

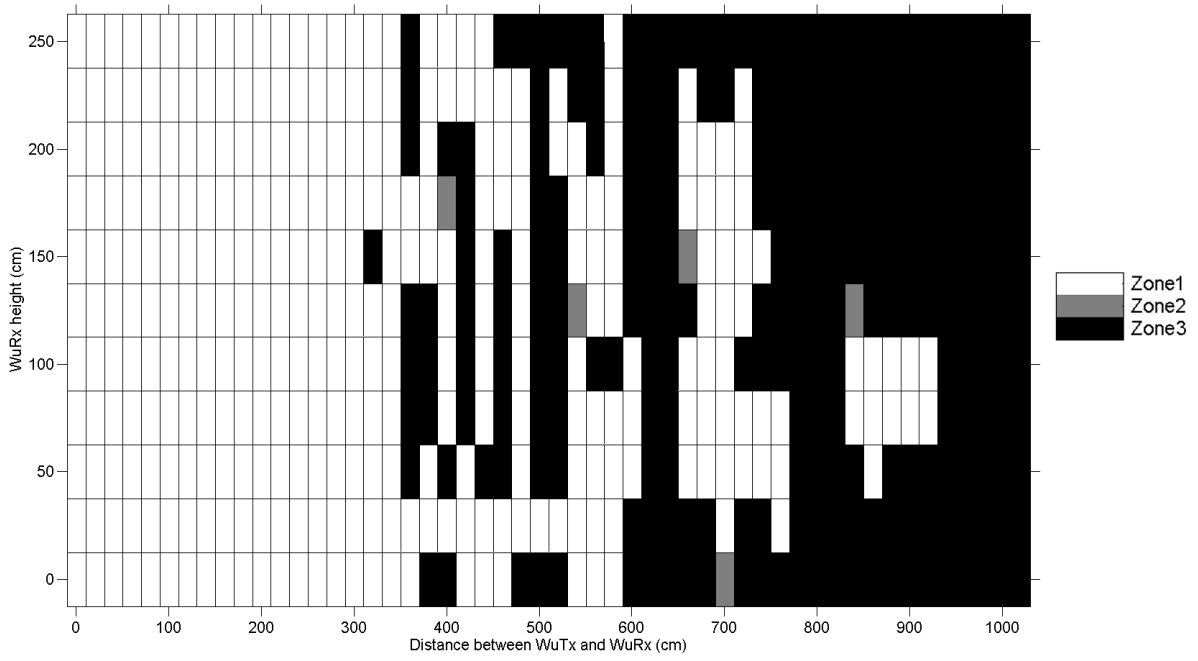

Figure 2.10: Wake-up zones for the outdoor scenario. WuTx: 10 cm x 10 cm ground plane, VCC = 5 V, antenna gain = 0.5 dBi. SμA-WuRx: 3.81 cm x 4 cm ground plane, no SAW filter, five-stage VM.

Although the gaps issue is still present in Figure 2.10, the overall operational distance effectively increases, even if in an irregular manner. The most noticeable change is the spreading of the multipath effect to higher heights for the WuRx placement. Since by employing the

10 cm x 10 cm ground plane the transmitter antenna is now placed in the center of a ground plane and distant from the board's edge, the bounce effect provokes more WuC to reach the WuRx. If enlarging the ground plane up to the recommended size is not acceptable for the motes of a deployed WSN, there is still the possibility of employing a different antenna for the WuTx, for example a more directional one.

2.2.2.4 The Effect of the WuTx Antenna Selection

The initial configuration of the WuTx under study features a Lynx Technologies ANT-868-CW-QW quarter-wavelength monopole antenna providing +0.5 dBi gain, as shown in Table 2.2. This antenna presents a typical monopole-like radiation pattern, with an omnidirectional performance for the H-plane. To evaluate a more directional antenna type, which can be useful for mobile data collection in certain application scenarios, the use of a printed patch antenna is considered. Reasons for this design choice are simple design and low-cost manufacturing. The developed antenna is shown in Figure 2.11a. The antenna's corresponding frequency response is measured with an Agilent Technologies E8364B PNA Network Analyzer and results shown in Figure 2.11b.

The fabricated patch antenna operates at the frequency of 870.9 MHz, which is slightly higher than the 870 MHz value found by simulation in Ansys HFSS electromagnetic software. This discrepancy is due to fabrication tolerances. However, the WuR system's frequency band is still covered due to the 30 MHz bandwidth. The new antenna presents directional behavior, which signifies longer operational distances. The radiation patterns of the developed antenna are extracted in an anechoic chamber to analyze its directivity and shown in Figures 2.12a, 2.12b and 2.13.

Because the input impedance value of the new antenna is also 50Ω, the power consumption of the WuTx remains unaffected. However, since the gain of the new antenna could make the WuTx surpass the power regulation limits, the transmission output power requires readjustment. The gain of the patch antenna is measured to be approximately +7 dB. By considering this gain and the power regulation limits mentioned in section 2.2.1, it can be seen from Figure 2.6b that the transmitter's VCC value must now be strictly set between 2.5 V and 2.8 V.

When attaching the new antenna design, the WuTx power output behavior is the same as Figure 2.6b, but taking into account a +37 dB value, which stands for the attenuator plus the new antenna gain. With these values, it is important to also consider the transmitter's ±1 dB possible variation stated in the datasheet [21]. Considering this potential variation and that fact that the VCC values of 2.5 V and 2.8 V are in the region of the Figure 2.6 with sharpest variations, the operational range tests are performed for both voltage levels.

Figure 2.14, shows wake-up activations as far as 13.5 meters for both voltage values evaluated. Employing the new antenna allows reducing the current consumption of the WuTx and increases the operational range by a multiple of four, a relevant improvement even for

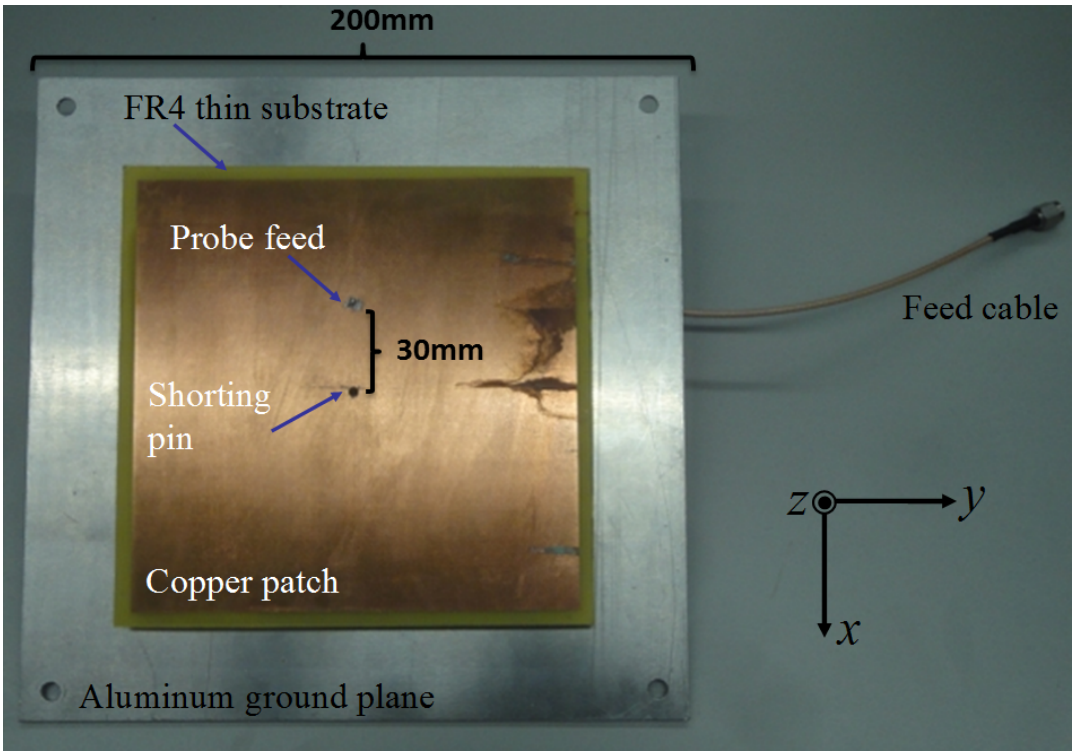

(a)

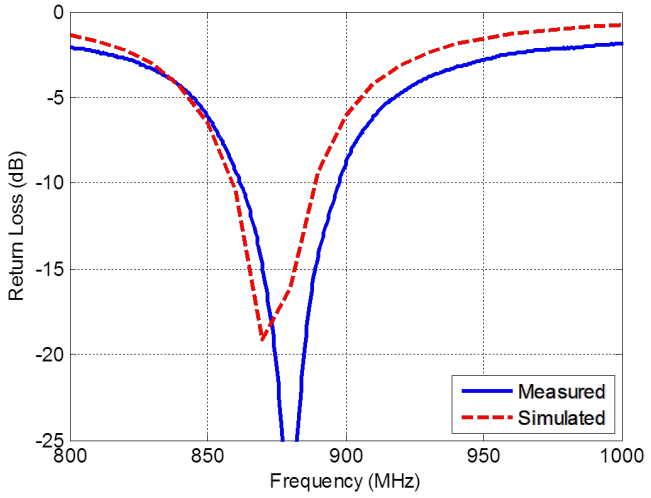

(b)

Figure 2.11: (a) Hardware design of the developed patch antenna. (b) Frequency response of the developed patch antenna design.

a configuration including the SAW filter. As expected, the best distance is obtained when WuRx is placed to a similar height to WuTx. Also, slightly higher distances are achieved and gaps contracted when using 2.8 V compared to 2.5 V.

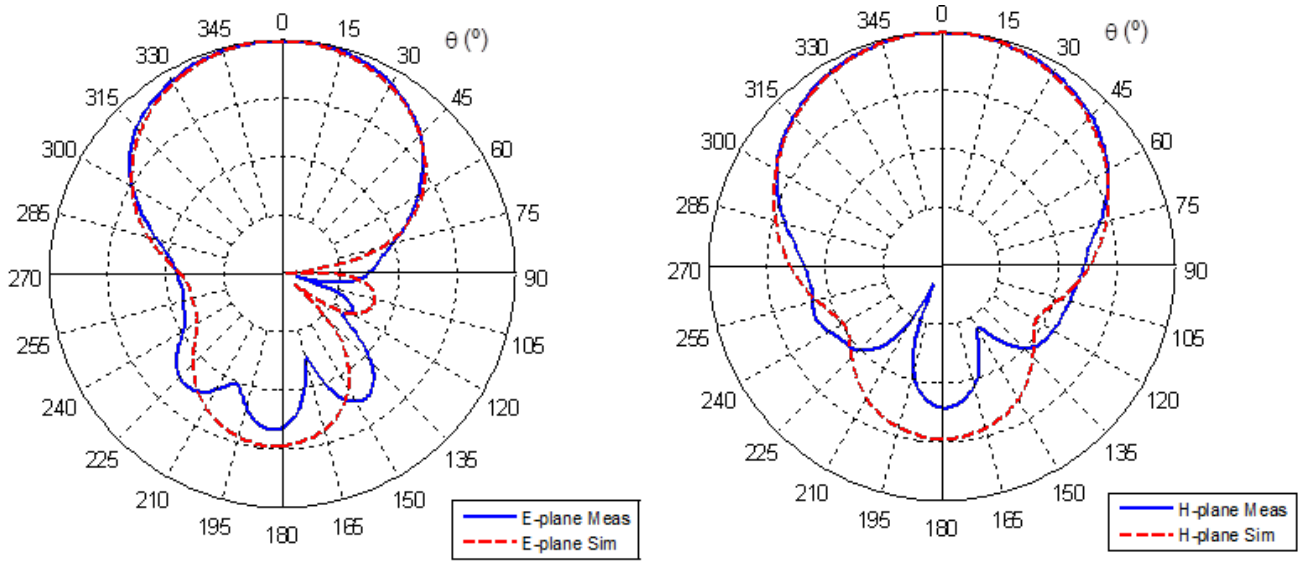

(a) (b)

Figure 2.12: Radiation patterns of the patch antenna: (a) E-plane; (b) H-plane.

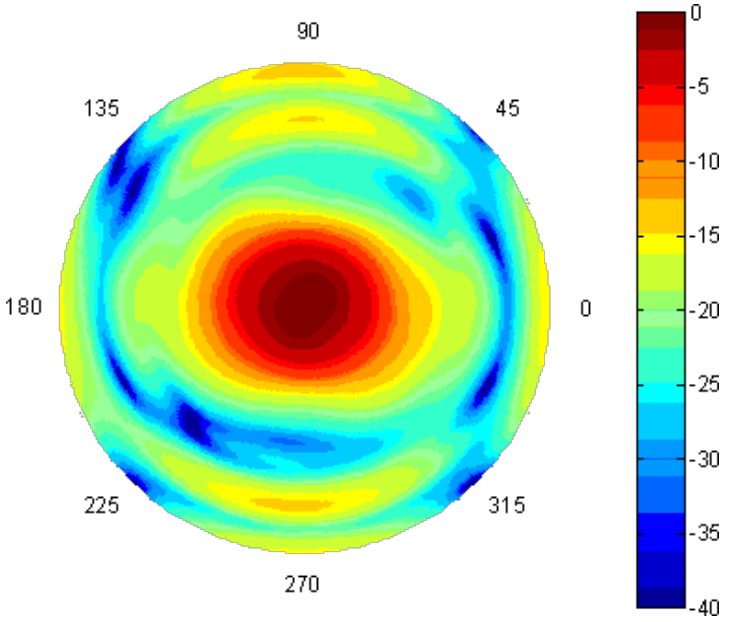

Figure 2.13: Front radiation pattern of the patch antenna (units: dB).

2.2.2.5 The Effect of the Number of VM Stages

Another investigated aspect of the WuR system is the effect of number of VM stages of the SμA-WuRx on the overall voltage gain and operational distances achieved. The simulations performed in Ansys HFSS electromagnetic software in Figure 2.15 analyze the voltage gain versus different number of VM stages. In the figure, Va, Vin and Vo stand for voltage at antenna, VM input and VM output, respectively. From the theoretical point of view, for the low voltage input values of around 0.1 V like the typical ones expected for WuRx, increasing the number of multiplication stages does not imply an observable difference in Figure 2.15.

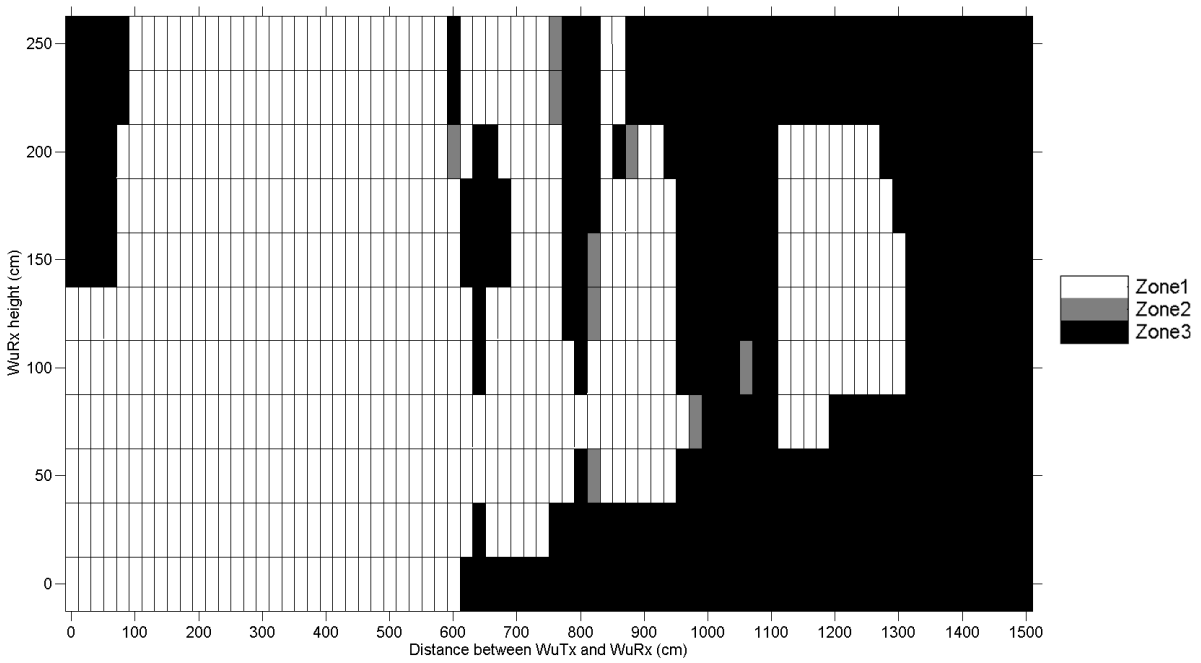

(a)

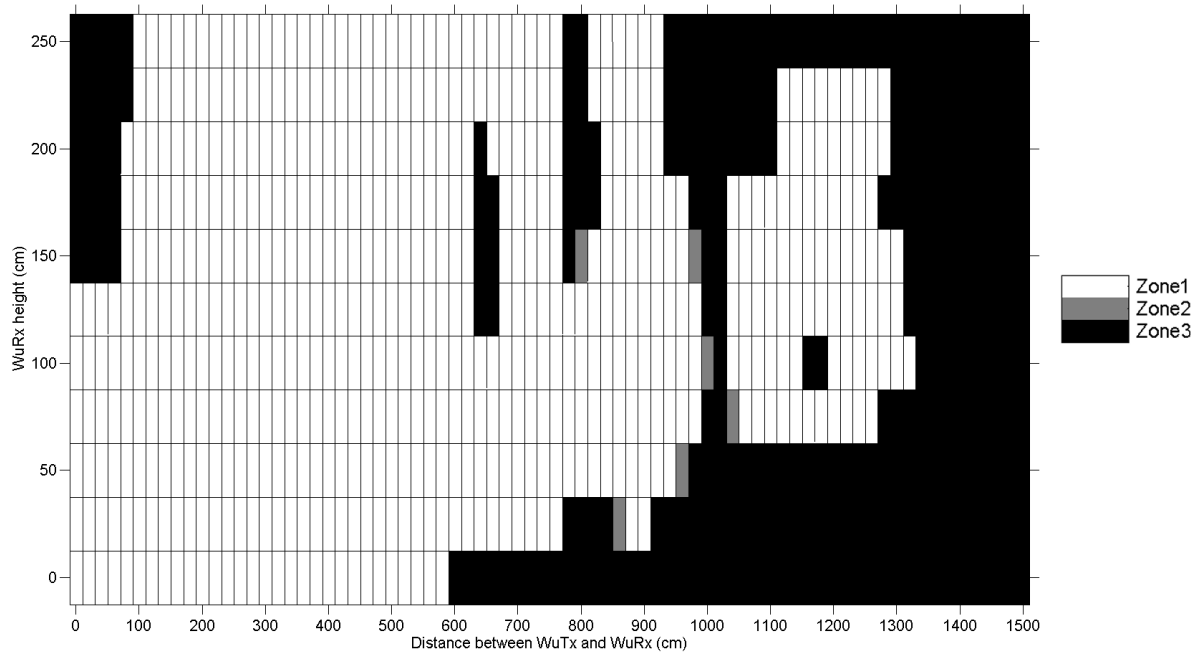

(b)

Figure 2.14: Wake-up zones for the outdoor scenario. WuTx: Patch antenna, gain = 7 dB for (a) VCC = 2.5 V, and (b) VCC = 2.8 V. SμA-WuRx: 3.81 cm x 4 cm ground plane, SAW filter, five-stage VM.

From physical experiments, it is reassured that for low RF input voltages, a 5-stage VM circuit is a good cascade value, while a 2-stage VM performs poorly in terms of the operational distances and there is hardly noticeable performance difference between 5-stage and 10-stage VM circuits. The reason for the similar performances between the latter two configurations is the cancellation between the voltage gain and voltage drops at each VM stage. Moreover, a

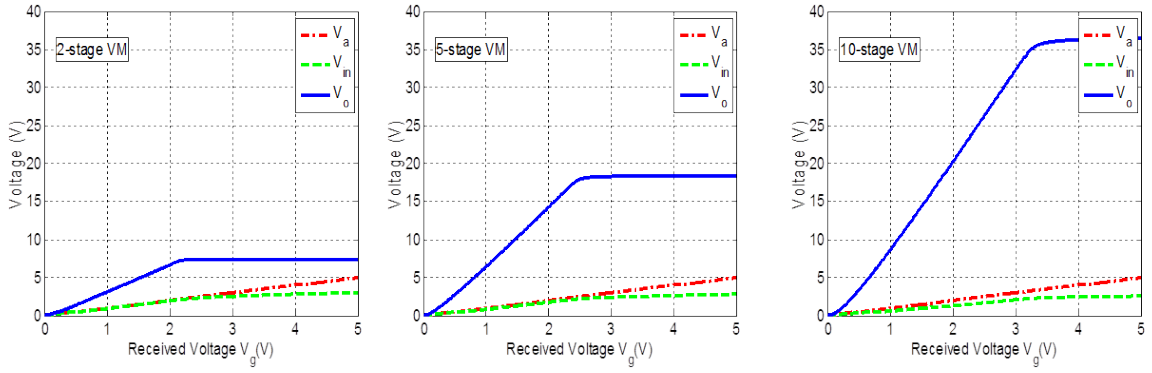

Figure 2.15: Simulated cumulative voltage results for 2, 5, and 10 VM stages, respectively.

drawback of higher number of stages is the amount of required circuitry and the consequent extra delay and economic cost introduced by them.

2.2.3 Latency Analysis

Although the timing aspect cannot be optimized, there is a need to know a few related particularities regarding both WuTx and WuRx designs. The first one is the option of setting the WuTx in low-power mode, which allows power-efficient operation. To do so, the ARF7243A features a PWRUP mechanism to turn the radio on. Data must be sent 2 milliseconds after the PWRUP pin is activated. After transmission the device is disabled to save energy. The direct timing relationship between when a WuC is transmitted by the WuTx and the instant it appears at the output of the comparator at the WuRx can be seen in Figure 2.16.

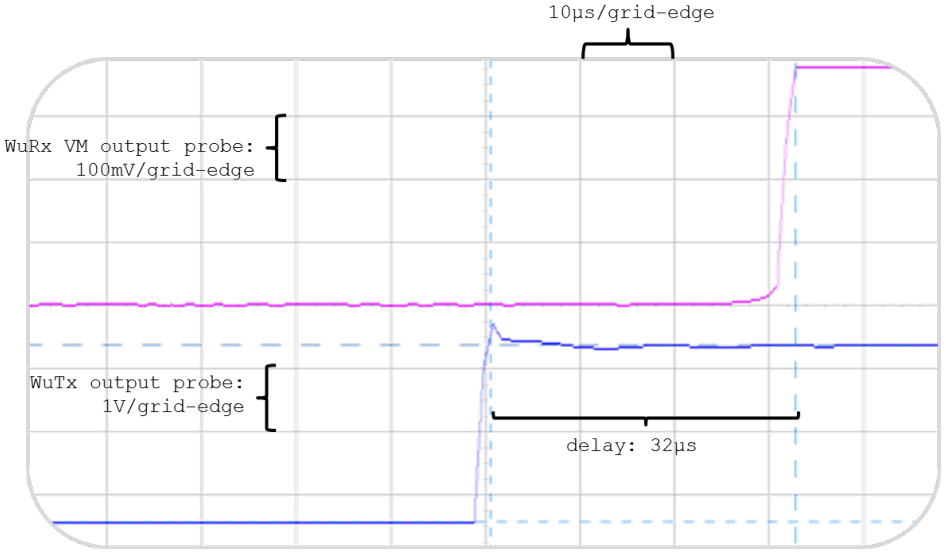

Figure 2.16: WuC delay shown at the output of the transmitter (bottom) and at the output of the VM on the WuRx (top).

The time delay is an important metric to quantify in case of delay-sensitive user applications. As seen in the figure, a 32 µs delay is observed between the input data pin of the WuTx

when sending a WuC and the output of the WuRx comparator. Note that the delay between WuTx and SμA-WuRx depends on many factors including the use or not of a of SAW filter, the number of voltage multiplying stages, and the response time of the comparator. In addition to the WuRx delay, the time needed for the activation of the MCU after the interrupt from WuRx may also have to be considered depending on the application. For a wireless sensor mote using a CC2430 transceiver based on a 8051 MCU, this value is 120 μs [23].

2.3 A Reference, Off-the-shelf WuR System

In this section, a commercial WuR solution is analyzed from a practical perspective as a reference to compare the proposed SμA-WuRx and WuTx system against. For such purpose, the so-called Austria MicroSystems AS3933 demokit, containing both one wake-up transmitter and one wake-up receiver boards, is studied from the power consumption and operational distance points of view.

2.3.1 Design and Specifications

The AS3933 [24] is a low-power Amplitude Shift Keying (ASK) receiver capable of generating a wake-up interrupt upon detection of a data signal at a carrier frequency between 15 kHz and 150 kHz. The WuRx board can operate using one, two, or three active channels, as shown in the block diagram in Figure 2.17. Enabling three channels, i.e., three orthogonal coil antennas, is a method to make reception independent of receiver orientation; the coil antenna with better reception is the one providing the input signal for the IC to work with. If such three-dimensional detection is not required, it is possible to deactivate one or more channels, or even operate them in a 50% , 33%, 20% or 11% duty cycle in order to save energy. The AS3933 WuRx includes an integrated correlator to optionally implement a 16/32 bit wake-up address decoding scheme. This WuRx features a maximum sensitivity of -69 dBm [24].

As for clocking signal (CLK), the WuRx system accepts an external clock, a crystal oscillator or its own internal one, named respectively LC-oscillator, Xtal RTC and RC-OSC. The chosen CLK signal source determines the WuRx current consumption. According to the datasheet specifications, the current consumption in standard listening mode with three active channels and crystal oscillator as CLK is 8.9 μA. Instead, the consumption is reduced down to 8.3 μA when employing a RC-OSC for clocking. This difference for a crystal oscillator matches the one obtained in section 1.3, Code 1.2 for a MCU configured to work with an internal oscillator instead of an external crystal.

The AS3933 WuRx IC is capable to detect the presence of an inductive coupled carrier and extract the envelope of the WuC. Next, the frame content is correlated with a programmed pattern. If the received value corresponds to the stored node address, a wake-up Interrupt ReQuest (IRQ label in Figure 2.17) is generated. Such correlation can be bypassed, in which

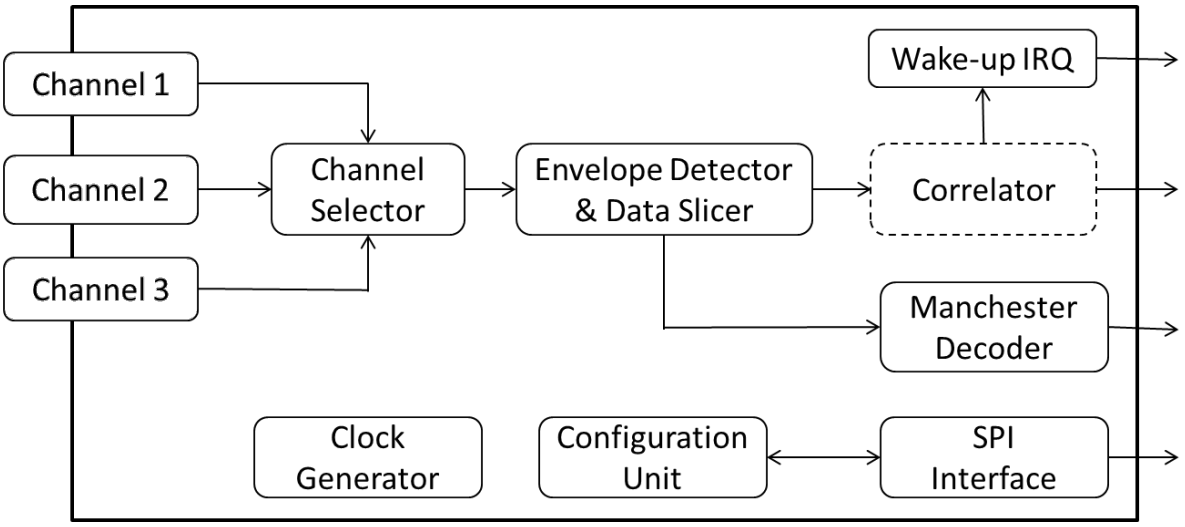

Figure 2.17: The AS3933 block diagram. The use of correlator is optional.

case the wake-up procedure performs only carrier frequency detection as in the SμA-WuRx case.

2.3.2 Performance Evaluation of AS3933

In this section, a current consumption analysis for both WuTx and WuRx boards of the AS3933 WuR system is performed. Operational range measurements are presented to quantify the wake-up zones, which is crucial to determine the applications that can benefit from this WuR system. The hardware boards are shown in Figure 2.18. Note the 3 dimensional coil system on the upper part of the WuRx.

2.3.2.1 Current Consumption Evaluations

Due to the physical enclosure of the AS3933 WuTx, it is not trivial to carry out a characterization of the provided transmitter in terms of power. Conducted measurements for the current consumptions of the entire WuTx board indicate a maximum current consumption of 0.8 A while transmitting one WuC.

Regarding the AS3933 WuRx board, it includes a specific jumper to allow measuring the current of just the IC, and not the entire board. The measured current consumption values of 6.3 μA and 6.4 μA are close to the 6.5 μA value in [24] for a configuration featuring three active signal channels and a crystal oscillator as CLK source. While decoding a WuC, the current consumption value rises up to 12 μA.

2.3.2.2 Operational Range Evaluations

The same testing scenario as in section 2.2.2 is set to quantify the operational distances of the AS3933 demokit. As done in the evaluations of the SμA-WuRx, the transmitter is fixed at a

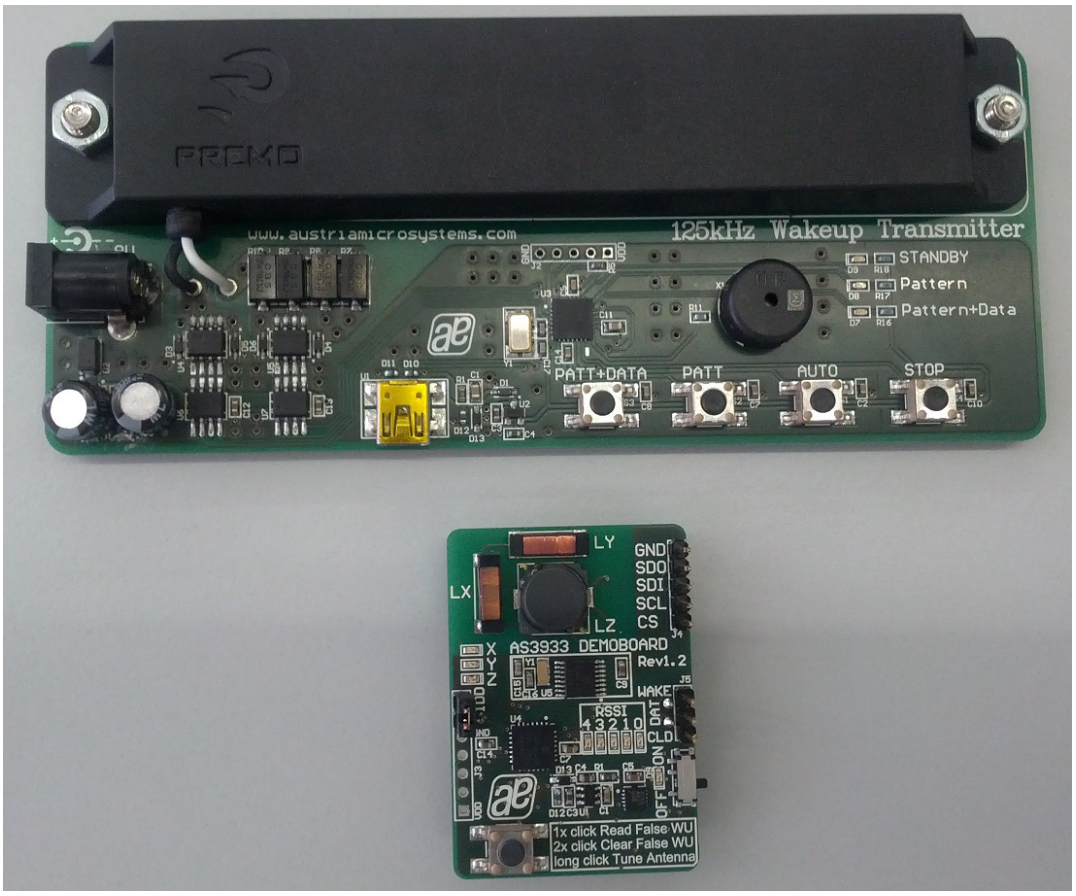

Figure 2.18: The AS3933 WuTx (top) and WuRx (bottom).

coherent, useful height of 100 cm and the receiver board is displaced vertically and horizontally to different heights and distances in 25 cm and 20 cm steps, respectively.

This section studies the achievable operating distances of the system for two VCC values for the WuTx: 5 V (default) and 12 V. A higher VCC value is expected to give better range results, since the output power increases. Several settings are applied at both devices to achieve the longest possible operational distance. For example the system's symbol-rate is reduced to its minimum (512 symbols/s), since it is expected that the lower the data-rate, the higher the distance. The comparator hysteresis of the data slicer at the WuRx is also lowered from 40 mV to 20 mV to detect weaker signals and its sensitivity increased by setting the channel amplifier gain to +3 dB. The field tests of AS3933 WuR system are performed in an outdoor environment, and the corresponding wake-up zones shown in Figure 2.19.

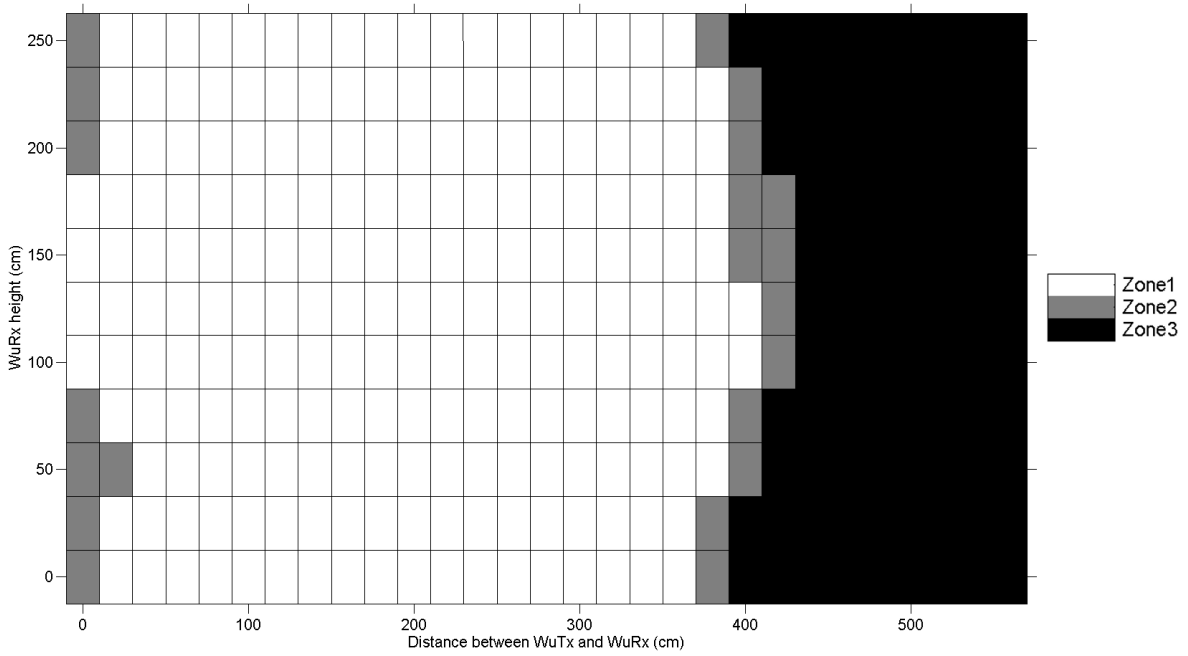

(a)

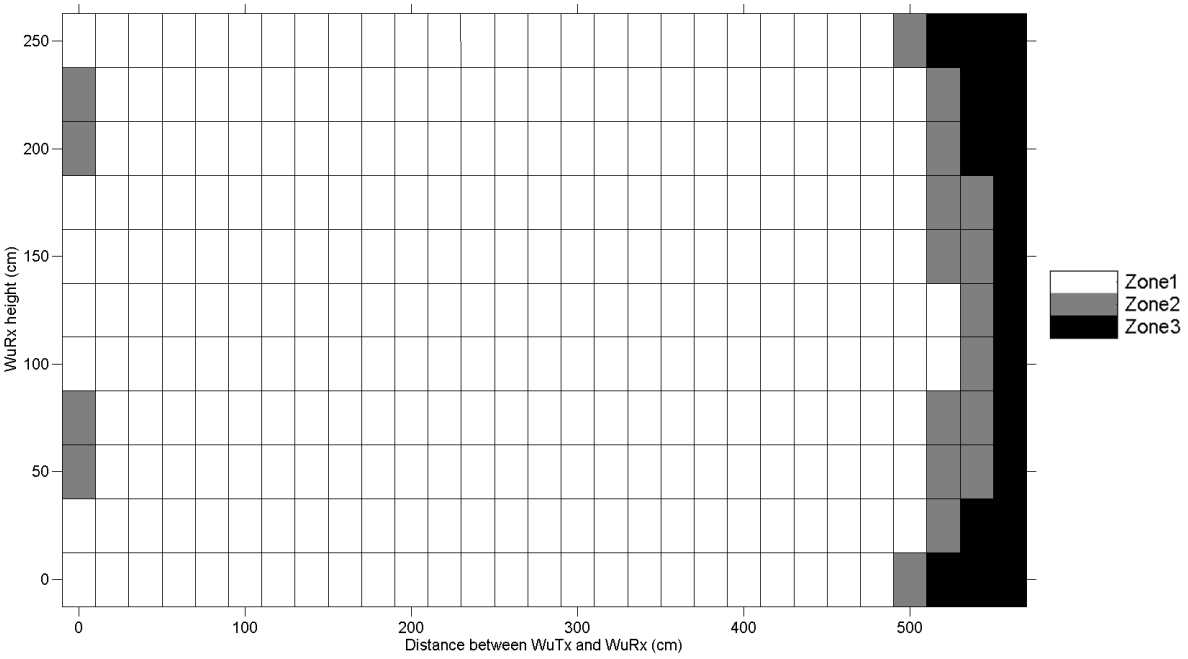

(b)

Figure 2.19: Wake-up zones of the outdoor scenario for the AS3933 demokit when WuTx power supply is (a) VCC = 5 V; (b) VCC = 12 V.

The AS3933 WuRx board provides RSSI values for the received WuC signal through a set of LEDs, allowing new measurements to be performed. In Figure 2.20, the highest normalized RSSI value is logged for each different distance and height pair. The logged value may belong to any of the three channels of the AS3933. Such RSSI values can be used to observe the expected behavior of the wake-up probabilities. Comparing Figure 2.20 to Figure 2.19, it is

seen that a persistent reception occurs up to 20% of the maximum RSSI value.

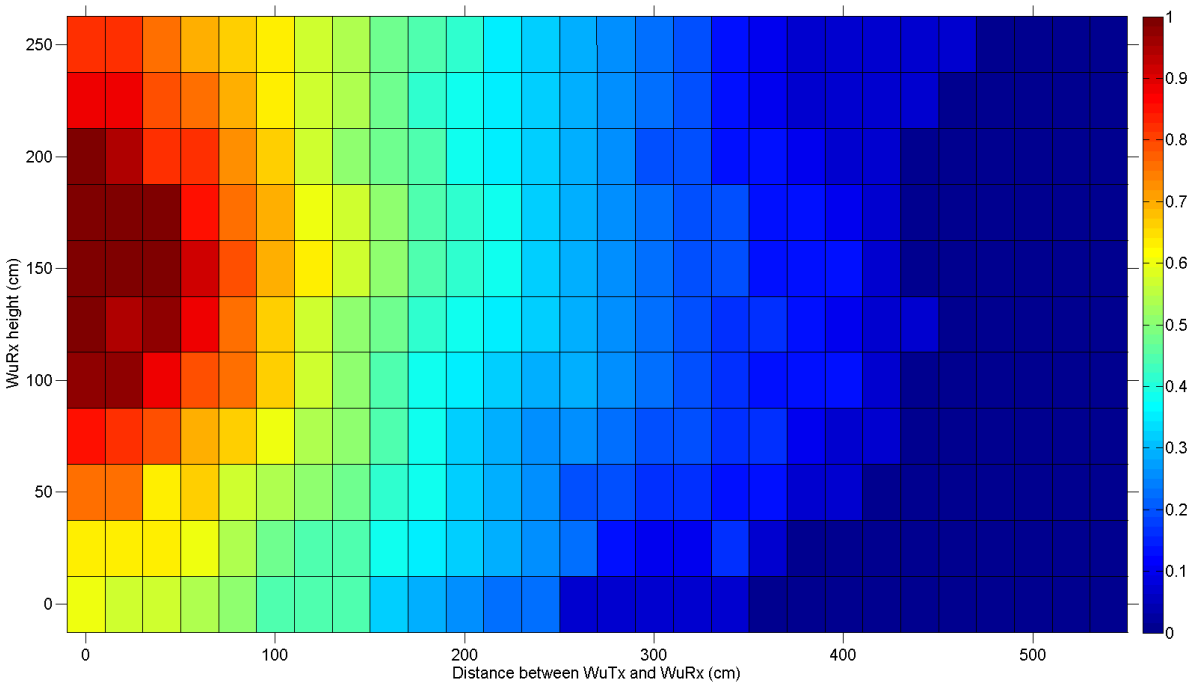

(a)

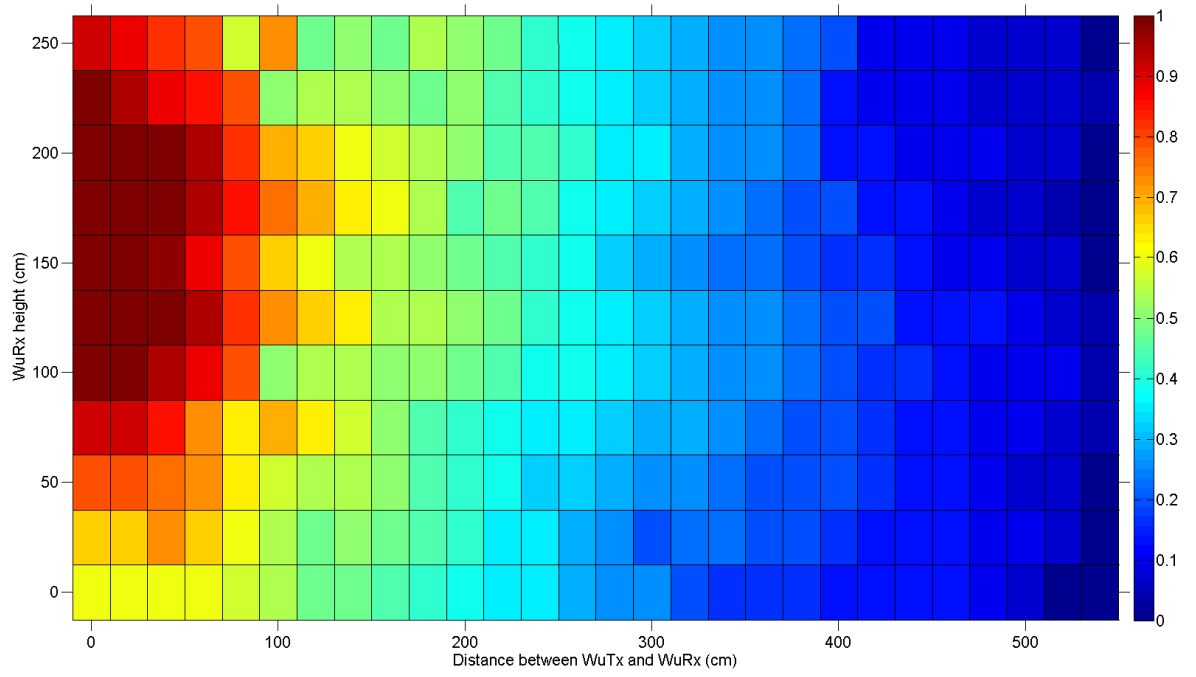

(b)

Figure 2.20: Normalized RSSI values measured by AS3933 WuRx when WuTx is powered at (a) VCC = 5 V; (b) VCC = 12 V.

2.4 Comparison between the Proposed WuR and the AS3933 WuR Systems

The WuR system proposed in this chapter is a successful prototype useful for many low-power wireless applications. However, the system can be further improved by including several features that would be desirable, such as longer operational ranges and/or addressing mechanisms. Ways to address these two issues, among many others, are addressed in next chapters of this thesis.

From the energy point of view, the SμA-WuRx clearly reduces the current consumption featured by the AS3933. Even if configuring the latter in a 50% duty cycle mode, where some WuCs may be missed by the AS3933, the SμA-WuRx features half the consumption (0.8 μA vs 1.7 μA). When in standard listening mode, the AS3933 requires around 7 μA for its 3-channel configuration and the corresponding signal amplifiers activated, thus the savings provided by the SμA-WuRx are even more pronounced.

Regarding operational distance evaluations, the AS3933 demokit achieves a maximum range of around 5.5 meters, whereas the proposed WuR system doubles this value when used with the developed WuTx antenna. The developed WuTx also employs less power to transmit the WuC (0.5 A vs 0.8 A).

In terms of hardware components, the SμA-WuRx is also far less complex than the AS3933, which in turn requires additional software to set its internal registers through its SPI interface each time it is powered off. From the monetary cost point of view, the SμA-WuRx achieves almost one third of the cost of AS3933-based WuRx when considering the costs for assembling the two WuRx devices (3€ vs. 9€). Apart of the typical components such as resistors, capacitors and diodes, the WuRx based on AS3933 needs the mentioned IC, a voltage regulator, a MCU and some input coils.

Finally, a functionality that is provided by AS3933 but not currently supported by SμA-WuRx is addressing. Although not all user applications require such functionality, in case of the need for it, there are several ways to enable SμA-WuRx to be individually addressed among a set of nodes. One well-known way is the use of correlator, as in the AS3933 case. Another one, namely Time-knocKing, is introduced in next chapter 3 of this thesis and exploits the MCU's low-power operation modes.

3 Time-knocKing: a Novel Low-Power Mechanism for WuR Addressing

Some of the advantages of using WuR over traditional duty cycling have already been introduced in Chapters 1 and 2. Still, if a WuR system is not enabled to distinguish an individual, unique node to wake-up among a set of them, the energy savings enabled by its use become minimized because of the overall network power consumption. In other words, the overhearing problem is still present in a network of nodes equipped with non-addressable WuRx, even in an order of magnitude lower than in the case the use of WuR is not contemplated.

In this chapter, a WuRx addressing scheme is proposed, namely Time-Knocking (TicK), to allow non-addressable WuRx designs to be individually queried. Section 3.1 introduces the addressing feature in WuR systems. Section 3.2 presents and describes the different WuRx addressing approaches. Section 3.3 introduces this novel WuRx addressing proposal, TicK, in detail and also provides an example execution trace and enumerates some hardware characteristics to implement TicK. Afterwards, section 3.4 provides theoretical analysis relating current consumption with the WuC arrival frequency of a node operating using TicK, MCU-decoding and the correlator approaches. Section 3.5 applies such theoretical analysis to different scenarios. Section 3.6 provides a snippet of TicK's source code. Finally, conclusions are presented in section 3.7.[1]

Contents

[1] The current chapter is based on and extends the work contained in the following publication: ≪J. Oller, I. Demirkol, J. Paradells, J. Casademont, and W. Heinzelman, 'Time-Knocking: A Novel Addressing Mechanism for Wake-up Receivers', in 8th IEEE International Conference on Wireless and Mobile Computing, Networking and Communications (WiMob), 2012, pp. 268-275.≫.

3.1 Introduction

In the basic operation of most addressable WuRx [3, 5, 25], upon WuC's carrier frequency detection, signal demodulation starts for the preamble and address decoding. Due to interference and noise sources, such carrier frequency may be detected for both correct and false WuCs. The TicK approach saves a significant amount of energy even when there are frequent WuC. A LPM-based approach like TicK also achieves less hardware complexity than using extra components such as a correlator for the address resolution task [3, 5, 26–29]. Also, due to the usual low bit-rate employed in WuR, and hence long bit durations, using the LPM of the MCU to resolve the address instead of, e.g., decoding the full-address through MCU processing [17], is far more energy-efficient.

The idea of encoding data within time intervals is the basis of Pulse Position Modulation (PPM). In this chapter, the use of PPM at the WuTx and LPM and hardware timers of a low-power MCU at the WuRx, respectively, enable WuC generation and node addressing in WuR systems not designed with this feature from scratch. LPMs are a common feature in low-power MCUs. For Texas Instruments' MCUs, they are simply called LPM. For Microchip MCUs, the feature is called eXtreme Low Power (XLP). LPM operation is introduced in chapter 1, section 1.3.

As an added value, TicK address mismatches are quickly determined, and non-intended nodes disable themselves from continuing the address resolution even before the sender node finishes transmitting the entire WuC, thus further optimizing energy savings. Another advantage of TicK is that the address construction is variable, and nodes can be assigned with temporary or local addresses, e.g., with short lengths to improve the energy-efficiency and reaction time, or with long ones to improve the system's resilience to interferences.

To evaluate the benefits of TicK, its expected current consumption is analytically derived along with the one for two common address resolution approaches: MCU-decoding [17] and correlation [3, 5, 26–29]. In order to obtain realistic parameter values to use in the formulae, physical measurements are performed. The results show that, by slightly sacrificing from the WuC duration, a WuRx using TicK-based addressing achieves better current consumption values than that of the other two traditional approaches investigated. However, such WuC delay does not represent a drawback in WuR systems since they do not require high bit-rates. Other important advantages of TicK is that it does not require any additional hardware, and

that all non-addressable WuRx proposals in the literature can be employed in a TicK manner. For example, the AS3933 in chapter 2 can be configured to use TicK by disabling its correlator via its SPI interface.

3.2 Related Work

The current section introduces various addressing approaches for WuR systems. When there is a need to discriminate the destination device among a set of WuRx-equipped nodes, addressing capabilities become a must for energy-efficient network operation. In WuR systems, the different addressing approaches mainly distinguish by the components employed for the WuC address decoding, since this aspect affects the overall energy consumption. For example, if during the address resolution process a high degree of MCU's intervention is required, power consumption is expected to be much higher than in the case where the addressing procedure is done entirely by a dedicated component such as a correlator.

3.2.1 WuRx Addressing Through Multiple Frequencies

A Radio-Triggered IDentification (RTID) WuRx scheme basically consists of hardware capable of detecting several simultaneous RF carriers at different frequencies. In [30], when a node wants to activate another one, it simultaneously transmits in several frequencies that code the address of the destination node. Thus, nodes must be equipped with several transceivers.

The RTID approach clearly has a very limited addressing space. Although, according to the authors, by distributing addresses in a non-duplicative manner RTID allows energy savings up to 88%. However, the requirement for transceivers capable of operating at different frequencies brings complexity to the WuRx.

3.2.2 WuRx Addressing through the MCU

When employing a MCU to decode an address, the WuRx acts as a simplistic RF receiver. Figure 3.1 depicts this MCU-based decoding approach. After detecting the WuC, the pulse train is decoded by the MCU to obtain the destination address.

In [31], when an external radio signal is detected at 868.5 MHz, the MCU is activated by an interrupt on one of its input pins to receive the WuC containing the WuRx address. Unfortunately, in [31] there is no explicit data about the current consumption of this MCU-decoding approach. However, the values are expected to be similar to other studies that also employ the MCU to decode the addresses embedded in the WuC. For example, in [17], the overall power consumption of such WuRx addressing approach is up to 819 µW, an unacceptable value for WuRx purposes, as indicated in chapter 1, section 1.6.

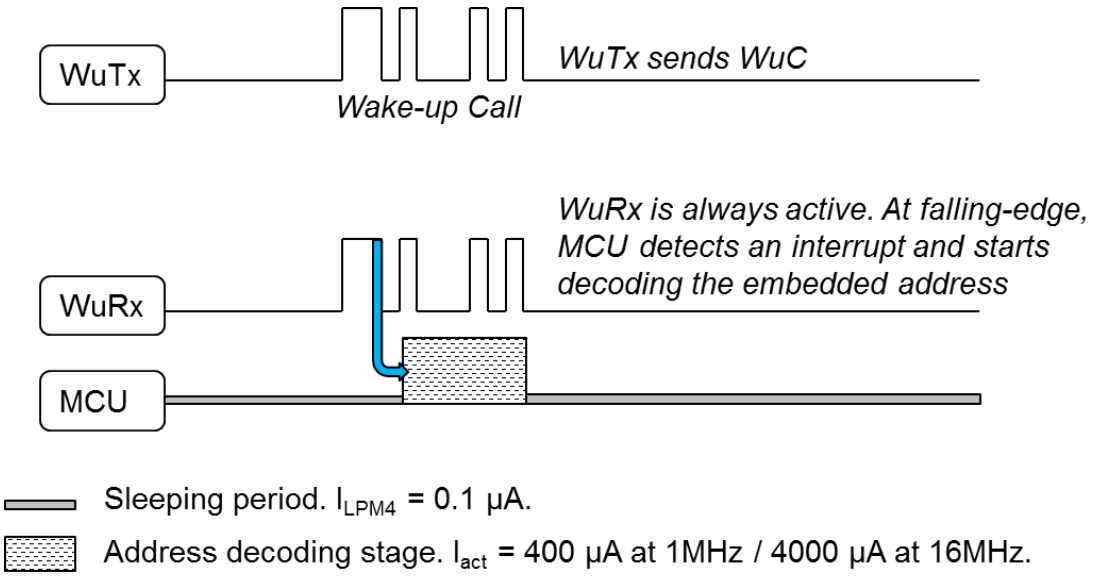

Figure 3.1: Time diagram for decoding the WuRx address by MCU.

3.2.3 WuRx Addressing through Correlation

A different approach to MCU-decoding is the use of a hardware correlator. Internally, a correlator circuit generates a parallel output of the bits contained in a buffer, which are shifted at each clock transition with a new bit incoming through the signal input. Such output value is compared to a pre-stored one.

In the WuRx case, the input shift register progressively hosts the demodulated address extracted from the WuC by analog to digital conversion (performed by envelope detection) and compares it with the node's own identifier. If both values are the same, the wake-up interrupt output pin is asserted. Figure 3.2 depicts the use of a correlator to decode an address in a WuC. Address correlators consume few µA when in idle state and approximately 10 µA when fully active decoding the WuC address [3, 24].

In [26, 27], one WuC decoding attempt is shown to require 75 µW by simulation. Similarly, the wake-up architecture in [28, 29] is composed of both an analog and a digital part, the latter comprising a correlator for address decoding. The proposal presents current consumption values of 12.4 µW and 368.1 µW when in idle listening and decoding the WuC address, respectively, considering a 1.8 V power supply and a bit-rate of 40 kbps. This bit-rate value is quite high for WuRx designs, since they use to keep it low in order to reduce current consumption.

A correlation approach is also found in the commercial AS3933 WuRx [24]. The AS3933 is described in chapter 2, section 2.3.2. Basically, it consists of a 3-channel low-power ASK receiver that generates an interrupt upon detection of a Low-Frequency (LF) carrier frequency at 15 kHz - 150 kHz. It operates in the 2.4 V - 3.6 V range with a current consumption of 2.78 µA when no address decoding is in progress. The AS3933 expects the WuC to arrive as Figure 3.3 depicts.

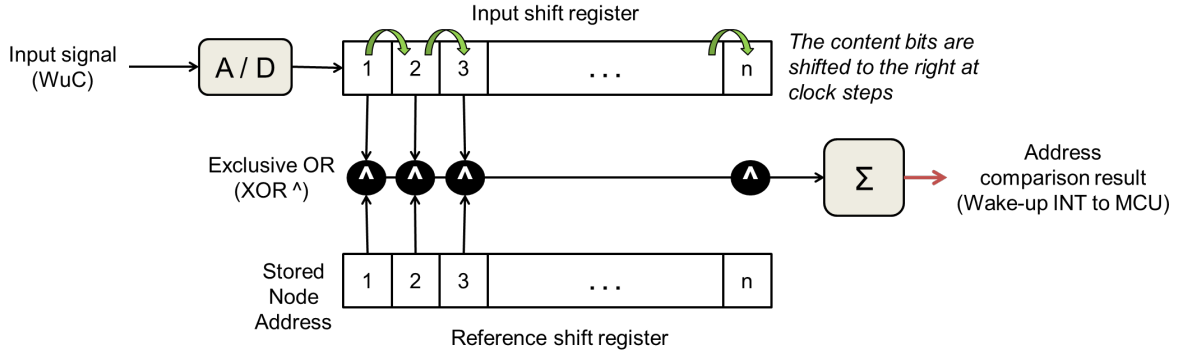

Figure 3.2: Address comparison by means of bit correlation.

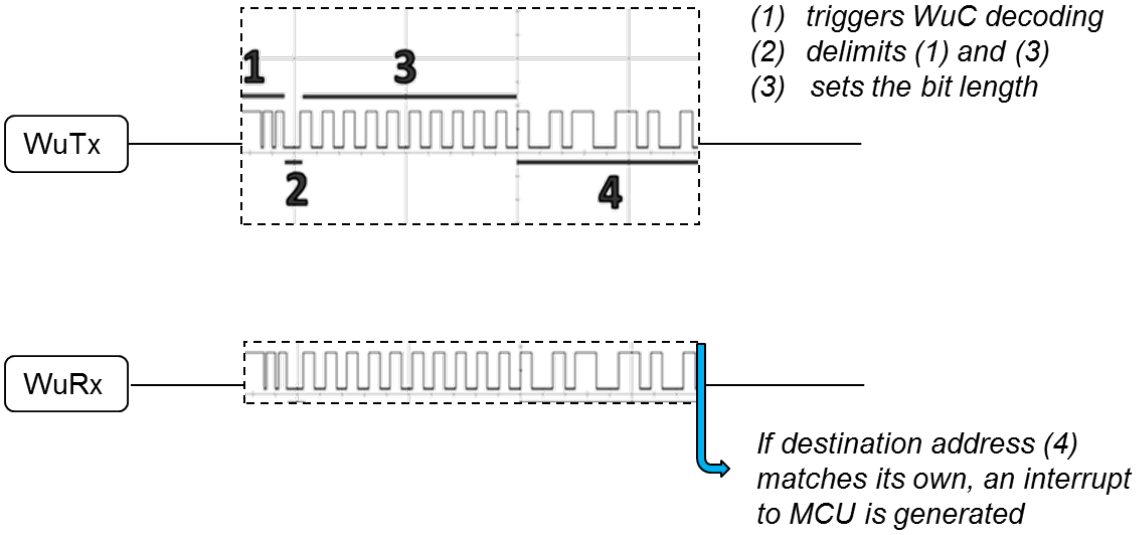

Figure 3.3: WuC decoding in the AS3933; (1) Carrier burst, (2) separation bit, (3) preamble, (4) destination node address.

The WuC format in Figure 3.3 is not fixed in length but may slightly vary when adjusting some parameters of the WuRx, as done in the following Code 3.1 for a MSP430G2452 MCU and two example arbitrary registers. When the AS3933 WuRx receives a properly built WuC, an IRQ is raised in the corresponding input pin of the MCU.

```
1  // #includes contain names for registers, constants, etc.
2  #include <msp430g2452.h>
3  #include <stdint.h>
4
5  /* chip SPI structure:
6      - 00b write / 01b read / 11b direct command
7      - __xxxxxb reg_number / direct command
8      - xxxxxxxxb data
9  */
10 #define WAIT_SPI_2_FINISH   while(!(USICTL1 & USIIFG));
11
```

```
12
13 volatile uint16_t SPI_answers[12];
14 volatile uint8_t i = 0;
15
16
17 void main(void)
18 {
19     WDTCTL  = WDTPW + WDTHOLD;  // Stop watchdog timer
20
21     P1DIR   =   0xFF;           // All P1.x outputs
22     P1OUT   =   0;              // All P1.x reset
23     P2DIR   =   0xFF;           // All P2.x outputs
24     P2OUT   =   0;              // All P2.x reset
25
26     // PORT 1 SPI CONF
27     // **************
28     P1SEL |= 0xE0;
29
30     // Port, SPI master
31     USICTL0 |=  USIPE7 +  USIPE6 + USIPE5 +
32                 USIMST + USIOE + USISWRST;
33     // divide SMCLK by 16
34     USICKCTL = USIDIV_4 + USISSEL_2;
35
36     // USI released for operation
37     USICTL0 &= ~USISWRST;
38     USICTL1 &= ~USIIFG;
39
40     // general interrupt enable for receiving the SPI responses when USICNT ↙
    ↳ has been emptied
41     USICTL1 |= USIIE;
42     __enable_interrupt();
43
44
45     // SPI WRITE SECTION
46     // -----------------
47     // write 00000000b R0, data  = 00000010b, Activate coil 1
48     P1OUT |= 0x10;  USISR = 0x0002; USICNT |= 0x50; // strobe CS, SPI WRITE &↙
    ↳  USI16B + 16 bits to transfer
49     WAIT_SPI_2_FINISH
50
51     // write 00000111b R7, data = 00101101b, Wake-up pattern, 1st byte
52     P1OUT |= 0x10;  USISR = 0x072B; USICNT |= 0x50; // strobe CS, SPI WRITE &↙
    ↳  USI16B + 16 bits to transfer
53     WAIT_SPI_2_FINISH
54
55     // SPI READ SECTION
56     // strobe CS, SPI READ & USI16B + 16 bits to transfer
```

```
57      // ----------------
58      // read 01000000b R0
59      P1OUT |= 0x10;  USISR = 0x4000; USICNT |= 0x50;
60      WAIT_SPI_2_FINISH
61
62      // read 01000111b R7
63      P1OUT |= 0x10;  USISR = 0x4700; USICNT |= 0x50;
64      WAIT_SPI_2_FINISH
65
66      // we are done with the demo, sleep
67      _BIS_SR(LPM4_bits + GIE);
68  }
69
70  // USI interrupt service routine, USIIFG set when USICNTx becomes zero
71  #pragma vector=USI_VECTOR
72  __interrupt void universal_serial_interface(void)
73  {
74      // CS is cleared here!
75      P1OUT &= ~0x10;
76      // recover all SPI answers in a vector
77      SPI_answers[i++] = USISR;
78      USICTL1 &= ~USIIFG;
79  }
```

Code 3.1: Example code to check correct SPI communications between a MSP430G2452 MCU and a AS3933.

The previous Code 3.1 follows the typical structure for SPI writes and reads to a memory. However, the AS393x chips do not feature such memory. Thus, this code has to be run upon each MCU boot process. Code 3.1 first configures a GPIO port to be used as SPI interface. Then, it sets the clock dividers in order to establish the bit-rate for read / write operations. Afterwards, it enables the interrupts from SPI, which indicate when a SPI write or read operation finishes to the MCU to prevent information being overwritten or read too early. A read / write operation consists in a *chip select* operation (`P1OUT |= 0x10`), specifying an operation indicator followed by a register address and a value to the USISR, and setting the number of bits to be written to USICNT.

3.3 WuRx Addressing through Time-Knocking (TicK)

TicK follows a different approach than waking up the MCU to decode the entire address of a WuC or including a dedicated hardware correlator. In TicK, the WuTx transmits several short WuCs at specific instants. The time durations between the WuCs encode the address bits. On the receiver side, the LPM of the MCU is both used when the WuRx is idle and also between WuC arrivals, which enables optimum energy savings. Different address values are coded depending on the time between the interrupts the WuCs provoke to the MCU. Since

the number of MCU instructions to capture the time value, perform some bit shifting and compare the WuC's address to the node's own is extremely small, the TicK approach enables the MCU to remain in LPM a large amount of time.

The low-cost and low-power MCU MSP430G2452 [32] from Texas Instruments is employed for performance evaluations of both MCU-decoding and TicK approaches in this chapter. This MCU consumes 0.1 µA in its deepest sleep mode LPM4. In LPM4, only interrupts coming from a WuRx can wake-up the MCU. This MCU features low-power hardware timers that require additional 0.4 µA when in LPM3, increasing the total power consumption to 0.5 µA. Finally, in active mode, i.e., when the MSP430G2452 is fully functional, it consumes between 400 µA and 4 mA depending on the MCU's core frequency used, which is an adjustable parameter.

The fundamentals of TicK are shown in Figure 3.4. TicK defines time blocks, which consist of time slots, where WuCs can occur. Let n_b be the number of time blocks used to represent an address and $n_s + 1$ the number of time slots in each block. During the first time slot in each block, a *Reference WuC* (black frames in Figure 3.4) is sent, which provides synchronization. Up to n_s possible addressing WuC locations exist for each block, enabling the representation of $\log_2(n_s)$ bits. Thus, with n_b blocks, a total address length of $n_b \log_2(n_s)$ bits can be represented.

Before addressing, sleeping nodes are at their lowest power mode LPM4. With the first reference WuC, the nodes are interrupted through the WuRx circuitry to go into active mode. The Interrupt Service Routine (ISR) serving such an interrupt consists of very few lines of code that start a MCU timer. Afterwards, the MCU goes into LPM3 mode to wait for a second WuC interrupt, which delimitates the block. If the WuC arrives in an instant not corresponding to the first part of the node's address during a certain time, the MCU discards the whole WuC and disables its interrupt pin until the end of the entire addressing duration. On the other hand, if a WuC is received in the correct time slot, then the current part of the incoming WuC address partially matches the node's address and the MCU goes to LPM4, until it is once again awakened with the reference WuC of the next block.

Figure 3.4 shows an example for a TicK block size of 4. If after the reference WuC another WuC arrives at time unit `4`, then this block currently addresses '`11`'. Next, the MCU goes to LPM4 again until the following reference WuC, which implies the start of the following address block. This is repeated until the full address length is reached. Thus, TicK allows setting the MCU in LPM even during the duration of the addressing phase, thus further reducing the energy needs for addressing.

For a given address bit-length, different tuples of number of blocks (n_b) and number of slots per block (n_s) are possible. However, the total addressing time in terms of total number of slots, namely d_{TicK}, changes depending on the chosen tuple. This is shown in Figure 3.5 for two other possible value combinations of n_s and n_b and their corresponding d_{TicK} values for coding the same 16 bit address in Figure 3.4 of '`1000100100101111`', i.e., `0x892F` in hexadecimal representation. For example, since each block encodes $log_2(n_s)$ bits of the

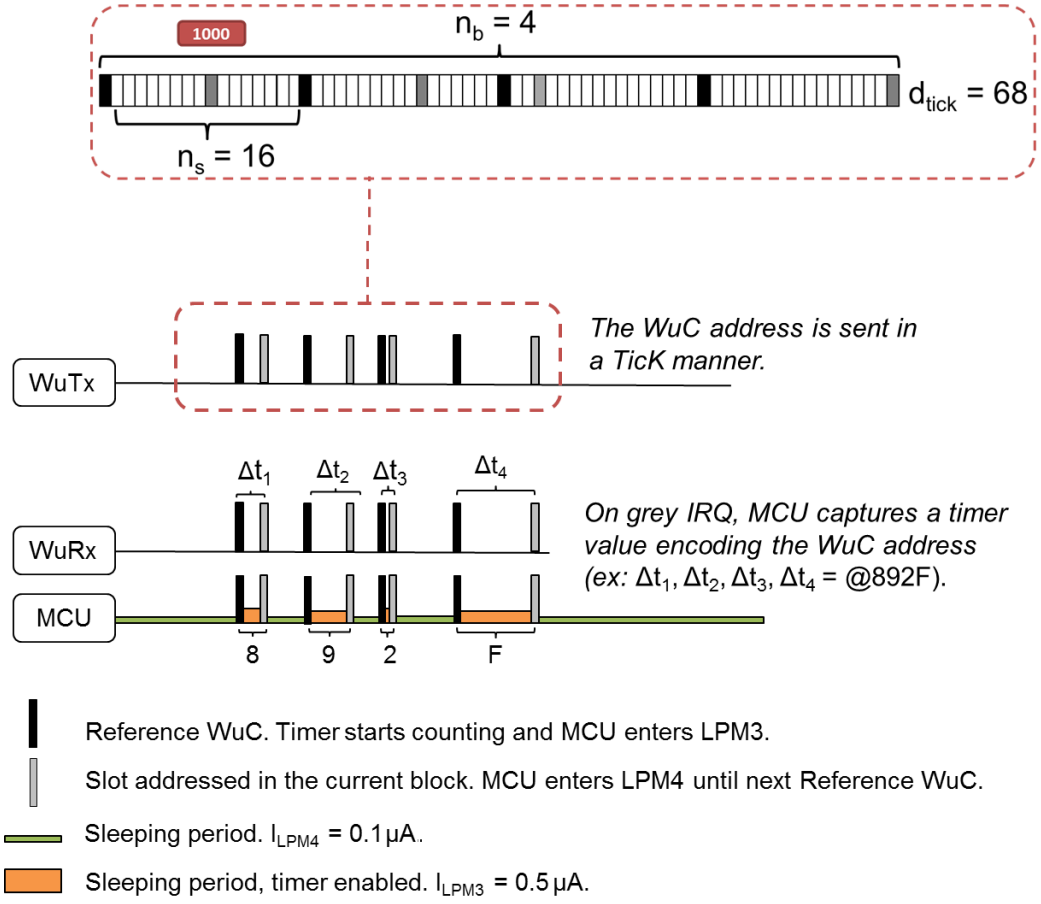

Figure 3.4: The TicK addressing approach.

address, to encode the first four bits, i.e., 1000, two blocks are needed for $n_s = 4$ and $n_b = 8$; the first representing 10, the second representing 00. Exactly the same fragment of address is coded in a single block with $n_s = 16$ and $n_b = 4$, since in this case, each block represents $\log_2(n_s) = 4$ bits, being the first one '1000'.

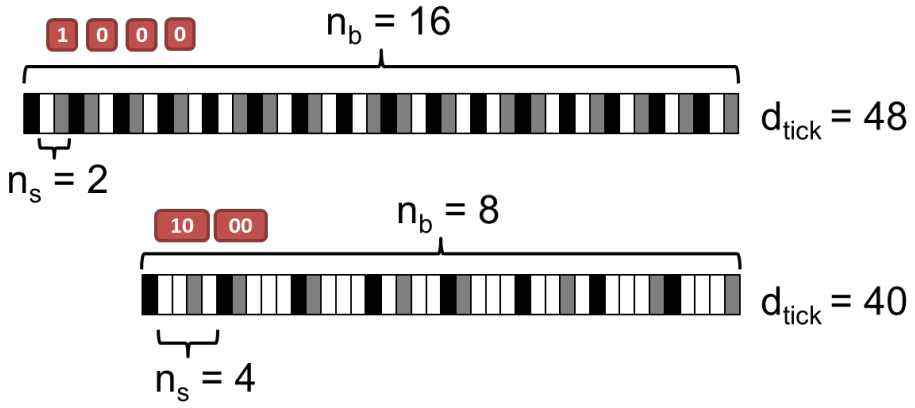

Figure 3.5: Different ways to code a WuRx address in TicK.

Theoretically, employing smaller t_{slot} values enables lowering the overall delay of TicK. A

t_{slot} of 1 ms is considered in the evaluations, which implies a bitrate of 1 kbps, a reasonable value for WuRx purposes and easily manageable by a low-power MCU. In fact, the time slot duration can be reduced up to the time needed to serve the ISR (t_{ISR}). In evaluations, a t_{ISR} = 100 µs is used. This value is calculated by multiplying the number of assembler language instructions of the ISR by 6. These values correspond to the maximum CPU cycles a single instruction can last in the MSP430G2452 and to the Instruction Cycle Time value in the MCU's datasheet [32], respectively.

The Very Low-power Oscillator (VLO) used by the MSP430G2452 to feed the timer in LPM3 consumes only 0.4 µA. The VLO can be considered a trustworthy clock source as long as it does not suffer significant voltage or temperature changes. According to the MSP430G2452 datasheet, the VLO frequency temperature drift is 0.5%/°C. In the experiments performed, no large clock drifts are observed by empirical tests.

3.4 Theoretical Analysis of the Addressing Approaches

This section presents performance analysis for each of the presented WuRx addressing strategies. The formulas for the required current consumption for each case consider both common and particular sets of parameters. The definitions of these parameters are provided in Table 3.1. The *scope* column indicates which approach the parameter applies to.

Name	Value	Scope	Description
I_{WuRx}	0.89 µA	MCU, TicK	CC of WuRx
I_{LPM4}	0.1 µA	MCU, TicK	CC of MCU, LPM4
I_{LPM3}	0.5 µA	MCU, TicK	CC of MCU, LPM3
I_{act}	400 µA	MCU, TicK	CC MCU at 1 MHz
I_{act}	4000 µA	MCU, TicK	CC MCU at 16 MHz
I_l	2.8 µA	Correlator	CC of AS3933, sleeping
I_d	8.7 µA	Correlator	CC of AS3933, decoding
n_s	2 / 4 / 16	TicK	number of slots
n_b	16 / 8 / 4	TicK	number of blocks
t_{slot}	1 ms	TicK	time slot duration
t_{ISR}	0.1 ms	TicK	time to serve interrupt
d_{MCU}	20 ms	MCU	Addressing duration
d_{Corr}	40 ms	Correlator	Addressing duration
d_{TicK}	48 / 60 / 68 ms	TicK	Addressing duration

Table 3.1: Operational parameters for the MCU-decoding, correlator and TicK addressing approaches.

The TicK approach allows significant energy savings, since nodes are in LPMs most of the time. While in LPM4, the node just dissipates the current resulting from the wake-up radio receiver circuitry (I_{WuRx}) and the MCU's lowest power mode (I_{LPM4}). For the TicK and MCU-decoding addressing tests, the WuR system from chapter 2 is used.

3.4.1 WuRx Addressing Through TicK

To better understand the current consumption of the TicK approach, it is useful to define two variables; one representing the current consumption per block for the decoding period (α), and one representing the current consumption during the sleep period (β). The current section 3.4 considers the current consumption of a TicK node in case of a correct address. Section 3.5, in turn, also contemplates the case of nodes which are not the intended receivers. This is the case of nodes detecting WuC addressed to other nodes or false addressing initiation procedures due to interference, noise, etc.

Figure 3.6 details the TicK operation within a block decoding. As seen in the figure, each block includes two WuCs, that will result in two ISR executions with active MCU current consumption, i.e., $2t_{ISR}I_{act}$. After the reference WuC, the MCU enters LPM3 mode on average for $(t_{slot} - t_{ISR}) + \frac{(n_s-1)}{2}t_{slot}$ duration, since the first slot represents the reference WuC and, based on uniformly random address value distributions, nodes will be in LPM3 mode for half of the rest of the block duration $(n_s - 1)t_{slot}$, and in LPM4 for the other half of it. Then, the average current consumption per block, α, can be expressed as:

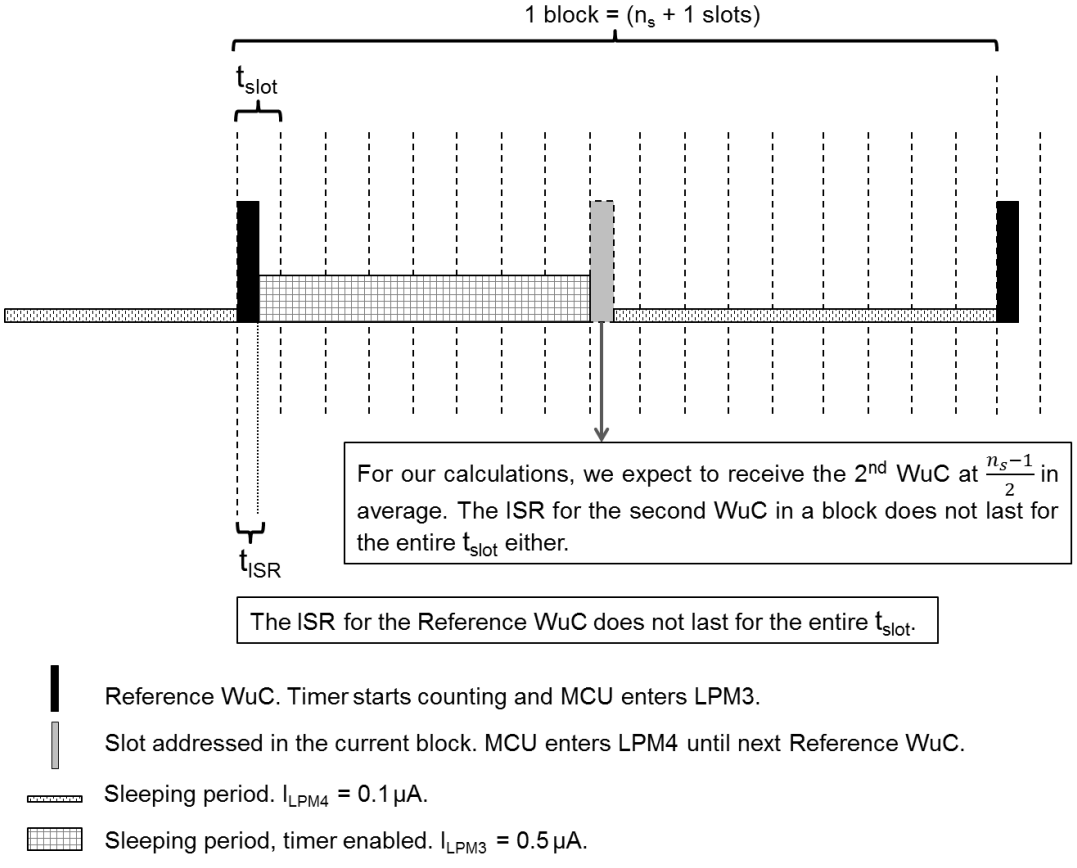

Figure 3.6: Detailed TicK operation within a time block.

$$\alpha = 2t_{ISR}I_{act} + \left[\frac{(n_s+1)t_{slot} - 2t_{ISR}}{2}\right](I_{LPM4} + I_{LPM3}) \tag{3.1}$$

For β, which represents the current consumption of a wake-up period while the node is not involved in addressing, the average current consumption is based on the frequency of WuC arrivals. Let T be the interarrival time of addressing initiations. Then,

$$\beta = [T - n_b(n_s + 1)t_{slot}]\, I_{LPM4} \tag{3.2}$$

Finally, considering the n_b blocks of a complete address along with the continuous current dissipation of the WuRx hardware, the overall average current consumption per time unit in TicK ($\overline{I}_{TicK}$) can be written as:

$$\overline{I}_{TicK} = \frac{n_b\alpha + \beta}{T} + I_{WuRx} \tag{3.3}$$

3.4.2 WuRx Addressing through MCU-decoding

There are several recommendations for energy-efficient MCU operation, as introduced in chapter 1. Some of these recommendations consist in employing interrupts to wake the processor and control program flow, properly configuring unused GPIO as output to prevent current consumption due to floating pins, and avoiding function calls. These recommendations are applied for both MCU-decoding and TicK approaches analyzed in this chapter.

The MSP430G2452 MCU has an adjustable frequency range between 1 MHz and 16 MHz. Although for WuRx addressing purposes it is more power-efficient to use the lowest frequency possible, calculations are provided for both MCU frequency values of 1 MHz and 16 MHz, to contemplate the cases where is not possible to reduce the MCU's frequency.

In WuRx addressing through MCU-decoding, a WuC duration d_{MCU} of 20 ms is considered as the result of adding the preamble `1110` before transmitting the 16 bits of the WuC. A bit duration t_{slot} of 1 ms is considered. When the WuC is transmitted, the one-to-zero transition at the end of the preamble acts as a falling edge at the WuRx, which triggers the interrupt for the MCU to start decoding the address.

For $(T - d_{MCU})$ time, the overall current consumption will be $I_{LPM4}+I_{WuRx}$, since the MCU is in LPM4 mode and the WuRx always on. However, during the address decoding duration the overall current consumption is $I_{act} + I_{WuRx}$. Then, the average current consumption of this MCU-decoding WuRx addressing approach is found to be:

$$\overline{I}_{MCU} = (I_{LPM4} + I_{WuRx})\frac{(T - d)}{T} + (I_{act} + I_{WuRx})\frac{d}{T} \tag{3.4}$$

First part of Equation 3.4 pertains to the sleeping period of the MCU and lasts for all the time the MCU is not decoding any address. During this period, the presented current consumption is the result of adding the one of the WuRx to the one of the MCU in LPM4. The second part of the formula relates the current consumption in active mode ($I_{act} + I_{WuRx}$)

and duration of the WuC. Both elements are divided by T in order to distribute the value along a WuC period.

3.4.3 WuRx Addressing through Correlation

For the performance evaluation of the addressing through correlation scheme, the AS3933 analyzed in chapter 2, section 2.3.2 is considered.

The correlator approach requires no MCU for address resolution. As for Equations 3.3 and 3.4, two stages of operation take place for address decoding: 1) *Listening*, where the WuRx waits for a carrier burst, which would be analogous to the LPM4 stage for MCU-based cases, and 2) *Decoding*, where after the carrier burst the preamble and address resolution starts. The current consumption of both stages is indicated by I_l and I_d, respectively. Thus, the average current consumption for the correlator approach can be derived in a similar manner as previously but considering a different WuC duration, d_{Corr}:

$$\overline{I}_{Corr} = I_d \frac{(T - d_{Corr})}{T} + I_l \frac{d_{Corr}}{T}. \tag{3.5}$$

3.5 Performance Comparison of the Addressing Approaches

Precise current consumption results can be obtained for each addressing method by applying the values of Table 3.1 to Equations 3.3, 3.4, 3.5. Values in Table 3.1 are obtained by laboratory measurements.

For the performance evaluation, different addressing interarrival times, T, are considered, ranging from 1 second to 1 minute. These interarrival times model frequent communications or frequent false addressing initiations due to interference or noise. Having an energy-efficient addressing mechanism becomes more important as the number of devices in a WuC range increases. In such cases, an addressing mechanism that manages the false WuCs rapidly and in a low-power manner is crucial. In the evaluations, a 16 bit addressing is considered, as it is the default configuration of the AS3933 WuRx. As illustrated in Figures 3.4 and 3.5, TicK enables three (n_s, n_b) value tuples: (2, 16), (4, 8), and (16, 4) for this address length.

The average current consumption values of TicK for the three (n_s, n_b) value alternatives are calculated by using Equation 3.3 and plotted in Figure 3.7. As seen in the figure, the choice of the (n_s, n_b) values is crucial for the overall performance, although they also result in different addressing durations, d_{tick}, as shown in Table 3.1. Specifically, for the 16 bit addressing in TicK, the best current consumption results are obtained for the tuple (16, 4).

For a MSP430G2452 MCU implementing TicK as in Figure 3.7, a 16 MHz operational frequency requires 10 times more current consumption than at 1 MHz. Obviously, the MCU frequency also drastically affects the MCU-decoding approach, where the WuC is entirely decoded by MCU. In the AS3933 case, among the possible configurations considering different

values for carrier frequency, the bit duration, and the preamble length indicated in the AS3933 datasheet [24], the default d_{Corr} duration is used, which is found to be around 40 ms. Calculations contemplate the most optimistic current consumption value when decoding, I_d, which is stated to be around 8.7 µA. Applying the maximum value in the datasheet (12 µA) would result in higher overall current consumption of this WuRx addressing approach.

Figure 3.8 depicts the relationship between the addressing interarrival time, T, and the maximum battery lifetime for the three approaches, considering the average current consumption values from (3.3)-(3.5) and a CR2032 230 mAh cell coin battery. In Figure 3.8, the most energy-demanding approach is MCU-decoding at 16 MHz. Note that this approach performs

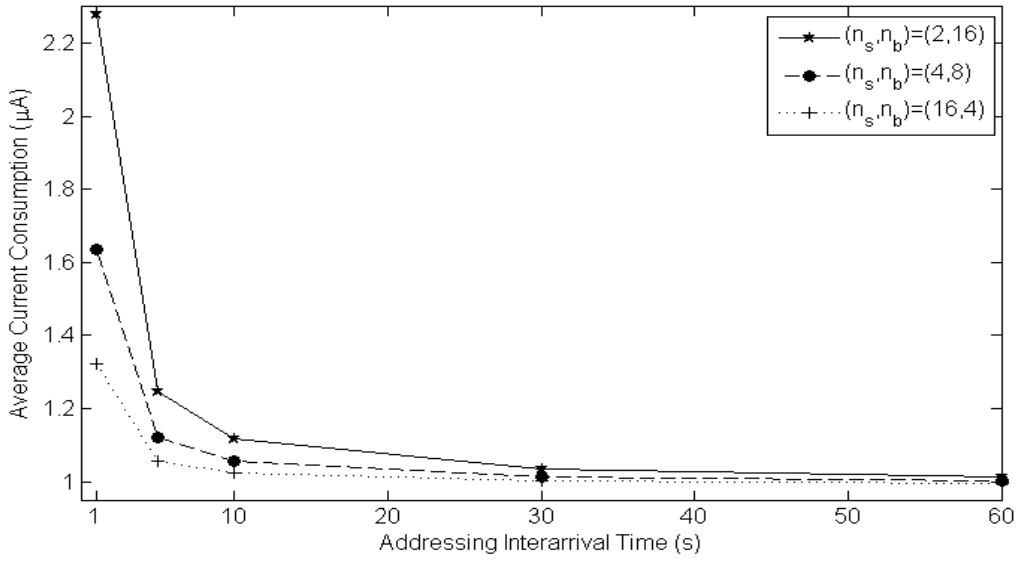

(a)

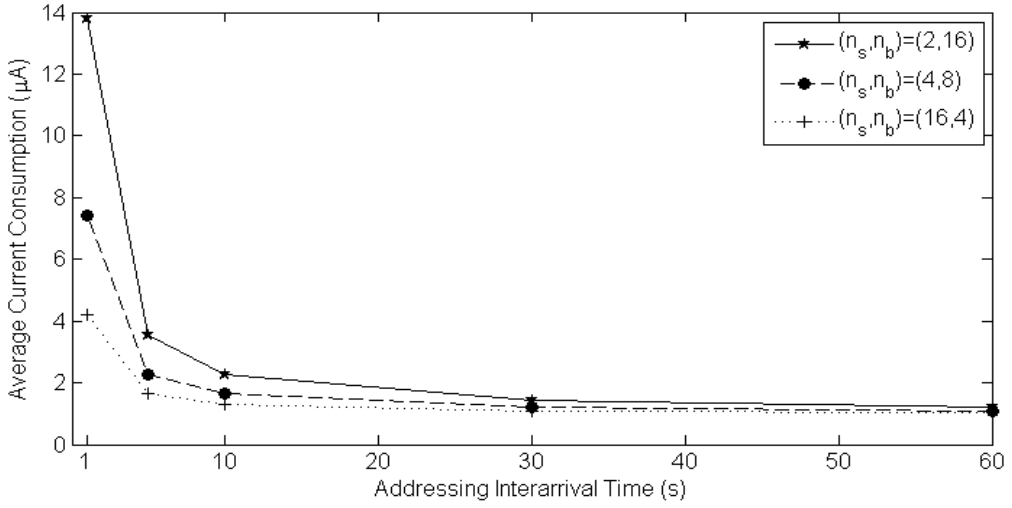

(b)

Figure 3.7: Average current consumption of TicK for different (n_s, n_b) tuples for 16 bit addressing, with MCU frequency of (a) 1 MHz and (b) 16 MHz.

the worst because of the MCU requiring more than 4 mA in active mode at this frequency. Indeed, reducing the intervention of the MCU in such mode as much as possible, as in TicK, improves the overall current consumption. In turn, the AS3933 WuRx presents a very constant current consumption result. Since the current consumption values when sleeping, I_l, and when decoding, I_d, are of the same order of magnitude, there is no big difference for different period values. The approach providing longer battery lifetime is TicK at 1 MHz, showing values close to 25 years even with addressing interarrival times, T, of 10 seconds, practically doubling the performance of the other approaches. TicK at 16 MHz follows as the next most energy efficient configuration.

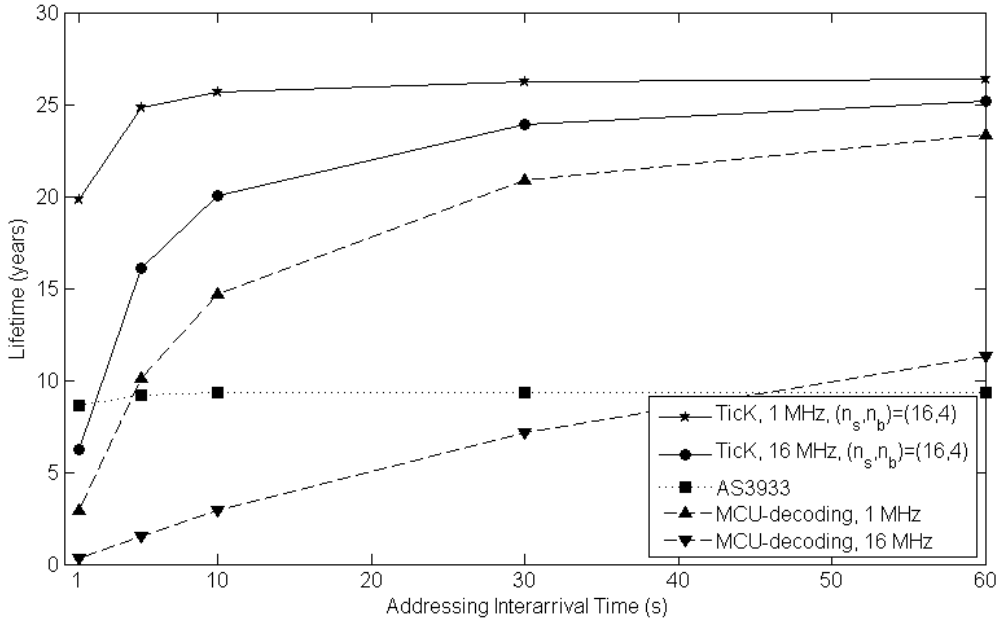

Figure 3.8: Battery lifetime of the three WuRx addressing approaches vs. interarrival times.

Figure 3.9 shows another set of evaluations performed for scenarios where several WuRx-equipped nodes are present and woken up one by one. Such approach corresponds to polling-style data collection and is common. In the case of TicK, all nodes within the WuC range are activated at the beginning of an addressing. Afterwards, they return immediately to sleep as soon as they detect a block with a WuC that does not correspond to their address. Then, the current consumption of the n nodes have the following consumption values and probabilities, depending on how long a node is being addressed; if a node is the intended one, $\overline{I}_{TicK}$, as given in Equation 3.3, is required. An unintended node, on the other hand, has a probability in Equation 3.6 of having the first $k-1$ address block's address bits in common with the node being addressed, and of having a different address at the kth block. Up until the kth block, the average current consumption per block is α as formulated in Equation 3.1, and the unintended node sets its timer until the end of the addressing, i.e., for $n_b - k$ blocks and disables its interrupt pin.

$$P(k) = \frac{1}{{n_s}^{k-1}} \frac{n_s - 1}{n_s} \tag{3.6}$$

Then, for n = number of nodes, the total current consumption can be expressed as:

$$\overline{I}_{TicK_n} = \overline{I}_{TicK} + (n-1) I_{WuRx} + (n-1) \times \sum_{k=1}^{k=n_b} \left[\frac{n_s - 1}{n_s^k} \left(\frac{(k-1)\alpha + \alpha' + (n_b - k)(n_s + 1) t_{slot} I_{LPM3}}{T} \right) \right]$$

where α' is the average current consumption for an unintended node within the block, the address bits of which are recognized to differ with the intended node. For the sake of brevity, this value is approximated with α.

Differently to TicK, both the MCU and AS3933 decoding approaches have to decode the entire address to decide whether a WuC targets them, thus the current consumption their networks present upon WuC detection is simply a multiplication by the number of nodes. Figure 3.9 depicts the network's total current consumption of the three approaches, with TicK showing the most benefit. It can be clearly seen that when the number of nodes in a network increases, employing a quick node-discarding address resolution scheme such as TicK is crucial to save as much energy as possible.

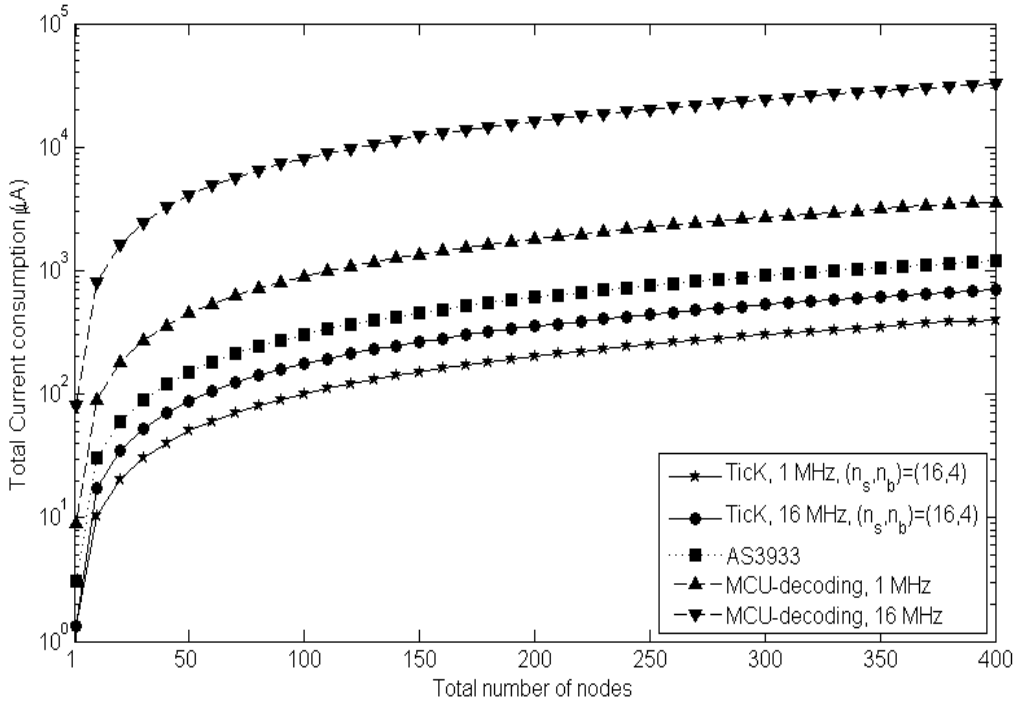

Figure 3.9: Total current consumption featured by the three WuRx addressing approaches for a varying number of nodes (T = 1000 ms).

3.6 TicK Source Code

Provided next is the TicK source code for a MSP430G2452 MCU. This code equips the SµA-WuRx in chapter 2 with an addressing mechanism.

```
// #includes contain names for registers, constants, etc.
#include <msp430g2452.h>
#include <stdint.h>

// MSP430 GPIO pins
#define BUTTON  BIT3
#define LED1    BIT6
#define LED0    BIT0
#define WURX    BIT4

// WuRx constants
#define STARTING_SIGNAL     0
#define ENDING_SIGNAL       1
#define MAX_INDEX_WUC       10
#define WUC_LENGTH          3
#define MY_WURX_ADDRESS     15
#define ADDRESS_PRECISION   2
#define INTERRUPT_FACTOR    1
#define WURX_TIMEOUT        MY_WURX_ADDRESS * 10
#define ENABLE_TIMEOUT      WUC_LENGTH + 2

// debug things
#define DEBUG_WURX

// WuRx variables
volatile uint16_t miliseconds = 0;
volatile uint8_t  WuRx_phase = STARTING_SIGNAL;
#ifdef DEBUG_WURX
volatile uint8_t  index_chain = 0;
volatile uint16_t chain[MAX_INDEX_WUC];
#endif


// main code, all based in interrupts
int main(void)
{
    WDTCTL = WDTPW + WDTHOLD;   // Stop watchdog timer

    // GPIO pins most energy saving configuration
    P1DIR = 0xFF;               // All P1.x outputs
    P1OUT = 0;                  // All P1.x reset
    P2DIR = 0xFF;               // All P2.x outputs
```

```
43      P2OUT = 0;                    // All P2.x reset
44
45      // P1IES = 0xFF by default = 1, INT is high-to-low
46      // Set P1.0 and P1.1 to output direction
47      P1DIR |= (LED0 + LED1);
48      P1DIR &= ~(BUTTON + WURX);  // launchpad: P1.3, P1.4 are inputs
49      P1OUT &= ~(LED0 + LED1);    // set LEDs to OFF
50      P1IFG &= ~WURX;             // WuRx IFG cleared
51      P1IE  |= WURX;              // WuRx interrupt enabled
52
53      BCSCTL1 = CALBC1_1MHZ;      // set core @ 1 MHz
54      DCOCTL = CALDCO_1MHZ;
55      // LFXT1 source: LFXT1S0 for 32KHz crystal, LFXT1S1 for VLO
56      BCSCTL3 |= LFXT1S1;
57
58      // If timerA uses ACLK (12kHz) then, respectively, the periods for TACCR0↙
        ↳  = 11 & TACCR0 = 119 are 12000/(TACCR0+1) = 1000Hz or 1ms & 100Hz or 10↙
        ↳ ms
59      TACCR0 = (11 * INTERRUPT_FACTOR) + 9 * (INTERRUPT_FACTOR / 10);
60
61      // enable int for CCR0, timer in ACLK, counter mode, clear timer
62      TACCTL0 = CCIE;
63      TACTL = TASSEL_1 + MC_1 + TACLR;
64
65      // Enter LPM4 & configure to leave it by interrupt, timer is OFF
66      _BIS_SR(LPM4_bits + GIE);
67  }
68
69
70  // Port 1 interrupt service routine
71  #pragma vector=PORT1_VECTOR
72  __interrupt void Port_1_ISR(void) {
73      // check if we have captured whole WUC
74      if (WuRx_phase == ENDING_SIGNAL) {
75          // recollect address = milliseconds and put to chain
76  #ifdef DEBUG_WURX
77          chain[index_chain] = miliseconds;
78          index_chain = (index_chain + 1 );
79          if (index_chain == MAX_INDEX_WUC) index_chain = 0;
80  #endif
81          // check address
82          if ((miliseconds <= MY_WURX_ADDRESS + ADDRESS_PRECISION) && (↙
        ↳ miliseconds >= MY_WURX_ADDRESS - ADDRESS_PRECISION)) {
83              P1OUT |= (LED0 + LED1);
84              // blink for one second
85              __delay_cycles(100000);
86              P1OUT &= ~(LED0 + LED1);
87          }
```

```
88      }
89      // for the next WuC
90      miliseconds = 0;
91
92      // disable meanwhile the GPIO INT sources
93      P1IFG &= ~(BUTTON + WURX);
94      P1IE   &= ~(BUTTON + WURX);
95
96      // pass to LPM3, we need OSC for next block
97      _BIC_SR_IRQ(LPM4_bits + GIE);
98      _BIS_SR_IRQ(LPM3_bits + GIE);
99  }
100
101
102 // Timer A interrupt service routine
103 #pragma vector=TIMER0_A0_VECTOR
104 __interrupt void CCR0_ISR(void) {
105     // we only use CCIFG, no need to diff between TAIFG and CCIFG
106     miliseconds += INTERRUPT_FACTOR;
107     if(miliseconds == ENABLE_TIMEOUT) {
108         // clear just-in-case and reenable INT
109         P1IFG &= ~(BUTTON + WURX);
110         P1IE |= (BUTTON + WURX);
111
112         // after the second WUC, pass to LPM4, no need for OSC
113         if (WuRx_phase == ENDING_SIGNAL) {
114             _BIC_SR_IRQ(LPM3_bits + GIE);
115             _BIS_SR_IRQ(LPM4_bits + GIE);
116         }
117
118         // next step
119         WuRx_phase ^= 1;
120     }
121     else if (miliseconds == (WURX_TIMEOUT)) {
122         // wake-up timeout!
123         WuRx_phase = STARTING_SIGNAL;
124         P1OUT &= ~(LED0 + LED1);
125     }
126 }
127
128 #pragma vector=PORT2_VECTOR, WDT_VECTOR, ADC10_VECTOR, COMPARATORA_VECTOR, \
129     NMI_VECTOR, TIMER0_A1_VECTOR, USI_VECTOR
130 __interrupt void ISR_trap(void)
131 {
132     WDTCTL = 0; // this means an access violation and a PUC reset
133 }
```

Code 3.2: TicK source code for the MSP430G2452 MCU.

3.7 Conclusions

Wake-up radio is a promising energy-efficient rendezvous method for wireless networks. However, for the energy efficiency of such approaches, all related operations, including the address decoding for WuRx, should also be energy-efficient due to the very limited power source in devices such as wireless sensors or actuators.

The so-called Time-Knocking approach enables energy efficient addressing by varying the sleep duration of MCUs through WuC to encode the address. In this chapter, the current consumption results of TicK are compared against two common addressing methods: MCU-decoding and correlator-based addressing. For all three methods, current consumption formulas are derived and evaluated using realistic system parameter values. The results show that TicK achieves much better current consumption values compared to the two other methods, while slightly sacrificing delay from the duration of addressing. TicK also enables variable length addresses, which can be used for temporary or local address assignments, and supports multicast or group-based wake-up inherently and in a very energy-efficient way because of addresses in TicK being encoded in a progressive manner. Moreover, address mismatches in TicK are determined without waiting for the end of addressing, hence surrounding non-intended nodes can go to sleep mode quickly. Evaluations in this chapter also contemplate scenarios comprising multiple nodes, where only one node is addressed but the WuC reaches the rest of the nodes, too. Such scenarios show the current consumption advantage of TicK even more significantly.

TicK allows employing a panoply of different hardware at WuTx and WuRx and is also implementable in many MCU and WuRx combinations. However, TicK being a PPM-based strategy makes it vulnerable to interferences, even if address mismatching is quickly detected by TicK. The problem of interferences gets worse as the sensitivity of the WuRx employed in TicK gets better, since more range means more false WuC triggering taking place. In addition, despite its versatility, TicK is designed with the WuTx and WuRx prototypes from chapter 2 in mind. Unfortunately, there are applications where a large antenna is not suitable and boards should be considered as designed as equal peer entities. Finally, longer ranges that the ones providing by designs in chapter 2 would be desirable.

In order to address the previous issues, chapter 4 presents and analyzes a WuR design developed at the University of Freiburg. During a research partnership, Universitat Politècnica de Catalunya thoroughly analyzed such system's performance in terms of time and energy, implemented several energy harvesting prototypes, provided an extensive state-of-the-art to the community (chapter 5), developed the first WuR simulator (chapter 6) and finally successfully extended the WuR concept to new research areas, like being capable of shifting WuR systems to IEEE 802.11 areas in chapter 8.

4 Analysis & Performance Evaluation of SubCarrier Modulation Wake-up Radio Systems (SCM-WuR)

This chapter analyzes a novel wake-up radio approach that integrates both data communication and wake-up functionalities into one platform, providing a reconfigurable single-radio operation. This differs from other systems since most require one radio for data communications and one for WuR purposes. The WuR platform is analyzed in section 4.1 for the delay, current consumption and overall operational range metrics under different transmit power levels in section 4.2. Section 4.3 presents an actual single-hop WuR application scenario, as well as demonstrates the first true multi-hop capabilities of a WuR platform and simulates its performance in a multi-hop scenario. Finally, section 4.4 concludes the chapter.[1]

Contents

4.1 Introduction to SubCarrier Modulation Wake-up Radio Systems

In order to be suitable for different types of applications, a good WuR design must enable long operational ranges, require very low or no power, present a reproducible and low-cost hardware

[1] Chapters 4 and 5 are based on and extend the work contained in the following JCR Q1 (2013) publication: ≪J. Oller, I. Demirkol, J. Casademont, J. Paradells, G. U. Gamm, and L. Reindl, 'Performance Evaluation and Comparative Analysis of SubCarrier Modulation Wake-up Radio Systems for Energy-Efficient Wireless Sensor Networks', Sensors, vol. 14, no. 1, pp. 22-51, Dec. 2013.≫.

design and preferably operate in the Industrial, Scientific and Medical (ISM) frequency bands. The WuR design introduced in this chapter, so called SubCarrier Modulation Wake-up Radio (SCM-WuR) satisfies all these requirements and presents itself as one of the best systems in the literature as of 2014.

The SCM-WuR idea, first introduced in [25], uses the off-the-shelf LF AS3932 WuRx integrated circuit [24], which is a streamed version of the AS3933. The AS3932 is a low-power Amplitude Shift Keying (ASK) receiver capable of generating a wake-up interrupt upon detection of a 110 kHz to 150 kHz signal. This frequency range differs from the 15 kHz to 150 kHz one of the AS3933. Depending on the application, or the WuTx capabilities, the proper IC should be chosen. Theoretically, the SCM-WuR system in this chapter could be implemented in any of both integrated circuits. However, the AS3933 is more expensive.

The SCM-WuR system design, illustrated in Figure 4.1a, allows switching between two radio modes that differ in their modulation schemes in order to implement both data and wake-up functionality in a single platform. In *wake-up mode*, the WuRx detects the envelope of the 868 MHz WuC signal sent by a remote WuTx, which results in the underlying raw LF signal expected by the AS3932 chip. This LF signal corresponds exactly to the one expected by AS3933 in Chapters 2 and 3. The AS3932 integrated circuit only requires a few µA of current to decode this LF signal. Afterwards, in *data mode*, an antenna switch is employed to bypass the AS3932 and communication is managed directly by the 868 MHz radio transceiver.

To incorporate the AS3932 into the SCM-WuR approach, it is important to clearly understand how its working principles fit in the SCM-WuRx design. The AS3932 can operate at a frequency of 125 kHz, and is usually employed as WuRx in short-range applications such as remote key locks, or automotive-related applications such as Tire Pressure Monitoring sensors. The block diagram of AS3932 WuRx board from the manufacturer's demokit is shown in Figure 4.1b, where the chip is connected to three input coil antennas that enable reception independent of the node's orientation, in the same manner as the AS3933 in Chapters 2 and 3. In such configuration, the AS3932 in the manufacturer's demokit consumes 8.3 µA. In turn, the corresponding WuTx requires up to +33 dBm, because of WuR communication relying not on electric but on magnetic coupling. Unfortunately, such RFID-like approach results in limited WuC detection distances of 5 m [4], as shown for the AS3933 in chapter 2, section 2.3.2.2 and requires up to 0.8 A.

In the SCM-WuR approach in Figure 4.1a, nodes differently route WuC and data communications by means of an antenna switch. This is needed because all RF transmissions, WuC and data, are performed at 868 MHz. Instead, the approach in Figure 4.1b detects WuC by magnetic coupling.

The SCM-WuR design in Figure 4.1a reuses in an effective way the characteristics of the AS3932 integrated circuit, and deploys an 868 MHz +2 dBi gain omnidirectional antenna instead of the three coil antennas of Figure 4.1b. By disabling two RF paths and the channel selector in Figure 4.1b, the current consumption of the AS3932 in Figure 4.1a is reduced from

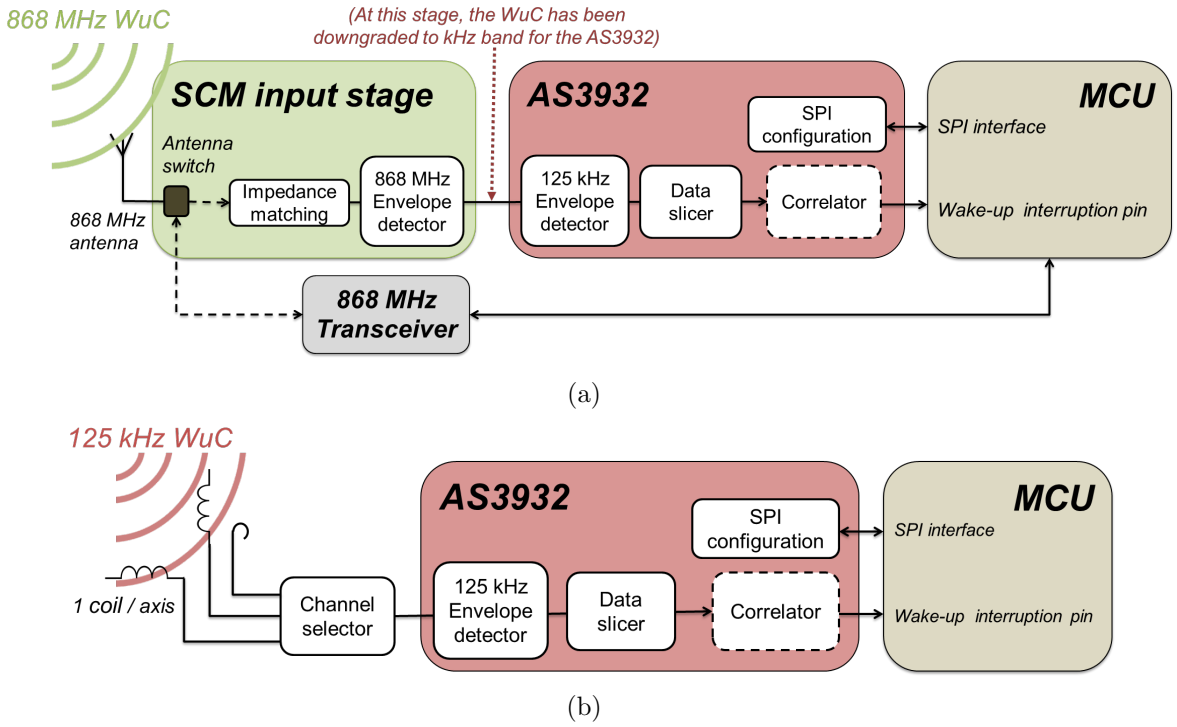

Figure 4.1: (a) Block diagram of the SCM-WuRx/WuTx. (b) Block diagram of the Austria MicroSystems AS3932 WuRx demoboard.

8.3 µA down to 2.6 µA. After the WuC reaching the antenna in Figure 4.1a, an external envelope detector demodulates the 868 MHz WuC to extract the 125 kHz signal. Afterwards, the integrated 125 kHz envelope detector of the AS3932 extracts the original data from the 125 kHz carrier as in the case in Figure 4.1b.

Thus, from the signal processing point of view, a double modulation strategy (also called SubCarrier Modulation or SCM) is used to wake-up a WuRx; the WuC is modulated in OOK resembling a 125 kHz signal, where as a carrier, and each cycle of this 125 kHz signal is modulated in OOK using an 868 MHz signal as a subcarrier. That is, to send each bit of information of the WuC, the MCU of the WuTx shapes a continuous RF wave at 868 MHz generated by a Texas Instruments CC1101 transceiver [33]. To transmit a bit value of '1', the CC1101 outputs the bit sequence of `1010` ... at 250 kbps, which appears as a 125 kHz signal after the envelope detector at the receiver. Each of these '1's is shaped using a modulated 868 MHz carrier (Figure 4.2). To transmit a '0', the CC1101 simply remains silent.

From the operational point of view, for a SCM-WuR node in sleep mode the RF switch is set by the MCU to route the wireless signal either from the 868 MHz transceiver to the antenna, in the case of a WuTx generating a WuC, or from the antenna to the AS3932, in the case of WuRx. In traditional data communication mode, the antenna is left connected to the 868 MHz transceiver. When in data communication mode, the node may transmit typical wireless data frames containing measures from any sensors attached to any of the several GPIO of the MCU. As a power-efficient WuR design, the hardware boards designed for the

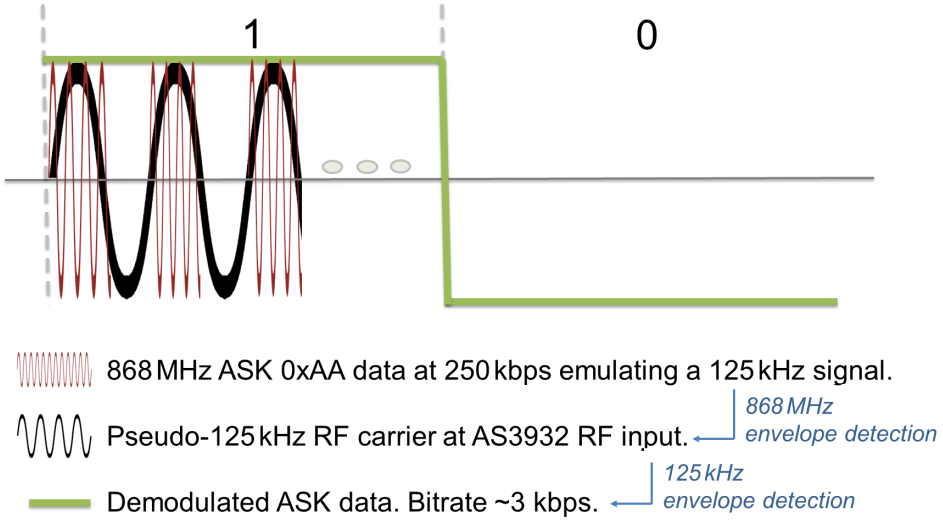

Figure 4.2: Bits of a WuC in a SCM-WuR system.

SCM-WuR system, shown in Figure 4.3, include a low-power MCU which enables the nodes to operate as either WuTx or WuRx. The CC1101 transceiver is in charge of both generating WuC and managing traditional data frames. In turn, the AS3932 receives the WuC. The node in the figure is powered by means of a simple coin cell battery with a capacity of 225 mAh (3 V).

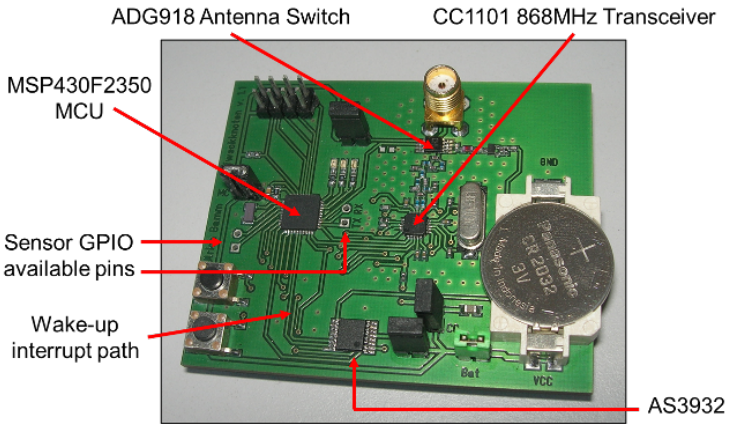

Figure 4.3: The SCM-WuR hardware board.

To ensure the validity of the SCM double modulation strategy, as well as to check the WuRx sensitivity, a signal generator is programmed to output an 125 kHz OOK modulation on a 868 MHz carrier, and connected directly to the WuRx board using a SMA cable. Down to a signal ouput level of -53 dBm of the signal generator, the Signal to Noise Ratio (SNR) lies in a range where the WuRx reliably detects the WuC. The idea behind the use of such double modulation for the WuC is to benefit from the reduced antenna size and better gain of sub-GHz frequency signals, and overcome the short operational range problem of the WuRx design in Figure 4.1b due to operating in the 125 kHz frequency band.

A good impedance matching stage is crucial for achieving the best possible sensitivity in WuRx designs. Following Figure 4.4 shows a non-optimized matching between the antenna, modeled as a load presenting an input impedance of Z_L = (R + Xj) = (20 - 40j)Ω, and the input WuC path, G = 50 Ω.

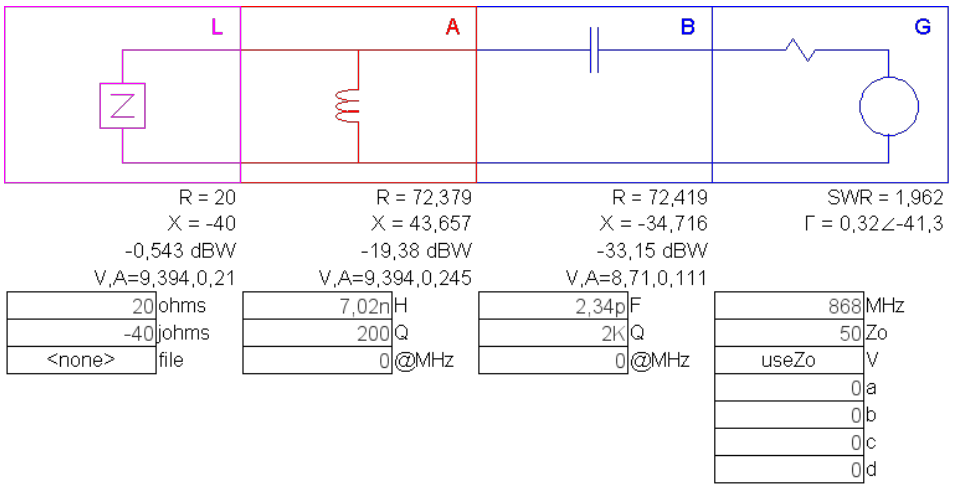

(a)

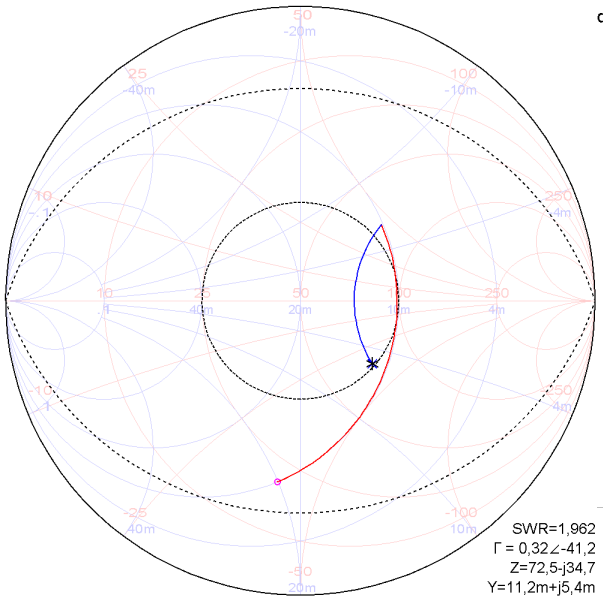

(b)

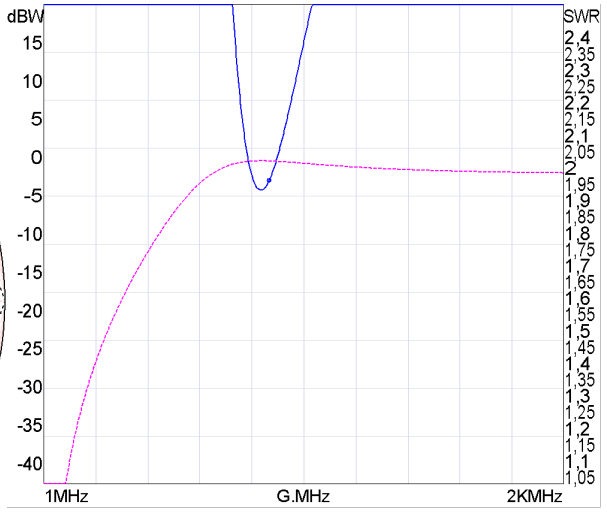

(c)

Figure 4.4: (a) L-matching network; (b) Smith Chart trajectories; (c) Dotted-line: power transferred. Flat line: VSWR.

The matching in Figure 4.4a could be perfectly valid for some applications. In fact, a Voltage Standing Wave Ratio (VSWR) ~ 2, as indicated in Figure 4.4c, represents a 11% of received power lost. However, for WuR applications, where operational ranges are critical compared to traditional applications, impedance adjustments may provide a huge difference. Instead, the matching in Figure 4.5 seems to provide optimum performance, with a VSWR

close to 1, which indicates perfect match and the consequent improved power transfer between Z_L and G, or between the antenna and the envelope detector in Figure 4.1a.

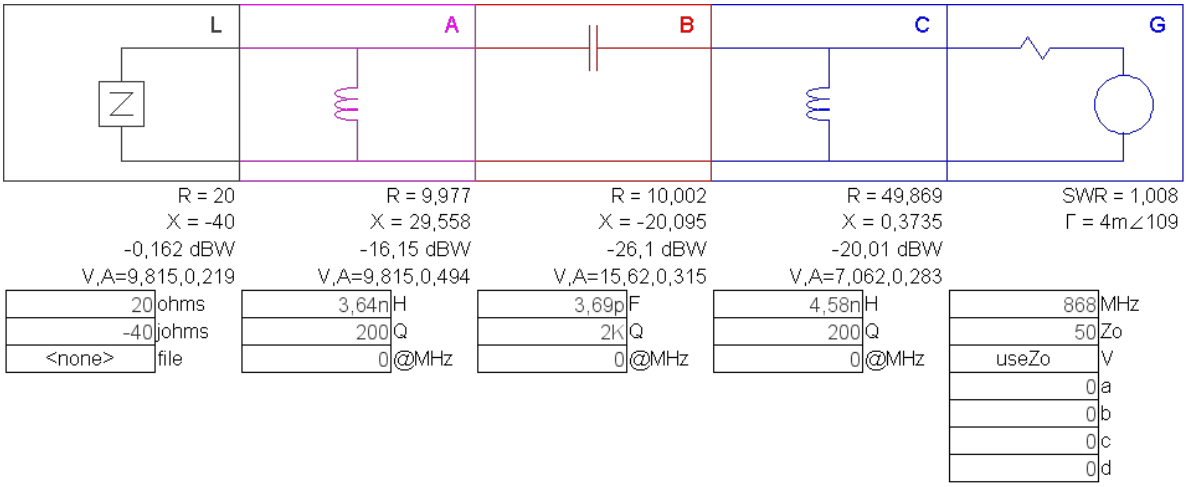

(a)

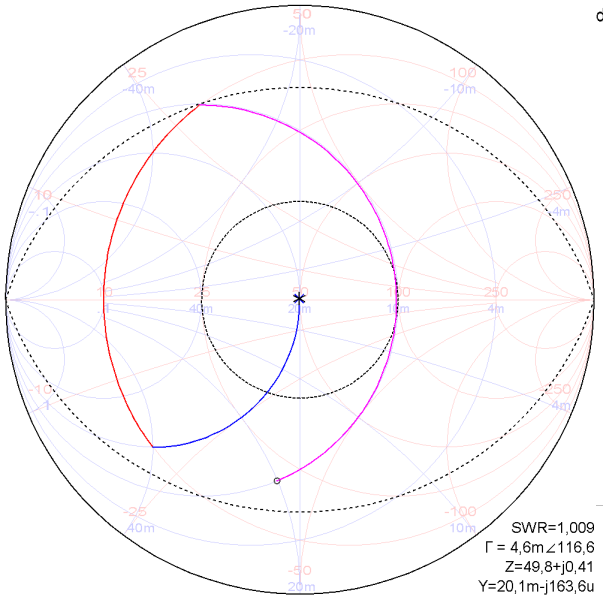

(b)

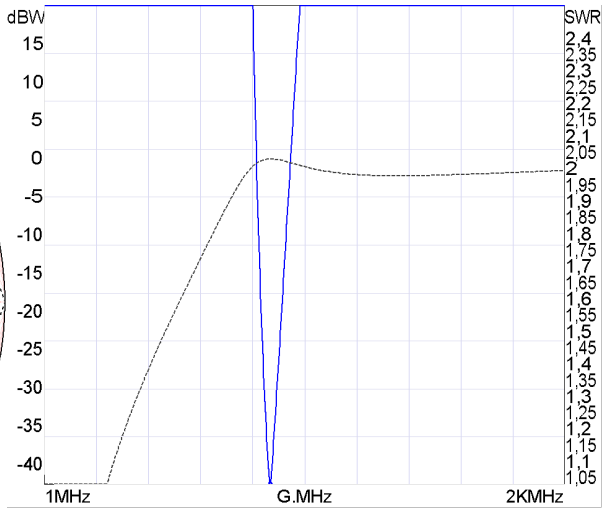

(c)

Figure 4.5: (a) π-matching network; (b) Smith Chart trajectories; (c) Dotted-line: power transferred. Flat line: VSWR.

The eye-shaped dotted line in the Smith Chart in Figure 4.5b delimits the Quality Factor, Q, of the circuit, expressed in Equation 4.1.

$$Q - factor = \frac{center\,frequency}{bandwidth} \tag{4.1}$$

Graphically, if the arcs built by the different trajectories in the Smith Charts are restricted in a small Q-eye, the WuRx presents wider band. L-networks as the one in Figure 4.4 do not

allow to adjust the Q of the circuit. π-networks as the one in Figure 4.5 allow for custom Q designs.

While simulations like the ones in Figures 4.4 and 4.5 are useful, the WuRx impedance matching can behave differently than expected if some design guidelines are not followed. For example, it is essential to have a proper ground plane when designing RF and to leave proper clearance in the RF trace.

In the developed SCM-WuR system, the last bits of the WuC contain the address of the intended receiver node. The AS3932 IC in the WuRx generates an interrupt only if the correlator matches the address in the WuC with the one set for that WuRx via SPI commands, as shown in chapter 3, Code 3.1. WuRx can either use unique address assignments or role-based assignments. For example, all router or relay devices can be assigned a specific role identifier. In a similar way, a WuC can be employed to activate only nodes attached to a particular sensor type, which can be humidity, fire, garbage, heart-rate, pressure, etc.

Interestingly, SCM-WuR can perfectly also be implemented without an AS3932 integrated circuit, since the main component it employs is an address correlator. Other WuRx proposals in the literature implement similar correlators by means of shift registers and parallel comparators. However, since the AS3932 already contains an efficient address correlator as well as a kHz envelope detector, this integrated circuit is conveniently reused and deployed in SCM-WuR boards for a high-performance and reproducible design. Another important feature of SCM-WuR is that, by deploying proper envelope detection stages in the RF input path, systems working at other frequencies such as 433 MHz or 2.4 GHz can be easily implemented, which makes the SCM-WuR design very flexible. A final advantage of the SCM-WuR is not requiring two separate wireless transceivers for data communication and for WuR, reducing the overall monetary cost of the system.

4.2 Performance Analysis of the SCM-WuR System

This section presents a complete performance analysis of the SCM-WuR system. The characterization is done for timing and wake-up delay analysis, current consumption of WuTx and WuRx boards at different communication stages, and operational distance ranges achieved for WuCs transmitted at different WuTx power levels.

4.2.1 Timing and Wake-Up Delay Analysis

In the SCM-WuRx, the AS3932 chip, found after the 868 MHz envelope detector, expects the WuC to be sent according to the format detailed in Figure 4.6. This format matches the one in chapter 3, Figure 3.3 for the AS3933 and is further detailed next. The WuC format consists of a carrier burst, a preamble containing several consecutive 0-1-0 bit transitions, a 16-bit address pattern and an optional data sequence. The data field allows two devices to exchange a small size data without leaving wake-up mode. If employed, such data reception requires

the MCU to monitor a pin labeled as DATA in the AS3932. Low-power pin monitoring can be done by means of energy-efficient strategies such as TicK [34] in chapter 3, which barely requires few µA on average.

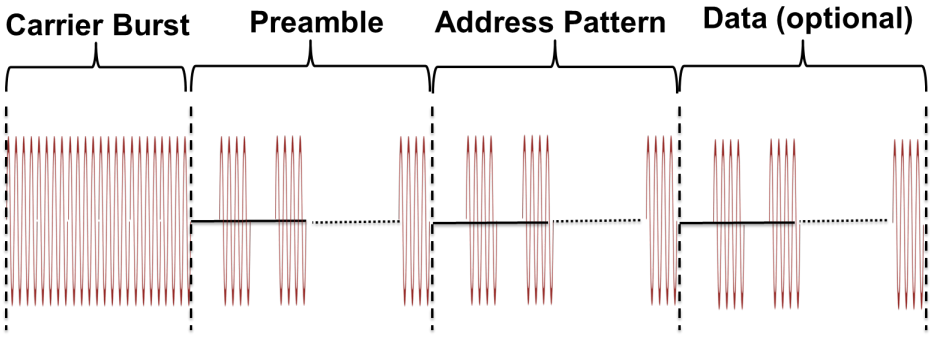

Figure 4.6: WuC format as in the AS393x datasheet.

The AS3932 generates a wake-up interrupt for the node's MCU only if the entire WuC protocol is fulfilled and the address pattern matches the node's address. Otherwise, the AS3932 can also be configured as a plain frequency detector to further reduce energy consumption if addressing is not needed or, again, if alternative energy-efficient wake-up addressing strategies such as TicK [34] are considered. In such frequency-detection case, only the carrier burst is needed. In the evaluations in this chapter, SCM-WuR boards are configured to use addressing but no trailing data.

In the SCM-WuR system, the WuC bit-rate can vary from 1024 bps to 8192 bps. Empirical evaluations show that WuCs sent at higher bit-rates than 2730 bps result in a challenging signal for the envelope detector and data slicer of the WuRx, which leads to both operational range and WuC detection rate decrease. At such bit-rate of 2730 bps, the transmission of a WuC is measured to last for 12 ms. In data communication, components are able to work at higher bit-rates than when used for WuR purposes. For example, the CC1101 is able to operate up to 600 kbps.

To quantify the total time required to activate an SCM-WuR board through a WuC, the total wake-up delay is measured by attaching one oscilloscope probe to the output of the WuTx and another to the GPIO wake-up input of the MCU. As shown in Figure 4.7, the wake-up delay is observed to be 13.08 ms, as a result of adding factors such as RF amplification settling time (250 µs) and the delay for the data slicer (366 µs) to the WuC duration.

4.2.2 Current Consumption Analysis

The power level at which a WuC is transmitted presents a trade-off between energy consumption at WuTx and the system's effective operational range. To quantify this trade-off, three different transmit power levels are tested, -10 dBm, 0 dBm and +10 dBm, for which the corresponding current consumption values are measured to be 13 mA, 14.4 mA and 19.1 mA,

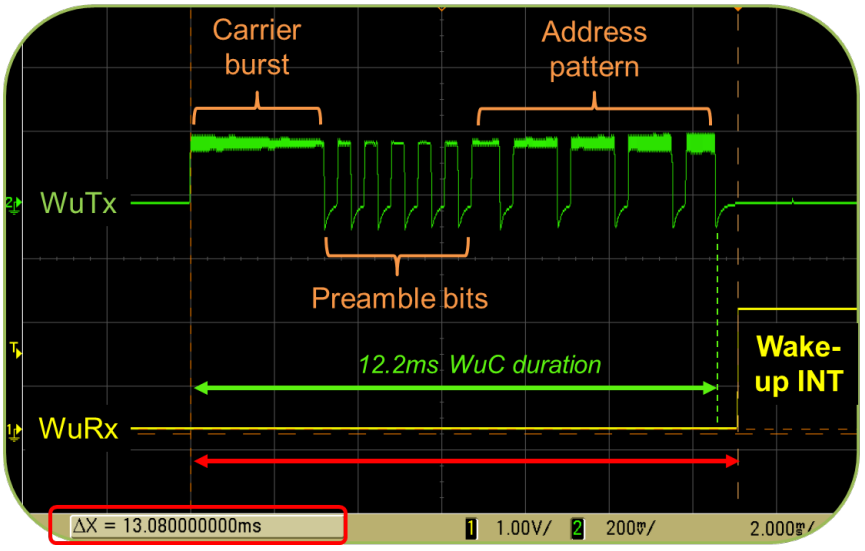

Figure 4.7: Incoming WuC from the SCM-WuTx and corresponding interrupt (INT) signal to the node's MCU in the receiving SCM-WuRx.

respectively. Considering the latter value, a WuTx employs a total of 0.68 mJ when transmitting a WuC and 0.23 mJ when transmitting one 100-bytes data packet.

Regarding the WuRx side, the CC1101 868 MHz transceiver is turned off in wake-up mode, while the antenna switch only requires a few nA, which is a negligible value compared to the current consumption levels in the µA order of the AS3932 chip (2.6 µA) and the MCU. The exact current consumption of the MCU depends on the LPM it is in. The MSP430F2350 MCU [35] employed in SCM-WuR boards can be configured to use LPM levels from 0 to 4. Different levels correspond to disabling/enabling the core, digital oscillators and different clock sources. As introduced in chapter 1, section 1.3, disabling all such elements enables reducing the current consumption of the MSP430 from 300 µA in 1 MHz active mode, to 0.1 µA when in its deepest sleep mode LPM4, where it can only be activated by an external interrupt on one of its configured GPIO pins. In sleep mode, the entire SCM-WuRx current consumption is ~2.7 µA. This value allows for up to 8 years of battery lifetime if considering a 230 mAh CR2032 cell coin battery.

An Agilent Technologies N6750A power analyzer is employed in Figure 4.8a to depict the stages of communication between WuTx and WuRx along the corresponding current consumption values experienced by SCM-WuR systems in detail. In the tests conducted, one SCM-WuR device is programmed to operate as WuRx. Upon reception of a WuC, it activates a LED for 100 ms and next switches from WuRx to WuTx mode role to send a WuC to a third node. As shown in Figure 4.8a, the WuRx in wake-up mode initially consumes as low as 2.7 µA (2.6 µA for the AS3932 + 0.1 µA for the MCU), since it is just waiting a possible incoming WuC carrier burst. When a carrier burst is detected, the WuRx starts decoding the address, which requires 8.8 µA. Comparatively, under duty-cycling schemes (e.g., IEEE 802.15.4, IEEE 802.11 or 3G/4G) the mobile device is periodically activated to check for a possible incoming

communication, requiring current consumption amounts in the order of mA, i.e., 1000 times higher than that of SCM-WuR. In Figure 4.8a, after the decoding of a matching address an interrupt is sent to the MCU and a signalling LED blinks for 100 ms. Then, the CC1101 is activated (240 µs, value not shown in the figure) and a new WuC is transmitted. Such WuC lasts 12 ms as in Figure 4.7 and requires 19.1 mA for an output power of +10 dBm. For further energy savings at the WuTx, and if the whole 16-bit addressable space is not required, the WuC duration value can be reduced by using node addresses ending with bit values of '0'.

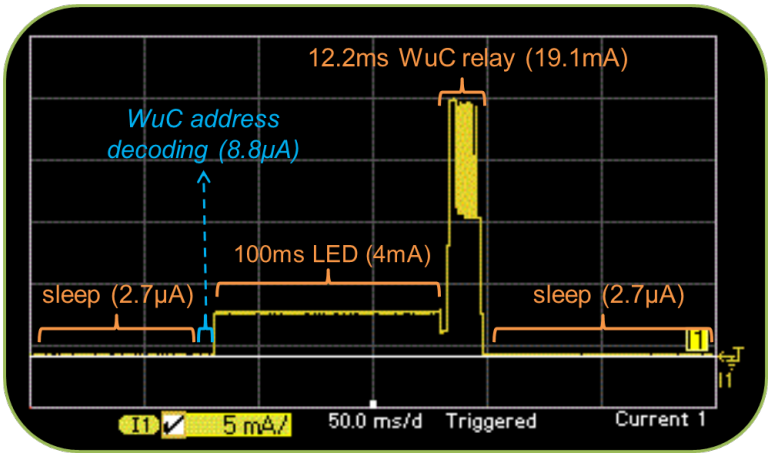

(a)

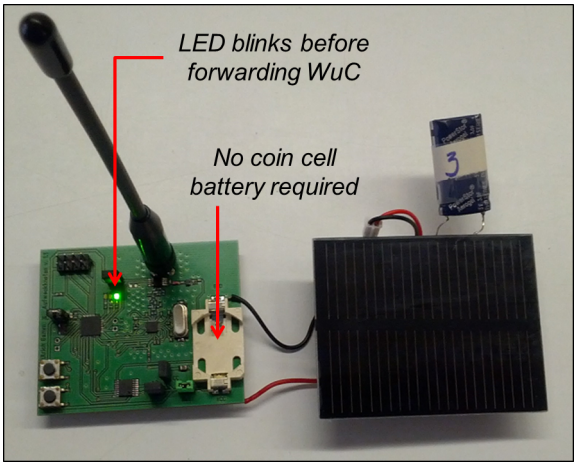

(b)

Figure 4.8: (a) Power analyzer trace of a SCM-WuR relay node; (b) Powering the relay SCM-WuR node by means of a solar cell and a supercapacitor.

The described application example represents a multi-hop wake-up through the use of SCM-WuR, which, to the best of the authors' knowledge, is being demonstrated in the literature for the first time in a real WuR hardware platform. A similar power profile is expectable for another type of application where a node sends back a transducer measure to a collector node originally sending the WuC.

The energy requirements of SCM-WuR nodes are so low that they can be easily powered by means of solar harvesting solutions. As a proof-of-concept, a novel functional prototype

implementing the WuR multi-hop procedure in Figure 4.8a is shown in Figure 4.8b.

4.2.3 Wake-Up Range Analysis

As in the case of the WuR system in chapter 2, a characterization of the operational distances achievable when employing different transmit power levels is essential to observe the trade-off between range and current consumption for the SCM-WuR system. This evaluation also enables devising adaptive transmitting power strategies for further energy efficiency.

In the test set-up of the wake-up range analysis, the WuTx is fixed at a coherent height of 1 m and the WuRx displaced vertically and horizontally relative to the WuTx, in steps of 40 cm and 50 cm, respectively. For the WuTx, three transmit power levels are evaluated: -10 dBm, 0 dBm and +10 dBm. In the evaluations, the WuRx is attached to a Bluetooth Low Energy (BLE) device. When the WuRx receives a WuC destined to it, it sends a wake-up interrupt to the input pin of the BLE device's 8051 MCU. Such MCU is programmed to stay in low-power mode when idle, and to generate a single BLE *Advertising frame* for every wake-up interrupt on its GPIO input pin. These BLE reply frames are detected over the air by the use of a BLE sniffer. Thus, in this scenario the main data communication and the wake-up communication are done in different frequency bands, i.e., it corresponds to an out-of-band WuR solution. If instead data frames are transmitted back by means of an integrated transceiver, such as the CC1101 in case of the SCM-WuR boards, the WuR solution is considered in-band.

The amount of sniffed BLE Advertising Frames matches the number of successfully decoded WuC. Based on this number, and analogously to the performance evaluations in chapter 2, three operational zones are defined in Figure 4.9. *Zone1* denotes a consistent reception of the WuCs and is represented by white color; *Zone2* denotes the zones with certain WuCs are detected, but reception is not 100% guaranteed and is represented by gray color; in *Zone3* the WuRx is not activated at all by any WuC, which is represented by black color.

As shown in Figure 4.9, the maximum operational distance achieved is approximately 41 m for a WuTx transmit power of +10 dBm, which is a significant improvement over the maximum range of most state-of-the-art WuR solutions, as thoroughly analyzed in the next chapter 5. For the other two tested transmit power levels of -10 dBm and 0 dBm, the maximum operational distances measured are 6 m and 24 m, respectively. A range of 6 m is adequate for several applications such as Wireless Body Area Networks (WBAN). By combining the patch antenna design in chapter 2 and a SCM-WuTx, about 100 m are observed at +10 dBm, which is among the best values in the literature.

Since the maximum allowed transmit power at the 868 MHz band is +27 dBm in Europe, the wake-up range of SCM-WuR can still be increased by using amplifiers such as the CC1190, with the counterpart of increasing energy consumption at the transmitter side. For a +20 dBm output power, more than 100 m range has been measured for SCM-WuR systems. Again, this operational wake-up range is among the longest ones in the literature for a WuRx current

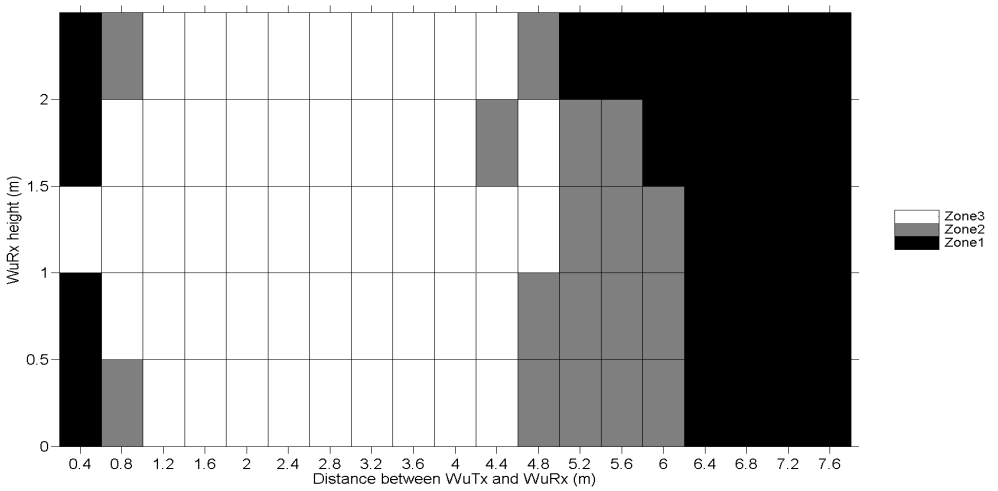

(a)

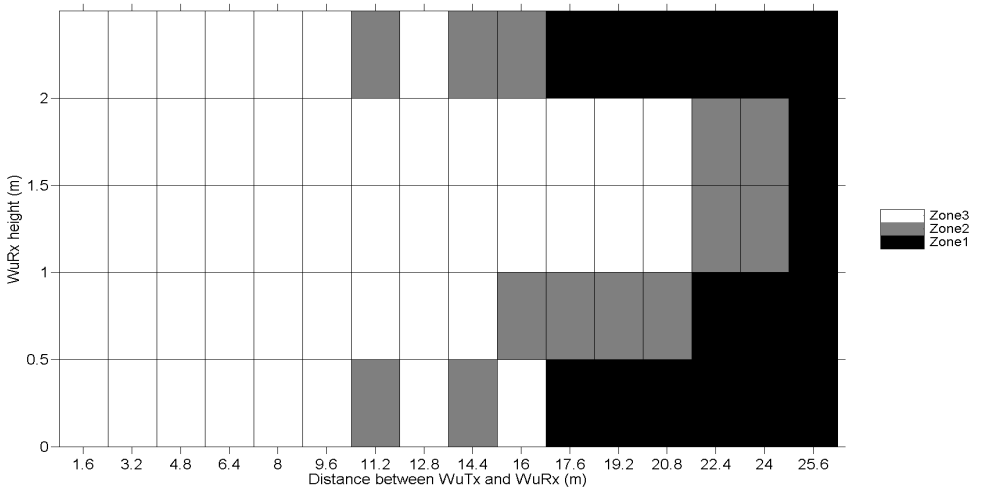

(b)

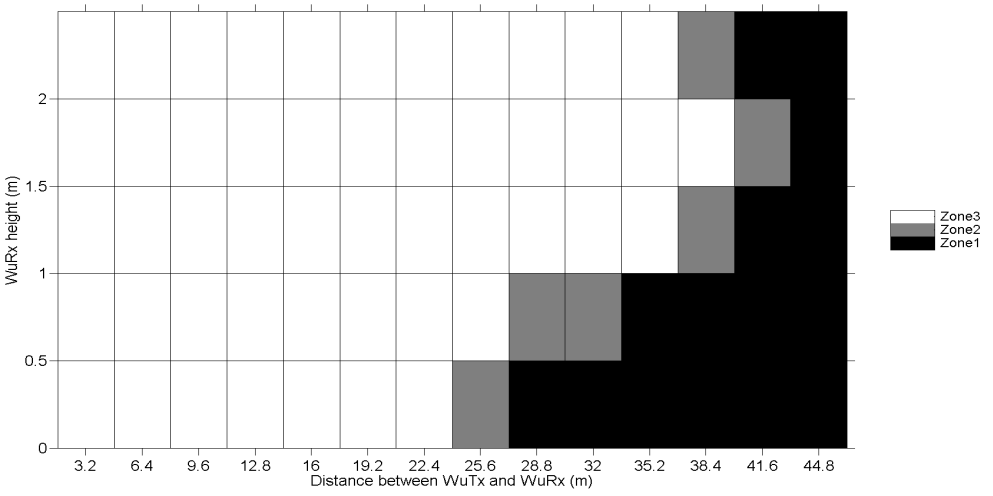

(c)

Figure 4.9: Wake-up distance evaluations for SCM-WuTx output power of (a) -10 dBm; (b) 0 dBm; and (c) +10 dBm.

consumption of few μA [36]. Choosing between the configuration comprising a power amplifier or one with a high-efficiency antenna depends on the application. The combination between the patch antenna and the amplifier-enabled WuTx has not been tested.

A Mathematica [37] simulation employing the values in Table 4.1 is conducted in order to compare the values featured by the SCM-WuRx to the maximum theoretical limits.

Parameter	Value
Frequency	868 MHz
WuTx Power	+10 dBm
WuRx Sensitivity	-53 dBm
WuTx Antenna gain	+2 dBi
WuRx Antenna gain	+2 dBi
WuTx Height	1 m
WuRx Height	1.25 m

Table 4.1: Parameters for the range simulation in Figure 4.10.

The results in Figure 4.10 show both the theoretical free-space Friis distance and the 2-ray ground reflection model for the described scenario. The dot in the figure depicts the WuRx real operational range results from Figure 4.9c.

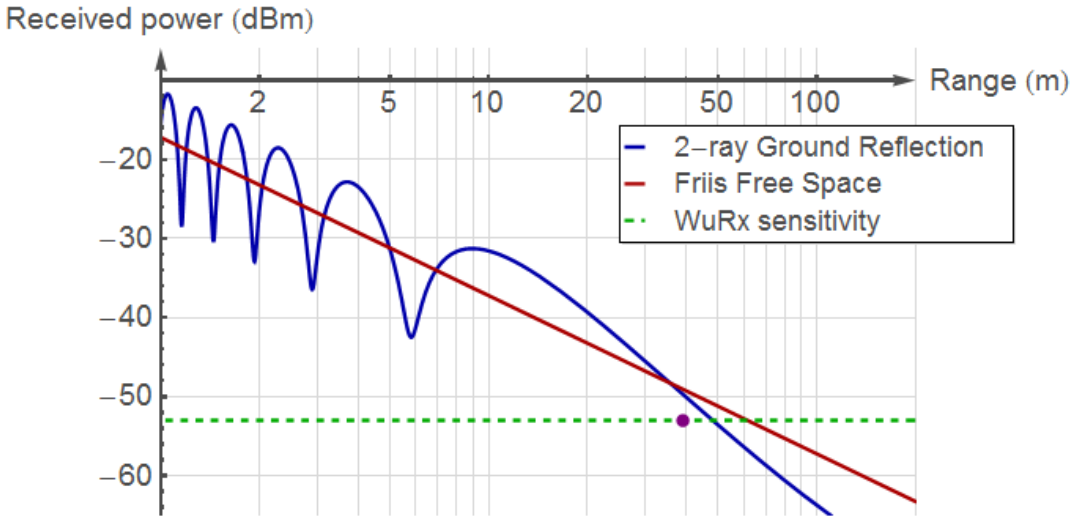

Figure 4.10: Simulation of the theoretical received power of SCM-WuRx vs. measured sensitivity.

4.3 Illustrative Application Scenarios and Multi-Hop Network Performance Evaluation of SCM-WuR

The characteristics of SCM-WuR make it suitable for a wide range of applications. This section illustrates two types of scenario, one single-hop and one multi-hop, and evaluates by simulation the network performance of the latter for nodes featuring the SCM-WuR system.

A possible single-hop scenario is urban sensing, for which a collector data-mule application is considered. Under this scenario, a SCM-WuR board acting as a collector node is placed in a non-power-restrained mobile node, which can be a public bus or a garbage truck. Such mobile node travels around the city and queries SCM-WuRx-equipped sensors placed along its route. Thus, the only moment that the deployed SCM-WuR boards get activated is when the mobile node passes nearby. Such behavior differs from typical duty-cycling wireless sensors, which activate periodically but are only really queried when the data-mule passes nearby, which can correspond to once in several hours.

Remote sensors may be placed or attached to any element in town, as illustrated in Figure 4.11. In addition, and as shown in Figure 4.8b, in case that such SCM-WuR sensor nodes are queried infrequently, they can even be powered by means of energy harvesting solutions, allowing a power supply capacitor to charge up between queries. The trash bin in Figure 4.11 can host an SCM-WuR-equipped ultra-sound sensor to transmit back the height of the garbage once queried. Also, trees can be equipped with humidity sensors in order to check they are being irrigated correctly during the day. Even the bus stop can be equipped with environmental sensors such as solar radiation and pollution sensors. Finally, panels may feature proximity sensors to be aware of how many users read the information, or advertisements, displayed in them. The SCM-WuR system can query any or all of these sensors by means of proper addressing. Such addressing may be not unique, thus the same address can be set for all the sensors of the same type, e.g., humidity, in a role-based addressing schema. Thus, the same address can be reused between several bus stops to just address certain types of sensors. A GPS-based application connected to the city database makes the mobile node aware of which kind of sensor is deployed in each area of the town. For this single-hop application, SCM-WuR boards capable of operating up to 40 m are adequate. As commented, this range can be reduced if shorter ranges are enough.

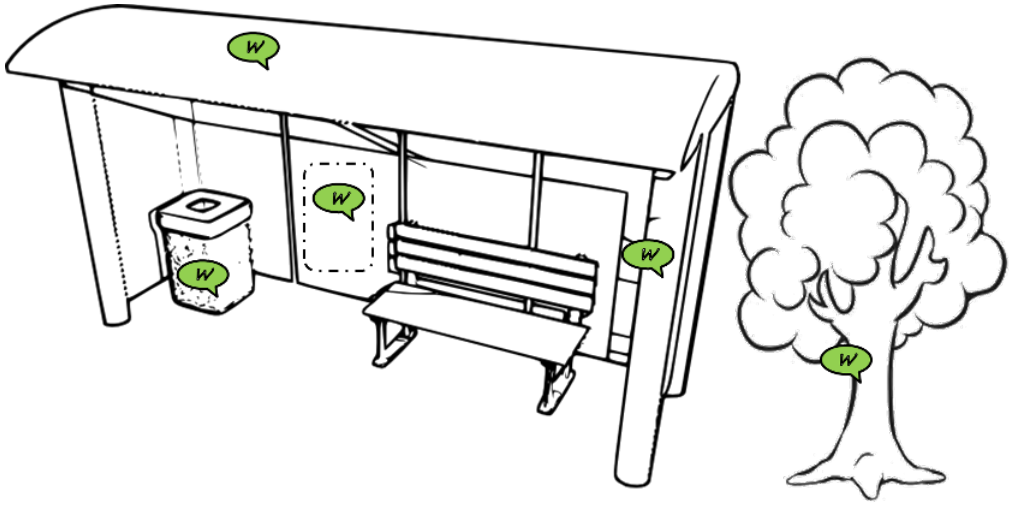

Figure 4.11: A bus stop equipped with SCM-WuR sensors.

For the multi-hop scenario, a slightly different version of the SCM-WuR boards is considered to enable them operating up to distances of 100 m and/or traverse walls. For this, the boards are equipped with a CC1190 output power amplifier for up to an output power of +20 dBm. In this configuration, the current consumption featured by SCM-WuRx only slightly increases up to 3.5 µA, while the current consumption for a WuC transmission noticeably raises up to 152 mA. Currently, there are ongoing research efforts to reduce such high value for WuC transmission. Comparatively, in case of the 40-m version of the SCM-WuR system, the ratio between the energy required to send a WuC (Section 4.2.2) and a 100-byte data packet and a WuC is calculated to be 0.68 mJ / 0.23 mJ = 2. In case of the 100-m capable SCM-WuR system, this value increases up to 5.5 mJ / 0.23 mJ = 24. The current consumption increment for boards in wake-up mode is due to a design modification to employ a CC430, which merges in a single integrated circuit both MSP430 and CC1101 components. While this change allows for less circuitry, the LPM4 for the CC430 SoC is not as efficient as the one for a standalone MSP430F2350 MCU. The 100-m version of the SCM-WuR boards is powered by 2 AA batteries for a capacity of 1500 mAh (3 V). This change also provides more robust management of current peaks. These values are indicated in Table 4.2.

In order to test the performance of the SCM-WuR approach in a the multi-hop network, an OMNET++ [38] model for the SCM-WuR boards is developed for the convergecast tree topology in Figure 4.12. SCM-WuR transmissions are empirically proven to be able to traverse up to three walls along their RF path. Therefore, sensors can be placed anywhere in three dimensions along the scenario, where nodes periodically send their vibration measurements to a sink. Intermediate nodes have to send their own measurements, as well as to relay the information they receive. The network's sink, i.e., Node 0, merely operates as a receiver until a mobile data-mule node, or a human operator, comes nearby. Then, the sink provides all the information collected in an aggregated fashion. A more extensive analysis comprising more topologies, applications and metrics evaluating the SCM-WuR system are included in chapter 6.

In the simulation results of Figure 4.13, the x-axis represents packet rates (λ) of 0.006, 0.01, 0.02, 0.03 and 0.1 packets per second. This values correspond to periods from 180 s to 10 s between two packets generated by the same node. Packets to be forwarded are sent immediately. The simulation is conducted for 10 000 s and up to 10 tests are performed for each packet rate. The rest of parameters of the scenario are shown in Table 4.2.

Figure 4.13a depicts lifetime values achieved by one of the bottleneck nodes, Node 1. Node 1, besides sending its own measures, is in charge of forwarding packets from half of the nodes in the network and hence, it is one of the two most power-demanding nodes. As seen in the figure, the lifetime values for this Node 1 decrease as more frequent sensor reports are required. For periods longer than one minute ($\lambda \sim 0.016$), the SCM-WuR network in Figure 4.12 allows for lifetimes longer than two years. In the network in Figure 4.12, each report from a sensor consists of one WuC followed by one regular data transmission, which approximately requires

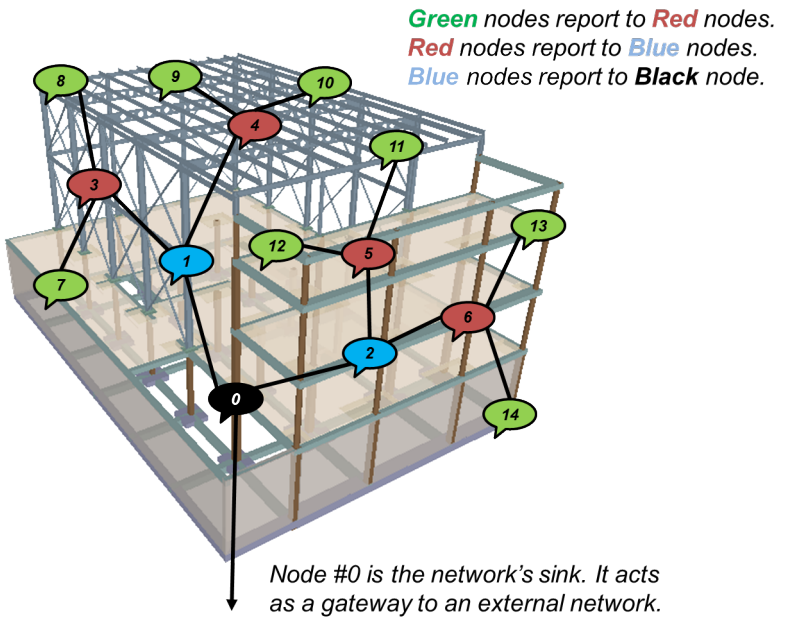

Figure 4.12: A network of SCM-WuR vibration sensor nodes along a multi-hop scenario.

Parameter	Value
Frequency	868 MHz
Inter-node Distance	100 m or up to 3 walls
Packet Payload	100 bytes
Battery Capacity	1500 mAh
Rx Current: Data Communications Mode	18.8 mA
Tx Current: Data Communications Mode	19.1 mA
Data Communications Radio Bit-rate	250 kbps
Joules to transmit one 100-bytes packet	0.23 mJ
Rx Current: Wake-up Mode	3.5 µA
Tx Current: Wake-up Mode	152 mA (+20 dBm)
WuC Duration	12.2 ms
Energy to transmit 1 WuC	5.5 mJ
Number of Nodes	15

Table 4.2: Parameters for the simulation in Figure 4.12.

12 ms (WuC) + 3 ms (data) ~ 15 ms channel access time. Numerically, for a reporting period of 180 s, or $\lambda = 0.006$, a SCM-WuR node is active during 0.000083% of the time. In contrast, duty cycled systems may be active up to 5% of the time [10]. The difference in percentages comprises several orders of magnitude. When the reporting period decreases, WuR lifetime performance logically gets closer to the ones typical for duty cycled solutions (e.g., lifetime is approximately 69 days for a reporting period of 10 s or $\lambda = 0.1$ packets per second). However, for many real-life applications reporting periods of several minutes are expectable.

The successful Packet Delivery Ratio (PDR) of the sensor readings to the sink is depicted in Figure 4.13b. As shown, for reporting periods longer than 10 s ($\lambda = 0.1$ packets per second) the

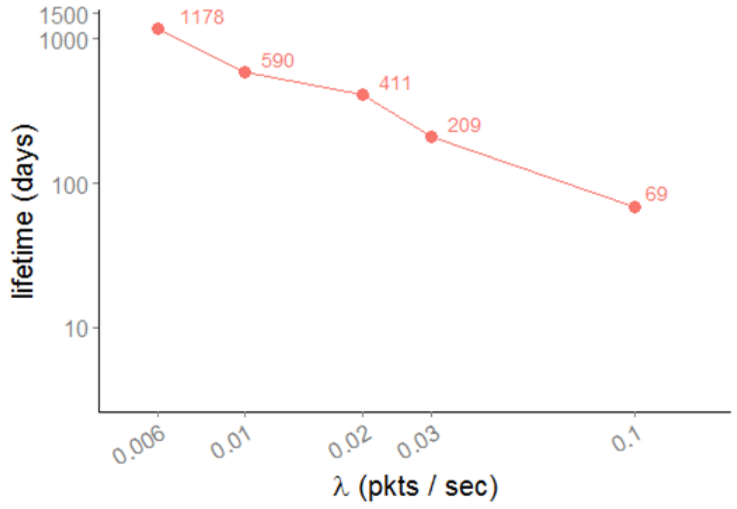

(a)

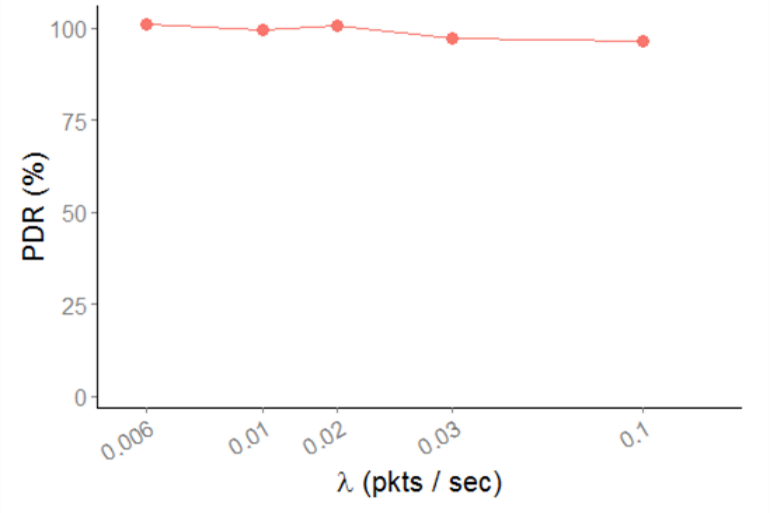

(b)

Figure 4.13: (a) Lifetime (days) and PDR (b) of Node 1 in Figure 4.12.

PDR for SCM-WuR in this scenario is practically 100%, i.e., all packets sent by the network nodes are successfully transmitted up to the sink.

4.4 Conclusions

Wake-up Radio (WuR) systems provide significant energy savings for wireless sensors when compared to conventional duty-cycling approaches. This chapter introduces and analyzes a promising novel WuR approach based on SubCarrier Modulation (SCM), which enables two radio operation modes. When the remote sensor node is in low-power wake-up mode, a WuC can trigger it remotely. Afterwards, the node switches to data communication mode to start the data exchange, e.g., wirelessly reply a transducer measure back.

As demonstrated through physical tests, measurements and simulations along this chapter, SCM-WuR systems feature an outstanding trade-off between hardware complexity, current consumption and operational range, and even enable multi-hop wake-up for long remote sensor measure collection. SCM-WuR systems may effectively implement a vast range of applications, both single and multi-hop. Instead, as shown in next chapter 5, other state-of-the-art proposals are restricted to short and medium-range scenarios and / or present several other drawbacks when compared to SCM-WuR.

5 Comparative Analysis of State-of-the-Art Wake-up Radio Systems

This chapter introduces the rest of the most relevant state-of-the-art WuR proposals as of 2014, as well as a comparison between them and the SCM-WuR approach in Chapter 4 in terms of current consumption, circuit complexity, operational range, addressing, application flexibility and WuC bit-rate. Because of this analysis, this chapter must be considered as a mere state-of-the-art, but a comparison based on the concepts and designs presented in previous chapters. To convey the overall picture of the state-of-the-art and to position the SCM-WuRx approach accordingly, the WuRx proposals are grouped by their distinctive features. Information for respective WuTx is provided when available. At the end, a global comparison table summarizes the most important characteristics of each approach (Table 5.1).

Contents

5.1 Radio Frequency IDentification (RFID)-based WuR Proposals

RFID technologies can be used as a basis for WuR systems, where the WuRx is an RFID tag and the WuTx is an RFID reader. However, their applicability and performance are strongly interrelated with the intended application.

A passive RFID-based solution is presented in [14], where a programmable RFID tag, so-called Wireless Identification Sensing Platform (WISP), is powered by an off-the-shelf UHF RFID reader to generate an interrupt on an input pin of a Tmote Sky wireless sensor mote [39]

(Figure 5.1). When the MCU gets activated, it transmits an IEEE 802.15.4 wireless frame back containing the sensor data by means of the mote's CC2420 2.4 GHz transceiver.

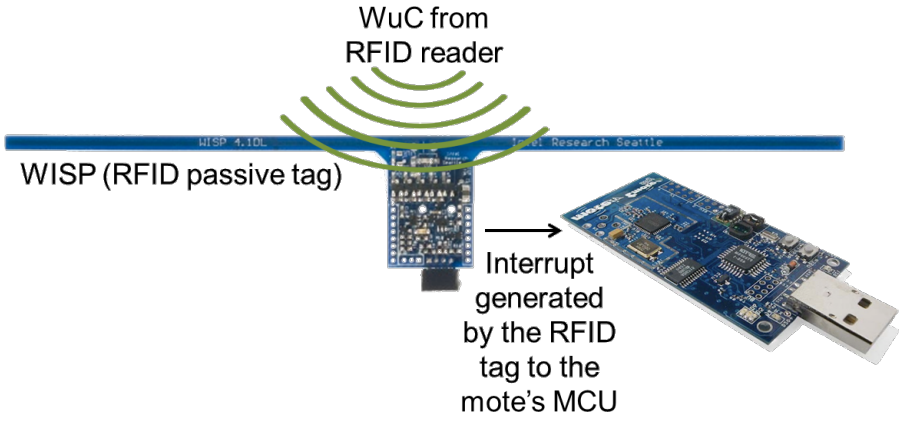

Figure 5.1: Passive RFID-based WuR system.

Since the power required by the WISP's MCU to operate is provided by the magnetic field from the RFID reader generating the WuC, the passive RFID-based WuRx proposal in [14] presents unbeatable power consumption values. Unfortunately, RFID-based WuR systems cannot provide operational distances larger than the typical ones for UHF RFID systems, about 5 m [14], an issue which limits their applicability. In addition, RFID readers, i.e., the WuTx, require power in the order of watts to achieve such distances and are considerable in size.

Other active RFID-based WuR proposals, such as RFID-Impulse [40], feature better WuTx current consumption and operational distance values of up to 30 m by employing commercial active RFID tags as WuRx. Such tags present higher current consumption than other state-of-the-art WuRx approaches and cost as much as an entire wireless sensor mote, which represents a downside for WuRx designs [41], as indicated in chapter 1, section 1.6. Besides, the proposal in [40] strongly relies on the capability of a 2.4 GHz active RFID tag to perform WuC detection by means of low-power Clear Channel Assessment (CCA). However, the applicability and performance of such mechanism are called into question in other studies [42]. In addition, it is not clearly stated if the proposal in [40] is a theoretical analysis, a simulation or a real implementation of a WuR system.

Medium-range applications appear to be the most suitable for RFID-based WuR systems. Such applications are related to data-mule scenarios, where a non-power-restricted mobile node, equipped with a RFID reader acting as the system's WuTx, travels around the application area to retrieve information from small sensors equipped with RFID-WuRx. This is the case of warehouse inventory or medical applications. One example of the latter case is that, instead of using traditional wired health monitoring devices, nursing staff of a hospital can easily gather all the sensor data from tags attached to patients' sensors by just entering their room and activating the RFID-WuTx. This application requires a range of few meters,

which RFID-based WuRx are capable to provide [43]. It is also important to note that RFID-WuR systems rely on magnetic rather than electric coupling for communication. Therefore, certain application areas may be restricted to RFID-based WuR because of security or health concerns.

Thus, even if they feature the lowest current consumption, and mostly because operational ranges related to RFID are closely related to antennae sizes, RFID-based WuR systems suffer from having a restricted number of application areas. Because of this, it is more common to find small RFID readers employed in short-range applications like access control systems, where the user approaches the tag for the communication to take place. Moreover, the use of RFID-WuR systems in small size communication devices is not possible because of the RFID-WuTx power requirements and antenna size. For example, an Ultra High Frequency (UHF) antenna is around 25 cm^2 in size and the associated reader may require up to +30 dBm [44] to activate a remote RFID tag several meters away.

When compared to SCM-WuR, RFID-WuR present no-power consumption at the receiver side for the passive RFID-tag. On the other hand, a SCM-WuRx design featuring about 3 µA and operational distances larger than few meters seem to enable many more use cases. Furthermore, such reduced current consumption value allows for very long lifetime for low data-rate applications, as described in chapter 4, section 4.2.2. Also, SCM-WuR nodes can even be powered by means of energy harvesting, which reduces the requirement of SCM-WuR to zero-power. Regarding operational distances, a SCM-WuTx only employs 0 dBm (1 mW) to wake-up a SCM-WuRx 10 m away (chapter 4, section 4.2.3), thus also medical applications as the ones enumerated for RFID-based WuR systems are perfectly feasible, even with a much lower power budget at the transmitter side than in the RFID case. Finally, SCM-WuR nodes also feature much smaller form factor for WuTx designs and can perform peer-to-peer communications, which are two crucial requirements for other applications.

5.2 Heterodyne WuRx Proposals

Heterodyning is the process by means of which an incoming radio frequency, a WuC in case of WuR systems, is downgraded by means of signal mixing to an intermediate lower frequency easier to be process by electronic components.

A 2 GHz heterodyne proposal with uncertain (1 MHz to 100 MHz) IF (Intermediate Frequency) capable to operate up to 200 kbps is analyzed in [2]. In the proposed WuRx (Figure 5.2), the WuC passes through a Bulk Acoustic Resonator (BAW) filter. Then, its frequency is down-converted to IF by means of mixers fed by a ring oscillator. Next, the signal is amplified and filtered again. Finally, the WuC envelope is extracted and presented as a baseband digital output in one of the GPIO inputs of the node's MCU. The heterodyne design in [2], while achieving good sensitivity values of -72 dBm, implies a WuRx's current consumption value

of 104 µA. Such value, even in the sub-mA order, is much higher than other state-of-the-art approaches.

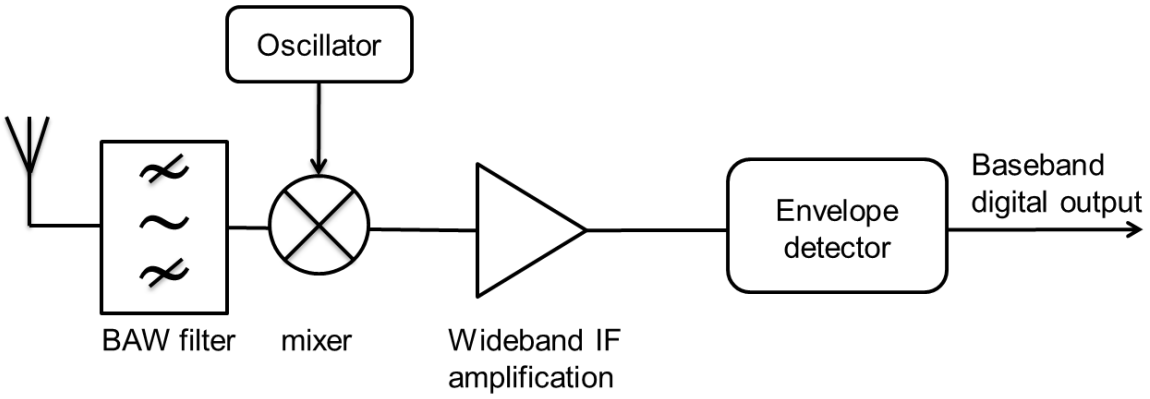

Figure 5.2: Block diagram of the heterodyne WuRx in [2].

A different heterodyne proposal for a crystal-less 2.4 GHz WuRx is presented in [45]. The WuC is modulated by means of Pulse Position Modulation (PPM). In order to reduce the power consumption of this WuRx, both the signal front-end and the oscillator are duty-cycled. However, the design still requires up to 350 µA.

A 45 MHz heterodyne WuRx proposal is presented in [46]. The performance of this design is evaluated by simulation. The WuRx targets WBAN applications, thus its purpose is to collect biometrical measurements after being activated. For signal amplification, the design employs an energy-efficient Injection-Locking Ring Oscillator (ILRO). An ILRO can effectively provide signal gain and restoration in certain low-power applications where there is the need to avoid high gain RF amplifiers. At the final stage of the front-end, the signal is processed by a low power Phase Locked Loop (PLL) demodulator. The WuRx in [46] features a sensitivity of +62.7 dBm and, similarly to [2], it can operate up to 200 kbps, but still cannot reduce its current consumption to less than 53 µA.

As shown in the previous heterodyne approaches, it is common to try to include few active components in WuRx designs in order to enhance them with better sensitivity or operational ranges than those of passive WuRx. However, WuRx containing active components tend to require excessive amount of energy. In fact, heterodyne approaches feature the highest power consumption and circuitry complexity among all the WuR types in this chapter because of including active components such as mixers and amplifiers. Such design paradigm, while enabling good sensitivity and bit-rate values, implies current consumption values of up to 50 µA [46], 104 µA [2], and 350 µA [45], which are out of the desired range for competitive WuRx designs. Nowadays, WuRx are commonly required to operate under the 10 µA threshold. Therefore, it seems that heterodyne approaches are not enough energy-efficient for WuRx designs. Furthermore, most heterodyne WuR proposals operate at non-ISM bands such as 2 GHz [2] or 45 MHz [46], a circumstance which potentially would require the WuR system to work out-of-band, or to include a special, dedicated transceiver.

A recent super-heterodyne proposal seems to target solving the previous issues. The WuRx in [47] features current consumption values of 1.2 µA, 3.2 µA and 86.7 µA for different WuC bit-rates, which allow for wake-up latencies of 484 ms, 121 ms and 3.8 ms, respectively. While all these combinations perform worse than SCM-WuR, they outperform existing heterodyne approaches.

Comparing heterodyne approaches to SCM-WuR is challenging, since most of the studies lack information about their application areas, addressing capabilities and/or achievable operational distances. For example, heterodyne WuRx proposals in the literature output a baseband sequence when receiving a WuC, thus they are not considered to feature embedded addressing. Despite this, they can still be compared for other metrics, such as bit-rate. In fact, heterodyne WuR system proposals provide WuC bit-rates noticeably higher than SCM-WuR. Nevertheless, because of the main function of a WuRx consists of activating an intended sleeping sensor node, SCM-WuR systems do not feature the hundreds of kbps of heterodyne WuR systems, thus can discount several active components. Such circumstance allows SCM-WuRx designs for less complicated and cheaper circuitry, which results in designs requiring up to ten times less power. Also, SCM-WuR systems operate in-band at 868 MHz, thus there is no need for additional transceivers.

5.3 MCU-Based WuRx Proposals

These proposals employ an additional independent MCU in a WuRx to perform several tasks, such as signal filtering. Unfortunately, such approach is as agile to implement as inefficient in terms of energy consumption. The design in [17], shown in Figure 5.3, features an AT-mega128L MCU to decode a WuC after signal rectification and amplification. The AT-mega128L is always kept in active mode requiring 801 µW at 3 V. If this MCU decodes the proper node address in the WuC, it wakes up a second and more powerful MCU from its sleep mode. Before the AT-mega128L, the WuRx deploys an energy-hungry but not very efficient amplifier stage, which provides operational ranges of barely 3 m.

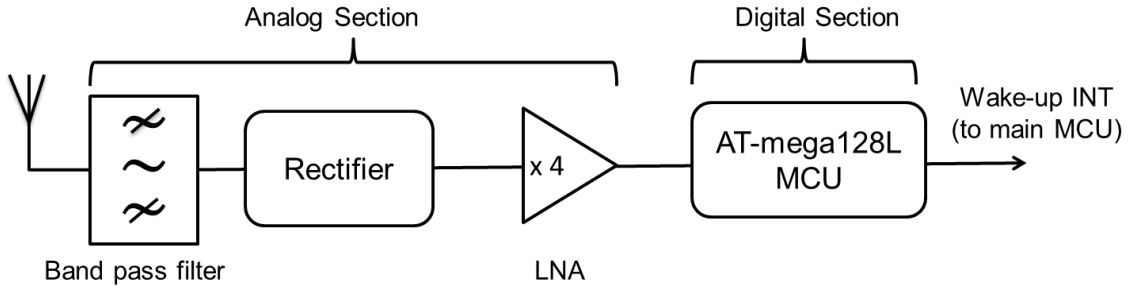

Figure 5.3: MCU-based WuRx design.

The design in [17] is not suitable for WuRx purposes because of requiring an always-active MCU, its high current consumption value and the mentioned limited operational range. SCM-WuR simply outperforms WuR systems based on a secondary MCU [17] in every metric. Clearly, MCU-based WuR systems cannot be considered for realistic applications, yet they are presented in this chapter as an alternative proposal in the literature.

5.4 Low-Complexity WuRx Proposals

The performance achieved in both the previously presented WuRx types, heterodyne and MCU-based, shows that precisely the most effective way to reduce energy need is trying to simplify the circuitry in a WuRx.

Chronologically, the first proof-of-concept WuRx is presented in [30], simply featuring a capacitor and a rectifying diode. Interestingly, this simplistic and low-complexity WuR system even considers a RTID addressing scheme described in chapter 3, section 3.2.1, where the WuTx transmits signals at different frequencies simultaneously to activate an intended WuRx. However, this WuR system features poor operational ranges of few meters.

Another low-complexity 868 MHz WuRx consisting of a voltage multiplier, a rectifier scheme and a voltage comparator is presented in [31]. The WuR system, while featuring an interesting WuRx current consumption value of just 900 nA, does not achieve operational distances larger than 3.5 m and is prone to false wake-ups caused by RF interferences at the mentioned frequency. To overcome these limitations, this thesis proposes several improvements to this system in chapter 2, such as adding a SAW filter to protect the WuRx from being activated by interferences and different WuTx designs to increase the operational distances up to 15 m, a value that effectively allows the WuR system to be employed for medium-range applications.

Another low-complexity WuRx proposal [48] can selectively operate at 915 MHz or 2.4 GHz depending on the chosen input stage configuration, which can be varied by means of different input coil configurations at the RF impedance matching stage. The described WuRx consumes 51 µA at 1 V and basically amplifies the WuC signal, extracts its envelope and, if a duty-cycled Analog to Digital Converter (ADC) considers the signal powerful enough, generates an interrupt destined to the node's MCU. Similarly, the WuRx presented in [48] splits its operation in a two-step fashion, the former one of which is also duty-cycled. In the so-called *monitoring mode*, WuC is detected by means of a duty-cycled comparator. This mode consumes as low as 4.7 µA from a 1.8 V power supply. Afterwards, upon detection of a WuC, the WuRx is switched to *identification mode* to decode the address in the WuC. Unfortunately, the high bit-rates employed by this WuR system drive the decoding of the address in the WuC to require up to 599 µA.

The most efficient low-complexity WuRx proposal to date is presented in [3]. The WuRx, which block diagram is shown in Figure 5.4, is designed for WBAN applications. The design provides operational ranges of up to 10 m for a WuTx output power of +10 dBm. Indeed,

the WuRx in [3] features one of the lowest current consumption of the all WuRx approaches (180 nA at 1.5 V), while still presenting a good trade-off between current consumption, hardware complexity and operational range. However, the WuC addressing feature is left to the MCU and its related current consumption not mentioned in the paper. In fact, the WuC is considered as the trigger to start the data slicer and the Pulse Width Modulation (PWM) demodulator, which provide a SPI translation of the incoming data to the MCU.

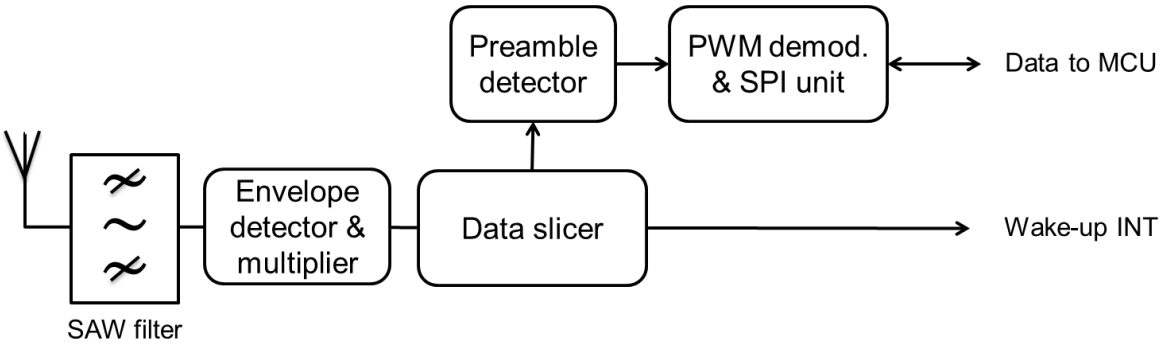

Figure 5.4: The low-complexity WuRX design in [3].

Yet another low-complexity WuRx design for WBAN is presented in [49]. Even though it also presents a minimal current consumption value of 82 nA at 1.2 V, the proposed 915 MHz design barely achieves operational distances of 1 m for 0 dBm. Thus, this latter WuRx is not considered for the comparison in this chapter.

Low-complexity WuR designs can be considered as an intermediate approach that combines the best of RFID-based and heterodyne approaches, since they feature less circuitry complexity than heterodyne approaches and, at the same time, better ratio between operational range and WuTx current consumption than RFID-based WuR systems. In addition, most low-complexity WuRx proposals provide full details in order to make designs reproducible and also operate at bit-rates much more adequate for WuR purposes than those of heterodyne approaches. As a proof-of-concept, the low-complexity WuR system in [31] fits in the short-range application area, like RFID-based WuRx designs. However, since the related WuTx can be implemented by means of a RF transceiver instead of a RFID reader, it presents much better possibilities in terms of peer-to-peer applications. In addition, in case some design improvements are incorporated in the WuRx design and more efficient antennae line the one in [4] are allowed in WuTx, the resulting WuR system may feature higher operational range values than that of RFID-based WuR. Such potential for larger operational distance values, along with a current consumption value as low as 0.9 µA, enables the WuRx to be employed in a larger number of applications. Figure 5.5 shows a wireless sensor platform based on the Texas Instruments CC2530EM [50] board equipped with a custom implementation of the low-complexity WuRx described in [4]. The design is empirically checked to feature operational distances around 13 meters by the same procedure in chapter 2, section 2.2.2.

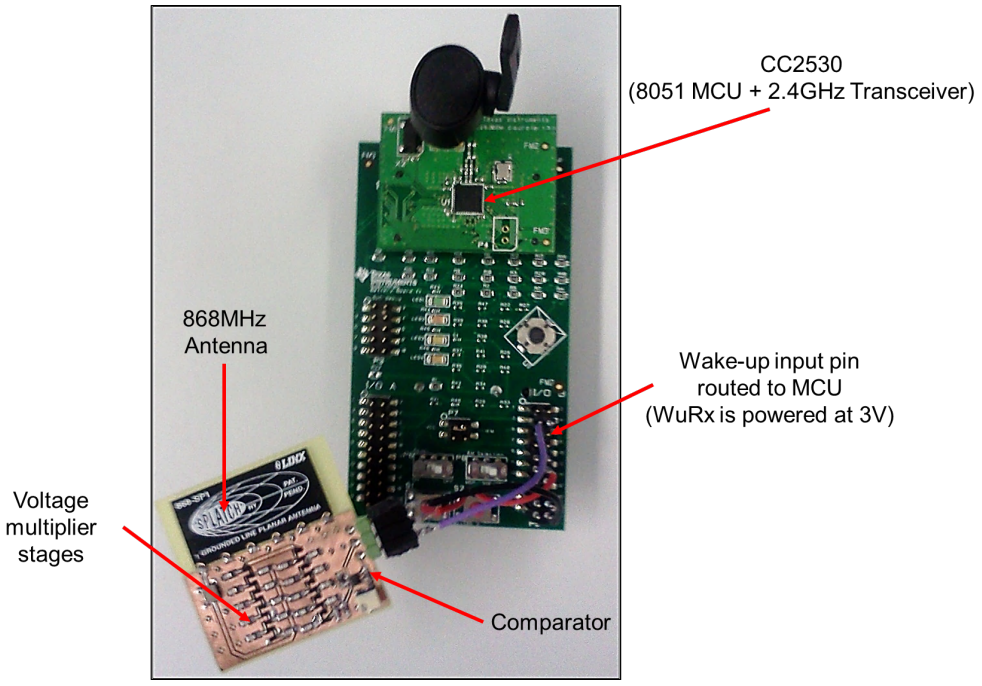

Figure 5.5: The low-complexity WuRx design in [4] attached to a wireless sensor node. When the WuRx detects a WuC, the main board is woken up from sleep mode to transmit back an IEEE 802.15.4 data frame.

Several low-complexity WuRx proposals [48, 51], duty cycle several WuRx components to reduce the current consumption. Such strategy cannot be performed without affecting WuTx transmissions, which need to be longer or repeated to ensure the duty-cycled WuRx is able to detect them, in a similar case as protocols like B-MAC [12]. Clearly, both circumstances imply either higher current consumption at the WuTx side, increased latency, or a reduction in the performance in terms of WuC detection, which may be not acceptable in certain WuR applications. Another drawback among all low-complexity WuR proposals is that they either lack addressing capabilities or require high amount of current to perform the address decoding procedure (up to 0.6 mA in [48]).

Unfortunately, most low-complexity WuR proposals lack of range-related information, thus their comparison to SCM-WuR is difficult. However, since their design includes few active components, operational distances around 10 m would be expectable. For example, the WBAN low-complexity proposal in [3] is stated to achieve 10 m for a WuTx output power of +10 dBm. However, due to the fact the WuTx already employs the maximum allowed power at 433 MHz, the design cannot achieve longer operational ranges. Compared to [3], SCM-WuR provides noticeably higher operational ranges and slightly higher sensitivity (-51 dBm vs. -53 dBm). As shown in Figure 4.9c, the maximum operational distance achieved by SCM-WuR is about 41 m for a WuTx transmit power of +10 dBm.

While low-complexity WuR systems present an evolution when compared to RFID-based, heterodyne and MCU-based ones, their limited operational distances and the fact that they lack an address correlator imply important performance issues. Instead, SCM-WuR systems

deploy a correlator in the WuRx expressly devoted to decode the address embedded in WuC while still requiring very few µA. In addition, the SCM approach allows for real operational ranges up to 100 m. Finally, SCM-WuR boards do not present duty-cycled components in their design. These characteristics allow SCM-WuR systems to be more efficient in every aspect and adequate for a wider range of application scenarios than low-complexity WuR.

5.5 Correlator-Based WuRx Proposals

The most efficient WuRx designs in the literature employ hardware correlators. Thus, all correlator-based WuRx designs implicitly feature addressing capabilities. For example, SCM-WuR boards only require 8.8 µA for their correlator to decode a WuC address.

A simulated correlator-based WuRx approach can be found in [52]. It features a current consumption value of 19 µA and operational distances of 4 m for a 0 dBm output power. This work is the basis of several newer proposals, since it depicts a complete WuC signal processing trace including all the sequential steps from envelope detection to the address comparison stages. Another simulated WuRx, but based on a Field Programmable Gate Array (FPGA), is presented in [53]. Because of both works being proposed only by simulation and featuring similar characteristics, only the proposal in [52] is considered for the comparison in this chapter.

A real correlator-based WuRx employing a FPGA for decoding the WuC is presented in [54]. It requires 8.4 µA and is powered by 1.5 V power supply. Prior the FPGA, the design deploys an envelope detector and a programmable amplifier. Unfortunately, the operational ranges achieved when varying the amplifier gain are not provided in the paper. Since the WuRx is stated to target short-range applications, probably distances from 3 m to 10 m are expectable.

The most efficient WuRx as of 2013 is presented in [5]. Such 868 MHz WuRx is based on a correlator capable of identifying addresses up to 64 bits in length. The power supply is 1.0 V and the total power consumption 2.4 µW. The study in [5] includes the total time for the WuRx to fully activate the MCU, which takes from 40 ms to 110 ms. This WuRx is stated to feature operational distances of up to 304 m for a WuTx transmit power of +6.4 dBm. However, the proposed design, shown in Figure 5.6, omits crucial design details of the WuRx and is presented as a black box. Because of this, the proposal in [5] is hardly reproducible and analyzable.

Because of the proposal in [52] merely simulates a WuRx circuit, its performance cannot be compared to SCM-WuR directly. Hence, the most relevant WuR proposals in the category of correlator-based WuRx to be compared to SCM-WuR are [5, 54]. The authors in [54] state the WuC address decoding is performed in FPGA for the sake of flexibility. This means the 8.4 µA consumption value featured by the WuRx can be reduced if addressing is implemented on-chip. Precisely, such modification is already performed in SCM-WuR boards, which only present a value of ~10 µA when decoding of a WuC address. Instead, during idle state, SCM-WuR boards feature a third of the current consumption of the proposal in [54]. Despite this,

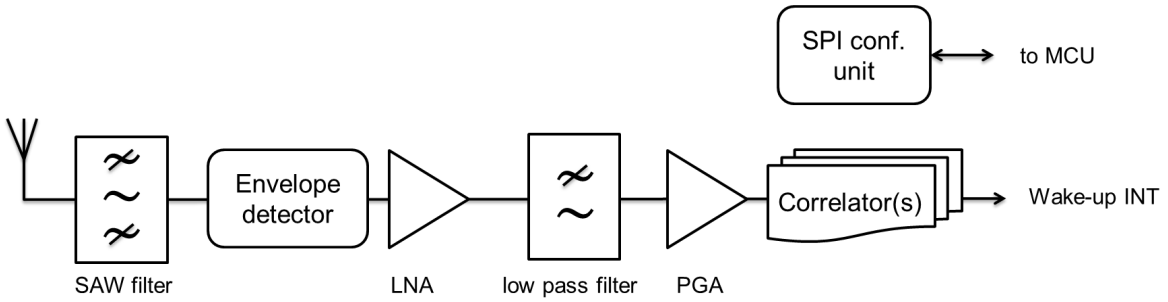

Figure 5.6: Block diagram of the correlator-based WuRx design in [5].

both designs can be considered similar, even if the proposal in [54] is designed with short-range applications in mind. In fact, because of decoding of the WuC being performed by FPGA, the proposal in [54] even outperforms SCM-WuRx in few metrics such as WuC bit-rate capabilities of up to 100 kbps, which in turn means shorter WuC latencies. However, usually such high bit-rates are neither common, nor required for WuR applications. Unfortunately, a WuRx design featuring a FPGA may present higher monetary cost. When compared to other high bit-rate WuR systems such as heterodyne ones, the FPGA-based proposal in [54] enables a drastic improvement in terms of current consumption.

On the other hand, the high performance WuRx presented in [5] features an 868 MHz impedance matching stage based on high-quality inductors for increased sensitivity as in SCM-WuR boards, along with operational ranges of 300 m for WuTx transmit power values below +10 dBm. Unfortunately, the WuRx design becomes hardly to reproduce due to the lack of details in the paper. In addition, the transmission of the WuC in [5] lasts for 4 to 10 times longer than that of SCM-WuR. Since during the WuC decoding the WuRx cannot handle any other input RF signal, such WuC time duration may seriously affect the PDR of a network comprising several WuRx-equipped nodes.

Some proposals are just cited but not analyzed in this section since they are either difficult to reproduce or their utility is limited. For example, the WuRx in [55] requires a 60 GHz WuTx. On the other part, some systems like [56], because of being designed as intra-vehicle systems, provide limited ranges of barely 2 meters.

5.6 Other Types of WuRx

Apart from RF WuR systems, there are also proposals based on different transmission medium. For example, the proposal in [57] utilizes Free Space Optical (FSO) communications to generate the WuC. It achieves operational ranges of up to 20 m for a WuTx power of 16.5 mW. The wake-up receiver requires 100 µA. Unfortunately, the system suffers from low bit-rates of 2 kbps even in data communication mode and requires Line-of-Sight (LoS) between nodes. The authors in [57] state that, in the case of optical wake-up systems, addressing is inherently

implemented by means of the directional nature of the optical medium. Yet, it is not clear the performance of this system for networks where nodes are not perfectly aligned.

Another FSO proposal is presented in [58], which features an ultra-low power consumption of 695 pW. This WuRx allows for operating distances up to 50 m when employing a fixed-position 3 mW laser as WuTx, of 6 m when employing a 3 W focusable LED and of 20 cm when employing a 0.5 W standard LED. Similarly to the design in [57], the wake-up system in [58] suffers from LoS requirements, even lower bit-rate (91 bps) and WuC detection capabilities extremely dependent on the physical alignment between the optical transmitter and receiver nodes. Each of these issues limits the application areas of optical systems. Differently from [57], the proposal in [58] features an embedded addressing scheme.

An infrared (IR)-light wake-up system is presented in [59]. The WuRx features an IR-LED energy harvester which provides the energy required by a WuC-detector and an external-noise current canceller to operate. The system allows to wake-up domestic electronic appliances up to 6 m away by a WuRx only requiring 40 pW. While this is an interesting value, the system also presents some issues like the lack of addressing, the traditional high current consumption of infrared transmitters and latency values of up to 50 ms, as well as the same line-of-sight requirements of any infrared communication.

The last type of wake-up systems employs ultrasonic communications between receiver and transmitter [60]. The receiver requires less than 1 µA when in idle state and up to 7 µA when active. The system may be employed to estimate distances up to 9 m between receiver and transmitter with a maximum error of 0.1 m. The WuTx consumes 37 mW (2 V) and takes about 0.5 s to specify an 8-bit address, thus its bit-rate is 16 bps.

Clearly, optical and ultrasonic WuR systems target different application scenarios than SCM-WuR. However, they can still be compared in terms of several metrics. In fact, the optical approach in [58] features the lowest power consumption among all the wake-up systems by only requiring 695 pW in sleeping mode. In turn, the related WuTx only consumes 3 mW to reach up to 50 m. Unfortunately, the number of applications which can benefit from two perfectly aligned nodes, as required by the optical system due to employing a laser as WuTx, is very restricted compared to SCM-WuR systems, which are not alignment-dependent. On the other hand, while the ultrasonic WuRx in [60] requires less than 1 µA to operate, its application areas are restricted to short-range distance estimation. In addition, its bit-rate is extremely low even for wake-up applications, making a single WuC to last for up to 500 ms.

5.7 Summary

The most relevant WuRx proposals in the literature are plotted in Figure 5.7 to allow a quick comparison of their features.

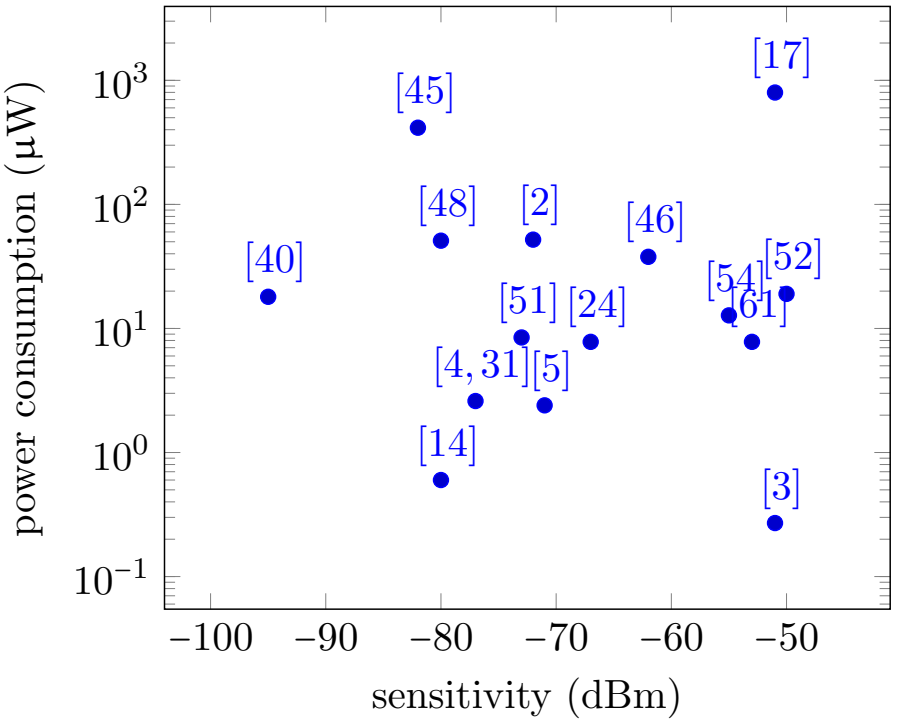

Full details are provided in summary Table 5.1. There are currently no standardization efforts for WuR systems, thus most of them operate on unlicensed Industrial, Scientific and Medical (ISM) frequency bands. Column labeled as @ in Table 5.1 indicates if the WuRx features embedded addressing capabilities. Due to missing information about RFID-WuR proposal in [40], values from the core RFID active tag employed in the WuRx design are indicated.

Ref.	Type	Frequency	Sensitivity	Current Consumption	@	Range	Bit-rate	Applications
[14]	RFID	900 MHz (ASK)	-80 dBm	0.2 µA (3 V)	Y	5 m (N/A)	N/A	Short-Range WBAN
[40]		2.4 GHz (ASK)	-95 dBm	6 µA (3 V)	Y	30 m (0 dBm)	250 kbps	Experimental
[2]	Heterodyne	2 GHz (OOK)	-72 dBm	104 µA (0.5 V)	N	N/A	200 kbps	WSN
[45]		2.4 GHz (PPM)	-82 dBm	346 µA (1.2 V)	N	N/A	500 kpbs	WSN
[46]		45 MHz (FSK)	-62 dBm	54 µA (0.7 V)	N	<10 m (N/A)	200 kbps	WBAN
[17]	MCU	868 MHz (OOK)	-51 dBm	266.6 µA (3 V)	N	3 m (+4.7 dBm)	N/A	Experimental
[30]	Low-complexity	433 MHz	N/A	100 µA (1.5 V)	Y	7 m (+10 dBm)	N/A	Experimental
[4, 31]		868 MHz (OOK)	-77 dBm	0.876 µA (3 V)	N	15 m (+27 dBm)	2 kbps	Short-Range Data-mule WBAN
[48]		2.4 GHz (OOK) 915 MHz (OOK)	-69 dBm -80 dBm	51 µA (1 V)	N	N/A	10 kbps	WSN
[51]		928 MHz (OOK)	-73 dBm	idle/decoding 4.7 µA/599 µA (1.8 V)	Y	N/A	1 kbps	WSN
[24]	Correlator	150 kHz (ASK)	-67 dBm	idle/decoding 2.6 µA/8.3 µA (3 V)	Y	5 m (+33 dBm)	0.5 to 8 kbps	Short-Range WBAN Keylock
[3]		433 MHz (PWM)	-51 dBm	180 nA (1.5 V)	Y	10 m (+10 dBm)	2 to 80 kbps	Data-mule WBAN Warehouse
[52]		2.4 GHz (PWM)	-50 dBm	19 µA (1 V)	Y	4 m (0 dBm)	50 kbps	Experimental
[54]		2.4 GHz (OOK)	-55 dBm	8.5 µA (1.5 V)	Y	N/A	100 kbps	Short-Range
[5]		868 MHz (OOK)	-71 dBm	2.4 µA (1 V)	Y	304 m (+6.4 dBm)	20 to 200 kbps	Data-mule Warehouse Environmental

Table 5.1: Comparative table of representative WuR proposals.

Ref.	Type	Frequency	Sensitivity	Current Consumption	@	Range	Bit-rate	Applications
[57]	Optical	Light	-53 dBm	25 µA (3.3 V)	Y	15 m (+12 dBm) 20 cm (0.5 W LED)	2 kpbs	WSN
[58]		Light (PWM)	37 lux	580 pA (1.2 V)	Y	6 m (3 W focus LED) 50 m (3 mW Laser)	91 bps	Experimental
[60]	Ultrasonic	Sound (OOK)	1 mV at 1 m	874 nA (2 V)	Y	9 m (+15.6 dBm)	16 bps	Distance measur.
SCM-WuR	Correlator	868 MHz (OOK)	-53 dBm	idle/decoding 2.7 µA/8.4 µA (3 V)	Y	40 m (+11 dBm) 100 m (+20 dBm)	0.5 to 8 kbps	Short-Range Data-mule WBAN Warehouse Environmental

Table 5.1: Comparative table of representative WuR proposals (cont).

6 Performance Comparison of WuR vs. Conventional WSN MAC Protocols: A Simulation Approach

The on-demand nature and the energy savings provided by WuR are decisive factors for rethinking applications from using traditional MAC protocols. This chapter targets to provide the necessary data to evaluate the feasibility of such change for different kinds of applications, either single-hop networks or static and mobile multi-hop networks. Practically any WSN fits in one of these categories. Hence, the results in this chapter reflect the performance offered by the five different communication methods for scenarios common in the literature. Trends and conclusions extracted from this chapter are applicable to other WuR designs as long as they present similar performance to SCM-WuR.

This chapter contemplates a real WuR design and compare its performance to four different widely known MAC protocols. The WuR model, corresponding to the SCM-WuR system from chapter 4 and adaptable to other WuR designs, builds on OMNET++ [38] and MiXiM [62] to avoid custom-built simulation software. Concretely, section 6.2, introduces the state of the art of WuR simulation and its comparison to traditional MAC protocols. Next, section 6.3 describes the complete employed simulation framework and the software implementations of the MAC protocols and WuR in OMNET++ and MiXiM. The proposed scenarios under evaluation are presented in section 6.4, along with a complete analysis on the performance in terms of numerous metrics for each approach under each use case. Finally, section 6.5 concludes the chapter.[1]

Contents

[1] The current chapter is based on and extends the work of a publication accepted and currently undergoing publication at at JCR Q1 IEEE / ACM Transactions on Networking:
≪J. Oller, I. Demirkol, J. Casademont, J. Paradells, G. U. Gamm, and L. Reindl, 'Has the time come to switch From Conventional MAC Protocols to Wake-up Radio for Wireless Sensor Networks?'≫.

6.1 Introduction

The purposes of the many Medium Access Control (MAC) protocols proposed in the literature for Wireless Sensor Networks (WSN) are diverse; while some focus on improving data throughput in bursty traffic conditions, others focus on maximizing energy efficiency. However, regardless of their target, most rely on duty-cycling for their implementation. Unfortunately, while the introduction of such duty-cycle provides important energy benefits over an always-on approach, MAC protocols for WSN still suffer, to a greater or lesser extent, from idle listening, overhearing and additional latency, as thoroughly commented in this thesis. Duty-cycling bounds MAC protocols' energy efficiency, and this in turn affects the network's performance. Designers have implemented a panoply of different MAC protocols to fit different application requirements, up to the situation of what is known as the MAC Alphabet soup for WSN [63].

As the number of MAC and WuR proposals grows in the literature, there are plenty of unknowns that remain unaddressed, being the different performance they feature when applied to realistic applications among the most important ones. In addition, since some designs are proposed entirely by simulation, their implementation and performance evaluations rely on custom-designed software solutions, a factor which limits the applicability and reproducibility of any obtained results. Instead, OMNET++, as used in this chapter, is publicly available and provides a reliable and complete set of primitives for wireless signal propagation, energy consumption, etc., as well as means to generate realistic application scenarios and extract complete simulation results. The framework MiXiM is employed on top of OMNET++ because of its focus on WSN purposes. Compared to OMNET++, MiXiM provides primitives specific of wireless sensor, body area and ad-hoc networks. MiXiM includes characterizations of known hardware radio transceivers such as CC2420 or CC1101, as well as implementations of two largely recognized MAC protocols for WSN, that is, B-MAC and unslotted IEEE 802.15.4. For higher significance of the results, the work in this chapter adds, by strictly following the design guidelines in their respective research papers, two implementations of broadly known MAC protocols, namely X-MAC [10] and RI-MAC [64], to the previous two, besides the implementation of SCM-WuR. For the WuR parameter characterization, empirical time and current consumption values measured from real evaluation boards are employed. The performance of

the five approaches is analyzed under three scenarios derived from real-life WSN use cases for numerous metrics such as power and energy consumption, battery lifetime, latency and PDR. Both individual node and global network contexts are studied.

6.2 Related Work

Because WuR being a recent research topic, the number of studies comparing their performance to the one achieved by WSN MAC protocols is limited. Few studies, e.g., [65], mainly focus on comparisons among WuR. However, such studies overlook relevant or novel WuR functions such as multi-hop WuR communications, and do not provide any information related to the different performance provided by WuR when compared to traditional MAC approaches. In addition, the employed simulation software is often not clearly described.

In [66], a comparison is performed between two WuRx designs requiring 50 µW and traditional preamble-sampling MAC protocols. Simulations are performed in MATLAB but node placements are considered random, thus the results in the paper are difficult to extrapolate to real-world applications such as mobile data-collectors and/or planned node deployments. Also, the WuRx designs in [66] require about 5 times more power than SCM-WuR and unfortunately do not provide any data related to the range achieved by the WuR operation. In addition, the work in [66] only focuses on analytical aspects, such as the required number of nodes to achieve full connectivity in an application area via multi-hop capabilities. However, such multi-hop capabilities are not even mentioned as feasible in the respective papers for the designs included and analyzed in [66].

The authors in [67] compare simulation and ideal mathematical analysis of wireless nodes when equipped with a real WuR system featuring a power consumption of 125 µW for the WuRx. The paper relates the number of hops in the communication with the related effective range and PDR achieved by nodes deployed in a random manner. Unfortunately, the paper does not contemplate other important aspects such as latency measurements, detailed energy distribution for the participating nodes or the effect of interferer nodes, among others. Instead, and in a similar manner to [65], the main purpose of the paper is to determine the coverage of WuR systems when compared to traditional approaches. While this subject is important because of the shorter range of WuR compared to traditional transceivers, a complete application analysis should consider the rest of concurrent aspects. In addition, the analyzed WuR system requires up to 15 times more power than the WuR system employed in this chapter, thus drastically reducing the network lifetime, the evaluation of which is in fact also omitted in [67].

A complete simulation for a binary-tree scenario comparing B-MAC, IEEE 802.15.4 and a WuR design, so-called RFID-Impulse, is presented in [68] and shortly described in chapter 5, section 5.1. While this work considers a real-world application and relevant MAC protocols, the design of the WuR is not even elaborated, nor its operation, or its range. As a result,

the reproducibility and applicability of the obtained results are limited. The work in [69] effectively solves the previous issue and represents the basis of this chapter.

6.3 Simulation Framework for MAC Protocols and Wake-up Radio

The SCM-WuR model in this chapter is developed on MiXiM because of 1) its integration to OMNET++ and 2) the characterizations it provides explicitly for WSN, such as models for common radio transceivers and for MAC protocols like B-MAC and IEEE 802.15.4. The WuR model is developed and compatible with the latest software versions of OMNET++ and MiXiM 4.3 and 2.3, respectively.

In order to achieve an architecture implementation as generic as possible, the node model depicted in Figure 6.1 is considered. Such model follows all OMNET++ guidelines. Addenda are illustrated as dotted line in the figure. The *Application* module contains the code for the user application, e.g., to initialize the node, generate packets or perform mobility-aware tasks, such as controlling the node speed if needed. Next, different routing protocols may be implemented in the underlying *Network* (NWK) layer module in Figure 6.1, which may also be omitted. To focus evaluations in this chapter to MAC protocols and WuR respective performances and to achieve fairness, the only changes among different simulation setups take place at the lower radio levels. That is, the MiXiM's configuration files for B-MAC and X-MAC are exactly the same and only differ in the parameter indicating the MAC protocol under analysis. Only when evaluating WuR, the *Wake-up Radio* module is enabled. Thus, Figure 6.1 respects MiXiM's basic node model and only contemplate additional software modules for WuR designs. *Wake-up Radio* addenda are just omitted in simulations of the MAC protocols. In other words, for B-MAC, X-MAC, RI-MAC or IEEE 802.15.4 simulations, the *Data radio* is the only radio module active. Instead, when evaluating WuR nodes, the main radio is managed by a transceiver controller module, depicted as *Control* block in Figure 6.1, which allows the application to monitor and control the status of the transceiver, as done in real WuR systems such as SCM-WuR. The *Battery*, *Mobility* and *Address* blocks in Figure 6.1 provide primitives for averaging the power consumption, setting the node mobility pattern and the address scheme featured by the network, respectively.

In order to evaluate the performance of the nodes in different applications, the parameters of Application and Data Radio modules of nodes are set accordingly. This simulation model allows for a panoply of combinations to test, which can be done in a plug-and-play manner.

6.3.1 Implemented MAC Protocols

The operation of the different MAC protocols simulated in this chapter is depicted in Figure 6.2. The first three approaches, i.e., IEEE 802.15.4, B-MAC and X-MAC, represent examples

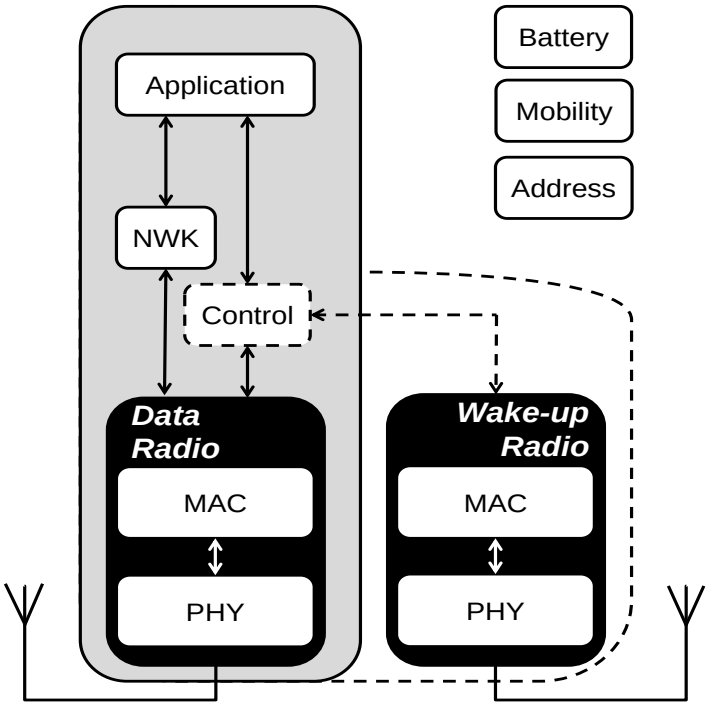

Figure 6.1: Node model proposed in OMNET++. WuR addenda indicated by dotted lines.

of Transmitter Initiated (TI) protocols. On the other hand, RI-MAC is the reference Receiver Initiated (RI) protocol. This terminology classifies the protocols depending on which node starts the data communication procedure. Regarding WuR, and because of the flexibility of the WuR model in this chapter, it is possible to implement any of the two approaches by just changing few lines of code. Hence, both WuR variants are included in the analysis in this chapter, namely TI-WuR and RI-WuR. In TI-WuR, a node first sends a WuC to wake up the remote node and sends a data frame afterwards. In RI-WuR, a node wakes up a remote node in order to receive back a data frame.

In the evaluations, the *Data Radio* module in Figure 6.1 contains an implementation of one of the four MAC protocols: unslotted IEEE 802.15.4, B-MAC, X-MAC and RI-MAC. The choose of these protocols is due to several reasons, enumerated next.

→ IEEE 802.15.4 is the most commonly employed protocol in WSN nodes, e.g., by ZigBee [70] and 6LoWPAN [71] devices. This standard specifies two different flavors for a) networks comprising a controller node, which coordinates the other nodes by means of beacon frames, and for b) networks without such controller. The *beacon-enabled* mode implements a so-called Contention Free Period (CFP), during which the nodes access the medium by using Time Division Multiple Access (TDMA), since the controller manages the scheduling. Thus, in this period, nodes may be duty-cycled. However, for peer to peer networks the *beaconless mode* is more common, since it does not depends on a special controller node. In addition, synchronization in beacon-enabled networks is not

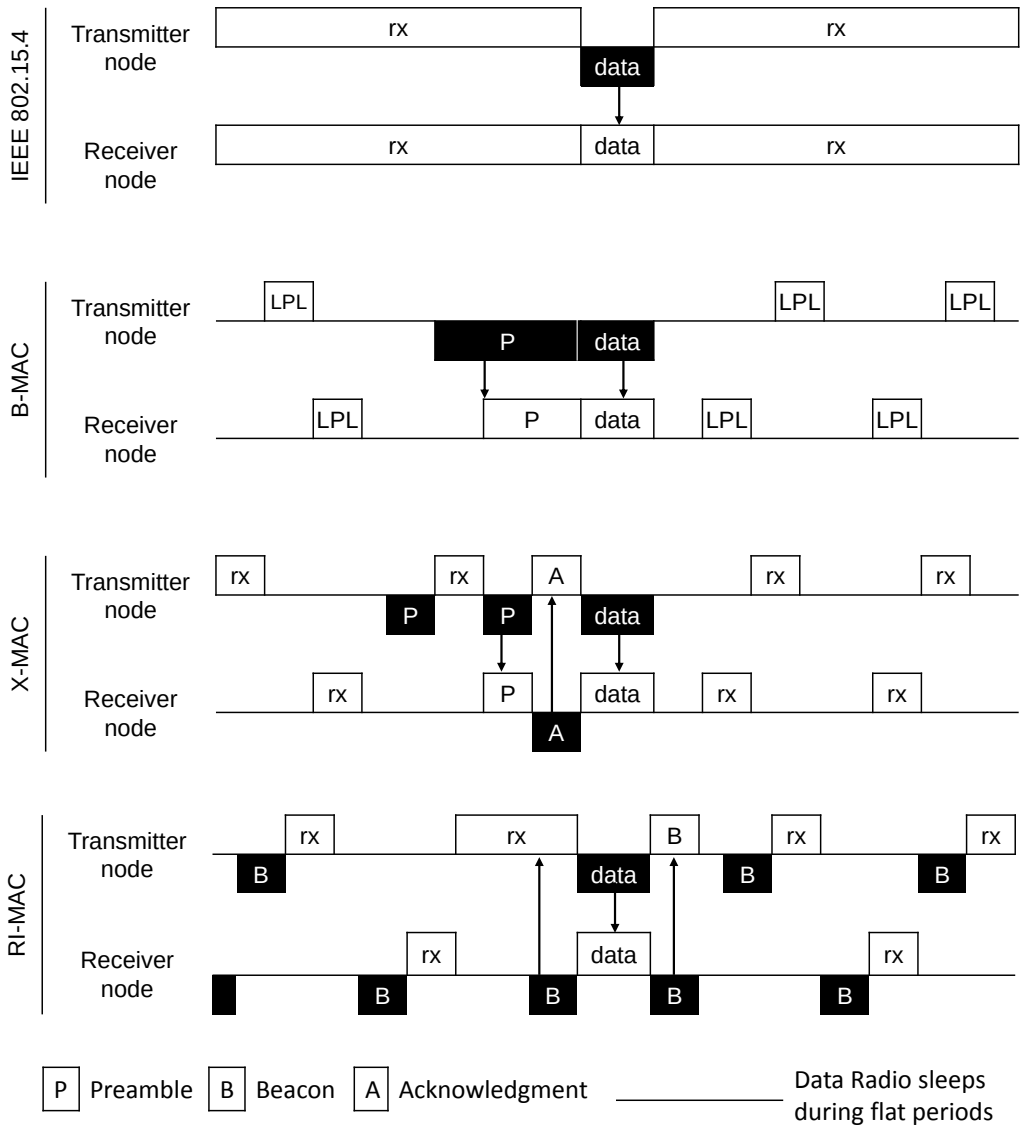

Figure 6.2: Working principles of evaluated MAC protocols.

trivial to achieve. In contrast, in beaconless mode, nodes have to either be *always awake*, or use some synchronization mechanism (which is out of the scope of IEEE 802.15.4) for duty-cycling. In the performance evaluations in this chapter, the unslotted or *non-beacon enabled* version of IEEE 802.15.4 provided by default by MiXiM and shown in Figure 6.2, is considered. Its performance establishes a common base reference for all the obtained results, since it will guarantees both the best results in terms of latency and the worse in terms of energy efficiency. In the rest of the chapter, this implementation is simply named IEEE 802.15.4. As a Carrier Sense Multiple Access (CSMA)-based approach, in a beaconless IEEE 802.15.4 network, a node desiring to access the channel must first assure no other transmitter is using the medium by means of Clear Channel Assessment (CCA). If the node senses the medium to be busy after CCA operation, it performs a randomized back-off and tries to transmit after the chosen back-off time. Since in

CSMA-based protocols, such as IEEE 802.15.4, no preamble or wake-up packet is needed, transmissions can be performed quicker than in preamble-based MAC approaches such as B-MAC and X-MAC introduced next:

→ B-MAC [12], also included in MiXiM by default, is a widely known WSN MAC protocol and the default MAC layer for several versions of operating systems for WSN nodes such TinyOS [72]. In B-MAC, as shown in Figure 6.2, a transmitting node first emits a preamble which is slightly longer than the entire sleeping period of duty-cycling nodes. This timing ensures the receiver node to detect the preamble after the sleeping period of its duty cycle. During such detection, and in order to save energy, the receiver's transceiver is not operated at full power, but it performs CCA to simply detect the presence of a radio transmission. Thus, the preamble is detected by a so-called Low Power Listening (LPL) strategy as a simple raw medium-busy indication by the receiver, which waits until the preamble's end. Afterwards, it switches to real data reception mode, where the transceiver presents higher current consumption since, from this point on, it requires demodulation and decoding capabilities to receive the intended node's address included in the data packet. This uninterrupted preamble approach of B-MAC implies severe medium occupancy levels and latency issues. These issues can be reduced by increasing the duty cycle ratio, i.e., by shortening the sleep period of the MAC protocol, which in turn increases the energy consumption. Because of its preamble, which is implemented as a constant and uninterrupted flow of bits, B-MAC is executed by byte-level radios such as the Texas Instruments CC1000, where the minimum transmission unit is not packet but byte. This implies that data packets need to be decomposed to bytes and reassembled from the received bytes. Nowadays, this popular radio transceiver has been replaced by the CC1101, which implements both byte-level and packet-level features.

→ X-MAC [10] shifts the operation of B-MAC to packet-level radios in order to solve the aforementioned problems. Its performance is known to be better than the one of B-MAC, thus it is an imperative protocol to evaluate and omnipresent in related literature. In fact, a variant of X-MAC, so called X-MAC-UPMA, is the base MAC protocol of the Contiki operating system for WSN [73]. Thus, performance evaluations of X-MAC in this chapter can be extrapolated to several similar protocols. In X-MAC, as shown in Figure 6.2, the preamble is sliced or strobed, which means that the transmitter alternatively sends short preamble packets and listens to the channel. Differently from B-MAC, such short preamble packets already include the address of the intended receiver of the communication. Thus, the surrounding nodes not being currently addressed can return immediately to sleep in order to reduce overhearing as soon as they detect that the on-going communication is not destined to them. In turn, the intended node must respond with an acknowledgment frame. This behavior solves the long preamble issue in B-MAC

and allows for a fairer channel usage. Once the transmitter receives back the ACK, it can proceed to send the data frame. Note that if no ACK is received back, the X-MAC preamble may be as long as in B-MAC. X-MAC can be implemented in packet-level radios such as in CC2420, CC2520 or CC1101 radios, the models of which are provided by MiXiM. The X-MAC implementation in this chapter strictly follows both X-MAC paper [10] and MiXiM design guidelines [62].

→ In some applications, it is convenient that the receiver node starts the communication. This paradigm is called Receiver Initiated communication. RI-MAC [64] in Figure 6.2 is the reference WSN MAC protocol for RI communications and presents a noticeably different performance for certain applications when compared to IEEE 802.15.4, B-MAC and X-MAC, which are all Transmitter Initiated protocols. In the active part of its duty cycle, a RI-MAC node without any packet to transmit indicates this condition by sending a beacon. Nodes that require delivering a data frame to this node proceed to listen to the medium for a prolonged time slot. The reception of the beacon from the ready-to-receive node precisely acts as the trigger to start communication. This procedure is effectively the reverse equivalent of a preamble. Upon reception of a beacon from the intended receiver, the transmitter node proceeds to send the data frame. Thus, RI-MAC achieves lower power consumption if the power for packet reception is higher than for transmission and the data traffic and node density are not high, since all the nodes without queued packets contend for sending their beacons during their active period. RI-MAC does not suffer from long preambles occupying the medium. However, as in B-MAC and X-MAC, RI-MAC also suffers from an unavoidable current consumption because of its periodic beacon sending.

By considering the following equations for X-MAC, the rest of the approaches can be expressed in an simplified, yet analogous and useful, manner. In X-MAC, the expected energy to send a packet E_s is:

$$\begin{aligned} E_s = [&(\textit{preamble energy} + \textit{energy per ACK listen}) \times \\ &(\textit{expected preamble iterations})] + \\ &\textit{energy to send packet} \end{aligned} \tag{6.1}$$

From Equation 6.1, an approximation for sending a packet in B-MAC can be obtained by considering *expected preamble iterations* = 1 and *energy per ACK listen* = 0:

$$\begin{aligned} E_s = [&(preamble\ energy\ +\ 0) \times \\ &(1)] + \\ &energy\ to\ send\ packet \end{aligned} \tag{6.2}$$

From Equation 6.1, an approximation for sending a packet in RI-MAC can be obtained by considering *expected preamble iterations* = 1 and *preamble energy* = 0:

$$\begin{aligned} E_s = [&(0\ +\ energy\ per\ beacon\ listen) \times \\ &(1)] + \\ &energy\ to\ send\ packet \end{aligned} \tag{6.3}$$

On the other hand, the expected energy to receive a packet E_r in X-MAC is:

$$\begin{aligned} E_r = [&(listen\ cycle\ energy\ +\ sleep\ cycle\ energy) \times \\ &(expected\ preamble\ iterations\ on\ reception)] + \\ &energy\ to\ send\ ACK\ + \\ &energy\ to\ receive\ packet \end{aligned} \tag{6.4}$$

From Equation 6.4, an approximation for receiving a packet in B-MAC can be obtained by considering *expected preamble iterations on reception* = 1 and *sleep cycle energy* = 0 and *energy to send ACK* = 0:

$$\begin{aligned} E_r = [&(listen\ preamble\ energy\ + 0) \times \\ &(1)] + \\ &0\ + \\ &energy\ to\ receive\ packet \end{aligned} \tag{6.5}$$

From Equation 6.4, an approximation for receiving a packet in RI-MAC can be obtained by considering *listen cycle energy* = 0 and *sleep cycle energy* = 0 and *expected preamble iterations on reception* = 0:

$$
\begin{aligned}
E_r = [(0 + \ 0) \times \\
(0)] + \\
energy\ to\ send\ beacon + \\
energy\ to\ receive\ packet
\end{aligned}
\tag{6.6}
$$

Thus, from Equations 6.1, 6.2 and 6.3, and by removing the common *energy to send packet* term, it can be deduced than sending a packet in X-MAC, B-MAC and RI-MAC, respectively, mainly depends on *expected preamble iterations* (related to contention), *preamble energy* and *energy per beacon listen parameters* . IEEE 802.15.4 presents a common maximum energy value.

Accordingly, from Equations 6.4, 6.5 and 6.6, and by removing the common *energy to receive packet* term, it can be deduced than receiving a packet in X-MAC, B-MAC and RI-MAC, respectively, mainly depends on *expected preamble iterations on reception* (related to contention), *listen preamble energy* and *energy to send beacon* . IEEE 802.15.4 presents a common maximum energy value.

6.3.2 Wake-up Radio Design Implementation

As seen in the node model in Figure 6.1, WuR nodes in the proposed model feature two radio transceivers; the main transceiver and the wake-up transceiver, respectively located in the Data and Wake-up Radio modules. This two-radio model enables the simulation of any kind of WuR system, either with two physically separated radio interfaces or with a shared transceiver, as in the SCM-WuR case. Independently of its hardware implementation, the operation of WuR in Transmitter and Receiver Initiated flavors is depicted in Figure 6.3.

In the general case of WuR, MCU and the main data communication transceiver are initially switched off to reduce the energy consumption, while the wake-up radio is left activated to monitor the channel. However, different to traditional transceivers, WuRx only employ few μA for such activity. The SCM-WuR MiXiM model in Figure 6.1 precisely emulates the behavior of a WuR system. When a node wants to communicate, it first transmits a WuC via its WuTx. At the receiver node, a WuRx receiving a WuC generates an interrupt to wake up the node's MCU, which in turn switches on the main transceiver so that upcoming data frames can be received in a traditional fashion through the main radio. After the MCU of the node is activated, it may perform several tasks before disabling the data transceiver and going to low-power WuR mode again, such as receiving an incoming data frame (TI-WuR approach), or obtaining a measurement from a sensor and sending back the data (RI-WuR approach). In Figure 6.1, incoming and outgoing WuCs are managed by the Wake-up Radio block, while traditional communications are done through the Data Radio block, which implements IEEE

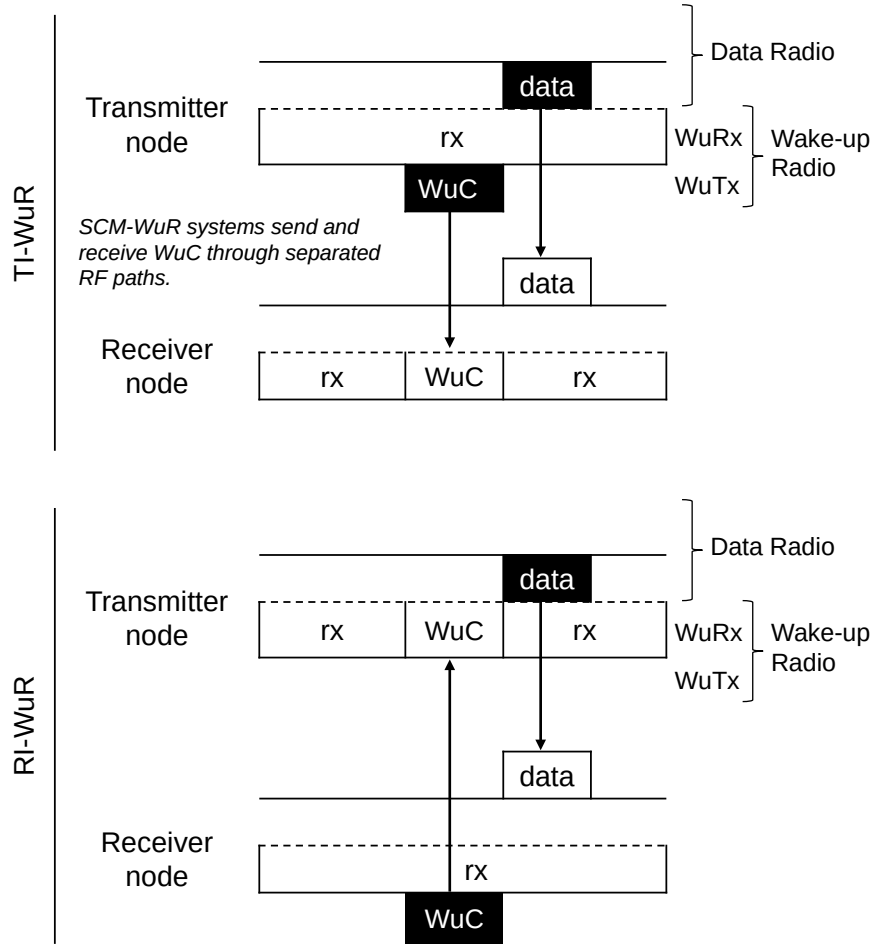

Figure 6.3: Working principles of the WuR approach. Differently to data Radios, WuRx only requires feu μA to operate.

802.15.4 during the short amounts of time it gets activated by the Control block in Figure 6.1 upon WuC detection by the WuRx.

As explained in chapter 4, a SCM-WuR node may dinamically operate as either WuRx or WuTx by simply adjusting its MCU's configuration. This flexibility is useful when the same node must be able to use both Transmitter and Receiver Initiated approaches. For example, some nodes may be interested in reporting notifications (e.g., sending sensor measurements without a previous query) or may provide responses to queries (e.g., about the last temperature measurement). Code 6.1 shows a fragment of the code of the Finite State Machine (FSM) of the Wake-up Radio implementation in OMNET++ / MiXiM. Along the code, comments also help identifying the different stages.

```
void Dual_Mode::handleSelfMsg(cMessage* msg) {

    // FSM for WuR acting as Transmitter-Initiated
    switch (FSM_STATE) {

    . . .

    // SLEEP_STATE (send OR receive WuC)
    // *********************************
    case SLEEP_STATE:
    // generating WuC
    // --------------
    if((msg->getArrivalGateId() == upperLayerIn_dual) && (msg->getKind() == APP_WUC_MESSAGE)) {
        send(msg, lowerLayerOutWuR_dual);
        FSM_STATE = WUC_TO_DATA_TX_STATE;
    }
    // WuR receiving WuC
    // -----------------
    else if(msg->getArrivalGateId() == lowerLayerInWuR_dual && (msg->getKind() == APP_WUC_MESSAGE)) {
        NetwPkt* incoming_wuc = static_cast<NetwPkt*>(msg);
        if (incoming_wuc->getDestAddr() == findHost()->getIndex()) {
            // main NIC on
            __MACRO_RADIO_RX_ON__
            cancelEvent(rx_timeout_msg);
            scheduleAt(simTime() + RX_TIMEOUT, rx_timeout_msg);
            FSM_STATE = RX_DATA_STATE;
            delete msg;
        }
    }
    // WuR receiving DATA_MESSAGES (not even possible)
    // -----------------------------
    else if(msg->getArrivalGateId() == lowerLayerInWuR_dual && (msg->getKind() == APP_DATA_MESSAGE)) {
        delete msg;
    }
    break;

    // WUC_TO_DATA_TX_STATE (send Data)
    // ********************************
    case WUC_TO_DATA_TX_STATE:
    // send Data
    // ---------
    if((msg->getArrivalGateId() == upperLayerIn_dual) && (msg->getKind() == APP_DATA_MESSAGE)) {
```

```
43          dual_to_phy = FindModule<MacToPhyInterface*>::findSubModule(this->↙
    ↳ getParentModule());
44          send(msg, lowerLayerOut_dual);
45          FSM_STATE = TX_DATA_STATE;
46      }
47      else if (msg->getKind() == RADIO_SWITCHED) {
48          delete msg;
49      }
50      break;
51
52      // TX_DATA_STATE (to end)
53      // **********************
54      case TX_DATA_STATE:
55      // when TX_over, return to sleep
56      // -----------------------------
57      if ((msg->getArrivalGateId() == lowerControlIn_dual) && (msg->getKind() ↙
    ↳ == TRANSMISSION_OVER)) {
58          FSM_STATE = INIT_STATE;
59          scheduleAt(simTime() + TIME_TO_GO_TO_SLEEP, init_msg);
60          delete msg;
61      }
62      else if (msg->getKind() == RADIO_SWITCHED) {
63          delete msg;
64      }
65      else if (msg->getKind() == MAC_ERROR) {
66          FSM_STATE = INIT_STATE;
67          // RESET
68          scheduleAt(simTime() + 0.1, init_msg);
69          delete msg;
70      }
71      break;
72
73      // RX_DATA_STATE (to end)
74      // **********************
75      case RX_DATA_STATE:
76      // main receiving DATA
77      // -------------------
78      if ((msg->getArrivalGateId() == lowerLayerIn_dual) && (msg->getKind() == ↙
    ↳ APP_DATA_MESSAGE)) {
79          NetwPkt* incoming_data = static_cast<NetwPkt*>(msg);
80          if (incoming_data->getDestAddr() == findHost()->getIndex()) {
81              cancelEvent(rx_timeout_msg);
82              recordPacket(PassedMessage::INCOMING, PassedMessage::LOWER_DATA, ↙
    ↳ msg);
83              send(msg, upperLayerOut_dual);
84              FSM_STATE = INIT_STATE;
85              scheduleAt(simTime() + TIME_TO_GO_TO_SLEEP, init_msg);
86          }
```

```
87      }
88      // main receiving WuC (not even possible)
89      // ------------------
90      if ((msg->getArrivalGateId() == lowerLayerIn_dual) && (msg->getKind() == ↙
        ↳ APP_WUC_MESSAGE)) {
91          delete msg;
92      }
93      // we have a timeout because no received DATA after being activated
94      // ---------------------------------------------------------------
95      else if (msg->getKind() == RX_TIMEOUT_MSG_TYPE) {
96          FSM_STATE = INIT_STATE;
97          scheduleAt(simTime() + TIME_TO_GO_TO_SLEEP, init_msg);
98      }
99      else if (msg->getKind() == RADIO_SWITCHED) {
100         delete msg;
101     }
102     break;
103     }
104     return;
105 }
```

Code 6.1: SCM-WuR message handling implemented in MiXiM.

The code is programmed as a FSM that the MCU of the node visits depending on the messages it receives. These messages can be both external (a WuC, a data frame) or internal (a timer, a CCA, a timeout, a message for the FSM to go to next state, etc.). Messages may arrive to *Wake-up Radio* module in Figure 6.1 from both upper and lower layers and can be data packets or control packets. For example, when in `SLEEP_STATE` the node may be required to wake-up a further node by the *Application* layer in Figure 6.1 generating a `APP_WUC_MESSAGE`. Thus, such message comes from *upperLayerIn*. If instead the node, when in `SLEEP_STATE`, is activated by a WuC incoming from a remote node, such message comes from the *lowerLayerInWuR* gate. As another example, the *lowerControlIn* entry point, or gate in OMNET++ terminology, represents the control channel from the lower PHY layer. Messages are parsed depending on the current FSM state. For example, in Code a SCM-WuR node which reaches the `RX_DATA_STATE` has correctly been woken up. At this point, since Code 6.1 refers to a transmitter initiated approach, the node may:

→ Receive a data packet `APP_DATA_MESSAGE`. This packet must contain the correct address of the node.

→ Receive a WuC. In this state, receiving a WuC does not imply any change in the FSM. However, the simulation framework does not allow to receive a data packet at the same time of a WuC.

→ Expire a radio time-out. After switching to `RX_DATA_STATE` upon detecting a WuC, the transceiver of node should remain in reception only for a limited amount of time. If no frame arrives during this time, in order to save energy the node must sleep again.

In this chapter, the 100-m version of the SCM-WuR is considered, that is the one implementing a power amplifier at the WuTx. A SCM-WuR board features as low as 3.5 µA when operating as WuRx in low-power wake-up mode and no WuC is present. This value increases up to 8 µA when the WuRx is decoding the address embedded in an incoming WuC. Regarding the transmitter side, the WuTx role requires up to 152 mA when sending a WuC to achieve the 100 meters range. This way, SCM-WuR transmissions present operational ranges comparable to traditional wireless sensor communications. However, due to the fact that WuRx designs are kept simplistic in order to operate in the mA order of magnitude, WuC transmissions in SCM-WuR require noticeably more power than conventional data frames to be detected. As a counterpart, and unlike duty-cycling systems, this energy for transmitting a WuC is only employed when really required, instead of employing it periodically, e.g., to check the wireless medium. In addition, the SCM-WuR platform is perfectly capable of performing multi-hop, as shown in chapter 4, Figure 4.8b.

Compared to MAC protocols, SCM-WuR only presents the consumption of a WuC per packet when sending and divides the consumption for receiving packets of any of the previous MAC approaches by at least a factor of 1000.

6.4 Performance Results

Three application scenarios are considered in this section; a single-hop scenario and two multi-hop scenarios, one with static topology and one with mobile topology. Each of the four WSN MAC protocols and the SCM-WuR approach are evaluated for every scenario.

6.4.1 Evaluated Scenarios

The three application scenarios are depicted in Figures 6.4a and 6.5. Network nodes are colored lighter, while darker ones represent interference sources modeled as contention generators that perform their own transmissions not intended for the current network. Contention nodes run the same protocol under evaluation as the network nodes. However, their transmissions are directed to a node address not present in the network evaluated. Thus, they can be considered as collocated networks deployed close to the one under evaluation that transmit packets in an uniform(1 s, 10 s) time distribution.

Several aspects for each scenario are studied along the performance evaluation in this chapter, such as the effect of diverse metrics like variable data-rates, the mobile node's speed or the duty cycle featured by nodes implementing the MAC protocols, where appropriate.

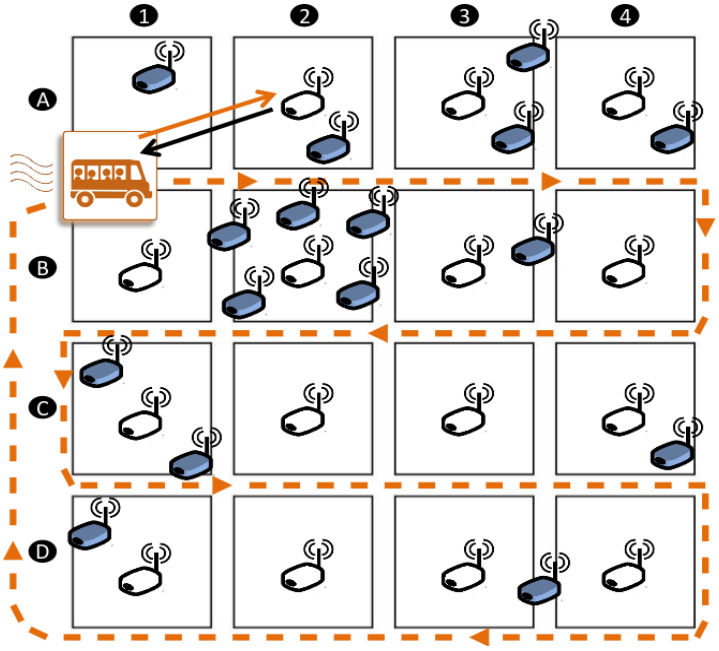

(a)

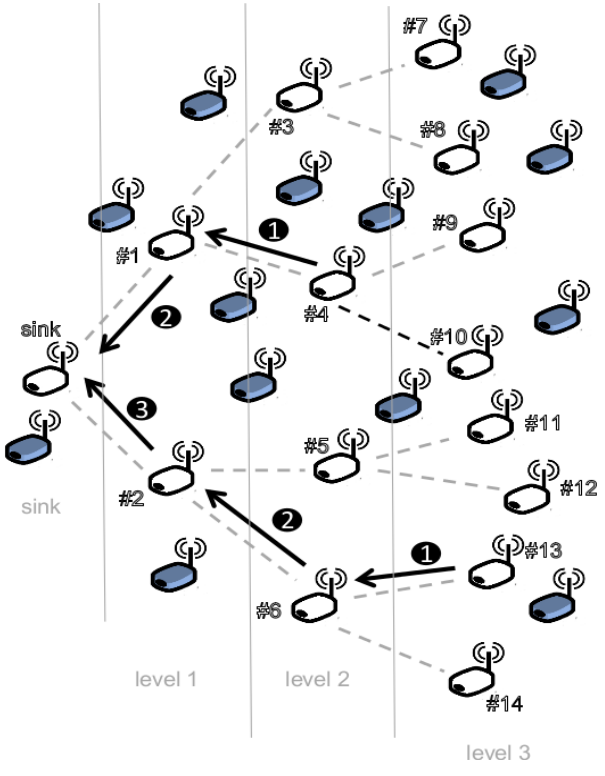

(b)

Figure 6.4: The two first scenarios analyzed in this chapter: (a) data-collector mobile single-hop; (b) converge-cast tree, or static multi-hop.

The first scenario in Figure 6.4a depicts a single-hop use case where a mobile data-collector, e.g., a bus, train, drone or robot, collects information from sensors deployed along its route. The collector node's mobility pattern of a *bus* is indicated by arrows in the figure and is periodic. Around a real city, the wireless sensors to be queried may be attached to trees,

garbage containers, or they may also represent energy utility meters installed inside nearby buildings. This simulation corresponds to an ongoing real project as of 2014 in Sant Vicenç dels Horts, Barcelona [74].

The scenario in Figure 6.4b depicts a WSN deployed as a multi-hop static binary tree topology, which is common in the WSN literature [68]. Basically, intermediate nodes are in charge of forwarding packets from their immediate child nodes and those ones, in turn, from their own descendant nodes. This network configuration is widely employed for monitoring applications, e.g., for precision agriculture.

Finally, the scenario in Figure 6.5 depicts a multi-hop mobile scenario where a mobile data-collector, e.g., a bus, train, drone or robot, collects information from chains of sensors. For example, sensor nodes can be attached at pillars of a bridge or along the side streets of a main road. Thus, this scenario can be considered to be a combination of the previous two. A variation of this use case is currently deployed and monitored in Germany. The bus, tree and bridge applications in Figures 6.4a, 6.4b and 6.5 may be considered respectively as networks that require an instantaneous response, a network with stable and constant throughput, and a mix between the previous two.

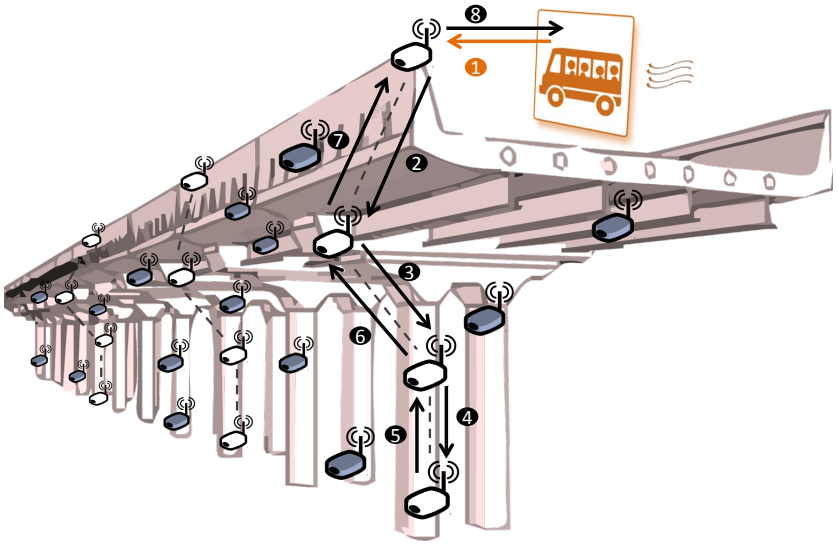

Figure 6.5: The third scenario analyzed in this chapter: (c) data-collector mobile multi-hop.

Table 6.1 summarizes the most important simulation parameters. Common parameters such as the maximum number of transmission attempts or the default duty cycle are set to usual values for WSN-related MAC protocols. Values for B-MAC and IEEE 802.15.4 are kept untouched from their MiXiM implementations. Only the current consumption of the B-MAC transceiver has been explicitly modified and set to be equal to the one used for the rest of MAC protocols for fair comparison. The parameters of the implementations of X-MAC, RI-MAC and WuR are taken from the respective reference papers [10], [64] and [61].

Table 6.1: Simulation Parameter Set.

Approach	Parameter	Value	Unit
Common	Supply Voltage	3	V
	Battery Capacity	1500	mAh
	Reception Current	18.8	mA
	Transmission Current	17.4	mA
	Sleep Current	0.02	µA
	Packet Payload	100	bytes
	Queue Buffer Length	10	packets
	Maximum Transmission Attempts	2	retries
	Distance between Nodes	150	m
	Scenario Duration w/ Interferers	3	hours
	Scenario Duration w/o Interferers	12	hours
	Default duty cycle	1	%
	Bit Error Rate	10^{-8}	%
	Signal Model	SimplePathLoss	
	Path Loss Exponent	3.2	
IEEE 802.15.4	Bit-rate	250	kbps
	Slot Duration	100	ms
	Backoff Exponent	3 to 8	slots
B-MAC	Bit-rate	15360	kbps
	Slot Duration	1	s
X-MAC	Bit-rate	250	kbps
	Slot Duration	1	s
RI-MAC	Bit-rate	250	kbps
	Slot Duration	1	s
Wake-up Radio	Sleep Current	3.5	µA
	Bit-rate	250	kbps
	WuC Duration	12.2	ms
	Reception Current (WuRx)	8	µA
	Transmission Current (WuTx)	152	mA

Ten simulation runs with different random seeds are performed for each parameter combination, which comprises scenario, communication protocol and metric under analysis. Confidence intervals of 95% are provided in the plots representing all these repetitions, as long as they are scientifically significant. Random seeds are used for different aspects, such as initial interfering nodes' placements or initial time offsets for periodic packet generation. The obtained results are processed by specific scripts for the R statistical software specifically developed for OMNET++, like the one in Code 6.2. In the code, the statements for initialization and fetching and loading of the result files have been intentionally omitted for the sake of brevity. Along the code, comments also help identifying the different stages.

Basically, Code 6.2 collects results such as time and energy from OMNET++ scalar files (**.sca*) and organizes them by node and variables under evaluation. Afterwards, mean values and confidence intervals are calculated. In this case, the network lifetime is obtained by

```
# initial vars cleanup
batt_capacity = 1500

# calculate mean and confidence intervals
averaged_scalars    <- cast(averaged_scalars, experiment+measurement+module+
    ↳ name ~ ., c(mean, sd, conf.int(0.95)), fill = NA)
colnames(averaged_scalars)[7] <- "ci"

# add the mean of all modules but SINK, and get confidence intervals
maxMeanCC <- averaged_scalars[averaged_scalars$name == "Mean current 
    ↳ consumption",]
maxMeanCC <- maxMeanCC[-grep("node[0]", maxMeanCC$module, fixed=TRUE),]
max_by_group  <- sqldf("select experiment, measurement, max(mean), module 
    ↳ from maxMeanCC group by experiment,measurement")
maxMeanCC <- ddply(maxMeanCC, experiment~measurement, summarise, maxim_CC = 
    ↳ max(mean))
maxMeanCCci   <- averaged_scalars[averaged_scalars$name == "Mean current 
    ↳ consumption",]
maxMeanCCci   <- maxMeanCCci[-grep("node[0]", maxMeanCCci$module, fixed=TRUE)
    ↳ ,]
maxMeanCCci   <- ddply(maxMeanCCci, experiment~measurement, summarise, maxim_
    ↳ ci = mean(ci))
maxCCstuff  <- maxMeanCC

# calculate lifetime
maxCCstuff$maxim_CC <- (batt_capacity / maxMeanCC$maxim_CC) / 24
maxCCstuff$ci       <- maxMeanCCci$maxim_ci

# get the range for the x and y axis, common for all nodes
xrange <- maxCCstuff$measurement
etiquetes = c("B-MAC", "IEEE 802.15.4", "RI-MAC", "SCM-WuR", "X-MAC")

# group means "common var to join the dots"
my_title <- "Minimum_lifetime_of_nodes_of_the_network"
my_plot  <- ggplot(maxCCstuff, aes(x=xrange, y=maxim_CC, shape=experiment, 
    ↳ lty=experiment, group=experiment, color=experiment)) +
    geom_errorbar(aes(ymin=maxim_CC-ci, ymax=maxim_CC+ci), width=.3) +
    geom_line() + geom_point(size=6) +
    scale_y_log10(breaks=c(0,10,100,1000,10000)) +
    scale_shape_discrete(name = "", labels=etiquetes) +
    scale_color_discrete(name = "", labels=etiquetes) +
    scale_linetype_discrete(name = "", labels=etiquetes) +
    ylab("Lifetime (days)") +
    #eliminates baground, gridlines, and chart border
    theme(
      plot.background = element_blank()
      ,panel.grid.major = element_blank()
      ,panel.grid.minor = element_blank()
      ,panel.border = element_blank()
      ,panel.background = element_blank()
      ,text = element_text(size=30)
      ,legend.key = element_rect(fill = "white",colour = "white")
      ,legend.background = element_rect(colour = "black")
      ,legend.position="top") +
    # draws x and y axis line
    theme(axis.line = element_line(color = 'black')) +
    scale_fill_hue(name = "", labels=c("B-MAC", "IEEE 802.15.4", "RI-MAC", "
    ↳ SCM-WuR", "X-MAC"))
```

Code 6.2: Calculating the minimum lifetime of a network in R.

considering the consumption of the most energy-demanding node (that is Node 1 or Node 2) and dividing such value by the capacity of the battery. Finally, the results are plotted. Similar scripts are obtained for the entire set of metrics under evaluation such as Packet Delivery Ratio, latency, etc.

6.4.2 Single-hop Scenario

The single-hop scenario, shown in Figure 6.4a, depicts the use case of a data-collector node which collects information from 15 sensors deployed along its route. The area for this simulation simulation scenario is ~1 km^2 and the vehicle moves at 10 m/s. Only statistics for the nodes pertaining to the evaluated network (in clear) are collected. Darker interferer nodes are considered to be part of coexisting systems which interfere with the system's network under evaluation.

The presented single-hop scenario is a very typical case, where the data-collector, or the node which starts the communication, has no power restrictions. Differently, the field-deployed nodes must save as much energy as possible, exploiting the infrequent nature of the data communications. Because of this, use of inefficient medium listening procedures must be minimized. Thus, this is a clear example of a Receiver Initiated scenario, where the receiver is the data collector. Accordingly, for the WuR approach the RI-WuR variant is considered. When querying a specific node by means of its node address, the data-collector transmits a packet and expects a response back. In real applications, the data-collector is equipped with a GPS application to determine the querying of the sensors in the area. If a response from the queried node does not arrive in time, the data-collector tries up to the *maximum packet retransmission attempts* value given in Table 6.1 before removing the query from the queue and proceeding to consult the next node in the grid as it approaches it. For this scenario, the Packet Delivery Ratio, or PDR, is defined as the ratio of responses received back at the mobile node, over the number of performed queries. Thus, the PDR metric represents in a very direct manner the global success of the communication protocol being evaluated.

6.4.2.1 Effect of the Duty Cycle Ratio

The ratio of time a node is active, i.e., its duty cycle, is varied in order to quantify the effect of such parameter on the PDR and average power featured by the MAC protocols in the single-hop scenario. Exactly 30 interferer nodes are randomly deployed along the scenario. The effect of these variations on different metrics can be observed in Figures 6.6 and 6.7, respectively.

As expected, the only approaches the change of the duty cycle ratio affects significantly in Figure 6.6 are Transmitter Initiated MACs, i.e., B-MAC and X-MAC, which practically double their PDR results when increasing the duty cycle to the maximum value studied. The rest of approaches under evaluation allow for 100% PDR in all cases.

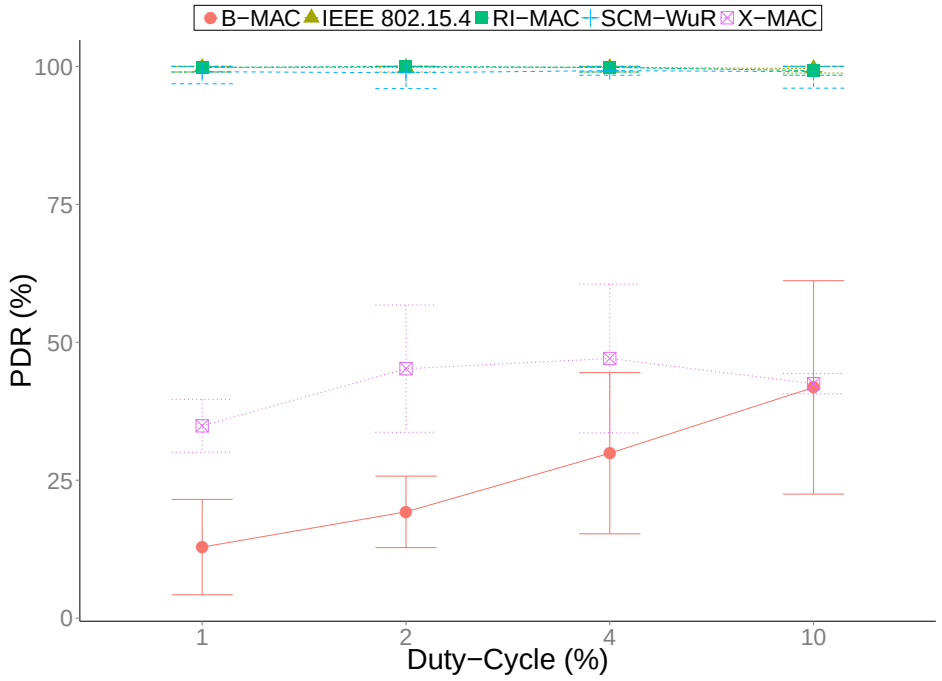

Figure 6.6: Effect of the duty cycle ratio on the network's PDR for the single-hop scenario from Figure 6.4a.

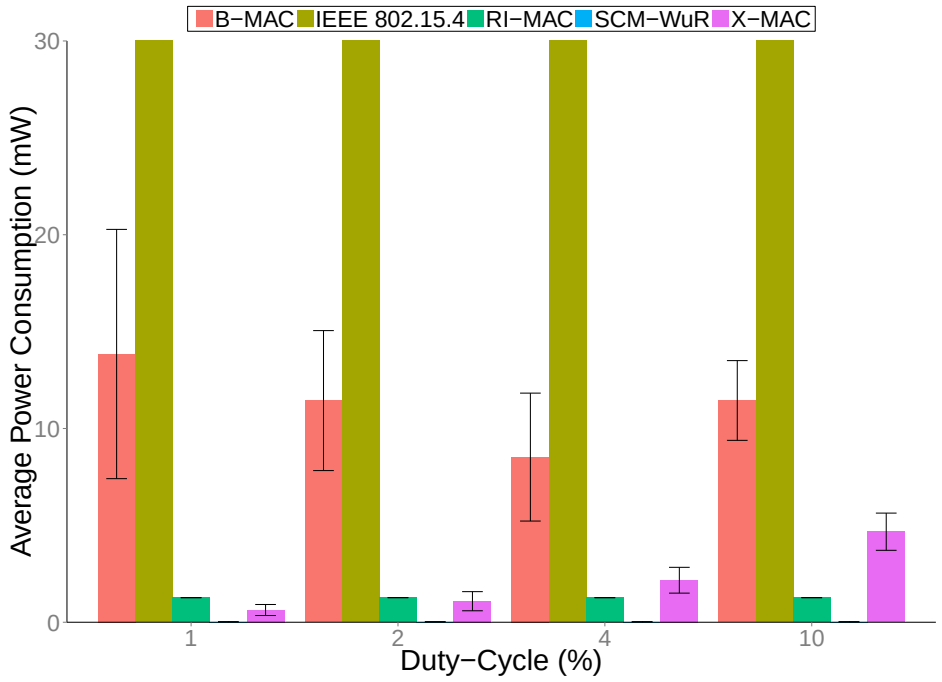

Figure 6.7: Effect of the duty cycle ratio on the overall average power consumed by the nodes for the single-hop scenario from Figure 6.4a.

B-MAC achieves this PDR doubling in a more linear manner than X-MAC since the latter, because of its strobed preamble, shows slightly better performance in terms of PDR immediately, even for low duty cycle ratios. However, B-MAC and X-MAC behave drastically different

in terms of power consumption. In Figure 6.7, while X-MAC, as it would be expected, slightly increases the average nodes' power consumption according to the duty cycle, B-MAC decreases its power consumption. This is because a larger duty cycle means shorter preambles, which effectively reduces the network contention and accordingly increases the PDR for B-MAC. IEEE 802.15.4 power consumption, in turn, is constant throughout all evaluated results and approximately 60 mW = 3 V × 17.4 mA, since no duty cycle takes place in this approach. By considering altogether graphs in Figures 6.6 and 6.7, it is clear that SCM-WuR provides the best trade-off between PDR and consumed power among all approaches.

6.4.2.2 Effect of Coexistent Network Interference

The effect of interferers on the network performance is modeled by varying the number of dark color nodes in Figure 6.4a, configured to generate and transmit packets in an uniform(1 s, 10 s) time distribution. These packets, not intended for any node in the evaluated network, generate contention as they occupy the wireless medium. Duty cycle of the MAC approaches is now set constant at 1%.

Again, PDR is defined as the ratio of responses received from network nodes by the mobile node, over the number of performed queries. The effect of the node contention over the network's PDR is clear in Figure 6.8 for protocols based on preambles. If a node is placed among several contenders, its response may not reach its way back to the collector node in time, even after several retransmissions.

B-MAC features 100% PDR as X-MAC only when no interferences are present. Because of its strobed preamble, X-MAC performs better than B-MAC under contention. When 30 interferers are present, in fact, PDR results are analogous to the ones in section 6.4.2.1 dor a duty cycle value of 1%, which reaffirms the consistence of the simulations. In turn, IEEE 802.15.4, RI-MAC and SCM-WuR, because of their better management of the wireless medium, provide a constant PDR very close to 100%.

For realistic and useful performance reviews, PDR results must be assessed along with the power consumed by the network nodes. Figure 6.9 precisely depicts the average lifetime of the network, understood as the average number of days a sensor node in the network in Figure 6.4a may last without requiring a battery replacement. Lifetime measurements in Figure 6.9 show that, when some degree of interference is expected, B-MAC is the approach performing worst in terms of lifetime. The figure shows how WuR extends lifetime by several orders of magnitude when compared to the duty-cycled approaches. B-MAC, due to its long preamble, features high power consumption. In turn, X-MAC's strobed preamble allows at least for some extended lifetime by detecting not intended preambles from surrounding nodes. However, as seen in Figure 6.8, this comes at the cost of slightly lower PDR. On the other hand, IEEE 802.15.4 achieves perfect PDR along the worse lifetime results. RI-MAC, appears to be the best MAC protocol approach in terms of PDR, mainly because of its clever management of

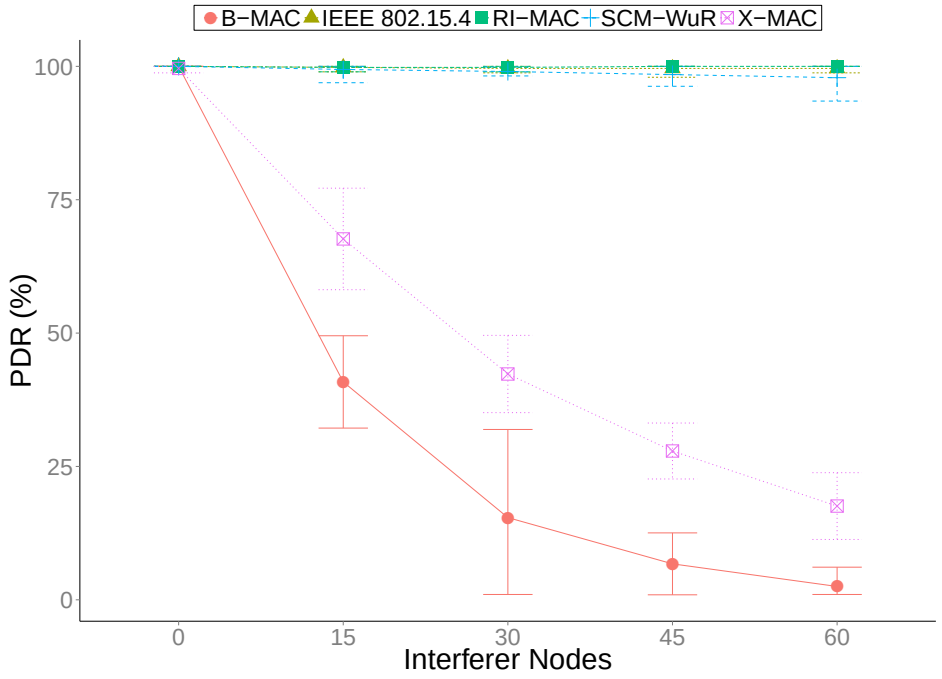

Figure 6.8: Effect of the number of interferer nodes on the PDR for the single-hop scenario.

the wireless medium. However, because of being based on duty cycle, RI-MAC power savings can never improve the mA order of magnitude. In this subject, SCM-WuR performs the best and offers the optimum trade-off. Globally, the WuR solution allows for the best results combination by providing both excellent PDR and lifetime results, thanks to its µA current consumption when in sleep mode and its implicit resilience to WuC generated by interferer nodes thanks to its hardware address correlation, explained in chapter 3, section 3.2.3.

6.4.3 Multi-hop Static Scenario

In order to effectively compare the performance of the studied approaches for multi-hop static scenarios, a binary tree as in Figure 6.4b is defined, where packets are sent in a regular manner towards the sink in a multi-hop fashion. Thus, differently from the single-hop scenario in section 6.4.2, this scenario follows a Transmitter Initiated paradigm where nodes constantly generate packets instead of waiting to be queried. For the WuR approach, TI-WuR is considered. Packet routes are predefined to do the performance comparison independently of the employed routing protocol, if any. Under this *tree topology*, the network nodes periodically generate data packets and send them to their parent nodes, which are in charge of forwarding the packets towards the sink. Along this scenario, PDR is defined as the number of packets received at the sink over the total number of packets generated during the experiment by all network nodes. Transmissions from interferer nodes are not accounted for PDR measurements. No data aggregation strategy is considered.

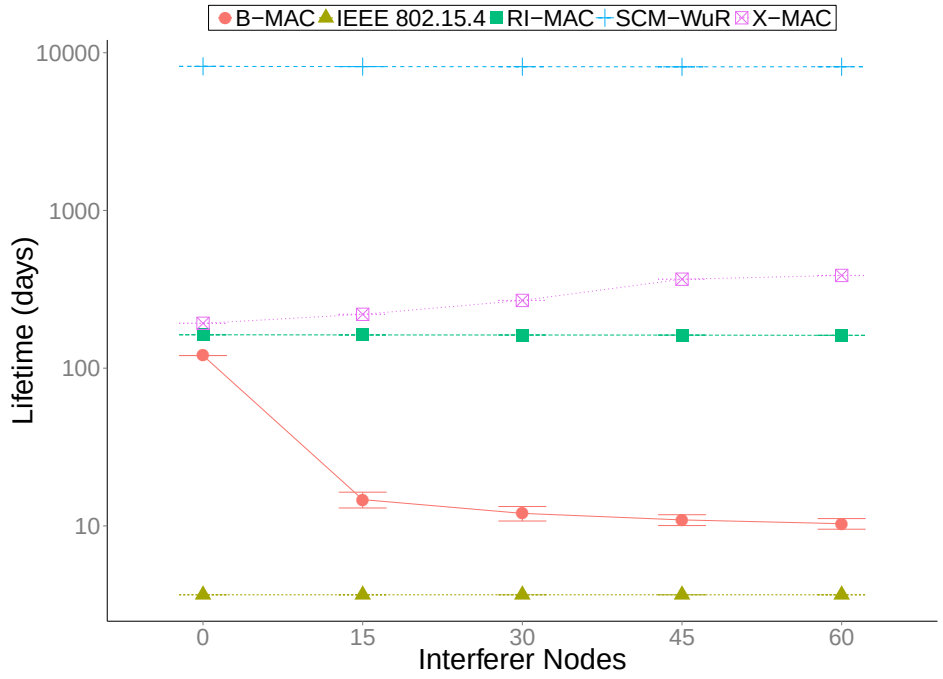

Figure 6.9: Effect of the number of interferer nodes on the network lifetime for the single-hop scenario (logarithmic graph).

6.4.3.1 Effect of the Duty Cycle Ratio

In this section, the network nodes are set to generate a packet every 10 seconds. Interestingly, when considering a number of retransmissions up to the *maxAttempts* parameter in Table 6.1, a 100% value for PDR is not achieved by any approach in this multi-hop static scenario even for no-contention circumstances, as shown in Figure 6.10. In addition, and differently to section 6.4.2.1, in this case RI-MAC performs as poor as any other duty-cycled MACs because in this tree application the duty cycle does not vary the network performance in terms of PDR. This is because the long preamble and high number of strobed preambles and beacons in B-MAC, X-MAC and RI-MAC respectively, prevent nodes running any MAC approach to successfully process the totality of both their own transmissions and the ones coming from the nodes they are in charge of. A node is also unable to process communication when performing a retransmission of one packet which has been unable to process previously. These issues result in poor PDR. Differently, in applications where transmission depends on a query, such as the single-hop scenario, the benefit of duty-cycling is clearer since nodes do not suffer of accumulating pending jobs.

Regarding power consumption, since for a packet generation rate of 10 seconds, Node 1 in Figure 6.4b, that is, one of the two most energy-demanding nodes in the network, is permanently busy, it does not change its power profile in Figure 6.11 when varying duty cycle ratios for MAC protocols.

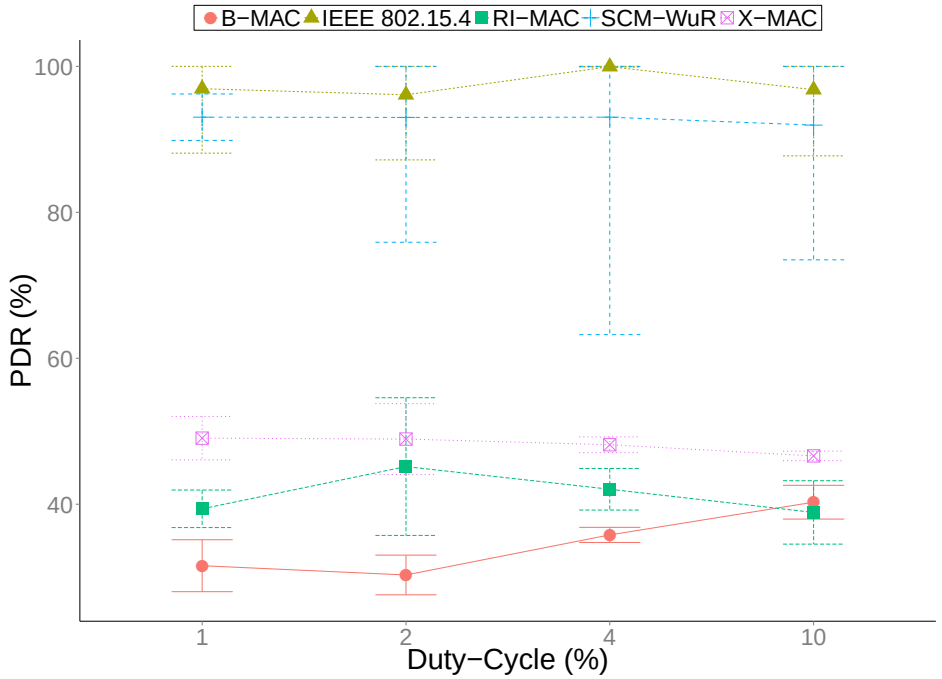

Figure 6.10: Effect of the duty cycle on the PDR for the multi-hop static scenario.

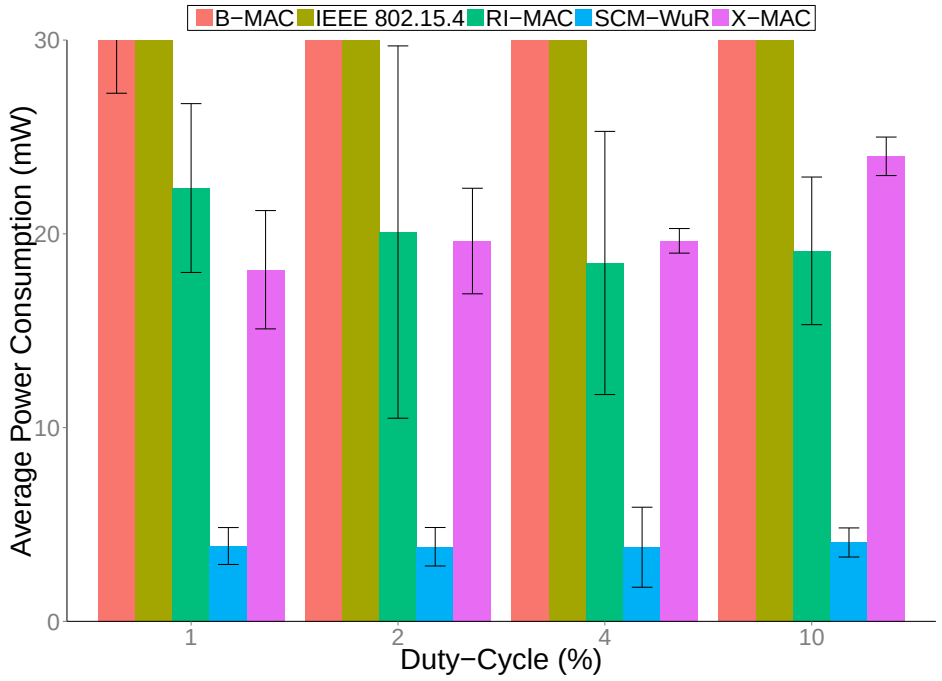

Figure 6.11: Effect of the duty cycle on the mean power consumption of Node 1 for the multi-hop static scenario.

In fact, Node 1's mean power consumption values are used to calculate the network lifetime, which is measured to be about 3 days, 12 days, 18 days, 20 days and 140 days in average for IEEE 802.15.4, B-MAC, X-MAC, RI-MAC and SCM-WuR, respectively. These lifetime values are much lower than the ones for the single-hop scenario due to the constant traffic load of

the tree scenario, much more persistent than the one for the single-hop scenario where nodes are allowed to sleep for much longer periods of time and only queried sporadically.

6.4.3.2 Effect of the Packet Generation Period

The time between consecutive packet generations by nodes in the network is varied in order to evaluate the tree network performance under different traffic loads, i.e., data rates. As a numerical example, if the packet generation period is 10 seconds, a node placed at penultimate level of the tree will have to forward 2 packets, 1 from each child, as well as to generate its own packet, for a total of 3 packets every 10 seconds. Nodes closer to the sink are naturally in charge of forwarding many more packets than the nodes closer to the leaf nodes. Packet generation periods are tested starting at 300 s and go down gradually to 1 s to increase the traffic load. Figure 6.12 shows the PDR achieved by the five approaches investigated for different packet traffic loads.

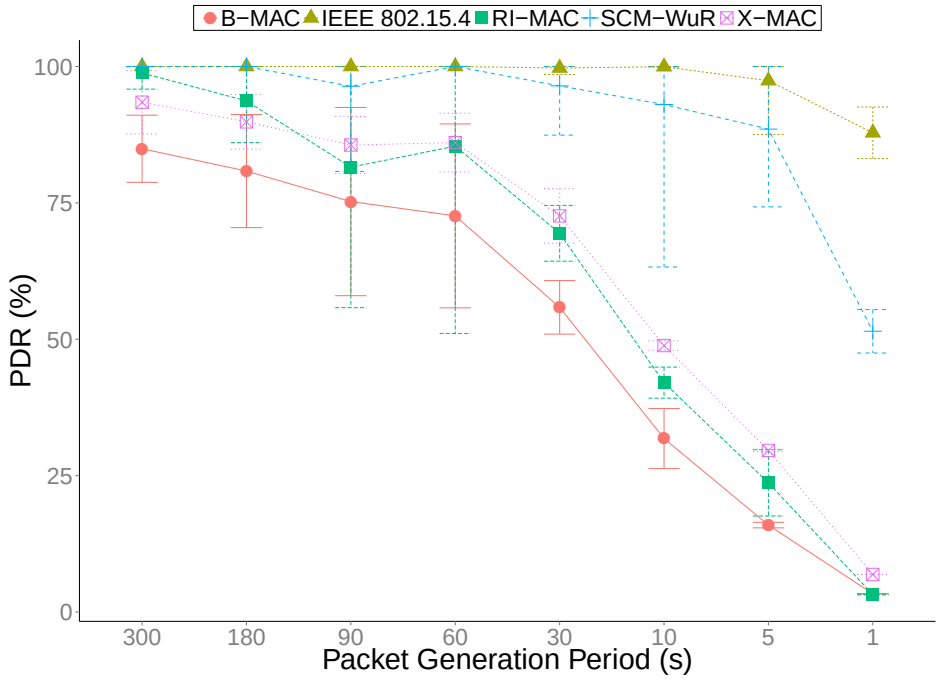

Figure 6.12: Effect of the packet generation period on the network PDR for the multi-hop static scenario.

As seen in the figure, B-MAC results in a PDR close to 0% when time between packet generations approximates 1 second. Since the B-MAC's preamble duration is also 1 second, this circumstance saturates the network. However, few WSN applications are required to transmit this often and packet generation periods longer than 30 seconds are much more common. In B-MAC, wait periods due to busy medium can be significant because of the long preamble duration and, in addition, during this procedure both transmitting node and nodes that are detecting the preamble cannot receive any packets from any other node. Moreover,

surrounding nodes' energy consumption is also increased, since in B-MAC they cannot sleep until receiving the data frame containing the address of the destination node, which comes after the preamble. For nodes in charge of forwarding packets from a greater number of descendants, this issue is even more pronounced. X-MAC suffers from the same issue as B-MAC, but thanks to its strobed preamble it slightly diminishes its effect and offers a better PDR. In turn, IEEE 802.15.4 and SCM-WuR provide good PDR values close to 100% except in the most demanding use case. In case of WuR, considering each data communication includes both WuC and data packet, Nodes 1 and 2 simply cannot attend all incoming transmissions taking place in the tree for packet generation periods of 1 and 5 seconds. On the other hand, while in the previous scenario RI-MAC offered similar performance in terms of average consumed power but much better PDR than B-MAC and X-MAC, because of the Transmitter Initiated nature of this current multi-hop static scenario this trend is no longer observed.

The mean power profile for Node 1 is analyzed for the different approaches and shown in Figure 6.13. As expected, IEEE 802.15.4 nodes consume the highest average power among all approaches due to the continuous listening of the channel. The purpose of duty-cycled protocols is precisely to reduce such energy-demanding continuous listening. X-MAC and RI-MAC effectively accomplish this for packet generation periods larger than 30 seconds.

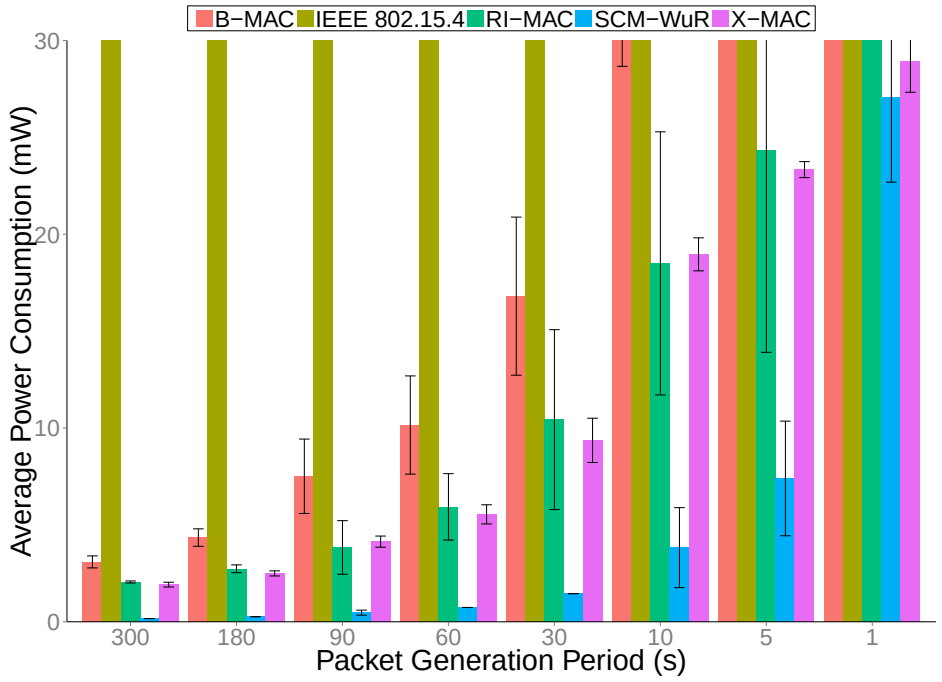

Figure 6.13: Effect of the packet generation period on the mean power consumption of Node 1 for the multi-hop static scenario from Figure 6.4b.

In a similar way, the mean power profile for the analyzed approaches is shown in Figure 6.14 for Node 11, yet this node is required to participate much less in the network.

The lifetime values of Node 1 and/or Node 2, as they are the ones in charge of performing most tasks in the tree from Figure 6.4b, indeed represent the global network's lifetime, shown

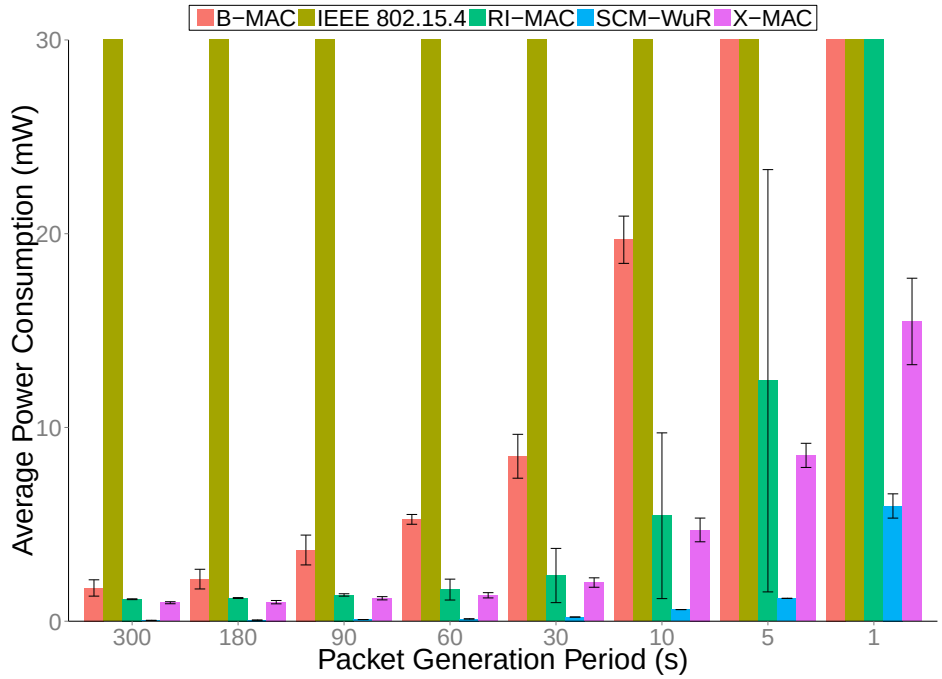

Figure 6.14: Effect of the packet generation period on the mean power consumption of Node 11 for the multi-hop static scenario from Figure 6.4b.

in Figure 6.15. For a packet generation period of 300 seconds, SCM-WuR guarantees network lifetimes of up to 1000 days of network operation time, RI-MAC and X-MAC around 100 days, B-MAC around 65 days and finally IEEE 802.15.4 can only provide around 3 days. Clearly, SCM-WuR outperforms any other approach.

Although they may seem to provide similar lifetime results, in this scenario RI-MAC performs worse than X-MAC's if considering the ratio between total energy featured by accounting all activities in the network nodes over the total number of payload bits received at the sink, as shown in Figure 6.16. Logically, the energy per bit performance of IEEE 802.15.4 improves as the data rate gets higher. The reason is that IEEE 802.15.4 consumes energy independently of the traffic rate because of its always-on state, thus the energy efficiency increases in accordance with the data load. However, although the energy efficiency of IEEE 802.15.4 is better than that of WuR for very high data rates, these are not common in WSN.

Clearly, WuR obtains its energy advantages in Figure 6.16 from the fact that the main radio interface is in the sleep mode most of the time. B-MAC, X-MAC and RI-MAC, due to the long preamble or receiving time they feature for each data packet, require more energy per bit than WuR but still less than IEEE 802.15.4 for low traffic loads. The energy per bit trends for these three MAC protocols are similar when increasing the data load, although the respective PDR values for the highest packet generation periods are so low that this subset of Figure 6.16 reports few relevance.

The network's latency is calculated in the tree scenario as the difference between the time a packet is generated and its reception time at the destination. Figure 6.17 shows the mean

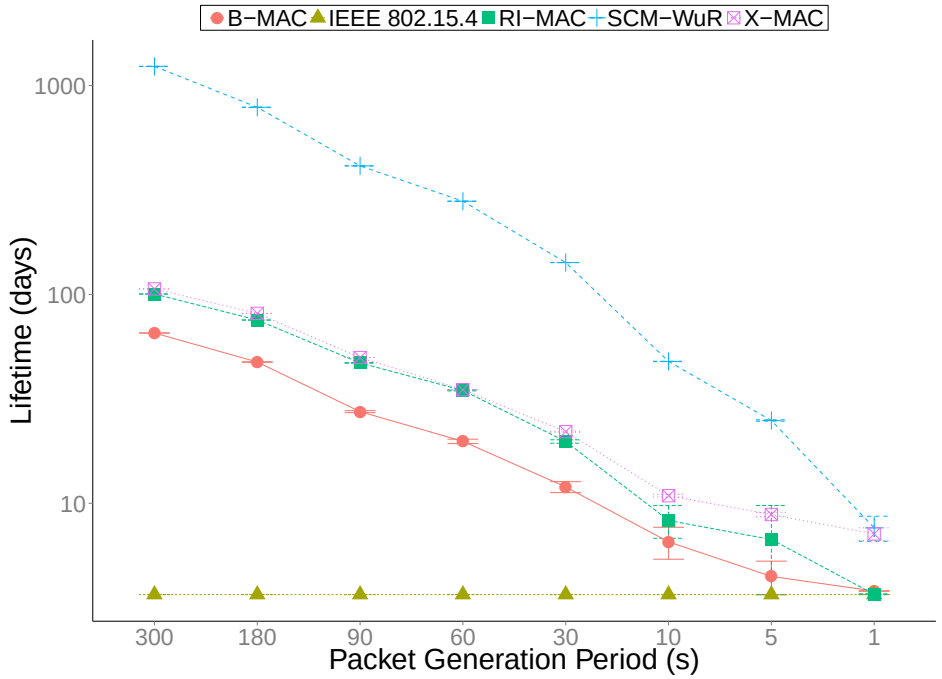

Figure 6.15: Effect of the packet generation period on the network lifetime for the multi-hop static scenario (logarithmic graph).

latency for packets to travel from the leaf Node 7 in Figure 6.4b to the network's sink. Such measure can be seen as the total time it takes for a packet generated at the furthest tree level to go through all the levels of the network's topology.

For preamble-based MACs, a preamble is generated at the same time of a data packet and sent just before it. In B-MAC, data packets may suffer long wait periods before being transmitted due to surrounding preamble transmissions. Such issue is repeated in all hops up to the sink, and becomes more and more important as the data load increases. Hence, MAC approaches saturate again for high data generation rates. IEEE 802.15.4 obtains the best latency results due to being constantly active for monitoring the channel and for not incurring in any delay overhead except the CCA prior the packet transmissions. However, this comes at the cost of high consumed power. For its part, SCM-WuR performs efficiently in terms of latency when compared to the other approaches, with values not higher than 60 ms for packets to go through the entire network. This value corresponds to the summation of the amount of time needed for the WuC (12.2 ms in Table 1, as obtained from measurements in chapter 4, section 4.2.1), the transition of the MCU and main network interface card from sleep to receiving state (1.79 ms), the reception of the data packet (time for a 100-byte packet at 250 kbps is 3.2 ms) and the average contention and processing-related times (1.5 ms) for a total of 18.5 ms. Such value, multiplied by 3 hops (4 levels) from Node 7 to reach the sink, sums up to a total of approximately 60 ms.

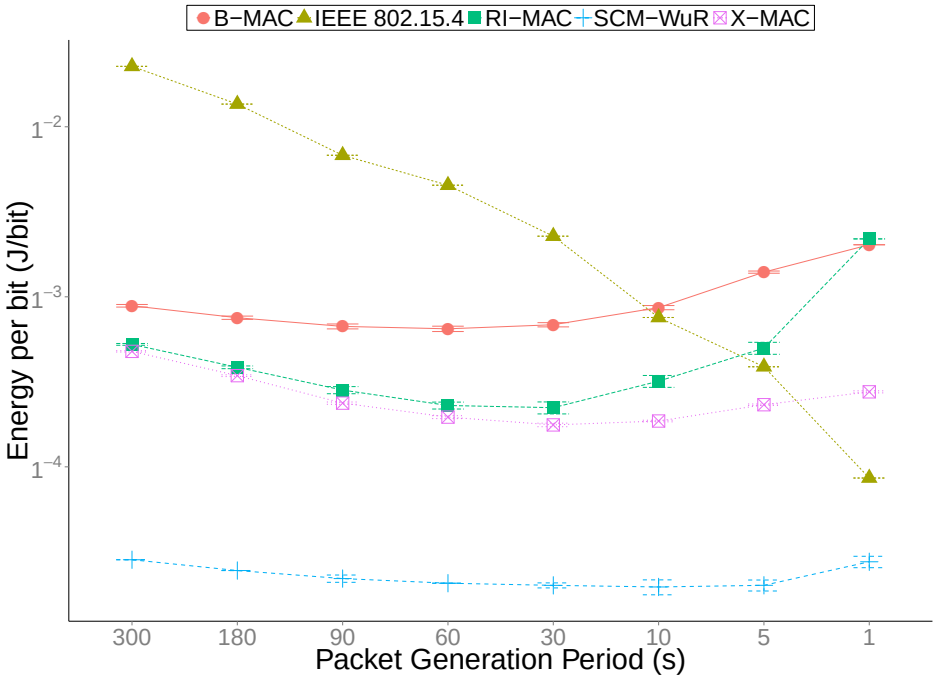

Figure 6.16: Effect of the packet generation period on the energy required per received bit by the sink's network for the multi-hop static scenario (logarithmic graph).

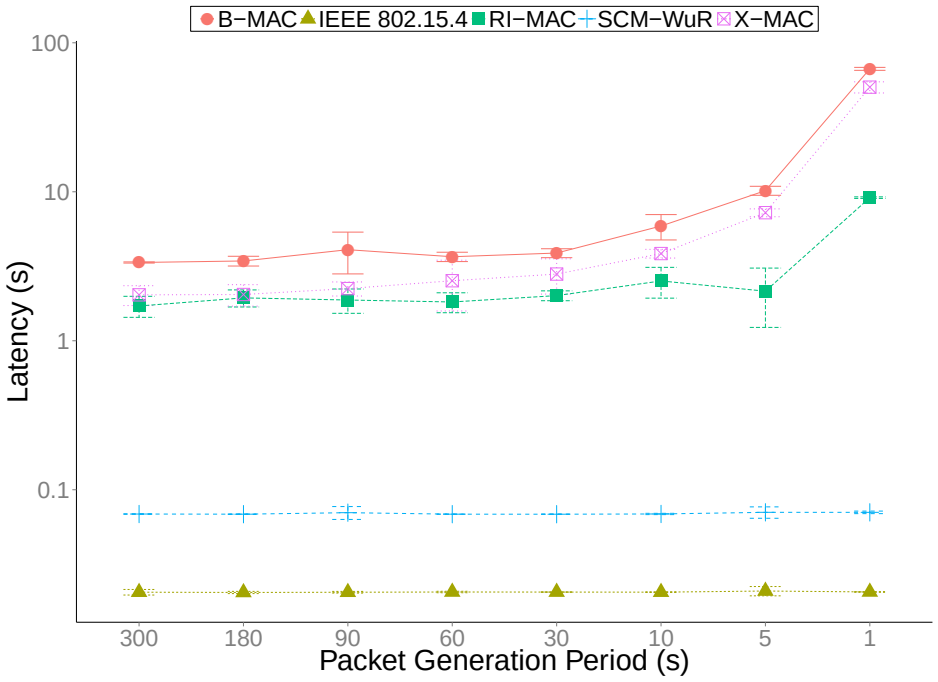

Figure 6.17: Effect of the packet generation period on the average latency observed by Node 7 for the multi-hop static scenario (logarithmic graph).

6.4.3.3 Effect of Coexistent Network Interference

The number of seconds between packet generations from network nodes is kept constant at 90 to isolate and evaluate the effect of the number of interferer nodes in this tree scenario.

Interferer nodes generate and transmit packets in an uniform(1 s, 10 s) time distribution. In this case, as shown in Figure 6.18, because of the multi-hop nature of the tree scenario, even SCM-WuR and RI-MAC suffer from the effect of interferer nodes and cannot provide PDR close to 100% any longer.

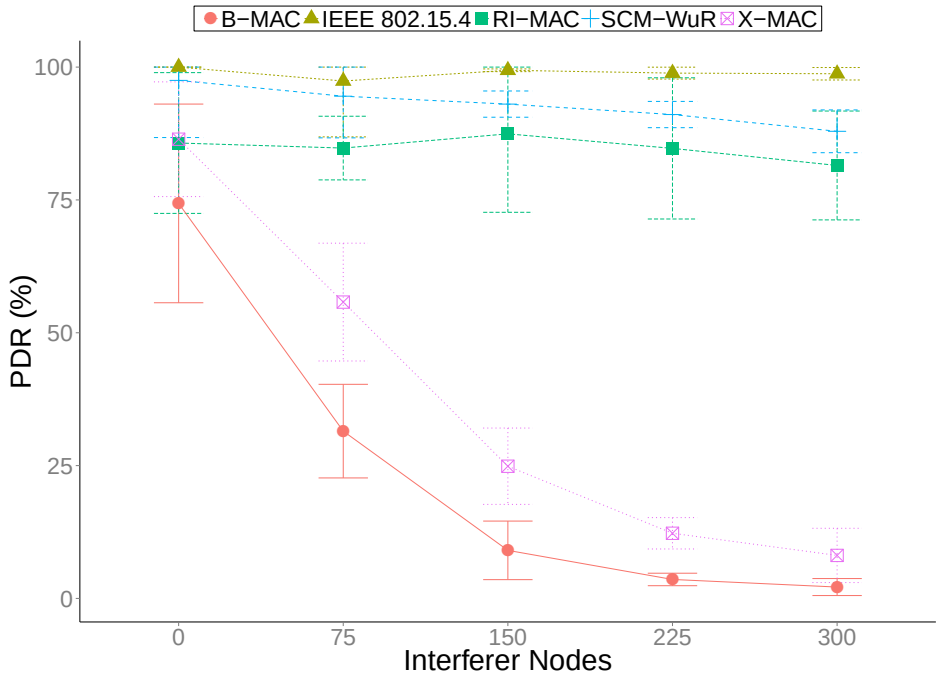

Figure 6.18: Effect of the number of interferer nodes on the network PDR for the multi-hop static scenario.

Regarding B-MAC and X-MAC, Figure 6.19 shows that in presence of interferers they feature the same poor lifetime of the single-hop scenario. Again, WuR achieves the best PDR-lifetime trade-off in this scenario.

6.4.4 Multi-hop Mobile Scenario

In the third application, nodes remain idle until the presence of a mobile data-collector on a bridge. Such mobile node queries the first node in a chain of four placed along the longitude of the bridge's pillars, as depicted in Figure 6.5. As in the single-hop scenario case, this third scenario is an example of a Receiver Initiated application and, accordingly, for the WuR approach the RI-WuR variant is considered. However, this RI scenario requires multi-hop communication as in the tree application. For this *bridge monitoring application*, the mobile node continuously travels on the bridge or target area, back and forth. The query from the mobile node travels in a multi-hop fashion down to the last node of the pillar and then returns back to the mobile node, which may be a bus or even a drone. Thus, 8 communication hops take place, 4 in each direction, to recover the information from a bridge's pillar. It is clear to see how this scenario mixes the nature of the previous two.

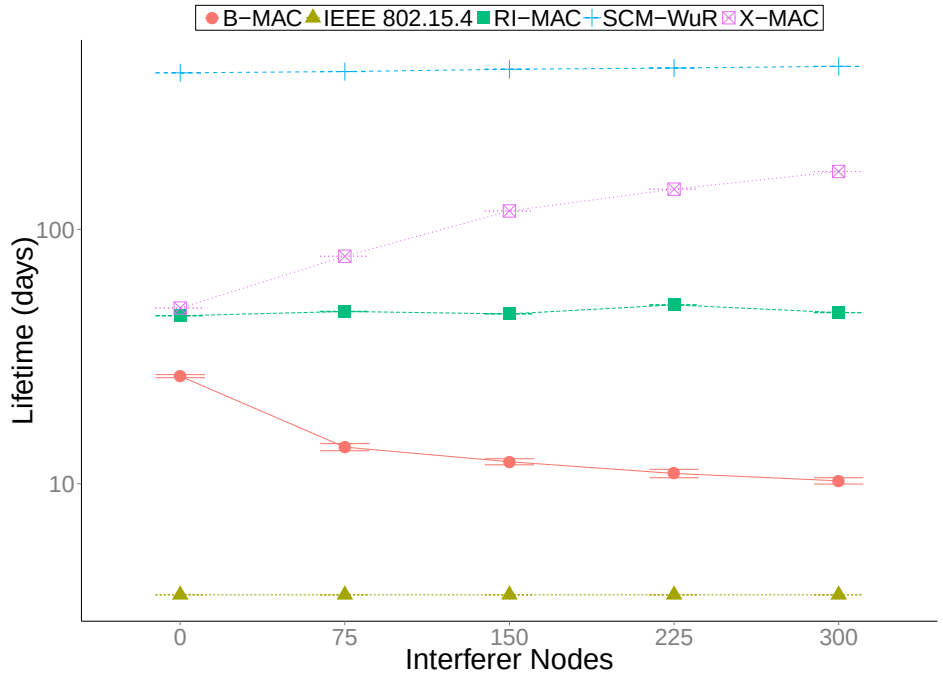

Figure 6.19: Effect of the number of interferer nodes on the maximum lifetime for the multi-hop static scenario (logarithmic graph).

This section studies the effect of the interferences, the effect of the duty cycle and the effect of the mobile node's speed. Considering the communication delay at each hop, situations may arise in this scenario where the answer from the bridge's pillar is not detected by the mobile node because of being already out of range due to its traveling speed.

6.4.4.1 Effect of the Duty Cycle Ratio

As in the tree example, in the current application an increase of the duty cycle does not signify an immediate performance improvement. The number of interferers is set to zero for the duty cycle evaluation, otherwise B-MAC and X-MAC cannot complete a single data transaction in this scenario even for the default mobile node's speed of 10 m/s (36 km/h). The effects of the variation of the duty cycle can be observed in Figures 6.20 and 6.21 for network's PDR and latency, respectively. Only if all the nodes in a chain can provide their results the entire query is accounted as successful for the application PDR.

In Figure 6.20, by increasing the duty cycle the PDR for X-MAC improves up to 100%. This behavior is consistent with the analogous in Figure 6.18 in the no-interferers case. In terms of latency, IEEE 802.15.4 performs the full up-down-up communication in 50 ms, while SCM-WuR, RI-MAC, X-MAC and B-MAC require 160 ms, 4000 ms, 4500 ms and 7500 ms, respectively. Communication is possible as long as the mobile node does not get extremely far away during the communication time, as analyzed in next section. These values correspond to the average single-hop latency multiplied by the number of hops. On average, RI-MAC and

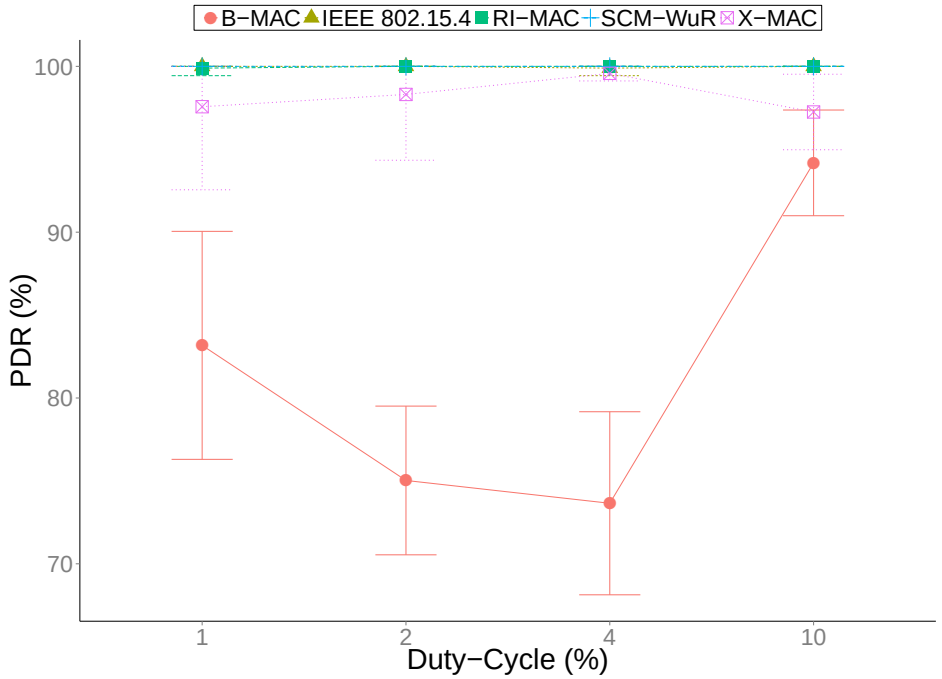

Figure 6.20: Effect of the duty cycle on the PDR for the bridge monitoring application.

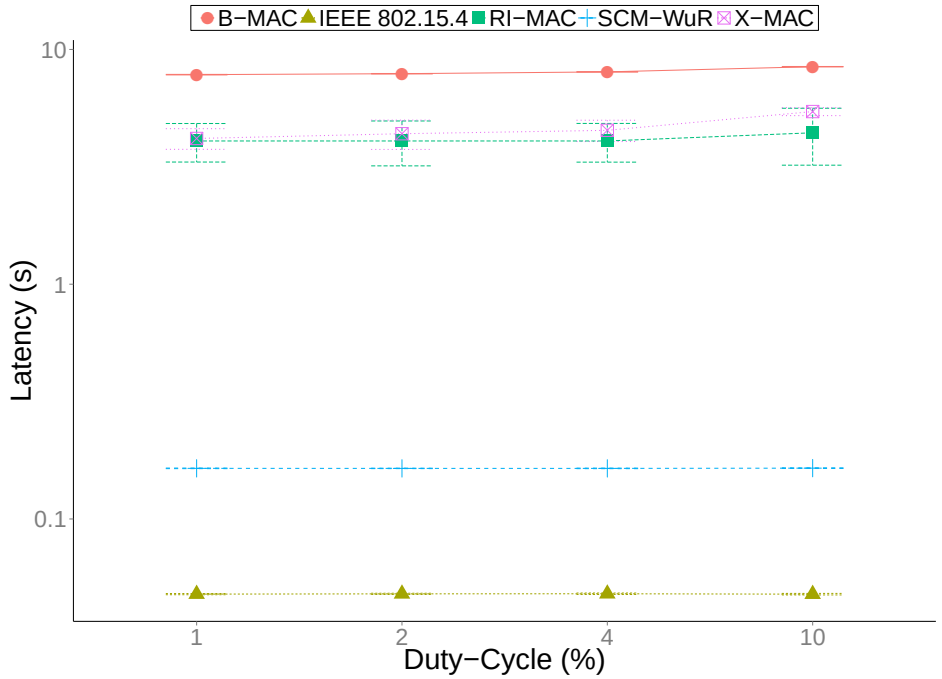

Figure 6.21: Effect of the duty cycle on the latency for the bridge monitoring application (logarithmic graph).

X-MAC require half the entire slot time of 1 second to communicate, differently to B-MAC which always needs 1 second.

Regarding battery lifetime, IEEE 802.15.4, B-MAC, X-MAC, RI-MAC and SCM-WuR are found to provide average node lifetimes of 3 days, 38 days, 82 days, 119 days and 1300 days

for this scenario, respectively. SCM-WuR improvements are constant for any duty cycle value of the MAC approaches.

6.4.4.2 Effect of Coexistent Network Interference

Differently from the tree application, the traffic generated by the current scenario is not constant. Again, interferer nodes generate and transmit packets in an uniform(1 s, 10 s) time distribution. However, communication must quickly take place once the first node in the bridge's pillar is queried in order to recover information from all the nodes in the chain. This measurement conditions allow for setting the performance of the evaluated approaches for applications requiring fast multi-hop response.

PDR and energy per bit results are shown respectively in Figure 6.22 and 6.23, from which it is easy to conclude that Transmitter Initiated MACs, such as B-MAC and X-MAC, do not fit well this type of application if a minimum contention degree may be present. The failure in delivering the requested information by B-MAC and X-MAC provokes their energy per bit ratio to drastically increase. For the other approaches, just slight PDR decreases and energy increments occur as the number of interferer nodes grows up.

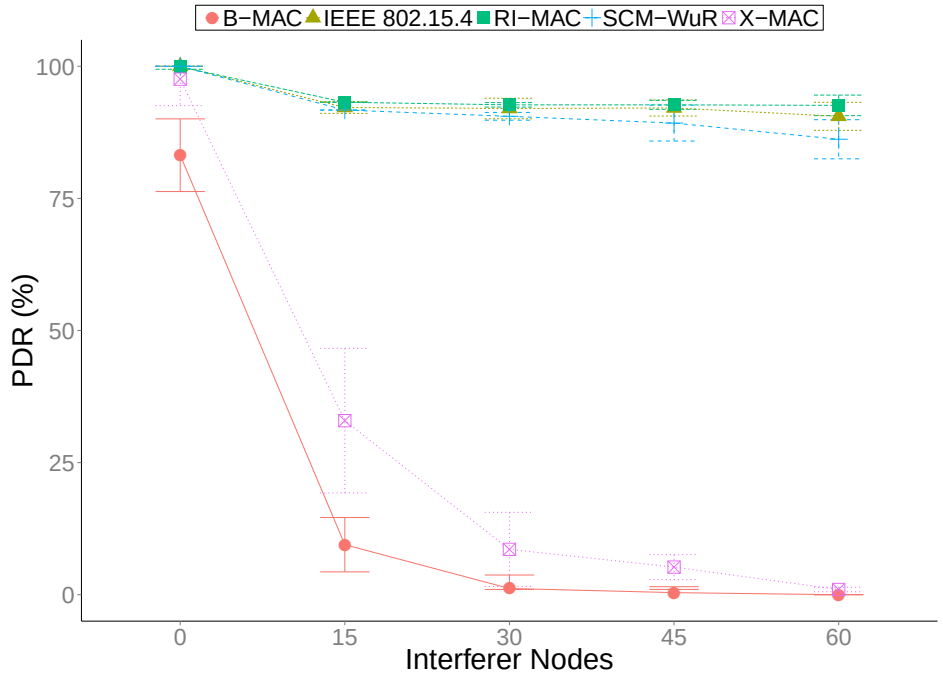

Figure 6.22: Effect of the number of interferer nodes on the PDR for the bridge monitoring application.

SCM-WuR overcomes the rest of approaches in terms of lifetime by a factor of 10, with up to 1000 days of battery life (not shown in figures). If a minimum amount of interferers is present, the PDR of B-MAC and X-MAC becomes very low because of their incapability in performing all the communication hops within time. The corresponding energy per bit increases accordingly with such incapability.

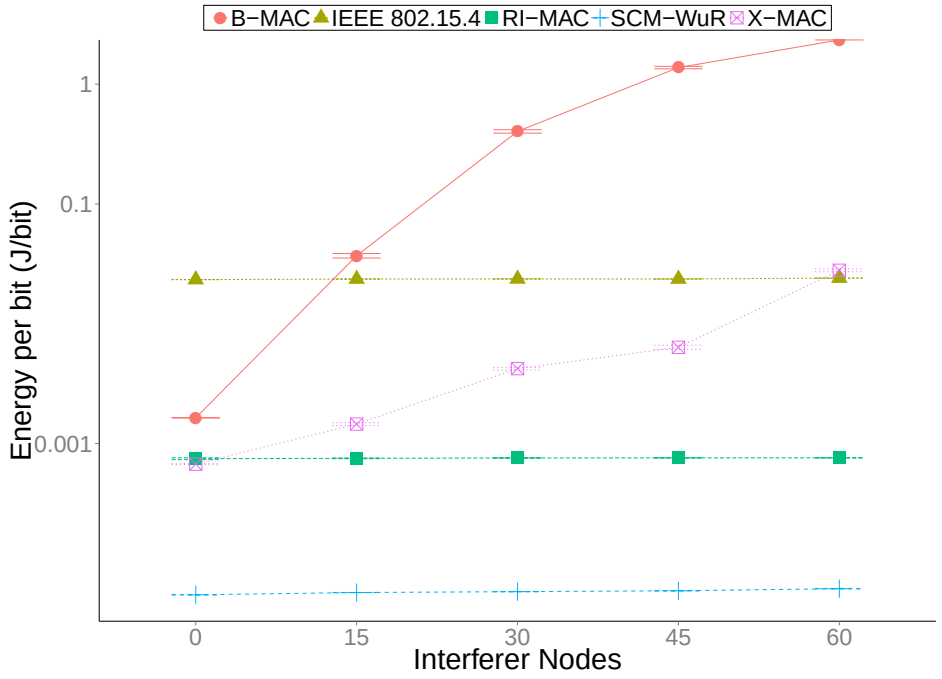

Figure 6.23: Effect of the number of interferer nodes on the energy/bit calculation for the bridge monitoring application (logarithmic graph).

6.4.4.3 Effect of the Mobile Node's Speed

Finally, the mobile node's speed is studied in order to determine how fast it can travel and still recover the information in the mobile multi-hop application. Again, the number of interferers is set to zero for B-MAC and X-MAC to be able to provide answers in time.

As shown in the plots, at around 25 m/s not all the packets are received back by the mobile node for any of the three duty-cycled MAC protocols. This speed limit may decrease in case of presence of interferences, as shown in previous sections. Because of this, it can be stated that duty-cycled MAC approaches cannot simply be deployed in applications demanding fast multi-hop to a mobile sink. SCM-WuR, in turn, performs the best for both energy and PDR metrics for all mobile speeds investigated.

6.5 Conclusions

The use of WuR systems provides drastic improvements to nowadays WSN, which are commonly based on duty-cycling MAC strategies. Even if duty-cycled approaches help reducing current consumption due to idle listening and overhearing, such reduction is not enough for new low-power application demands, where nodes should save as energy as possible as long as their intervention is not required. In this chapter, throughout evaluations of such use cases for numerous metrics, it is clearly observable that SCM-WuR permanently allows for remarkable energy savings, higher PDR, lower latencies and less complicated software implementations

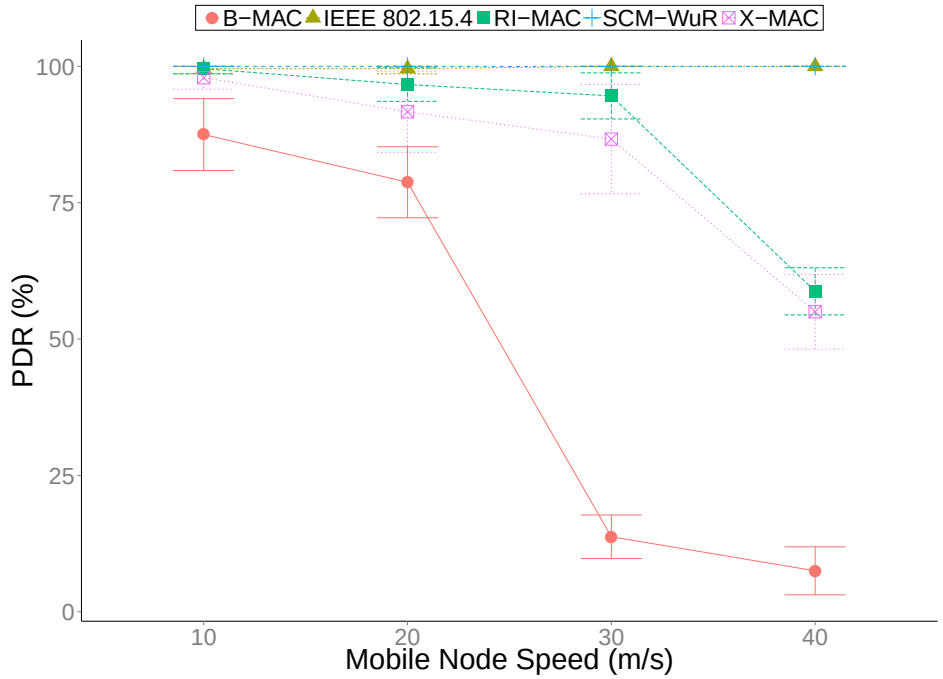

Figure 6.24: Effect of the mobile node's speed on the PDR for the bridge monitoring application.

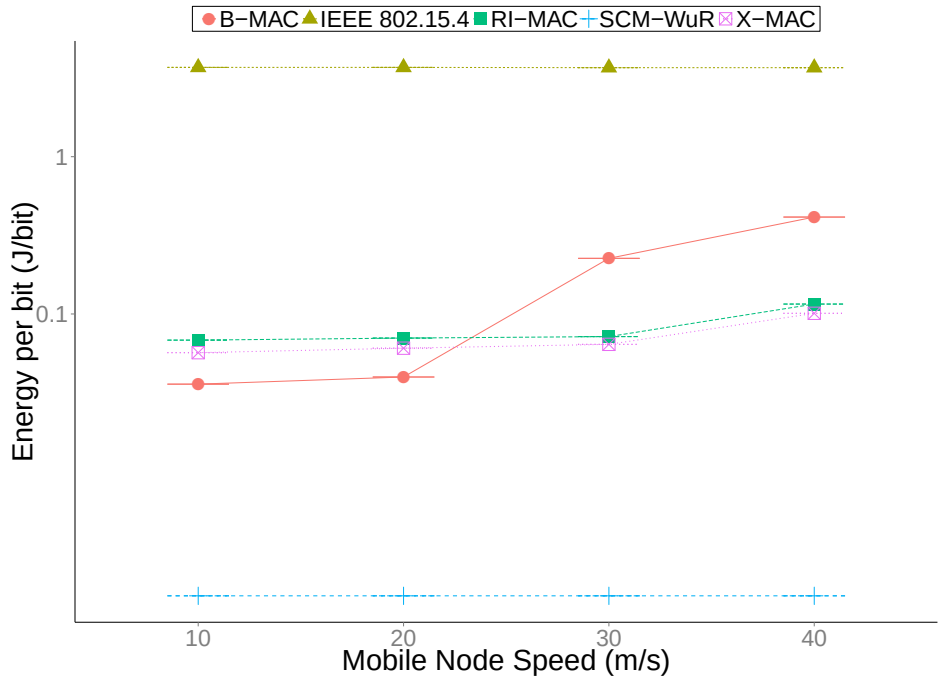

Figure 6.25: Effect of the mobile node's speed on the energy per bit calculation for the bridge monitoring application (logarithmic graph).

than duty-cycled MAC protocols. In fact, the only disadvantage of WuR systems appears to be the need for extra hardware development.

Results in this chapter enable network designers with the fundamentals to firmly consider

switching from currently dominant duty-cycled networks to a WuR approach, mostly because any MAC protocol may fit the high ecosystem of different possible applications. That is, developing a MAC protocol which performs acceptably in a wide range of diverse applications is a very difficult task, and achieving good performance in one application directly implies the other way around for others. This issue gets worse when considering single-hop and multi-hop use cases.

With the previous issues in mind, Bluetooth Low Energy, or BLE, appears as a duty-cycled MAC protocol mainly targeting single-hop applications. Because of this, and also because of its extreme integration with its upper application layers, BLE appears as an extremely energy-efficient protocol that cannot be easily replaced by WuR. The performance of BLE is analyzed in the following chapter 7, as well its application areas.

7 Evaluating Bluetooth Smart: a Novel Commercial Low-Power Technology

Bluetooth Low Energy (BLE) is an emerging wireless technology developed by the Bluetooth Special Interest Group (SIG) for short-range communication. In contrast with previous Bluetooth flavors, BLE has been designed as a low-power solution for control and monitoring applications and is the distinctive feature of the Bluetooth 4.0 specification [75].

As previous chapters do for WuR systems and several low-power MAC protocols, this chapter describes the main features of BLE, investigates the impact of critical parameters on its performance, and explores its potential applications. Section 7.1 overviews the BLE protocol stack and describes the operation and main characteristics of each layer; section 7.2 evaluates the energy consumption, latency and network size of BLE and discusses application layer BLE throughput; section 7.3 explores the market adoption possibilities for BLE and provides a comparison with other wireless low-power technologies. Finally, section 7.4 concludes the chapter with the main remarks.[1]

Contents

[1] The current chapter is based on and extends the work contained in the following JCR Q1 (2012) publication: ≪C. Gomez, J. Oller, and J. Paradells, 'Overview and Evaluation of Bluetooth Low Energy: An Emerging Low-Power Wireless Technology', Sensors, vol. 12, no. 9, pp. 11734-11753, 2012.≫.

7.1 Bluetooth Low Energy Protocol Stack

The advent of BLE, renamed as of 2014 as Bluetooth Smart for commercial reasons, has occurred while other low-power wireless solutions, such as ZigBee, 6LoWPAN or Z-Wave, have been steadily gaining momentum in application domains that require multi-hop networking [76]. However, BLE constitutes a single-hop solution applicable to different use cases such as healthcare, consumer electronics, smart energy and security. The widespread use of Bluetooth technology (e.g., in mobile phones, laptops, automobiles, etc.) fuels adoption of BLE, since implementation of the latter can leverage similarities with classic Bluetooth. BLE is expected to be used in billions of devices in the near future. In fact, the IETF 6LoWPAN Working Group (WG) has already recognized the importance of BLE for the so-called Internet of Things.

BLE is a perfect example of a low-power MAC protocol which allows for use cases which fall out of the scope of Wake-up Radio systems. Indeed, WuR cannot easily replace BLE in its target applications and thus is worth studying in this thesis as one of the most energy-efficient MAC protocols as of 2014. This supports the idea in chapter 1; since BLE is designed from scratch from the application point of view, WuR cannot provide the same benefits as over the MAC protocols in chapter 6, which all focus in improving the MAC layer's performance. BLE, while also restricted by the omnipresent duty cycle ratio, provides undeniable benefits at the application level.

This section presents the BLE protocol stack, and describes the main mechanisms and features of each layer. As in classic Bluetooth, the BLE protocol stack is composed of two main parts: the Controller and the Host. The Controller comprises the Physical Layer and the Link Layer, and is typically implemented as a small System-on-Chip (SOC) with an integrated radio transceiver. The Host runs on an application processor and includes upper layer functionality, i.e., the Logical Link Control and Adaptation Protocol (L2CAP), the Attribute Protocol (ATT), the Generic Attribute Profile (GATT), the Security Manager Protocol (SMP) and the Generic Access Profile (GAP). Communication between the Host and the Controller is standardized as the Host Controller Interface (HCI). Finally, non-core profiles (i.e., application layer functionality not defined by the Bluetooth specification) can be used on top of the Host. Figure 7.1a illustrates the BLE protocol stack. Figure 7.1b depicts the structure and size of the different fields contributed by each layer to a Physical Layer data unit when application data are transmitted. Subsections 7.1.1 to 7.1.7 focus on each layer of the BLE protocol stack.

Although some of the BLE Controller features are inherited from the classic Bluetooth Controller, both types of Controller are incompatible. Hence, a device that only implements

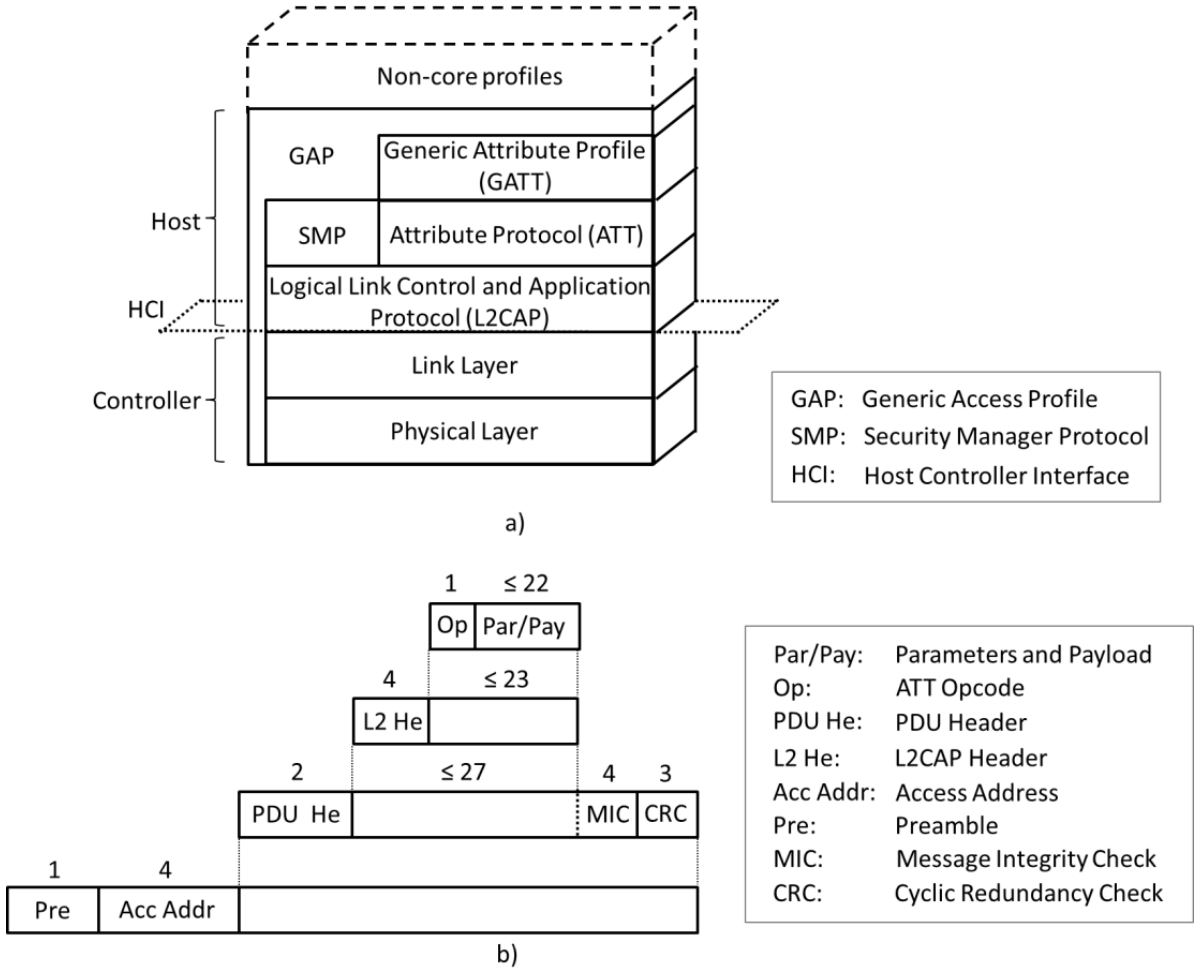

Figure 7.1: (a) BLE protocol stack; (b) structure of a BLE data unit. Field sizes in bytes.

BLE (which is referred to as a *single-mode* device) cannot communicate with a device that only implements classic Bluetooth. An example of a single-mode device is the Texas Instruments' CC2540 [77]. Some devices as Texas Instruments' CC2564 [78] implement both the classic Bluetooth and the BLE protocol stacks. These devices are called *dual-mode* devices.

7.1.1 Physical Layer

BLE operates in the 2.4 GHz Industrial Scientific Medical (ISM) band and defines 40 RF channels with 2 MHz channel spacing. There are two types of BLE RF channels: *advertising channels* and *data channels*. Advertising channels are used for device discovery, connection establishment and broadcast transmission, whereas data channels are used for bidirectional communication between two connected devices.

Three channels are defined as advertising channels. These channels have been assigned center frequencies that minimize overlapping with IEEE 802.11 channels 1, 6 and 11, which are commonly used in several countries. An Adaptive Frequency Hopping (AFH) mechanism is used on top of the data channels in order to face interference and wireless propagation issues,

such as fading and multipath. This mechanism effectively chooses one of the 37 available data channels for communication during a given time interval.

All physical channels use a Gaussian Frequency Shift Keying (GFSK) modulation. The modulation index (related to tolerance) is in the range between 0.45 and 0.55, which allows reduced peak power consumption. The physical layer data rate is 1 Mbps. The receiver sensitivity is defined in BLE as the signal level at the receiver for which a Bit Error Rate (BER) of 10^{-3} is achieved. The BLE specification mandates a sensitivity better than or equal to -70 dBm. The coverage range is typically stated to be over various tens of meters. However, empirical tests show that BLE can easily communicate up to 150 meters at +4 dBm.

7.1.2 Link Layer

The Link Layer in BLE is equivalent to the MAC protocol analysis of B-MAC, IEEE 802.15.4, X-MAC and RI-MAC in previous chapter 6.

In BLE, when a device only needs to broadcast data, it transmits the data in advertising packets through the advertising channels. Any device that transmits advertising packets is called an *advertiser*. The transmission of packets through the advertising channels takes place in intervals of time called advertising events. Within an advertising event, the advertiser sequentially uses each advertising channel (numbers 37 to 39) for packet transmission. Devices that only aim at receiving data through the advertising channels are called *scanners*.

Bidirectional data communication between two devices requires them to connect to each other. The creation of a connection between two devices is an asymmetric procedure by which an advertiser announces through the advertising channels that it is a connectable device, while the other device (referred to as an initiator) listens for such advertisements. When an initiator finds an advertiser, it may transmit a *Connection Request* message to the advertiser, which creates a point-to-point connection between the two devices. Both devices can then communicate by using the physical data channels. The packets for this connection will be identified by a randomly generated 32-bit access code.

BLE defines two device roles at the Link Layer for a created connection: the *master* and the *slave*. These are the devices that act as initiator and advertiser during the connection creation, respectively. A master can manage multiple simultaneous connections with different slaves, whereas each slave can only be connected to one master. Thus, the network composed by a master and its slaves, which is called a piconet, follows a star topology. As of 2014, a BLE device can only belong to one piconet. Next version of the specification, that is v.4.1, targets to enhance this feature by allowing a slave to be part of several piconets.

In order to save energy, slaves are in sleep mode by default and wake up periodically to listen for possible packet receptions from the master. Upon connection, the master first provides the slave with the information needed for the frequency hopping algorithm (including the map of data channels to be used) and for the connection supervision. The parameters related with

the management of a connection are transmitted in the *Connection Request* message and can be updated during the connection for various reasons (e.g., using a new data channel map due to a change of the interference pattern). Once a connection between a master and a slave is created, the physical channel is divided into non-overlapping time units called *Connection Events*.

A Connection Event takes place in a single frequency hop. Thus, all packets in a connection event are transmitted using the same data channel frequency. Every connection event starts with the transmission of a packet by the master. If the slave receives a packet, the slave must send a packet to the master in response. However, the master is not required to send a packet upon receipt of a packet from the slave. While master and slave continue to alternate in sending packets, the connection event is considered to be open. Data channel packets include a More Data (MD) bit which signals whether the sender has more information to transmit. If none of the devices has more data to transmit, the connection event will be closed and the slave will not be required to listen until the beginning of the next connection event. Other circumstances that force the end of a connection event include the reception of two consecutive packets with bit errors by either the master or the slave, and the corruption of the access address field of a packet sent by any device. In order to allow bit error detection, all data units include a 24-bit Cyclic Redundancy Check (CRC) code. Figure 7.2 shows an example trace of a BLE connection procedure.

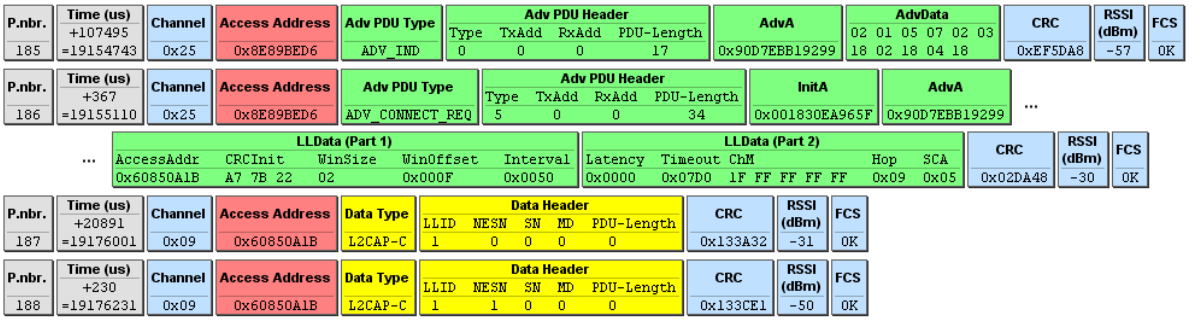

Figure 7.2: Fast connection establishment in BLE. Packet 185 shows an advertisement event and 186 shows the connection request to the slave device in the same event. This is followed 20 ms later by the master's poll packet in 187, and by the slave's answer in 188 in the same connection event [6].

For consecutive connection events, master and slave use a new data channel frequency, which is computed by using the frequency hopping algorithm. The time between the start of two consecutive connection events is specified by the *connInterval* parameter, which is a multiple of 1.25 ms in the range between 7.5 ms and 4 s. Another important parameter is *connSlaveLatency*, which defines the number of consecutive connection events during which the slave is not required to listen to the master and thus can keep the radio turned off. This parameter is an integer between 0 and 499 and should not cause a supervision timeout. A supervision timeout happens when the time since the last received packet exceeds the

connSupervisionTimeout parameter, which is in the range between 100 ms and 32 s. The purpose of this mechanism is to detect the loss of a connection due to severe interference or the movement of a device outside the range of its peer.

7.1.3 L2CAP

The L2CAP used in BLE is an optimized and simplified protocol based on the classic Bluetooth L2CAP. In BLE, the main goal of L2CAP is to multiplex the data of three higher layer protocols, ATT, SMP and Link Layer control signaling, on top of a Link Layer connection. The data of these services are handled by L2CAP in a best-effort approach and without the use of retransmission and flow control mechanisms, which are available in other Bluetooth versions. Segmentation and reassembly capabilities are not used, since upper layer protocols provide data units that fit into the maximum L2CAP payload size, which is equal to 23 bytes in BLE.

7.1.4 ATT

The ATT defines the communication between two devices playing the roles of *server* and *client*, respectively, on top of a dedicated L2CAP channel. The server maintains a set of attributes. An attribute is a data structure that stores the information managed by the GATT, the protocol that operates on top of the ATT. The client or server role is determined by the GATT, and is independent of the slave or master role.

The client can access the servers attributes by sending requests, which trigger response messages from the server. For greater efficiency, a server can also send to a client two types of unsolicited messages that contain attributes: (i) *notifications*, which are unconfirmed; and (ii) *indications*, which require the client to send a confirmation. A client may also send commands to the server in order to write attribute values.

7.1.5 GATT

The GATT defines a framework that uses the ATT for the discovery of services, and the exchange of characteristics from one device to another. A characteristic is a set of data which includes a value and properties. The data related to services and characteristics are stored in attributes. For example, a server that runs a *temperature sensor service* may account with a *temperature characteristic* that uses an attribute for describing the sensor, another attribute for storing temperature measurement values and a further attribute for specifying the measurement units.

7.1.6 Security

In order to provide a complete point-of-view, this section provides insights about BLE security, even if this thesis does not focus on communications security but in MAC aspects.

BLE offers various security services for protecting the information exchange between two connected devices. Most of the supported security services can be expressed in terms of two mutually-exclusive security modes called *LE Security Mode 1* and *LE Security Mode 2*. These two modes provide security functionality at the Link Layer and the ATT layer, respectively.

The BLE Link Layer supports encryption and authentication by using the Cipher Block Chaining-Message Authentication Code (CCM) algorithm and a 128-bit AES block cipher. When encryption and authentication are used in a connection, a 4-byte Message Integrity Check (MIC) is appended to the payload of the data channel PDU (see Figure 7.1b). Encryption is then applied to the PDU payload and MIC fields.

It is also possible to transmit authenticated data over an unencrypted Link Layer connection. In this case, a 12-byte signature is placed after the data payload at the ATT layer. The signature is computed by applying an algorithm that uses 128-bit AES as the block cipher [75].

In addition to the described services, BLE supports a mechanism called privacy feature, which allows a device to use private addresses and frequently change them. The privacy feature mitigates the threat by which an adversary can track a BLE device. The private addresses are generated by encrypting the public address of the device, which can be resolved by a trusted device that has been provided with the corresponding encryption key.

Each security mode accounts with different levels, which express requirements as to the type of pairing that has to be used. Pairing is a procedure by which the devices generate and distribute key material. Table 7.1 summarizes the security services and the type of pairing (if any) required by each security mode and level.

Security Mode	Level	Pairing	Encryption	Data Integrity	Layer
Mode 1	Level 1	No	No	No	Link Layer
	Level 2	Unauthenticated	Yes	Yes	
	Level 3	Authenticated	Yes	Yes	
Mode 2	Level 1	Unauthenticated	No	Yes	ATT Layer
	Level 2	Authenticated	No	Yes	

Table 7.1: Security services and features for BLE security modes and levels.

Pairing comprises three phases. In the *first phase*, the two connected devices announce their input/output capabilities and, based on these, they choose a suitable method for the second phase.

The *second phase* has the purpose of generating the Short-Term Key (STK), which will be used in the third phase to secure the distribution of key material. In the second phase, the pairing devices first agree on a Temporary Key (TK), by means of the *Out Of Band*, the *Passkey Entry* or the *Just Works* methods. The Out of Band method uses out of band communication means (e.g., NFC) for the TK agreement. NFC pairing is nowadays easily enabled by the so-called NFC dynamic tags. The M24SR from STMicroElectroncs [79] is an

example of this. Figure 7.3 is an example execution trace for an Freescale MCU configuring and recovering a password previously stored in the memory of a NFC dynamic tag.

```
 M24SR init
************
0x02 -> 0x00 -> 0xA4 -> 0x04 -> 0x00 -> 0x07 -> 0xD2 -> 0x76 -> 0x00 -> 0x00 -> 0x85 -> 0x01 -> 0x01 -> 0x00 -> 0x35 -> 0
xC0 ->
0x02 <- 0x90 <- 0x00 <- 0xF1 <- 0x09 <-
0x03 -> 0x00 -> 0xA4 -> 0x00 -> 0x0C -> 0x02 -> 0xE1 -> 0x03 -> 0xD2 -> 0xAF ->
0x03 <- 0x90 <- 0x00 <- 0x2D <- 0x53 <-
0x02 -> 0x00 -> 0xB0 -> 0x00 -> 0x00 -> 0x02 -> 0x6B -> 0x7D ->
0x02 <- 0x00 <- 0x0F <- 0x90 <- 0x00 <- 0x44 <- 0x45 <-
0x03 -> 0x00 -> 0xB0 -> 0x00 -> 0x00 -> 0x0F -> 0xA5 -> 0xA2 ->
0x03 <- 0x00 <- 0x0F <- 0x20 <- 0x00 <- 0xF6 <- 0x00 <- 0xF6 <- 0x04 <- 0x06 <- 0x00 <- 0x01 <- 0x20 <- 0x00 <- 0x00 <- 0
x00 <- 0x90 <- 0x00 <- 0xA9 <- 0xF3 <-
0x02 -> 0x00 -> 0xA4 -> 0x00 -> 0x0C -> 0x02 -> 0x00 -> 0x01 -> 0x3E -> 0xFD ->
0x02 <- 0x90 <- 0x00 <- 0xF1 <- 0x09 <-
0x03 -> 0x00 -> 0xB0 -> 0x00 -> 0x00 -> 0x02 -> 0x40 -> 0x79 ->
0x03 <- 0x00 <- 0x20 <- 0x90 <- 0x00 <- 0xFC <- 0x07 <-
0x02 -> 0x00 -> 0xB0 -> 0x00 -> 0x02 -> 0x20 -> 0xCB -> 0x4C ->
   password    0xDF572AEC
0xC2 -> 0xE0 -> 0xB4 ->
0xC2 <- 0xE0 <- 0xB4 <-
```

Figure 7.3: Execution trace of a low-power MCU reading a password from a NFC dynamic tag. Legend: $\Rightarrow$ I^2C from MCU to tag $\Leftarrow$ I^2C from tag to MCU.

In the Passkey Entry method, the user passes six numeric digits as the TK between the devices.

When none of the first two methods can be used, the Just Works method is employed, although it is not authenticated and it does not provide protection against Man In The Middle (MITM) attacks. Based on the TK, and on random values generated by each pairing device, the STK is obtained by both devices, which leads to the end of the second phase.

In the *third phase*, each endpoint of the connection may distribute to the other endpoint up to three 128-bit keys called the Long-Term Key (LTK), the Connection Signature Resolving Key (CSRK) and the Identity Resolving Key (IRK). The LTK is used to generate the 128-bit key employed for Link Layer encryption and authentication. The CSRK is used for the data signing performed at the ATT layer. The third key (i.e., the IRK), is used to generate a private address on the basis of a device public address. The message exchange required for distributing the LTK, the CSRK or the IRK is encrypted by using the STK obtained in the second phase.

The Security Manager Protocol (SMP) carries out the message exchange of the three described pairing phases. SMP operates on top of a fixed L2CAP channel.

7.1.7 GAP and Application Profiles

At the highest level of the core BLE stack, the GAP specifies device roles, modes and procedures for the discovery of devices and services, the management of connection establishment and security.

The BLE GAP defines four roles with specific requirements on the underlying controller: *Broadcaster*, *Observer*, *Peripheral* and *Central*. A device in the Broadcaster role only broadcasts data (via the advertising channels) and does not support connections with other devices. The Observer role is complementary for the Broadcaster, i.e., it has the purpose of receiving the data transmitted by the Broadcaster. The Central role is designed for a device that is in charge of initiating and managing multiple connections, whereas the Peripheral role is designed for simple devices which use a single connection with a device in the Central role. In consequence, the Central and Peripheral roles require that the devices controller support the master and slave roles, respectively. A device may support various roles, but only one role can be adopted at a given time.

Finally, since certain types of applications may benefit from reusing common functionality, additional profiles can be built on top of the GAP. Bluetooth follows a profile hierarchy, whereby a new profile including all the requirements of an existing profile can be defined. A highest-level profile that specifies how applications can interoperate is called an application profile. Application profiles, which are also specified by the Bluetooth SIG, favour interoperability between devices from different manufacturers.

7.2 Performance Evaluation

This section evaluates the performance of BLE in terms of energy consumption, latency and piconet size, for various use cases and configurations, and discusses application layer BLE throughput. The size of the notification, command and response messages considered in this study is the maximum one (i.e., 37 bytes at the Physical Layer), whereas polls sent by the master and acknowledgments are assumed to be empty PDUs (i.e., PDUs without payload). Latency results have been obtained by exploiting simulation tools developed in the C language for this purpose (given that publicly available simulators such as OMNET++ do not support BLE yet), and have been complemented by means of experimental measurements. Error probabilities are introduced by means of randomization. The simulation tools model two connected BLE devices that communicate with each other, taking into account all the BLE stack layers and their behavior in the presence of bit errors. Piconet size results have been obtained theoretically, whereas energy consumption has been analyzed both theoretically and empirically. Further details about the evaluation methods are provided in each corresponding subsection.

7.2.1 Energy Consumption

First, the theoretical lifetime of a slave that is connected to a master in a data collection application is investigated. Note that a slave is typically a device with limited energy supply, whereas a master may not suffer from the same energy constraints. This section considers two different methods by which the master obtains sensor measurement readings (which are

handled as attribute values) from the slave, which is assumed to act as the attribute server. These methods are named *one-way ATT communication* and *round-trip ATT dialogue*, respectively. In the one-way ATT communication, the slave sends a notification in response to a poll from the master. In the round-trip ATT dialogue, the master sends a request (not an empty PDU as in the case of a poll) to the slave, which transmits a response to the master (and both the request and the response trigger Link Layer acknowledgments). For the two methods described, the first packet transmission from the master takes place at the beginning of each connection event.

The evaluation is carried out theoretically by assuming current consumption values obtained from measurements for the CC2540 radio chip, for a transmit power of 0 dBm [7]. Specifically, for the one-way ATT communication, the study takes into account the energy consumed during each one of the following states:

→ device wake up,

→ radio turn on,

→ reception of the initial BLE packet from the master,

→ radio switch to transmit mode,

→ notification transmission,

→ and final post-processing before the device returns to sleep mode.

For the round-trip ATT dialogue, the additional energy consumption due to:

→ response transmission,

→ radio switch to receive mode,

→ and acknowledgment reception, is also considered.

The energy consumption during sleep periods is considered as well for both types of ATT transactions. For the evaluation of the device lifetime, an ideal CR2032 battery with a capacity of 230 mAh is assumed as input of the calculation chart in Figure 7.4 for two different connection events typologies.

The study considers the impact of *connInterval* and *connSlaveLatency* parameters. The whole range of valid *connInterval* values (i.e., from 7.5 ms to 4000 ms) is covered. For *connSlaveLatency*, values in the range between 0 and 7 are considered, since these values can be used for any permitted *connSupervisionTimeout* setting. The study is also carried out for the maximum possible *connSlaveLatency* value, which is given for the maximum *connSupervisionTimeout* value (i.e.,32 s), and depends on the *connInterval* value. For this study, a BER equal to zero is assumed, which gives an upper bound on the slave lifetime under the described

Battery capacity (mAh):	230
Connection Interval (ms):	1000
Sleep Current with timer running (mA)	0,001

	Case 1				Case 2			
	Time (us)	Current (mA)	Percent of events		Time (us)	Current (mA)	Percent of events	
			50				50	
State 1 (wake-up)	400	6		2400	400	6		2400
State 2 (pre-processing)	315	7,4		2331	340	7,4		2516
State 3 (pre-Rx)	80	11		880	80	11		880
State 4 (Rx)	275	17,5		4812,5	190	17,5		3325
State 5 (Rx-to-Tx)	105	7,4		777	105	7,4		777
State 6 (Tx)	115	17,5		2012,5	115	17,5		2012,5
State 7 (post-processing)	1325	7,4		9805	1280	7,4		9472
State 8 (pre-sleep)	160	4,1		656	165	4,1		676,5
				23674				22059
Total time of connection event	2775				2675			
Average Current draw during connection event (mA):		8,5311712				8,246355		
Average current draw accounting for sleep (mA):				0,024671				0,023056

Average current draw during connection (mA):	**0,023863775**
Expected battery life (hours):	**9638,039246**
Expected battery life (days):	**401,5849686**

Figure 7.4: Lifetime calculator of a connection event for two different energy traces [7].

conditions. The results are shown in Figure 7.5. The two upper traces in the figure follow a different trend because in these cases the maximum *ConnSlaveLatency* value, that is, the most energy-saving approach, is considered. Note that for applications that can exploit the maximum *connSlaveLatency* values (i.e., applications that do not require frequent measurements) slave lifetime does not exhibit a monotonical tendency with *connInterval*. This happens because the maximum *connSlaveLatency* is defined as an integer value and cannot be greater than 499.

The calc sheet in Figure 7.4 allows to extract the values for Figure 7.5 to illustrate the trade-off between slave lifetime and *connInterval* and *connSlaveLatency* parameters. The maximum slave lifetime obtained is 14.1 and 12.4 years for the one-way and round-trip methods, respectively. These values are achieved for both options for a *connInterval* of 86.25 ms and a *connSlaveLatency* of 370. With these settings, the master obtains one sensor measurement reading every 32 s. On the other hand, the most energy-intensive settings (i.e., *connInterval* of 7.5 ms and *connSlaveLatency* of 0) yield a slave lifetime of 2.6 and 2.0 days for each method, respectively. In this case, the time between consecutive readings is equal to 7.5 ms. Thus, BLE offers the flexibility for accommodating a wide range of measurement reading frequencies, which trade for slave lifetime. This is an interesting characteristic not present in other MAC protocols for WSN.

In order to complement the previous study, the average current consumption of a CC2540 node configured as a slave for the one-way ATT communication is measured. The distance

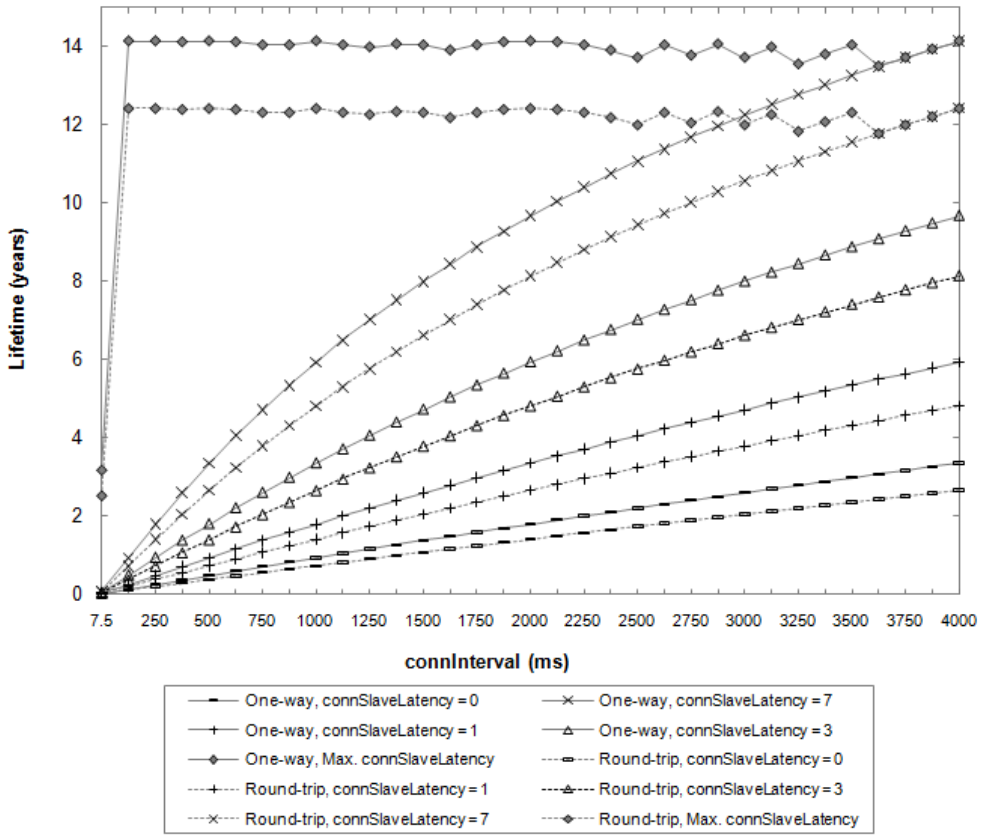

Figure 7.5: Theoretical lifetime of a BLE slave for one-way and round-trip ATT message exchanges, and for different parameter configurations, based on CC2540 current measurements [7].

between the slave and the master is 0.5 m, and the transmit power of both devices is 0 dBm. The slave is powered by a coin cell battery that has a capacity of 230 mAh and a nominal voltage of 3 V. Measurements are carried out by using an Agilent Technologies Power Analyzer (N6705A model). Figure 7.6 shows a picture of the experimental setup used to perform the described current consumption measurements. In the figure, the display in the power analyzer clearly shows the pwoer trace of a slave transmitting 3 advertising frames.

Figure 7.7 plots the measurement results obtained, for a set of *connInterval* values within the range from 7.5 ms to 4000 ms, and for a *connSlaveLatency* of 0. The device's lifetime values in Figure 7.5 are consistent with the average current consumption in Figure 7.7. As *connInterval* increases, the average current consumption decreases, since the slave remains in sleep mode for a greater fraction of the connection event.

It is possible to perform multiple configurations of the *connInterval* and *connSlaveLatency* parameters which yield the same rate of message exchanges between master and slave under ideal conditions (i.e., BER = 0). However, bit errors may significantly affect performance, depending on each particular *connInterval* and *connSlaveLatency* tuple. When a slave does not receive a packet from the master at the beginning of a connection event (e.g., due to bit

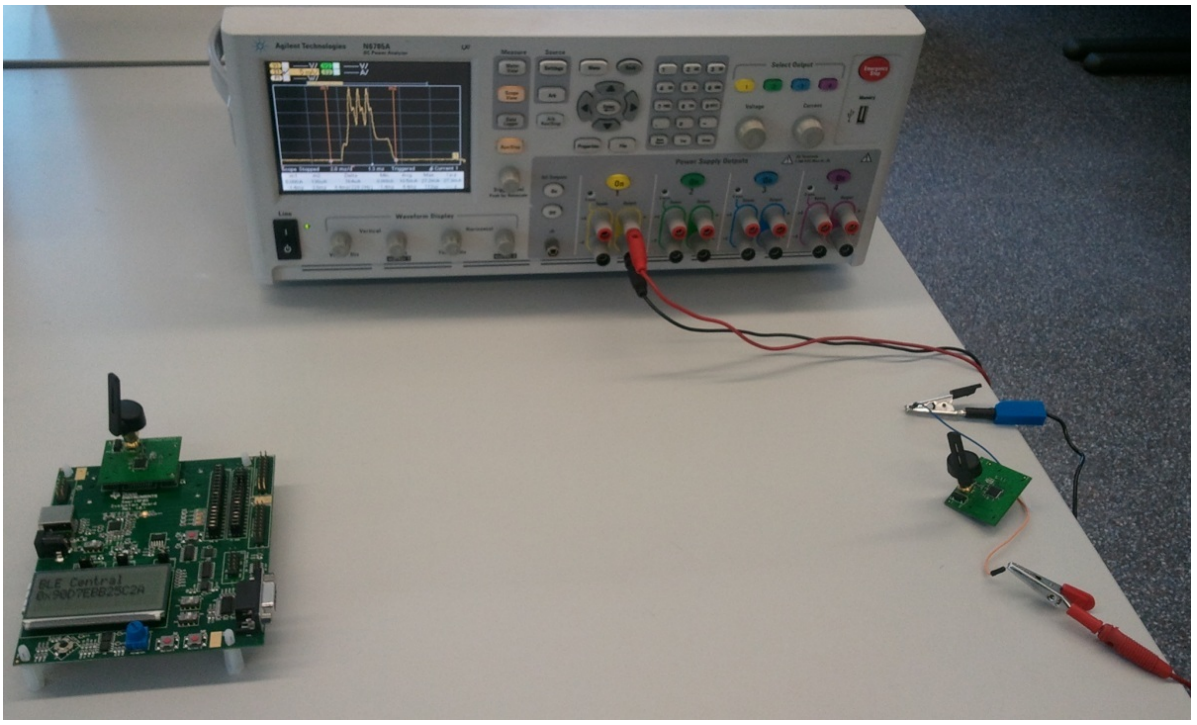

Figure 7.6: Experimental setup used for measuring the current consumption of a CC2540 slave. The devices on the left and on the right of the picture are configured as the master and the slave, respectively. The slave is connected to the Agilent N6702 power analyzer.

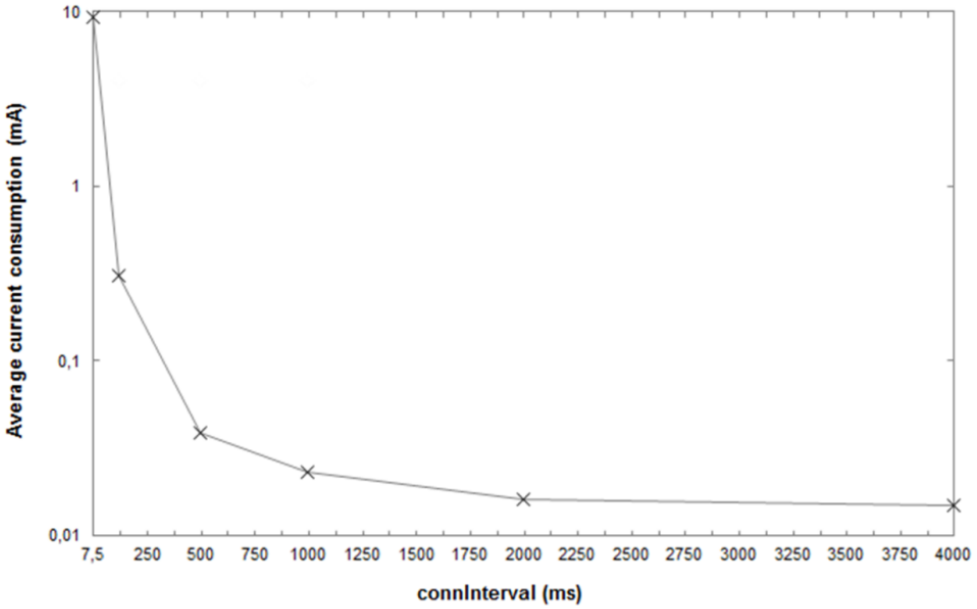

Figure 7.7: Average current consumption measured in a CC2540 slave, for the ATT one-way communication and $connSlaveLatency = 0$.

errors in the access address of the packet), the slave cannot apply latency and must listen for a packet from the master at the beginning of every connection event, until a packet from the master is received. This mechanism allows a fast resynchronization between master and

slave, so that data can be exchanged incurring low delay, at the expense of increased energy consumption. Figure 7.8 illustrates the theoretically expected lifetime of a slave that transmits a notification after each poll from the master for BER values up to 10^{-3} (i.e., the BER for which the sensitivity is defined in BLE). Note that if BER is equal to 0, the notification rate is 0.5 Hz for all the different parameter settings considered.

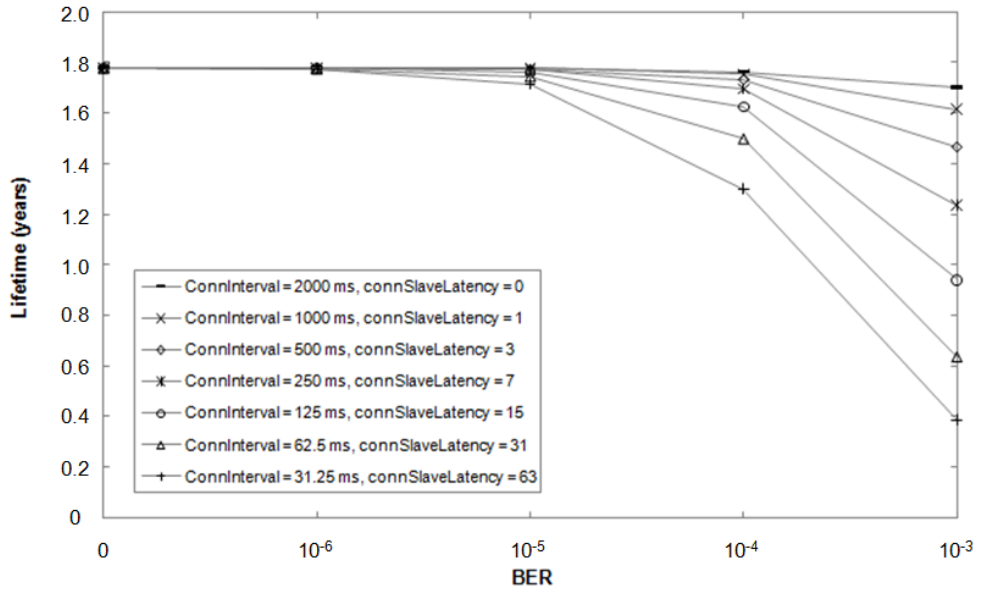

Figure 7.8: Theoretically expected slave lifetime for various *connInterval* and *connSlaveLatency* settings (which yield a notification rate of 0.5 Hz for BER = 0), for different BER values.

The choice of appropriate parameter values should be made by taking into consideration application requirements. While delivery delay may be tolerated for certain sensor measurement reading applications, a user that presses a button in a remote control is sensitive to delays greater than 500 ms [80]. Hence, if a slave is expected to react to commands sent by the master, setting *connInterval* to a low value is a safe approach. In sensor measurement transmission applications, the *connSlaveLatency* parameter can be tuned to offer the desired frequency of measurement readings and minimize energy consumption.

7.2.2 Latency

This section studies the average latency of one-way ATT communications and round-trip ATT dialogues between a master and a slave, as a function of the *connInterval* parameter, and for various BER values. Examples of the one-way ATT communications considered include the following: (i) the master polls the slave and the slave replies with a notification or a command; (ii) the master sends a notification or a command, and the slave acknowledges the master's

message at the Link Layer. The round-trip ATT dialogue considered is the same as that assumed in the energy consumption evaluation.

The latency of each message exchange is measured as the time difference between the start of the transmission of the first message and the end of the correct reception of the last message. The premise that a connection has been created between the two BLE devices before the ATT message exchange is assumed. Figure 7.9 illustrates the results, which are obtained as the average latency from ten million simulated message exchanges for each set of conditions. A *connSlaveLatency* equal to 0 is assumed. Results do not include the latency for the first packet of the connection. In fact, the master has flexibility in selecting the start time of the first packet transmission, which can occur between 1.25 ms and 11.25 + *connInterval* ms after the transmission of the *Connection Request* message.

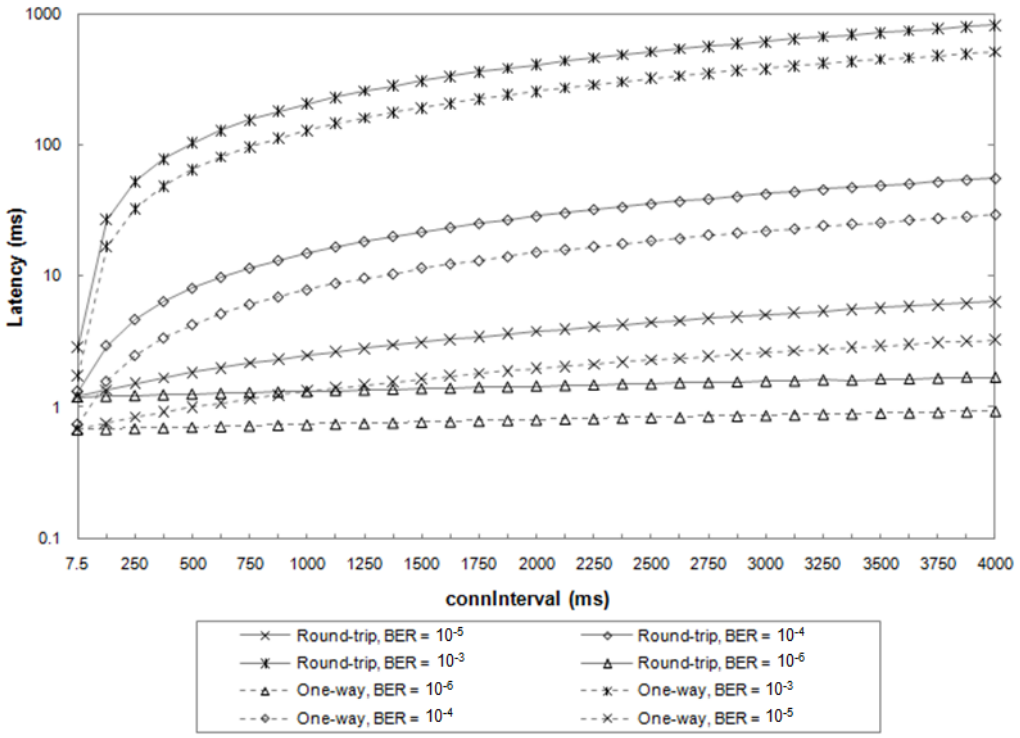

Figure 7.9: Average latency for one-way and round-trip message exchanges, for various *connInterval* and BER values.

For very low BER values (e.g., 10^{-6}), the average latency of round-trip and one-way ATT message exchanges are smaller than 2 ms and 1 ms, respectively, for any *connInterval* value. However, for greater BER values, the influence of *connInterval* becomes significant, since on average more than a single connection event is required for successful transmission of each ATT message. For high BER values (e.g., 10^{-3}), the average latency increases by up to three orders of magnitude.

On the other hand, also the measured latency of an error-free one-way ATT exchange during the experiments is measured. The measurement has been performed on the basis of

a CC2540 slave current consumption plot, which is illustrated in Figure 7.10. The obtained value is 676.7 µs, which is consistent with the delay expected to transmit a maximum-sized notification, receive the corresponding acknowledgment and wait for two IFS intervals.

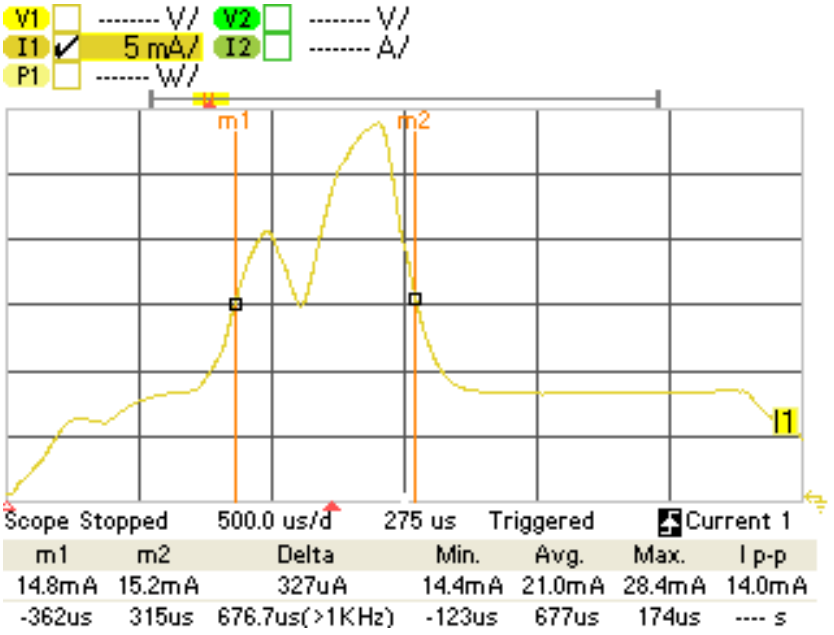

Figure 7.10: Latency measurement of a one-way ATT exchange, performed on the basis of a CC2540 slave current consumption plot. Marker *m1* is placed at the start of the reception of the poll packet from the master. Marker *m2* is placed at the end of the notification transmission.

7.2.3 Maximum Piconet Size

The maximum piconet size is next investigated, i.e., the maximum number of slaves that a master can handle. In BLE, each connection between a master and a slave is identified by a 32-bit access address. Beyond this fact, the Bluetooth 4.0 specification does not impose further limits on the number of slaves that can be connected to a master. However, there exist practical limits on that number depending on the type of communication between master and slave, on the physical memory of the devices, on the *connInterval* parameter setting and the BER that can be assumed. The maximum piconet size is independent of the *connSlaveLatency* parameter, because the inactive connection events due to slave latency cannot be used for connections with other slaves.

Figure 7.11 depicts the theoretical maximum number of slaves that a master can handle for various configurations. This upper bound limit represents the most optimistic case, where no retransmissions are needed, and is evaluated for the one-way and round-trip ATT interactions considered in the latency study. Thus, such upper bound on the maximum number of slaves per master is obtained by considering ideal communications (i.e., BER = 0). In addition, a

pessimistic scheduling scheme has also been included in the figure, whereby the communications between a master and two different slaves cannot overlap even because bit errors lead to retransmissions.

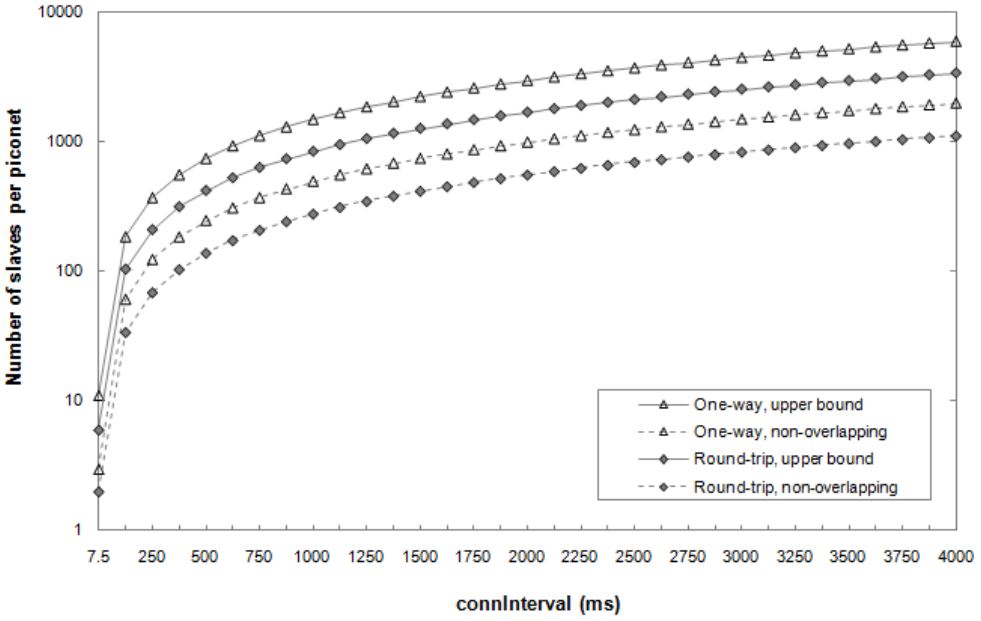

Figure 7.11: Theoretical maximum number of slaves per piconet for various types of interactions between devices and scheduling schemes.

As shown in Figure 7.11, the maximum number of slaves that a master can handle varies significantly depending on the setting of the *connInterval* parameter as Equation 7.1 indicates:

$$\lfloor max.slaves \rfloor = \frac{connInterval}{communicationduration} \tag{7.1}$$

The most energy-demanding configurations (i.e., those that use the lowest *connInterval* values) yield a limited piconet size. For example, for *connInterval* equal to 7.5 ms, the number of slaves per master is between 2 and 11, depending on the scheme considered. On the other hand, the maximum number of slaves a master can obtain data from is 5917, in the one-way ATT communication and for *connInterval* equal to 4 s.

Nevertheless, the maximum piconet size in a real scenario may be smaller than the theoretical one, due to limitations in terms of memory or antenna availability in the master. It is expected that a computer or a smartphone acting as a master will not suffer significant memory limitations. However, in some current smartphone models, the antenna is used by the classic Bluetooth and the WiFi stacks in addition to the BLE one, which reduces the available antenna time for BLE, hence the number of possible simultaneous BLE connections.

7.2.4 Throughput

Whereas the physical layer data rate is 1 Mbps, the maximum application layer throughput is calculated to be 236.7 kbps as a function of *connInterval* and BER [81]. This value is to be shared among all the participant devices in the piconet. On the other hand, recall that if any of the two connected devices receives two consecutive packets with an invalid CRC check, the connection event ends. Thus, the transmission of data cannot be resumed until the beginning of the next connection event, whereby a new data channel (i.e., a new frequency) is used. This behavior prevents any unnecessary waste of energy while bit errors are being found in one data channel. However, this scheme degrades the effective throughput of BLE in the presence of bit errors. In such conditions, moderate to high throughput can only be achieved for very low *connInterval* values.

Also hardware constraints, such as the number of application layer messages a device can send per connection event (due to memory limitations), as well as processing delays, limit the BLE throughput.

The maximum achievable throughput in a BLE link composed of two connected CC2540 devices is next measured. The distance between both devices is 0.5 m and their transmit power is 0 dBm. According to measurements, in these conditions, the BER of the BLE link is lower than 10^{-5}. In each experiment, the slave has been programmed to send the maximum number of notifications allowed by the BLE stack currently used in the CC2540 (i.e., 4 notifications per connection interval). Accordingly, *connInterval* and *connSlaveLatency* parameters are set to the smallest possible values (i.e., 7.5 ms and 0, respectively). Each notification has the maximum size (i.e., 20 bytes of application layer payload). The experiment is carried out for 1000 connection events. In the described conditions, the maximum application layer throughput measured for the piconet is 58.48 kbps. This low result can be explained by the following two facts: (i) whereas, in theory, up to eleven such notifications can be transmitted within a connection event of 7.5 ms, only 4 notifications are allowed per connection event, as aforementioned; and (ii) less than 4 notifications are actually transmitted in most connection events during the experiment (however, the same phenomenon occurs less frequently for connection intervals greater than 7.5 ms). These observations show that high throughput has not been a primary goal in the design of the BLE implementation used in the evaluation, considered as the reference platform in 2012.

7.3 BLE Application Areas

BLE may benefit from the widespread use of Bluetooth technology, since BLE easily integrates into classic Bluetooth circuitry, and hence it is likely that future Bluetooth devices will be dual-mode devices. According to published forecasts, BLE is expected to be used in billions of devices in the near future. In view of the important role that BLE may play in the Internet of

Things, the IETF 6LoWPAN WG is developing a specification in order to enable end-to-end IP communications for BLE devices [82]. For example, BLE-equipped smartphones can act as IP routers for BLE-enabled sensors and actuators. IP connectivity may dramatically increase the potential space of services and added value for BLE devices.

While BLE is emerging, other low-power wireless technologies, such as ZigBee, 6LoWPAN or Z-Wave, have already achieved significant presence in several market segments. Most of them work on top of the MAC protocols analyzed in chapter 6 or a variation of them. However, they do not have high deployment expectations in devices such as smartphones. BLE, on the other hand, is expected to have a strong position in these. Table 7.2 shows the main characteristics of BLE and the aforementioned technologies (classic Bluetooth has been included for comparison purposes).

Layer	Parameter	ZigBee	6LoWPAN	Z-Wave	BLE	Classic Bluetooth
PHY	RF Band (MHz)	868/915/2400		868/908 (all chips) 2400 (serie 400)	2400	
	Bit rate (kbps)	20/40/250		9.6/40 (all chips) 250 (serie 400)	v4: 1000	v1.2: 721 v2: 3000 v3: 24000
	Modulation	BPSK/BPSK/O-QPSK		BFSK	v4: GFSK	v1.2: GFSK v2: *PSK v3: 802.11
	Spreading Technique	DSSS		No	FHSS 2 MHz ch.	FHSS 1 MHz ch.
	Receiver Sensitivity (dBm)	min. -85 (2.4 GHz band) min. -92 (868/915 MHz bands)		-101 (at 40 kbps)	-87 to -93	-90
	Transmit Power (dBm)	-32 to 0		-20 to 0	-20 to +10	0/+4/+20
Link	MAC mechanism	TDMA+CSMA/CA (beacon mode) CSMA/CA (beaconless mode)		CSMA/CA	TDMA	
	Message bytes	max. 127		max. 64	8 to 47	max. 358
	Error control	16-bit CRC, optional ACKs		8-bit checksum optional ACKs	24-bit CRC. ACKs	header: 8-bit CRC payload: 16-bit CRC & 2/3 FEC ACKs
	Latency (ms)	<5 (beaconless mode 250 kbps)		<39 (at 40 kbps)	<3	<100
Identifiers		16 & 64-bit MAC @ 16-bit NWK @	16 & 64-bit MAC @ 16-bit IPv6 @	32-bit (home ID) 8-bit (node ID)	48-bit public @ 16-bit random @	48-bit public @

Layer	Parameter	ZigBee	6LoWPAN	Z-Wave	BLE	Classic Bluetooth
NWK	Multi-hop	Mesh routing Tree routing Source routing	RPL	Source routing	Currently not supported	Scatternet
	Hop limit	Mesh 30 Tree 10 Source 5	255	4	1	Not specified
Security		Integrity, confidentiality access control Key management	Integrity, confidentiality access control No Key management	AES-128	Security Modes. Pairing Key Gen. / Distrib. Confidentiality Authentication & Integrity	Pairing & Link Key Authentication Confidentiality Trust & Service Levels Authorization E_x Algorithms
Implementation Size		45 - 128 kB (ROM) 2.7 -12 kB (RAM)	24 kB (ROM) 3.6 kB (RAM)	32 - 64 kB (Flash) 2 - 16 kB (SRAM)	40 kB (ROM) 2.5 kB (RAM)	100 kB (ROM) 30 kB (RAM)

Table 7.2: Main characteristics of ZigBee, 6LoWPAN, Z-Wave, BLE and classic Bluetooth. The data of ZigBee, 6LoWPAN and Z-Wave has been obtained or adapted from the literature [76].

Healthcare, wellness and sports constitute an application domain where classic Bluetooth has already been used, and for which BLE constitutes an improvement. In fact, the Continua Health Alliance, an industry coalition of healthcare and technology companies, announced the selection of BLE for activity monitors and heart rate sensors to be used to monitor a users health and fitness levels.

Another opportunity for BLE is the possibility that the mobile phone may constitute a universal remote control for the domestic devices in a home. Smart energy and home security applications may further exploit BLE-enabled mobile phones. The single-hop scope of BLE may require proper transmit power tuning. In fact, most Wireless Home Automation Network (WHAN) technologies support the formation of multi-hop networks [76]. The dimensions of a home and signal propagation therein determine the appropriate transmit power setting for BLE devices and whether or not BLE can be the only technology used.

On the other hand, BLE can be used for contactless applications, such as mobile payment, ticketing or access control. However, NFC was primarily designed for this use case space, and since then, the panoply of device models that support NFC has been growing at a moderate but steady rate. NFC defines a subhundred-millisecond setup, two-way wireless technology based on the principle of magnetic inductive coupling, which allows for very short range (typically, below 10 cm). Therefore, NFC offers very limited device physical location flexibility in comparison with BLE, while it also offers significantly reduced security threat scope. Since transactions in the aforementioned application space are critical from a security viewpoint, the use of BLE would require the Passkey Entry or an adequate Out of Band pairing method. Given the properties of NFC, it constitutes a powerful candidate as Out of Band technology for BLE pairing, which additionally avoids the need to enter a key by the user. This combination of BLE and NFC provides advantages of both technologies. On the other hand, NFC does not impact on BLE use cases whereby communication range is greater than a few centimetres.

BLE is also adequate for industrial environments, which are challenging due to multipath fading and radio interference from machinery. Inherited from classic Bluetooth, BLE accounts with adaptive frequency hopping, which offers a robust solution to the aforementioned problems.

Comparatively, while the payment use-case cannot be implemented by means of WuR, the other two application cases can. In fact, this thesis contemplates in chapter 5 several WuR implementations for WBAN purposes [3] and practically all of them may be employed for WHAN purposes, and also for smart metering. However, the fact that WBAN devices are currently being connected to smartphones, makes BLE a more attractive alternative to users than WuR, even if less energy-efficient; numerically, the minimum average power consumption of BLE lies in the 20 µA, as shown in Figure 7.7. This value is about 10 times more than for the SCM-WuR system. Indeed, choosing one or another alternative really depends on the application case.

7.4 Conclusions

This chapter describes the BLE protocol stack, provides a performance evaluation of this technology and explores its potential applications. In BLE, there exists a trade-off between energy consumption, latency, piconet size, and throughput that mainly depends on the *connInterval* and *connSlaveLatency* parameters. Evaluation results show how these parameters can be tuned wisely in order to meet application requirements. This chapter also points out several implementation constraints that may reduce BLE performance in a real scenario, in comparison with the theoretically expected one. BLE emerges as a strong low-power wireless technology for certain single-hop applications which may be difficult to be covered by the use of WuR.

Another advantage of BLE is the high degree of integration it provides with consumer electronics. This is an aspect to be improved in WuR systems, which traditionally require custom WuTx. Next chapter 8 provides an initial approximation to solving this problem, by employing commercial IEEE 802.11 devices as WuTx, which helps shifting the WuR application areas from research to domestic environments.

8 Extending the WuR Functionalities to IEEE 802.11: Rethinking WuTx

This chapter proposes a novel WuR system that enables any IEEE 802.11-enabled device to be used as a WuTx without requiring any hardware modification. The accompanying low-cost and ultra-low-power WuRx hardware to be attached to any device (personal communication devices, sensors, actuators, etc.) for its remote wake-up is also presented. This way, both the gaps between WuR systems and MAC protocols and the one between research hardware and consumer electronics are filled.

In this chapter, section 8.2 describes the IEEE 802.11-enabled WuR system. Its performance, is analyzed in section 8.3 in terms of power consumption, latency and operational distances through physical experiments, as for previous platforms in this thesis. Section 8.3 also describes demonstrative use-cases showing the capability of the proposed WuR system to achieve significant energy-gains without the need for additional WuTx hardware. [1]

Contents

[1] The current chapter is based on and extends the work contained in the following JCR Q3 publication: ≪J. Oller, E. García-Villegas, E. López-Aguilar, I. Demirkol, J. Casademont, J. Paradells, G. U. Gamm, and L. Reindl, 'An IEEE 802.11-enabled Wake-up Radio System: Design and Performance Evaluation', IET Electronics Letters, vol. 50, no. 20, 2014.≫.

8.1 Introduction and Related Work

Different works focus on energy saving for IEEE 802.11 devices. However, albeit there are WuR solutions proposed for Wireless Sensor Networks [3]- [4], only the proposal in [83] contemplates the use of an IEEE 802.11 transceiver as WuTx. The work in [83] employs Frame Length Modulation (FLM) to map different frame durations to WuC addresses. However, this design requires a high WuRx sensitivity of up to -93 dBm. Such high value entails employing active circuit components such as signal amplifiers, and thus, increasing the WuRx power consumption up to 30 mW.

In [84], authors propose a system similar to [25], but shifting the WuRx from 868 MHz to 2.4 GHz. Besides, the approach in [84] requires building a custom WuTx, whereas the system in this chapter enables any legacy IEEE 802.11 device to operate as WuTx.

The IEEE 802.11 WuR system presented in this chapter outperforms the designs in [83] and [84] by providing longer operational ranges and lower power consumption at the WuRx. The proposed system is evaluated through physical experiments in different environments for realistic performance results. This contrasts with the operational distance evaluation of the system proposed in [83], which is only done through simulations.

On its part, Wake on Wireless LAN (WoWLAN) by Intel [85] represents a software-based approach that allows a system such a desktop PC to be put in sleep mode, while only keeping the IEEE 802.11 interface active. Events such as receiving a special packet, namely *magic-packet*, or being disconnected from an access point (AP) provoke the interface to wake up the system. However, according to [86], an IEEE 802.11 Network Interface Card (NIC) typically consumes around 500 mW in receiving mode. While this value represents an important energy saving compared to the power consumption of tens of watts featured by laptops and desktop computers in active mode, it still leaves room for drastic improvements when compared to WuRx.

Employing the Clear Channel Assessment (CCA) capability of an IEEE 802.15.4 sensor node as a low-power mechanism to detect 2.4 GHz signals has been proposed in [87]. Unfortunately, the performance of such hardware-based approach is found to be limited in [42], where a CC2420 is employed for such purpose. Since the CC2420 is designed for 5 MHz-wide IEEE 802.15.4 communications and the energy of an IEEE 802.11 frame is spread over 20 MHz, the receiver sensitivity is observed to degrade by 6 dB. In addition, this mechanism does not support WuC addressing, which is crucial to prevent the energy waste in the network caused by overhearing.

8.2 An IEEE 802.11-enabled WuR System

This section provides the design details of the WuRx and WuTx for the proposed IEEE 802.11 WuR system, along with the method to build the WuC.

8.2.1 IEEE 802.11-enabled WuRx Design

The WuRx for the IEEE 802.11-enabled WuR system is based on AS3933 chip [24] from Austria Microsystems. Tests in chapter 2, section 2.3.2.2 performed with the WuTx provided in the manufacturer's demokit, which transmits up to 1 W, show a limited wake-up range of ~5 m. Nevertheless, the AS3933 WuRx chip features a kHz-level high-performance envelope detector and an address correlator.

The IEEE 802.11-enabled WuRx is built by preceding an AS3933 integrated circuit with a 2.4 GHz antenna and the corresponding impedance matching stage. As for the 868 MHz WuRx in chapter 4, this shifts the WuR system's communication from magnetic to electric coupling and enables the system to use efficient microwave antennas, which require less transmission power and provide longer operational ranges.

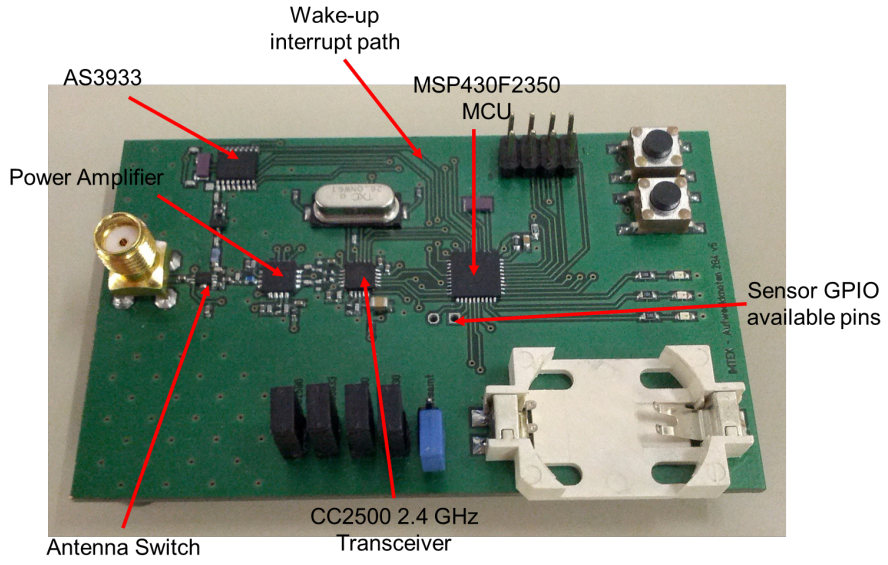

Figure 8.1: IEEE 802.11-enabled WuRx hardware.

The block diagram of the proposed IEEE 802.11-enabled WuRx is shown in Figure 8.2. After the impedance matching network, the RF received signal is down-converted from the GHz to the kHz level by means of an envelope detector. To match the 50 Ω output impedance of the antenna to the input impedance of the Schottky diode employed in the envelope detector, an L-network consisting of one inductance and two capacitances is employed. After first envelope detection, a second envelope detector, embedded in the AS3933, extracts the information modulated in the WuC, such as the address of the destined WuRx. Bits are output according to the bit-rate of the WuR system, which has to be set equally both at WuTx and WuRx for proper communication. As in any other WuRx design, if the final address correlator detects that the bits of the WuC contain the device's address, an IRQ signal is generated, which is used to wake up the device's MCU from its sleep mode. This IEEE 802.11-enabled WuRx design is measured to feature a sensitivity value of −52 dBm.

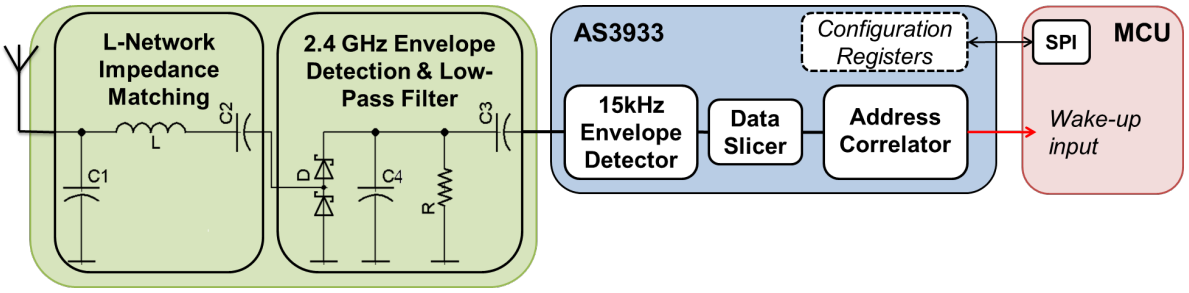

Figure 8.2: IEEE 802.11-enabled WuRx block diagram.

Note that the proposed IEEE 802.11-enabled WuRx is not restricted to the use of the AS3933, but can be implemented by means of any address correlator consisting in a shift register and a parallel comparator.

8.2.2 IEEE 802.11 WuTx

For the IEEE 802.11 WuTx to generate the WuC, which keeps the format for the 868 MHz in chapter 4, Figure 4.6, a Linux user-level application is programmed that emulates both the frequency and the timing by means of the SubCarrier Modulation, or SCM, strategy. In this case, the SCM strategy is employed by using of 2.4 GHz Wi-Fi signals emulating 15 kHz signals. Empty Link Layer IEEE 802.11 broadcast data frames (only including preamble and MAC headers) are used to generate the desired signal. Unlike unicast frames, broadcast transmissions are not followed by an ACK frame and, therefore, are suitable for the generation of a train of consecutive minimum-length frames. These broadcast frames are separated by 28 µs, which corresponds to the standard DCF Inter-Frame Space interval (DIFS). The time duration of a broadcast frame is 34 µs in the fastest IEEE 802.11g Modulation and Coding Scheme (MCS) of 54 Mbps. Note that broadcast frames must be sent at a basic rate, and that 54 Mbps is not usually included in the basic rate set. However, such basic set can be easily configured to include any standard value.

The generation of a neat train of IEEE 802.11 frames for the WuC from a Linux device requires some modifications at driver level. For such purpose, the MadWifi [88] open source NIC driver is modified to disable the CCA mechanism to both prevent interfering sources in the channel from deferring the transmission of the IEEE 802.11 frames conforming the WuC, and also to be able to keep the 16.1 kHz frequency.

As shown in Figure 8.3, alternating IEEE 802.11 frames and DIFS silence periods precisely emulates a carrier frequency of $(34\,\mu s + 28\,\mu s)^{-1} = 16.1\,kHz$, the repetition of which is the basis for the generation of the binary '1' of the OOK scheme employed for WuCs. In turn, binary '0' is generated by means of a prolonged silence period.

As long as the NIC driver's source code is available, the development in this chapter can be ported to any device featuring an IEEE 802.11-compliant transceiver such as tablets, smartphones, laptops or Wi-Fi APs, enabling their use as WuTx.

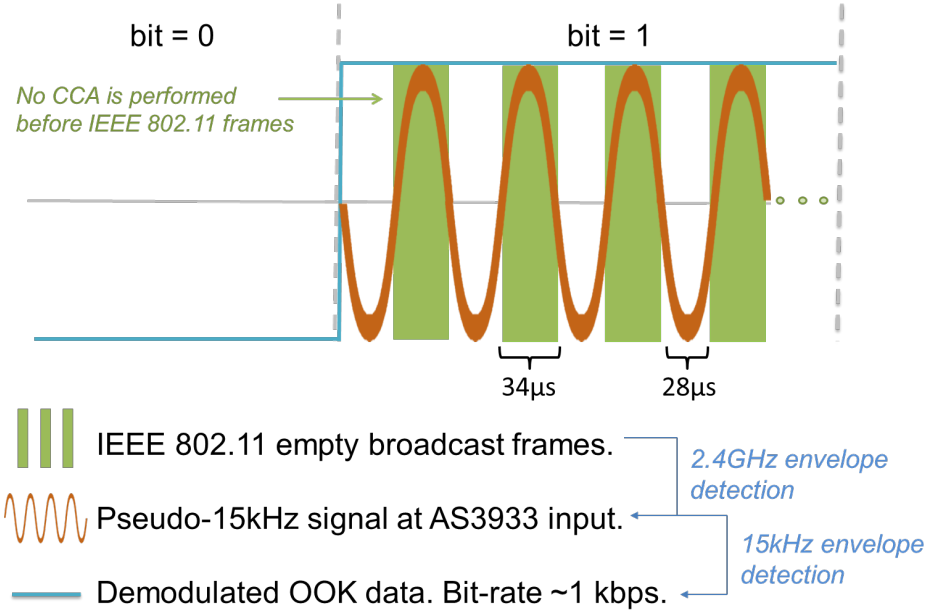

Figure 8.3: Shaping a 15 kHz signal with 2.4 GHz by means of SubCarrier Modulation.

8.3 Performance Evaluation of the WuR system

In order to evaluate the performance of the IEEE 802.11-enabled WuR system, the latency, the power consumption and the operational range it features are measured.

8.3.1 Latency Analysis

For WuR systems, the total time required to wake up a node, i.e., the wake-up delay, is a distinctive metric. For the proposed IEEE 802.11-enabled WuR system, the duration of a WuC is measured to be 44.7ms, as shown in Figure 8.4. WuR communications typically feature ms-level latency values due to their associated low bit-rates; for example, the high-performance WuRx in [5] features WuC duration of 40 ms to 110ms.

Figure 8.4 shows the WuC generated by the NIC matches the format in Figure 4.6 for SCM-WuR designs.

In the evaluations in this chapter, the AS3933 in the IEEE 802.11-enabled WuRx is configured to operate at 0.9 kbps, which corresponds to a single-bit duration of 1.12 ms. The bit duration achieved by the WuTx is exactly the same, as shown in Figure 8.5. The figure also shows the processing delay of the WuRx along with the IRQ generated on an input pin of the sleeping device. Specifically, the IRQ is generated 1.17 ms after the ending of the WuC processing, mainly due to factors such as RF amplification settling time (250 µs) and other internal delays. This 1.17 ms value contrasts with the calculated one of 0.88 ms (13.08 ms - 12.2 ms) of the 868 MHz SCM-WuR system. This latter value is lower because of the superior bit-rate of 2.730 kbps of the 868 MHz compared to the 0.9 kbps of the system proposed in this chapter.

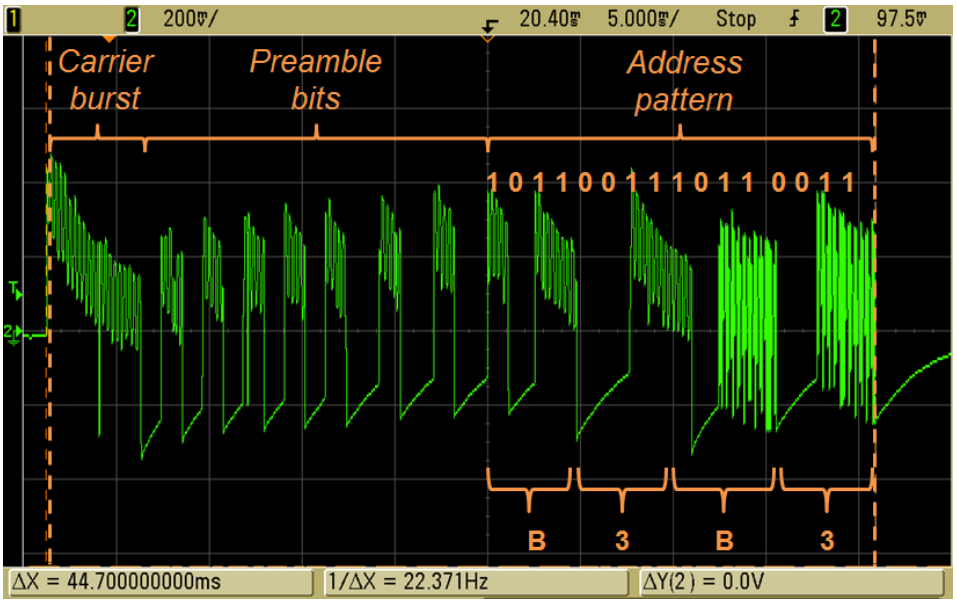

Figure 8.4: A 2.4 GHz WuC containing a node address of 0xB3B3.

Hence, a total wake-up latency of 45.87 ms (44.7 ms + 1.17 ms) is measured for a WuRx in the proposed IEEE 802.11-enabled WuR system to detect and completely decode a WuC.

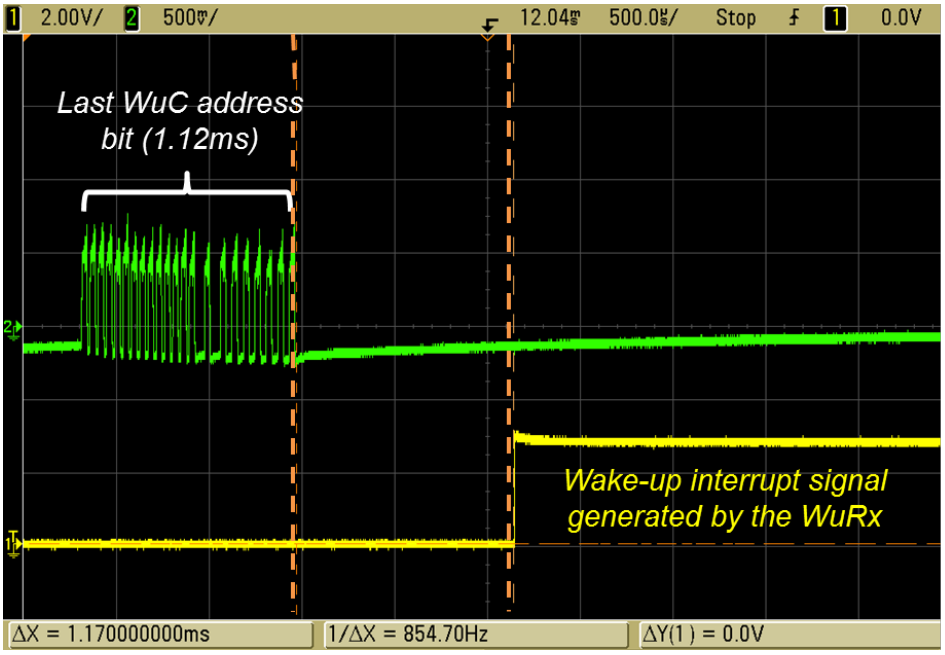

Figure 8.5: Latency to assert the wake-up pin after decoding a WuC in the IEEE 802.11-enabled WuR system.

8.3.2 Power Consumption Analysis

The WuRx board is powered by a single CR2032 3V cell button battery. As MCU, it includes a low-power MSP430F2350 from Texas Instruments, which requires as low as 0.3 µW in its lowest power mode, i.e., in LPM4. The measurements show that the total power consumed by the

WuRx board is 10.8 µW in sleep mode and 24 µW during WuC decoding. These measurements include the energy required by the MCU and by the AS3933. Given a common capacity of 230 mAh for CR2032 batteries, the proposed WuRx board features between 3 and 7 years of lifetime, depending on how frequently the WuCs arrive. This represents a significant battery lifetime for many user applications even for low-profile batteries such as cell coin ones.

In the evaluations, the WuTx, i.e., the IEEE 802.11 NIC, is configured to transmit at +18 dBm using a +2 dBi gain antenna. This transmitting power value, together with the WuC duration, results in an energy consumption of 1.5 mJ per WuC.

To illustrate the potential power savings that can be achieved by use of the IEEE 802.11-enabled WuR system, calculations are done considering the power consumption of commercial APs and workstations. In an office environment, where devices are in active state for 8 hours and in inactive state for 16 hours, deploying WuRx allows to put these devices in sleep state during such inactive times, while still enabling data communication addressed to them. The DELL Optiplex 9010 desktop computer features 66 W and 1 W in active and sleep states, respectively [89]. Also the active power consumption of two commercial wireless AP platforms, the Cisco WRT160N and Laguna GW2380, is measured to be 4.02 W and 1.9 W, respectively. The latter features a sleep mode, where the power consumption is reduced down to 1 µW. Using this as a reference value for both APs, by featuring the IEEE 802.11-enabled WuRx they can be put in sleep mode and still be activated remotely by only presenting a power consumption of 11.8 µW. In such an office environment scenario, the WuRx proposed allows power savings of 64.32 Wh/day, 30.4 Wh/day and 320 Wh/day for the Cisco WRT160N, Laguna GW2380, and the Dell Optiplex 9010, respectively. Such saving values are significant considering that they correspond to per device values.

8.3.3 Operational Range Analysis

The wake-up range analysis is done with a test setup, where an IEEE 802.11 workstation operating as WuTx and a WuRx are both placed at a height of 1 m. The WuRx is progressively displaced away from the WuTx in steps of 2 m. In Figure 8.6, the average time for the WuRx to decode a valid WuC sent by the WuTx is shown for two environments: an outdoor campus environment with high interference (several Wi-Fi networks per frequency channel) and one interference-free indoor environment. In the tests, 10 WuCs are transmitted per second, up to a maximum number of 100 WuCs.

Figure 8.6 shows the delay for the WuRx to detect the first valid WuC, averaged over up to 5 test repetitions for each distance point. Since the 2.4 GHz frequency band hosts many wireless technologies, WuC are susceptible to interference from surrounding transmissions, which delays the wake-up of the WuRx. As shown in Figure 8.6, it takes longer to activate a remote WuRx in a crowded environment than in a Wi-Fi free environment. Beyond 40 m, no WuC is detected by the WuRx, thus this value is considered to be the maximum operational

distance for the WuR system. On average, delays are found to be 0.9 s and 2.3 s for indoor and outdoor scenarios within the entire operational range, respectively, which are acceptable values for many user applications.

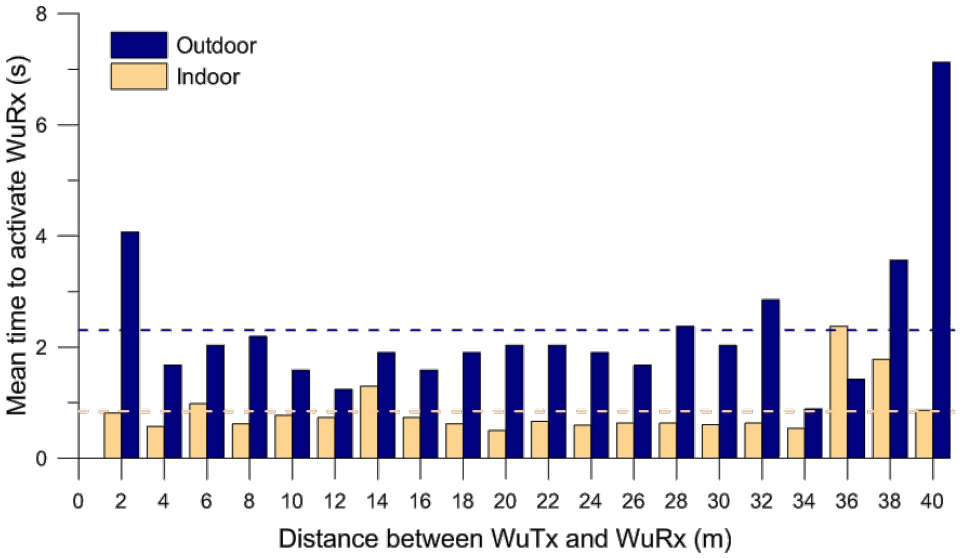

Figure 8.6: Field operational ranges achieved by the proposed IEEE-enabled WuR system.

Regarding the low latency values around 34 m, they may be due to beneficial signal propagation conditions, as shown in the simulation in Figure 8.7 for exactly the same scenario. In the figure, the values represent the received signal power levels at the WuRx when considering the *2-ray Ground Reflection* and *Friis Free Space* radio propagation models. In the figure, the real WuRx sensitivity valuel of the WuRx is indicated as a dot. Because of the uncertainty of the wireless medium, multipath reflection, non-ideal antennae, etc., the real maximum operational ranges of the WuR system, shown in Figure 8.6, are 20 m and 35 m shorter, respectively, than the simulated limits of the two models in Figure 8.7.

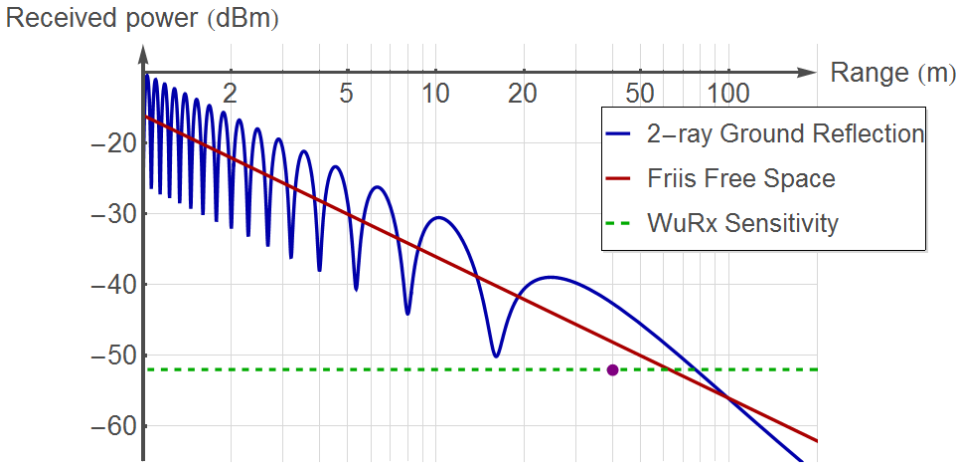

Figure 8.7: Field operational ranges corresponding to two theoretical propagation models. The dot indicates the maximum distance observed in Figure 8.6.

8.4 Conclusions and Future Work

This chapter presents the design and the implementation of an IEEE 802.11-enabled WuR system. In this system, the WuRx consumes as low as 10.8 µW. The WuTx works at 2.4 GHz and can be implemented on any IEEE 802.11-enabled device, such as a smartphone or tablet PC, without any hardware modification. The proposed WuR system is demonstrated to provide drastic energy savings for the realistic use cases depicted.

As possible future system enhancements, the use of IEEE 802.11n aggregated frames is contemplated, which is expected to provide faster low-rate carriers (~35 kHz) and, consequently, shorter WuCs. The effect of forging the Duration/ID field of IEEE 802.11 frames, thus preventing any other Wi-Fi transmission from interfering ongoing WuC, is also worth studying.

Conclusions

This thesis intensively shows along its chapters how the use of WuR systems provides drastic improvements over the power saving mechanism of nowadays WSN, which are commonly based on duty-cycling MAC strategies. Even if such duty-cycled strategies help reducing current consumption due to idle listening and overhearing, nowadays such reduction is simply not enough for new low-power application demands, where nodes should save as much energy as possible as long as their intervention is not required. WuR systems fulfil this requirement, among many others, up to the point that current designers should hesitate about its inclusion in new network designs.

WuR systems present additional benefits, such as being easier to program in terms of software. They also provide implicit synchronization. Because of this, no clocks have to be taken into account, since the node originating the communication explicitly activates the remote sleeping node. Therefore, even timers can be stopped for further energy savings.

As in the case of MAC protocols, WuR systems may strongly differ depending on the application. A system to collect remote information from sensors placed 20 meters away may certainly benefit of a different design than a WuR system for WBAN. Basically, WuR systems target to solve the overhearing problem. In fact, if a WuR system features a so-called addressing mechanism even the overhearing issue is solved, since it is possible to wake up a single node among several of them. Finally, since the wake-up procedure can be performed in a short time, the latency duty-cycled systems suffer from is also diminished.

The only disadvantage of WuR systems appears to be the need for extra hardware development. Since the employment of power amplifiers and energy consumption elements is restricted, achieving a good WuRx design may become a challenge. In fact, every chapter of this thesis targets to address some of these challenges. Thus, it is interesting to review and extend them in an incremental fashion.

The WuR system proposed in chapter 2 is a successful prototype useful for many low-power wireless applications. This development allowed our research group moving from approaches based on duty-cycled 802.15.4 to WuRx-enabled designs. The so-called SμA-WuRx is less complex than commercial WuR systems, does not require SPI communication, is cheaper from the monetary point of view, requires several times less energy and allows for up to 15 meters of WuR communication. However, the system can still be further improved by including several desirable features, such as longer operational ranges and/or addressing mechanisms.

To address the mentioned issues of the SμA-WuRx, we developed the so-called Time-Knocking (TicK) addressing strategy, analyzed in chapter 3. TicK enables energy efficient addressing by varying the sleep duration of MCUs through WuC to encode the address. TicK allows for variable length addresses, which can be used for temporary or local address assignments, and supports multicast or group-based wake-up inherently and in a very energy-efficient way. Moreover, address mismatches in TicK are determined without waiting for the end of addressing field, hence surrounding non-intended nodes can go to sleep mode quickly. Results in chapter 3 show that TicK achieves much better energy efficiency compared to other addressing methods, while slightly sacrificing delay from the addressing duration. Thus, Tick results in a valuable *add-on* to our first SμA-WuR system design.

As mentioned, a WuR system may not fit any possible application. Thus, while the SμA-WuRx and TicK efficiently solved many of the requirements of single-hop and data-collector applications, they lack of flexibility. Instead, SCM-WuR systems in chapter 4, as demonstrated through physical tests, measurements and simulations, feature an outstanding trade-off between hardware complexity, current consumption and operational range, and even enable multi-hop wake-up for long remote sensor measure collection. In addition, SCM-WuR systems effectively implement a vast range of applications, both single and multi-hop.

To place in context the performance of both SμA-WuR and SCM-WuR systems, chapter 5 provides an overview of the most important WuR systems as of 2014. It can be seen how both designs are among the most efficient of their kind.

Results in chapter 6 reconfirm the good performance of SCM-WuR in several use cases, and enable network designers with the fundamentals to firmly consider switching from currently dominant duty-cycled networks to a WuR approach. Developing a MAC protocol which performs acceptably in a wide range of diverse applications is a very difficult task, and achieving good performance in one application directly implies the other way around for others. This issue gets worse when considering single-hop and multi-hop use cases. However, WuR systems circumvent these issues and perform properly in all the use cases presented in chapter 6.

A clear circumstance where a MAC protocol can be considered more suitable than a WuR system is one where the system operates for a specified set of time and is completely shut down when not used. This is the case of health or sport monitoring, where the device is used exclusively during the activity. In these cases, the device does not stand by for long periods of time, as in the data-collector case, or to instantly react on an event detection. Instead, the MAC protocol operates only as long as the activity lasts, and each transceiver operation is meant to be indispensable. Bluetooth Low Energy, or BLE, appears as a duty-cycled MAC protocol mainly targeting single-hop applications. BLE operates as soon as the user requires it, and the device is completely shut down when not used. Nowadays, WSN based on BLE are not being considered. If this situation changes in the near future, probably multi-hop WSN based on BLE nodes will face the same limitations as the MAC protocols analyzed in this thesis. Meanwhile, because of its clearly defined use cases and its integration with its upper

application layers, BLE appears as an extremely energy-efficient protocol that cannot be easily replaced by WuR. Because of all these aspects, the performance of BLE is analyzed in chapter 7.

Finally, chapter 8 tries to solve one of the issues affecting WuR systems, that is, the need for extra hardware. While this issue seems difficult to solve for WuRx, the chapter provides ideas to use IEEE 802.11-enabled devices as WuTx. This idea is currently under research efforts and its development seems promising.

Thus, this thesis provides a complete research from initial WuR designs to the newest MAC protocols, as well as analysis of their throughput. The research is performed in an incremental fashion and includes hardware, software, simulation and documentation topics. A great effort has also been made to precisely characterize low-power MCU designs. This allows reaching the whole ecosystem of components which build a low-power wireless node.

Bibliography

[1] Analog Devices, "Diode Application Topics," 2013. [Online]. Available: http://wiki.analog.com/_export/pdf/university/courses/electronics/text/chapter-7

[2] N. M. Pletcher, S. Gambini, and J. Rabaey, "A 52uW Wake-Up Receiver With -72 dBm Sensitivity Using an Uncertain-IF Architecture," *IEEE Journal of Solid-State Circuits*, vol. 44, no. 1, pp. 269–280, 2009.

[3] S. J. Marinkovic and E. M. Popovici, "Nano-Power Wireless Wake-Up Receiver With Serial Peripheral Interface," *IEEE Journal on Selected Areas in Communications*, vol. 29, no. 8, pp. 1641–1647, 2011.

[4] J. Oller, I. Demirkol, J. Paradells, and J. Casademont, "Design, Development and Performance Evaluation of a Low-Cost, Low-Power Wake-Up Radio System for Wireless Sensor Networks," *ACM Transactions on Sensor Networks*, vol. 10, no. 1, 2013.

[5] C. Hambeck, S. Mahlknecht, and T. Herndl, "A 2.4uW Wake-up Receiver for wireless sensor nodes with -71 dBm sensitivity," in *IEEE International Symposium on Circuits and Systems (ISCAS)*, 2011, pp. 534–537.

[6] Texas Instruments, "Wiki: BLE sniffer guide," 2014. [Online]. Available: http://processors.wiki.ti.com/index.php/BLE_sniffer_guide

[7] S. Kamath, "Measuring Bluetooth Low Energy Power Consumption," Texas Instruments, Tech. Rep., 2012. [Online]. Available: http://www.ti.com/litv/pdf/swra347a

[8] Cambridge Silicon Radio, "Comparisons between Low Power Wireless Technologies: Bluetooth low energy, ANT, ANT+, RF4CE, ZigBee, Wi-Fi, Nike+, IrDA and NFC," p. 29, 2012.

[9] M. Jensen, "Coin cells and Peak Current Draw," 2012. [Online]. Available: http://www.ti.com/lit/wp/swra349/swra349.pdf

[10] M. Buettner, G. V. Yee, E. Anderson, and R. Han, "X-MAC: a short preamble MAC protocol for duty-cycled wireless sensor networks," in *Proceedings of the 4th international conference on Embedded networked sensor systems*. ACM, 2006, pp. 307–320.

[11] A. El-Hoiydi and J. D. Decotignie, "WiseMAC: an ultra low power MAC protocol for the downlink of infrastructure wireless sensor networks," in *Proceedings of the 9th IEEE International Symposium on Computers and Communications (ISCC)*. IEEE, 2004, pp. 244–251.

[12] J. Polastre, J. Hill, and D. Culler, "Versatile low power media access for wireless sensor networks," in *Proceedings of the 2nd international conference on Embedded networked sensor systems*. ACM, 2004, pp. 95–107.

[13] Y. Sun, S. Du, O. Gurewitz, and D. B. Johnson, "DW-MAC: a low latency, energy efficient demand-wakeup MAC protocol for wireless sensor networks," in *Proceedings of the 9th ACM international symposium on Mobile ad hoc networking and computing*. ACM, 2008, pp. 53–62.

[14] H. Ba, I. Demirkol, and W. Heinzelman, "Feasibility and Benefits of Passive RFID Wake-Up Radios for Wireless Sensor Networks," in *IEEE Global Telecommunications Conference (GLOBECOM'10)*, 2010, pp. 1–5.

[15] Y. Zhang, L. Huang, G. Dolmans, and H. de Groot, "An analytical model for energy efficiency analysis of different wakeup radio schemes," in *IEEE 20th International Symposium on Personal, Indoor and Mobile Radio Communications (PIMRC'09)*. IEEE, 2009, pp. 1148–1152.

[16] I. Demirkol, C. Ersoy, and E. Onur, "Wake-up receivers for wireless sensor networks: benefits and challenges," *IEEE Wireless Communications*, vol. 16, no. 4, pp. 88–96, 2009.

[17] B. Van der Doorn, W. Kavelaars, and K. Langendoen, "A prototype low-cost wakeup radio for the 868 MHz band," *International Journal of Sensor Networks*, vol. 5, no. 1, pp. 22–32, 2009.

[18] Linx Technologies, "ANT-868-SP Datasheet," 2008. [Online]. Available: https://www.linxtechnologies.com/resources/data-guides/ant-868-sp.pdf

[19] Atmel Corporation, "ATA5283: Interface IC for 125 kHz Wake-up Function Datasheet," 2005. [Online]. Available: http://www.datasheetcatalog.org/datasheet/atmel/doc4598.pdf

[20] J. L. Ferrer, "Diseño e implementación de un módulo hardware de bajo coste para redes basadas en el estándar IEEE 802.15.4 para la Internet Futura." Ph.D. dissertation, Universitat Politècnica de Catalunya, UPCommons, 2010. [Online]. Available: http://upcommons.upc.edu/pfc/bitstream/2099.1/9872/1/PCF_JLFerrer_Dise%C3%B1o_e_imp_nodo_IEEE_802.15.4_para_la_Internet_Futura.pdf

[21] Adeunis RF, "ARF27 Transmitters and Receivers: User Guide." 2007.

[22] Linx Technologies, "ANT-868-CW-QW Datasheet," 2008. [Online]. Available: https://www.linxtechnologies.com/resources/data-guides/ant-868-cw-qw.pdf

[23] Texas Instruments, "CC2430: 2.4 GHz IEEE 802.15.4 / ZigBee-ready RF Transceiver Datasheet," 2007. [Online]. Available: http://www.ti.com/lit/ds/symlink/cc2430.pdf

[24] Austria Microsystems, "AS3932/AS3933 LF detector ICs Datasheet," 2010. [Online]. Available: http://www.ams.com/eng/acceptpolicy/information/66224/570460/AS3933_Datasheet_EN_v2.pdf

[25] G. U. Gamm, M. Sippel, M. Kostic, and L. M. Reindl, "Low power wake-up receiver for wireless sensor nodes," in *6th International Conference on Intelligent Sensors, Sensor Networks and Information Processing (ISSNIP)*. IEEE, 2010, pp. 121–126.

[26] S. von der Mark, R. Kamp, M. Huber, and G. Boeck, "Three stage wakeup scheme for sensor networks," in *International Conference on Microwave and Optoelectronics (IMOC)*. IEEE, 2005, pp. 205–208.

[27] S. von der Mark and G. Boeck, "Ultra low power wakeup detector for sensor networks," in *Microwave and Optoelectronics Conference (IMOC)*. IEEE, 2007, pp. 865–868.

[28] S. Ishida, T. Takiguchi, S. Saruwatari, M. Minami, and H. Morikawa, "Evaluation of a wake-up wireless module with bloom-filter-based ID matching," in *8th Asia-Pacific Symposium on Information and Telecommunication Technologies (APSITT'10)*. IEEE, 2009, pp. 1–6.

[29] T. Takiguchi, S. Saruwatari, T. Morito, S. Ishida, M. Minami, and H. Morikawa, "A novel wireless wake-up mechanism for energy-efficient ubiquitous networks," in *Proceedings of the First International Workshop on Green Communications (GreenComm09)*, 2009, pp. 1–5.

[30] L. Gu and J. A. Stankovic, "Radio-Triggered Wake-Up for Wireless Sensor Networks," *RealTime Systems*, vol. 29, no. 2, pp. 157–182, 2005.

[31] J. Ansari, D. Pankin, and P. Mähönen, "Radio-triggered wake-ups with addressing capabilities for extremely low power sensor network applications," *International Journal of Wireless Information Networks*, vol. 16(3), no. 3, pp. 118–130, 2009.

[32] Texas Instruments, "MSP430G2x52 Mixed Signal Microcontroller," 2010. [Online]. Available: http://www.ti.com/lit/ds/symlink/msp430g2452.pdf

[33] ——, "CC1101: Low-Power Sub-1 GHz RF Transceiver Datasheet," 2012. [Online]. Available: http://www.ti.com/lit/ds/symlink/cc1101.pdf

[34] J. Oller, I. Demirkol, J. Paradells, J. Casademont, and W. Heinzelman, "Time-Knocking: A Novel Addressing Mechanism for Wake-up Receivers," in *8th IEEE International Conference on Wireless and Mobile Computing, Networking and Communications (WiMob)*, 2012, pp. 268–275.

[35] Texas Instruments, "MSP430F2350," 2010. [Online]. Available: http://www.ti.com/lit/ds/symlink/msp430f2350.pdf

[36] G. U. Gamm and L. M. Reindl, "Range extension for wireless wake-up receivers," in *9th International Multi-Conference on Systems, Signals and Devices (SSD)*, 2012, pp. 1–4.

[37] Wolfram Research, "Mathematica, Technical and Scientific Software," 2013. [Online]. Available: http://www.wolfram.com/mathematica/

[38] V. András and H. Rudolf, "An overview of the OMNeT++ simulation environment," in *Proceedings of the 1st international conference on Simulation tools and techniques for communications, networks and systems & workshops (Simutools)*. ICST, Brussels, Belgium, Belgium: ICST (Institute for Computer Sciences, Social-Informatics and Telecommunications Engineering), 2008, pp. 1–10.

[39] MoteIV Corporation, "T-mote sky: Ultra low power IEEE 802.15.4 compliant wireless sensor module," 2006. [Online]. Available: http://www.eecs.harvard.edu/~konrad/projects/shimmer/references/tmote-sky-datasheet.pdf

[40] R. Jurdak, A. G. Ruzzelli, and G. M. P. O'Hare, "Radio Sleep Mode Optimization in Wireless Sensor Networks," *IEEE Transactions on Mobile Computing*, pp. 955–968, 2010.

[41] N. M. Pletcher, "PhD Thesis: Ultra-low power wake-up receivers for wireless sensor networks," Ph.D. dissertation, University of California, Berkeley, 2008.

[42] H. Yomo, Y. Kondo, N. Miyamoto, S. Tang, M. Iwai, and T. Ito, "Receiver Design for Realizing On-Demand WiFi Wake-up using WLAN Signals," in *IEEE Global Telecommunications Conference (GLOBECOM'12)*, 2012, pp. 5206–5211.

[43] H. Ba, I. Demirkol, and W. Heinzelman, "Passive wake-up radios: From devices to applications," *Ad Hoc Networks*, vol. 11, no. 8, pp. 2605–2621, 2013.

[44] Alien Technology, "Alien ALR-9900+ Enterprise Reader," 2010.

[45] S. Drago, D. M. W. Leenaerts, F. Sebastiano, L. J. Breems, K. A. A. Makinwa, and B. Nauta, "A 2.4 GHz 830 pJ/bit duty-cycled wake-up receiver with -82dBm sensitivity for crystal-less wireless sensor nodes," in *Solid-State Circuits Conference Digest of Technical Papers (ISSCC), 2010 IEEE International*. IEEE, 2010, pp. 224–225.

[46] H. Cho, J. Bae, and H.-J. Yoo, "A 37.5 uW Body Channel Communication Wake-Up Receiver With Injection-Locking Ring Oscillator for Wireless Body Area Network," *IEEE Transactions on Circuits and Systems I: Regular Papers*, vol. 60, no. 5, pp. 1200–1208, 2013.

[47] H. Milosiu, F. Oehler, M. Eppel, D. Fruhsorger, S. Lensing, G. Popken, and T. Thones, "A 3 uW 868-MHz wake-up receiver with -83 dBm sensitivity and scalable data rate," in *ESSCIRC (ESSCIRC), 2013 Proceedings of the*, Sep. 2013, pp. 387–390.

[48] X. Huang, S. Rampu, X. Wang, G. Dolmans, and H. De Groot, "A 2.4 GHz/915 MHz 51 uW wake-up receiver with offset and noise suppression," in *IEEE International Solid-State Circuits Conference Digest of Technical Papers (ISSCC'10)*. IEEE, 2010, pp. 222–223.

[49] N. E. Roberts and D. D. Wentzloff, "A 98 nW wake-up radio for wireless body area networks," in *Radio Frequency Integrated Circuits Symposium (RFIC)*. IEEE, 2012, pp. 373–376.

[50] Texas Instruments, "CC2530EM Reference Design," 2010. [Online]. Available: http://www.ti.com/tool/cc2530em

[51] D. Y. Yoon, C. J. Jeong, J. Cartwright, H. Y. Kang, S. K. Han, N. S. Kim, D. S. Ha, and S. G. Lee, "A New Approach to Low-Power and Low-Latency Wake-Up Receiver System for Wireless Sensor Nodes," *IEEE Journal of Solid-State Circuits*, vol. 47, no. 10, pp. 2405–2419, 2012.

[52] P. Le-Huy and S. Roy, "Low-Power Wake-Up radio for wireless sensor networks," *Mobile Networks and Applications*, vol. 15, no. 2, pp. 226–236, 2010.

[53] P. Jean-François, B. Jean-Jules, and S. Yvon, "Modeling, design and implementation of a low-power FPGA based asynchronous wake-up receiver for wireless applications," *Analog Integrated Circuits and Signal Processing*, pp. 1–14, 2013.

[54] M. S. Durante and S. Mahlknecht, "An Ultra Low Power Wakeup Receiver for Wireless Sensor Nodes," in *3rd International Conference on Sensor Technologies and Applications (SENSORCOMM)*, 2009, pp. 167–170.

[55] T. Wada, M. Ikebe, and E. Sano, "60-GHz, 9 uW wake-up receiver for short-range wireless communications," in *Proceedings of the ESSCIRC (ESSCIRC)*, Sep. 2013, pp. 383–386.

[56] T. Terada, M. Kikuchi, A. Kudo, T. Yamazoe, and T. Takeuchi, "Low power and high receiving sensitivity wireless wake-up receiver with 2-stage power-supply control scheme for lithium-ion battery systems," in *29th Applied Power Electronics Conference and Exposition (APEC)*, vol. 1. IEEE, 2014, pp. 3397–3400.

[57] J. Mathews, M. Barnes, A. Young, and D. K. Arvind, "Low Power Wake-Up in Wireless Sensor Networks Using Free Space Optical Communications," in *4th International Conference on Sensor Technologies and Applications (SENSORCOMM)*, 2010, pp. 256–261.

[58] G. Kim, Y. Lee, S. Bang, I. Lee, Y. Kim, D. Sylvester, and D. Blaauw, "A 695 pW standby power optical wake-up receiver for wireless sensor nodes," in *Custom Integrated Circuits Conference (CICC), 2012 IEEE*, 2012, pp. 1–4.

[59] F. Utsunomiya, A. Tanaka, and T. Douseki, "A self-powered photosensor switch detects only rising edge of infrared-light pulse for wireless zero-standby-power wake-up receiver," in *IEEE Sensors*, Nov. 2013, pp. 1–4.

[60] E. Lattanzi, M. Dromedari, V. Freschi, and A. Bogliolo, "A Sub-uA Ultrasonic Wake-Up Trigger with Addressing Capability for Wireless Sensor Nodes," *ISRN Sensor Networks*, vol. 2013, 2013.

[61] J. Oller, I. Demirkol, J. Casademont, J. Paradells, G. U. Gamm, and L. Reindl, "Performance Evaluation and Comparative Analysis of SubCarrier Modulation Wake-up Radio Systems for Energy-Efficient Wireless Sensor Networks," *Sensors*, vol. 14, no. 1, pp. 22–51, Dec. 2013.

[62] A. Köpke, M. Swigulski, K. Wessel, D. Willkomm, P. T. K. Haneveld, T. E. V. Parker, O. W. Visser, H. S. Lichte, and S. Valentin, "Simulating wireless and mobile networks in OMNeT++ the MiXiM vision," in *Proceedings of the 1st International Conference on Simulation Tools and Techniques for Communications, Networks and Systems & Workshops (Simutools)*, Mar. 2008, p. 71.

[63] K. Langendoen, "The MAC Alphabet Soup." [Online]. Available: http://www.st.ewi.tudelft.nl/~koen/MACsoup/protocols.php

[64] Y. Sun, O. Gurewitz, and D. B. Johnson, "RI-MAC: a receiver-initiated asynchronous duty cycle MAC protocol for dynamic traffic loads in wireless sensor networks," in *Proceedings of the 6th ACM conference on Embedded network sensor systems (SenSys)*. ACM Press, Nov. 2008, p. 1.

[65] V. Jelicic, M. Magno, D. Brunelli, V. Bilas, and L. Benini, "Analytic comparison of wake-up receivers for WSNs and benefits over the wake-on radio scheme," in *Proceedings of the 7th ACM workshop on Performance monitoring and measurement of heterogeneous wireless and wired networks (PM2HW2N '12)*. ACM, 2012, pp. 99–106.

[66] R. Su, T. Watteyne, and K. S. J. Pister, "Comparison between Preamble Sampling and Wake-Up Receivers in Wireless Sensor Networks," in *IEEE Global Telecommunications Conference (GLOBECOM)*, 2010, pp. 1–5.

[67] Y. Zhang and G. Dolmans, "Wake-up radio assisted energy-aware multi-hop relaying for low power communications," in *IEEE Wireless Communications and Networking Conference (WCNC)*. IEEE, Apr. 2012, pp. 2498–2503.

[68] R. Jurdak, A. G. Ruzzelli, and G. M. P. O'Hare, "Adaptive Radio Modes in Sensor Networks: How Deep to Sleep?" in *5th Annual IEEE Communications Society Conference on Sensor, Mesh and Ad Hoc Communications and Networks*. IEEE, Jun. 2008, pp. 386–394.

[69] J. Oller, I. Demirkol, J. Casademont, J. Paradells, G. U. Gamm, and L. Reindl, "Wake-up Radio As an Energy-efficient Alternative to Conventional Wireless Sensor Networks MAC Protocols," in *Proceedings of the 16th ACM International Conference on Modeling, Analysis & Simulation of Wireless and Mobile Systems*, ser. MSWiM '13. ACM, 2013, pp. 173–180.

[70] D. Gislason, *ZigBee Wireless Networking*. Newnes, 2004.

[71] Z. Shelby and C. Bormann, *6LoWPAN: The Wireless Embedded Internet*. Wiley Subscription Services, 2009.

[72] P. Levis, S. Madden, J. Polastre, R. Szewczyk, A. Woo, D. Gay, J. Hill, M. Welsh, E. Brewer, and D. Culler, "TinyOS: An operating system for sensor networks," in *Ambient Intelligence*. Springer Verlag, 2004.

[73] A. Dunkels, B. Gronvall, and T. Voigt, "Contiki - A Lightweight and Flexible Operating System for Tiny Networked Sensors," in *Proceedings of the 29th Annual IEEE International Conference on Local Computer Networks*, ser. LCN '04. Washington, DC, USA: IEEE Computer Society, 2004, pp. 455–462.

[74] I. Demirkol, J. Paradells, J. Oller, J. Casademont, and A. Calveras, "Energy Efficient Wireless Networking of Sensor Nodes," in *AMA Conferences*, 2013, pp. 452–456.

[75] Bluetooth Special Interest Group, "Specification of the Bluetooth System, Covered Core Package," 2010.

[76] C. Gomez and J. Paradells, "Wireless home automation networks: A survey of architectures and technologies," *IEEE Communications Magazine*, vol. 48, no. 6, pp. 92–101, 2010.

[77] Texas Instruments, "CC2540: 2.4-GHz Bluetooth Low Energy System-on-Chip," 2010. [Online]. Available: http://www.ti.com/lit/ds/symlink/cc2540.pdf

[78] ——, "CC2564 Bluetooth and Dual-Mode Controller," 2012. [Online]. Available: http://www.ti.com/lit/ds/symlink/cc2564.pdf

[79] STMicroElectronics, "M24SR02-Y: Dynamic NFC/RFID tag IC with 2-Kbit EEPROM, NFC Forum Type 4 Tag and IC interface," 2014. [Online]. Available: http://www.st.com/web/en/resource/technical/document/datasheet/DM00097458.pdf

[80] J. Ko, A. Terzis, S. Dawson-Haggerty, D. E. Culler, J. W. Hui, and P. Levis, "Connecting low-power and lossy networks to the internet," *IEEE Communications Magazine*, vol. 49, no. 4, pp. 96–101, 2011.

[81] C. Gomez, I. Demirkol, and J. Paradells, "Modeling the Maximum Throughput of Bluetooth Low Energy in an Error-Prone Link," *IEEE Communications Letters*, vol. 15, no. 11, pp. 1187–1189, 2011.

[82] J. Nieminen, C. Gomez, M. Isomaki, T. Savolainen, B. Patil, Z. Shelby, M. Xi, and J. Oller, "Networking Solutions for Connecting Bluetooth Low Energy Enabled Machines to the Internet of Things," *IEEE Communications and Networks*, 2014.

[83] Y. Kondo, H. Yomo, S. Tang, M. Iwai, T. Tanaka, H. Tsutsui, and S. Obana, "Energy-efficient WLAN with on-demand AP wake-up using IEEE 802.11 frame length modulation," *Computer Communications*, vol. 35, no. 14, pp. 1725–1735, 2012.

[84] P. Pursula, V. Viikari, and J.-M. Saari, "Wake-up radio architecture utilizing passive down conversion mixing," *Microwave and Optical Technology Letters*, vol. 55, no. 5, pp. 1038–1041, 2013.

[85] Intel Corporation, "Intel Centrino Mobile Technology Wake on Wireless LAN (WoWLAN) Feature," 2006.

[86] F. I. Salvatore Chiaravalloti and L. Budzisz, "Power consumption of WLAN network elements," 2011. [Online]. Available: http://www.tkn.tu-berlin.de/fileadmin/fg112/Papers/TR-WLAN-Power.pdf

[87] K. Chebrolu and A. Dhekne, "Esense: communication through energy sensing," in *Proceedings of the 15th annual international conference on Mobile computing and networking*, ser. MobiCom '09. New York, NY, USA: ACM, 2009, pp. 85–96.

[88] "The Madwifi project." [Online]. Available: http://madwifi-project.org/

[89] University of Pennsylvania, "Computer Power Usage," 2013. [Online]. Available: https://secure.www.upenn.edu/computing/resources/category/hardware/article/computer-power-usage